IAEA-TECDOC-947

Waste treatment and immobilization technologies involving inorganic sorbents

Final report of a co-ordinated research programme
1992-1996

INTERNATIONAL ATOMIC ENERGY AGENCY

The originating Section of this publication in the IAEA was:

Waste Technology Section
International Atomic Energy Agency
Wagramerstrasse 5
P.O. Box 100
A-1400 Vienna, Austria

WASTE TREATMENT AND IMMOBILIZATION TECHNOLOGIES
INVOLVING INORGANIC SORBENTS
IAEA, VIENNA, 1997
IAEA-TECDOC-947
ISSN 1011–4289

Printed by the IAEA in Austria
June 1997

FOREWORD

A Co-ordinated Research Programme on the Use of Inorganic Sorbents for Treatment of Liquid Radioactive Waste and Backfill of Underground Repositories was initiated by the IAEA in 1987. This CRP brought together researchers from twelve different countries who were studying both the use of naturally occurring sorbents for waste treatment and backfill of underground repositories, and the preparation, characterization, sorption properties and kinetics of synthetic and composite sorbents for the treatment of liquid waste. The results of these investigations were summarized and published in IAEA-TECDOC-675, issued in November 1992.

Taking into account a growing application of inorganic sorbents in liquid waste treatment and immobilization and increasing activities of the Member States in this field, a new CRP was initiated in 1992 on Waste Treatment and Immobilization Technologies Involving Inorganic Sorbents. The results of this new CRP, which lasted for four years, are presented in this report.

The summary report on this CRP was prepared by the consultant, E.W. Hooper of the United Kingdom. The Scientific Secretary of the Programme was A. Tsarenko of the IAEA's Division of Nuclear Fuel Cycle and Waste Management.

The report was prepared for publication with the assistance of V.M. Efremenkov of the IAEA, Division of Nuclear Power and the Fuel Cycle. The IAEA would like to express its thanks to all those who participated in this programme and contributed to this report.

EDITORIAL NOTE

CONTENTS

SUMMARY OF THE CO-ORDINATED RESEARCH PROGRAMME

1. INTRODUCTION

The increasingly stringent safety requirements for release of liquid radioactive effluents to the environment and for disposal of conditioned waste demand improvement of technologies for treatment and conditioning of radioactive wastes. Intensive research and development work has been undertaken in different Member States, especially in the area of treatment and conditioning of liquid radioactive waste. New materials and technologies are under consideration for improving current practices in waste treatment and conditioning. Inorganic sorbents and ion-exchangers are among these materials.

The specific properties of inorganic sorbents important for treatment of specific waste streams can be designed during sorbent synthesis, and this makes their practical application very attractive.

A Co-ordinated Research Programme (CRP) was initiated by the IAEA in 1992 to promote greater co-operation in the field of radioactive waste treatment and immobilization using inorganic sorbents. Fifteen institutions from fourteen countries were involved in the research and development work in the framework of this programme, which lasted for a period of 4 years. The results obtained by the participants during the implementation of this programme are reported in this publication.

The main goal of the programme was to promote the exchange of information on the results obtained in different Member States in searching for reliable, cost-effective and integrated technologies for treatment and immobilization of liquid radioactive wastes involving inorganic sorbents. In the framework of this CRP it was intended:

- to conduct fundamental studies to obtain information on sorbent structure and sorption mechanisms that will be required in order to be able to select the best materials for sorption of particular radionuclides;
- to obtain thermodynamic and kinetic data necessary for the design of suitable treatment processes;
- to conduct further investigations to define sorption mechanisms of radionuclides on different soil samples and to provide data which can be used to predict radionuclide behaviour in the environment;
- to identify individual sorbents or sorbent mixtures appropriate and effective for the treatment of liquid waste streams with complex characteristics and compositions;
- to develop a series of simple standard tests that can be used universally in order to be able to compare the results of different groups of investigators.

This CRP contributed to all of the above areas of activity. The research work within the framework of this CRP involved the use of naturally occurring sorbents in waste treatment and immobilization technologies, preparation and characterization of synthetic and composite sorbents for waste treatment and initial studies on the sorption of caesium by soil fractions.

The CRP provided opportunities for close co-operation and information exchange between institutions involved in this work. Twenty-five collaborative actions were agreed and at the final RCM in January 1996, 19 were reported as having taken place with another 6 still in progress. All participants expressed their intentions of continuing to collaborate and exchange information in the future.

A general summary of the results achieved by this CRP during the four years of its implementation is provided below, followed by the individual reports of the CRP participants.

2. SCIENTIFIC AND TECHNICAL RESULTS OF THE PROGRAMME

The research carried out during this CRP has included the separation of fission products, activation products and alpha-emitting radionuclides from both simulated and real radioactive waste streams. A wide range of sorbents, including naturally occurring materials, synthetic inorganic sorbents and composite sorbents have been examined for these purposes. Table I lists the sorbents that were examined during this CRP, the country where they were examined and the radionuclides they were tested with. The research included synthesis, characterization and testing of different sorbents and study of their application for treatment of different waste streams. Some investigations were carried out on application of naturally occurring inorganic sorbents in the immobilization processes.

The following sections provide a brief summary of and the key conclusions of the research carried out. More information can be found in the individual reports.

2.1. USE OF INORGANIC SORBENTS FOR THE TREATMENT OF RADIOACTIVE WASTES

2.1.1. Naturally occurring sorbents

Various kinds of natural inorganic materials such as phosphates, oxides and magnetite minerals were studied in China in batch and column experiments to determine the efficiency of Pu, Am, Ce, Cs and Sr removal from a simulated reprocessing waste stream (with high acidity and salts content). Slow sorption kinetics were observed for most of them. But one material, an apatite, showed a high sorption capacity for Pu, Am and Ce.

Natural clinoptilolite has been studied in the Czech Republic for sorption of Cs, Co and Ru. It was demonstrated that treatment of clinoptilolite with an NaOH solution improves its ion exchange capacity for Cs and Co. The highest exchange capacity for Co was obtained with clinoptilolite treated with 5M NaOH. Natural clinoptilolite has also been used to remove RuO_4 vapour from gas streams at 50^0C and ambient temperature.

Studies undertaken in Belarus on Cs and Sr sorption by different fractions of soil have indicated that almost 90% of them are concentrated in a fine clay fraction of soil. These data are important for development of an effective methodology for soil decontamination.

2.1.2. Synthetic inorganic sorbents

A number of synthetic sorbents have been tested for the removal of different radionuclides from liquid waste streams.

A study of the properties of hexacyanoferrate sorbents for Cs and Sr sorption has been undertaken in The Russian Federation and Belarus. A nickel hexacyanoferrate sorbent was found to be the best, among those studied for the removal of Cs from solutions containing detergents. The data obtained has been used to develop a method for treating liquid wastes generated by decontamination of equipment affected by the Chernobyl accident.

Synthetic mordenite mixed with glass frit has been used in the Czech Republic to remove Cs from solutions containing boric acid. Good removal (>95%) was obtained by passing 600 bed volumes through a small packed bed of sorbent. Mordenite has also been tested for absorption of RuO_4 vapour from gas streams at temperatures of 50 and 100°C. Greater than $50\mu g$ Ru per gram of sorbent was attained before 1% breakthrough.

In Egypt, antimonates of Sn and Ce have been used, either pre-formed or formed in situ, to remove Na, Cs, Sr, Co and Eu from solution. The ion exchange properties were better the greater the Sb/Ce or Sb/Sn molar ratios used during sorbent synthesis.

TABLE I SORBENTS STUDIED DURING THE CRP

Country	**Sorbents**	**Radionuclides**
Belarus	Clinoptilolite	^{90}Sr, ^{137}Cs
Belarus	KU-2 cationite	^{90}Sr, ^{137}Cs
Belarus	AV-17 anionite	^{90}Sr, ^{137}Cs,
Belarus	Ni FC	^{137}Cs
Belarus	Mn FC	^{137}Cs
Belarus	Cellulose	^{90}Sr
China	Natural Materials (7)	^{60}Co, ^{90}Sr, ^{137}Cs, ^{144}Ce, ^{155}Eu, $^{239+240}$Pu, ^{241}Am
China	Synthetic Materials (1)	^{90}Sr, ^{137}Cs, ^{144}Ce, $^{239+240}$Pu, ^{241}Am
Cuba	Natural Materials (10)	^{60}Co, ^{137}Cs
Czech Rep	Natural Clinoptilolite	^{60}Co, ^{106}RuO$_4$, ^{137}Cs
Czech Rep	Synthetic mordenite	^{90}Sr, ^{106}RuO$_4$, ^{137}Cs
	Composite sorbents	
Czech Rep	Molybdophosphate (AMP)	^{137}Cs
Czech Rep	Hexacyanoferrate (NiFC)	^{60}Co, ^{137}Cs
Czech Rep	Manganese Dioxide (MnO)	^{54}Mn, ^{60}Co, ^{125}Sb, ^{137}Cs, ^{224}Ra, ^{228}Th, U
Czech Rep	Sodium Titanate (NaTiO)	^{54}Mn, ^{60}Co, ^{125}Sb, ^{137}Cs, ^{224}Ra, ^{228}Th, U
Czech Rep	Synthetic Mordenite (M315)	^{54}Mn, ^{60}Co, ^{125}Sb, ^{137}Cs
Czech Rep	Synthetic Zeolite (Na-Y)	^{54}Mn, ^{60}Co, ^{125}Sb, ^{137}Cs
Czech Rep	Cobalt Hexacyanoferrate	^{137}Cs
Czech Rep	Pot Cobalt Hexacyanoferrate	^{137}Cs
Czech Rep	Hydrated Titanium Oxide	^{224}Ra, ^{228}Th, U
Czech Rep	Barium-Calcium Sulphate	^{224}Ra, ^{228}Th
Egypt	Cerium (IV) Antimonate	^{22}Na, ^{60}Co, ^{90}Sr, ^{137}Cs, ^{152,154}Eu
Egypt	Tin (IV) Antimonate	^{22}Na, ^{60}Co, ^{90}Sr, ^{137}Cs, ^{152,154}Eu
Finland	Hexacyanoferrate	^{137}Cs
Finland	Activated Carbon	^{60}Co
Finland	Modified Titanium Oxide	^{90}Sr
India	Synthetic Zeolite 4A	^{90}Sr, ^{137}Cs, ^{60}Co
India	Synthetic Zeolite 13X	^{90}Sr, ^{137}Cs, ^{60}Co
India	Synthetic Zeolite AR1	^{90}Sr, ^{137}Cs, ^{60}Co
India	Amm Molybdophosphate	^{137}Cs
India	CaSO$_4$ - BaSO$_4$ eutectoid	^{90}Sr
India	Ferric Oxide-Active Carbon	^{90}Sr, $^{239+240}$Pu
India	Hydrous Titania	^{90}Sr
India	Hydrous Manganese Dioxide	^{90}Sr
Indonesia	Zeolite (Java)	^{137}Cs
Korea, Rep	Potassium Titanate	^{90}Sr
Korea, Rep	Hydrous Titanium Oxide	^{90}Sr
Poland	Manganese Dioxide	^{24}Na, ^{42}K, ^{86}Rb, ^{137}Cs, ^{85}Sr, ^{133}Ba, ^{223}Ra, ^{45}Ca
Russian Fed	Zinc Hexacyanoferrate/clinoptilolite	^{137}Cs, ^{90}Sr
Russian Fed	Copper Hexacyanoferrate/clinoptilolite	^{137}Cs, ^{90}Sr
Russian Fed	Nickel Hexacyanoferrate/clinoptilolite	^{137}Cs, ^{90}Sr
Ukraine	Tetraazaderivatives	^{51}Cr, ^{56} Ni, ^{60}Co, ^{66}Cu
Ukraine	Crown Ether Derivatives	^{90}Sr, ^{137}Cs
UK	Nickel Hexacyanoferrate	^{54}Mn, ^{51}Cr, ^{60}Co, ^{106}Ru, ^{110}Ag, ^{125}Sb, ^{137}Cs
UK	Zirconium Phosphate	^{54}Mn, ^{51}Cr, ^{60}Co, ^{106}Ru, ^{110}Ag, ^{125}Sb, ^{137}Cs, ^{59}Fe
UK	Novel Absorber Tests (38 sorbents)	^{54}Mn, ^{51}Cr, ^{59}Fe, ^{60}Co, ^{65}Zn, ^{90}Sr, ^{106}Ru, ^{109}Cd, ^{110}Ag, ^{125}Sb, ^{137}Cs, ^{203}Hg, $^{239+240}$Pu, ^{241}Am

In Finland, studies have covered the testing of a hexacyanoferrate sorbent for Cs removal, of active carbon materials for Co removal and the testing of a modified titanium oxide for Sr removal from liquid waste streams. Modelling of static and dynamic ion exchange in zeolites has also been undertaken.

In India, synthetic zeolites and ammonium molybdophosphate have been used to remove Cs from solution. A $CaSO_4$-$BaSO_4$ eutectoid, a hydrous titania and MnO_2 were found to be promising sorbents for Sr. The performance of the titania and MnO_2 sorbents were confirmed in tests with real waste. A ferric oxide-activated carbon sorbent performed well in the removal of Sr and Pu from an alkaline waste with high salt content.

Potassium titanates have been prepared by several methods in the Republic of Korea. It has been found that the ion exchange capacity of these sorbents towards Sr depends on the sorbent preparation method. The prepared titanates have been extensively characterized.

Synthesis of MnO_2 to produce a good sorbent for Ra has been carried out in Poland. Strong affinity for Ra is only shown by MnO_2 precipitated from solutions containing ions of similar size to the Ra^{2+} ion, i.e. K^+, NH_4^+, Rb^+.

The "seeded ultrafiltration" process was developed in the United Kingdom with pilot scale operations using a combination of hydrous titanium oxide, zirconium phosphate and sodium nickel hexacyanoferrate in combination with cross-flow ultrafiltration to reduce radionuclide concentrations in a boric acid waste stream to very low levels.

2.1.3. Composite sorbents

The Technical University of Prague, Czech Republic, has produced a wide range of polyacrylonitrile composite sorbents in which an inorganic sorbent is incorporated into a polyacrylonitrile matrix. Testing of these sorbents has included chemical and radiation stability examination. These sorbents have been applied for sorption of Cs, U, Ra, Th and Sr both from real and simulated wastes.

Na, K and NH_4 forms of nickel and copper hexacyanoferrate deposited onto clinoptilolite have been examined in The Russian Federation for Cs and Sr removal from solutions of different composition.

In Ukraine, sorbents obtained by attaching macrocyclic groups to inorganic and polymeric substrates have been tested for sorption of a range of elements. SiO_2, Al_2O_3, TiO_2 and ZrO_2 substrates were selected. Crown ethers or tetra-and penta-aza macrocyclic ligands were attached to the surface of the substrate.

2.2. USE OF INORGANIC SORBENTS IN IMMOBILIZATION TECHNOLOGIES

In both Cuba and Indonesia the addition of local zeolites to cemented waste forms has been examined using simulated and real wastes. It was found that the leaching of caesium was significantly reduced by addition of zeolite to the cement mix. Since substitution of zeolite for sand reduces compressive strength of cemented form a zeolite to solids ratio in it should not exceed 0.2.

Cementation of the composite sorbents produced in the Czech Republic with and without addition of clinoptilolite has been studied. Optimal conditions for spent sorbent immobilization into a cement matrix were identified.

Vitrification has been tested in the Czech Republic as an alternative method for immobilization of these composite sorbents. Mordenite-glass frit mixes at 1050^0C have been found to be a possible composition for the process of immobilization.

3. CHARACTERIZATION OF INORGANIC SORBENTS

Characterization by the Radon Emanation Method, of sorbents supplied by other participants, was undertaken by the Nuclear Research Institute in Řež, Czech Republic. These tests were carried out as part of the collaboration within the CRP. To provide a fair and meaningful comparison between different sorbents a standardized testing programme has been established in the UK. The Novel Absorber Evaluation Club operated by AEA Technology at their Harwell Laboratory was formed to implement this work. The results of the tests undertaken were presented to the CRP participants together with a description of the reference model waste streams used in the tests and also the test procedure. More information on this test procedure is presented in the report of E. Hooper of the United Kingdom.

4. CONCLUSIONS AND RECOMMENDATIONS

The results of research and development work undertaken in the framework of this CRP have indicated that inorganic sorbents in many cases have proven advantages for treatment of liquid radioactive waste. Natural zeolites, for example, are good selective sorbents for Cs removal from different liquid waste streams. Some specific properties of synthetic inorganic sorbents could be design and control during the process of their synthesis, which allows preparation of a range of sorbents suitable for treatment of many specific liquid waste streams. Application of inorganic sorbents (zeolites) for immobilization of radioactive waste into cement improves leaching resistance of the solidified waste forms.

The main activity of the CRP was concentrated on sorption of the most problematic and dangerous radionuclides, such as ^{60}Co, ^{90}Sr, ^{106}Ru, ^{137}Cs, ^{144}Ce, ^{155}Eu, $^{239+240}$Pu, ^{241}Am. Effective sorbents and optimal conditions for sorption of these radionuclides have been identified.

The variety of inorganic sorbents produced in different institutions require establishment of standardized procedures for their evaluation and comparison. In discussions at the end of the final RCM, participants confirmed their previous recommendation that actions have to be taken to establish such standard test procedures to enable the comparative testing of sorbents produced by different establishments for an identical purpose. It was agreed that standard testing procedures and a set of reference waste streams established by the Novel Absorber Evaluation Club could form the basis of a test procedure, which may be recommended for more broad application.

With regard to future work on the use of inorganic sorbents, the participants agreed that a programme with an objective of improving the decontamination efficiency in the treatment of liquid wastes, both aqueous and organic, would be of interest. These could be achieved both by combining sorption with other treatment processes such as precipitation, ion exchange, membrane filtration, photocatalytic oxidation and by combination of different sorbents and their application in a single stage for removal of different radionuclides from solutions. Substantial advantage can be accrued by selecting a combination of two or more processes and their consecutive or simultaneous application for treatment of liquid waste. The multiple or combined process approach may allow resources and materials recovery, provide volume reduction or allow processing in a single equipment unit. Special attention should be paid to any synergistic or inhibiting effects of combined methods and sorbent mixtures. The programme should aim at proving, possibly up to pilot plant scale, the effectiveness of the combined processes for treatment of real radioactive wastes.

XA9744274

SORPTION BEHAVIOUR OF Cs, Sr RADIONUCLIDES IN THE PRESENCE OF VARIOUS ANIONS AND SURFACTANTS IN SOLUTIONS

Yu.P. DAVYDOV, I.G. TOROPOV, T.V. VASILEVSKAYA, L.M. ZEMSKOVA,
V.N. ZABRODSKII, V.V. TOROPOVA, N.I. VORONIK, N.N. SHATIL,
N.E. PROKSHIN, I.V. KLIMENCOVA, Dm.Yu. DAVYDOV
Institute of Radioecological Problems,
Academy of Sciences of Belarus,
Minsk, Belarus

Abstract

The state of ^{137}Cs and ^{90}Sr radionuclides was studied in solutions of different compositions to develop appropriate methodology and technology for treatment of spent decontamination solutions. Complex physico-chemical methods were used for this study. Particular attention was paid to the sorption of ^{137}Cs and ^{90}Sr on different natural and synthetic inorganic sorbents, as the most specific and selective sorbents for separation of these radionuclides from different solutions Sorption of Cs and Sr on different fractions of soil was also studied in connection with development of rehabilitation methods for contaminated territories.

1. INTRODUCTION

At present, the protection of the environment, in particular from radioactive contamination, is one of the main problems in Belarus. As a result of the accident at the Chernobyl Nuclear Power Plant (NPP), nearly 1.5×10^5 TBq of radionuclides have been deposited on the territory of Belarus. At present, 10 years after the accident, the radioecological situation in the Republic is determined mainly by the Cs, Sr, Pu and Am radionuclides. Large territories - soil, forests, water systems, towns, settlements, industrial installations and social institutions, located in these places are contaminated. Despite the large quantity of radionuclide fall-out on Belarus, the concentration in objects is relatively low (<40 kBq/kg) but at the same time the contaminated areas are large. For example, it has been determined that the volume of domestic ash is about 8 thousand tons annually with a specific activity greater than 40 kBq/kg, and 32 thousand tons with activity greater than 4 Bq/kg.

The development of decontamination agents is needed for the effective decontamination of wooden structures, slate, brick and concrete. The compositions for decontamination of motor transport, railway transport, agricultural machinery and industrial enterprises are also required.

As the number of decontamination agents increase a corresponding need for techniques for the management of decontaminating solutions arises. Data on the speciation of radionuclides in solutions containing complexing agents and surfactants are the scientific basis for such technologies.

The data given in this report on the sorption of Cs and Sr are necessary both for the development of treatment processes for liquid radioactive wastes produced during the decontamination and for development of soil decontamination technology. At present it is clear that the problem of rehabilitation of Belarus territories contaminated with radionuclides cannot be solved without development of soil decontamination technology.

The problem of decontamination of soils is particularly important. The matter of necessity, possibility and advisability of such work can be solved on the basis of detailed radiochemical studies of the radiocontamination patterns, forms and behaviour of radionuclides in soils .

2. EXPERIMENTAL

The speciation of radionuclides in solutions containing complexing agents and surfactants has been studied over the pH range 1 to 12, using a number of methods - dialysis, ultrafiltration, centrifugation and ion exchange. The experiments have been carried out according to generally accepted methods [1-2].

Clinoptilolite was washed with distilled water and then dried. The KU-2 cation exchanger was converted into the Na - form. The sorption experiments were batch contacts with agitation of the solution and sorbent. The extent of sorption was determined by the change in concentration of the radionuclide in the solution and calculated in terms of the distribution coefficient, Kd [2].

The amount of ^{90}Sr in solution was determined by radiochemical separation using a carrier followed by determination of the activity of the separated precipitate and the yield of the carrier.

3. RESULTS AND DISCUSSION.

3.1. THE SPECIATION OF RADIONUCLIDES IN SOLUTIONS.

A knowledge of the species of radionuclides in aqueous solutions of various compositions is the scientific basis for solving the technical problem of development of sorption options for liquid waste treatment.

To determine the effect of surfactants and complexing agents on Cs and Sr forms in solution, experiments using ultrafiltration or ion exchange have been made. The data obtained are given in Tables I and II. From the data presented in these Tables it can be seen that Cs and Sr in decontaminating solutions can be both in ionic forms (predominantly Cs) and as colloids (Sr). It also follows from this data, that Cs sorption is independent of the pH value of the solution, but is affected by the presence of complexing agents and surfactants. The results indicate that Cs is predominantly present as $Cs(H_2O)_n^+$ -cations in solution.

The results obtained for Sr indicate that the speciation of Sr changes when the concentration of complexing agents and surfactants is varied. It is probable that interaction between Sr^{2+} and the components of the decontamination solutions occurs.

The above data shows that in the solutions containing surfactants and complexing agents, the fraction of ionic forms of Cs and Sr can be up to 100%. Therefore, for the removal of radionuclides from decontamination solutions, it is necessary to use sorbents which selectively sorb Cs and Sr.

TABLE I. THE STATE OF ^{90}Sr IN SOLUTIONS. ULTRAFILTRATION METHOD

Composition of solution	pH	Filter	Retention, %
Surfactant 0.3 g/L $NaNO_3$ 0.05 mol/L	2.0-9.0 10,0 11,0	Vladipor UPM-P	0 12.0 49.0
$H_2C_2O_4$ 5 g/L $Na_6P_6O_{18}$ 3.5 g/L sulphonol 1.5 g/L	1,0-10,0	-"-	13,0
Exhausted decontaminating solution		Paper	85,0
Effluent solution of the special laundry	9,9	Vladipor UPM-P	0

TABLE II. THE STATE OF Cs AND Sr IN SOLUTIONS. ION EXCHANGE METHOD

Composition of solution	pH	KU-2 cation exchanger		AV-17 anion exchanger	
		Kd		Kd	
		Cs	Sr	Cs	Sr
Surfactant 3g/L $NaNO_3$0.05 g/L	2.0 6.0 8.0 10.0	0 0 0 0	0 0 0 0	0 0 0 0	$1\ 10^2$ $1\ 10^2$ $1\ 10^2$ $1\ 10^2$
Surfactant 0,3 g/L $NaNO_3$ 0.05 g/L	2.0 6.0 8.0 10.0	$1.0\ 10^2$ $2.5\ 10^2$ $1.5\ 10^2$ $2.5\ 10^2$	$1.5\ 10^3$ $5.0\ 10^2$ $1.0\ 10^2$ 0	0 0 0 0	$1.5\ 10^2$ $6.0\ 10^2$ $5.0\ 10^2$ $8.0\ 10^2$
$H_2C_2O_4$ 5 g/L $Na_6P_6O_{18}$ 3.5g/L sulphonol 1.5 g/L	1.8 6.0 10.0	- - -	$3.0\ 10^1$ $2.0\ 10^2$ $4.0\ 10^2$	0 0 0	$2.0\ 10^1$ $1.0\ 10^2$ $4.0\ 10^2$

3.2. SORPTION OF Cs, Sr RADIONUCLIDES IN THE PRESENCE OF VARIOUS LIGANDS.

It follows from the data obtained on the speciation of Cs and Sr in solution that they are in an ionic state over a wide range of pH both in the absence and in the presence of complexing ligands.

The sorption behaviour of Sr and Cs by KU-2 cationite, AV-17 anionite, clinoptilolite, hexacyanoferrates and others has been investigated in the present work.

Since clinoptilolite is the most specific sorbent for Cs, experiments have been carried out with this sorbent. The data obtained are given in Table III.

TABLE III. SORPTION OF ^{137}Cs AND ^{89}Sr FROM SOLUTION BY CLINOPTILOLITE

Composition of solution	pH	K_d	
		^{137}Cs	^{89}Sr
$H_2C_2O_4$ - 5.6 10^{-2} mol/L	1.8	2 10^3	-
$Na_6P_6O_{18}$ - 5.7 10^{-3} mol/L	4.0	5 10^2	-
sulfonol - 1.5 g/L	6.0	4 10^2	-
	8.0	3 10^2	-
	10.0	3 10^2	-
surfactant - 3 g/L	2.0	8 10^2	5 10^1
$NaNO_3$ - 0,05 mol/L	6.0	8 10^2	1 10^2
	8.0	8 10^2	-
	10.0	8 10^2	0
surfactant - 0,3 g/L	2.0	7 10^2	5 10^1
$NaNO_3$ - 0,05 mol/L	6.0	6 10^2	6 10^1
	8.0	6 10^2	-
	10.0	9 10^2	3 10^2
NO_3^- - 0,1 mol/L	1.2	9.6 10^3	2 10^2
	5.0	1.2 10^{+}	5.5 10^3
	7.8	1.6 10^{+}	5.8 10^3

It follows from the data presented in Table III that clinoptilolite is a better sorbent Cs than KU-2. However, dependence of Cs sorption on pH and composition of the solutic can lead to insufficient extraction of caesium by both KU-2 and clinoptilolite under some conditions. It is necessary to obtain more effective sorbents.

The sorption properties of nickel(II) and manganese(II) hexacyanoferrates have been studied in the present work. The data obtained are given in Table IV.

Comparison of the data in Tables III and IV show, that nickel (II) and manganese (II) hexacyanoferrates are better sorbents for ^{137}Cs than clinoptilolite.

3.3. STUDY OF KINETICS OF SORPTION OF Cs AND Sr BY DIFFERENT SORBENTS

Both equilibrium data (thermodynamics) on sorption of radionuclides by various sorbents and data on the kinetics of sorption are needed for the development of effective technologies for radionuclide extraction from decontamination solutions. The size of the treatment plant will be greatly dependent on the time necessary for sorption of radionuclides from solutions. In case of Cs sorption by nickel hexacyanoferrate, the extent of sorption is dependent on the concentration of the macrocomponent in the solution and also on the time of contact of the solution with the sorbent.

In case of Cs and Sr radionuclides there are not many complex forms in solutions. Kinetic peculiarities of sorption processes will be defined by the chemical properties of these radionuclides, and the properties and structure of sorbents. The experimental data on sorption kinetics of Cs and Sr by several sorbents using solutions containing detergents or complexing are presented in Table V-XIII.

TABLE IV.THE SORPTION OF ^{137}Cs FROM SOLUTIONS

Composition of solution	Sorbent, mol/L	pH	Sorption of ^{137}Cs, (%)
$H_2C_2O_4$ - $5.6 \cdot 10^{-2}$ mol/L $Na_6P_6O_{18}$ $5,7 \cdot 10^{-3}$ mol/L sulfonol 1.5 g/L	nickel(II) hexacyanoferrate $3 \cdot 10^{-5}$	1.8	25
		4.0	38
		6.0	21
		8.0	17
The same	nickel(II) hexacyanoferrate $1.5 \cdot 10^{-3}$	1,8	91-99
The same	manganese(II) hexacyanoferrate $5 \cdot 10^{-5}$	1.8	22
	$2.5 \cdot 10^{-4}$	1.8	71
	$5 \cdot 10^{-4}$	1.8	96
	$5 \cdot 10^{-3}$	1.8	98
The same	manganese(II) hexacyanoferrate $K_4Fe(CN)_6$ - $1 \cdot 10^{-3}$ Mn^{2+} - $2.5 \cdot 10^{-3}$	1.8	99.9-99.99
surfactant - 0.3 g/L $NaNO_3$ - 0.05 mol/L	nickel(II) hexacyanoferrate $3.4 \cdot 10^{-3}$	8-11	96-99

TABLE V. KINETICS OF Cs AND Sr SORPTION FROM A SOLUTION, CONTAINING 0.3 g/L SURFACTANT AND 0.05 mol/L $NANO_3$

Time	Cs		Sr	
	Sorbent-clinoptilolite, pH 8.0		Sorbent- cationite KU-2, pH 6.0	
	Distribution coefficient, K_d	Sorption, %	Distribution coefficient, K_d	Sorption, %
10 min	0	0	-	-
1 hr	0	0	40	5
3 hr	80	26	70	12
24 hr	5 10^2	66	2 10^2	22
48 hr	7 10^2	68	6 10^2	52
72 hr	1 5 10^3	86	6 10^2	55

When cationite KU-2 is used as a sorbent, equilibrium of sorption can be reached during 1-2 hours.

In the case of sorption of Cs by clinoptilolite, sorption from H_2O and HCl solutions is rather fast, but when the complexing anions - SO_4^{2-} , PO_4^{3-} , CO_3^{2-} are present in solution sorption kinetics are rather slow.

TABLE VI. KINETICS OF Cs SORPTION FROM SOLUTIONS CONTAINING EDTA AND 0,1 mol/L HCL. SORBENT-CLINOPTILOLITE

pH	K_d						
	Time						
	30 min	1 hr	3 hr	6 hr	16 hr	24 hr	72 hr
	[EDTA]= 1 10^{-4} mol/L						
1.0	59	106	306	489	570	956	2370
4.0	32	40	67	124	204	230	420
6.0	24	21	48	139	197	209	404
9.5	32	64	109	126	313	238	430
[EDTA]= 1 10^{-3} mol/L							
1.0	154	217	226	300	322	1280	2230
4.0	63	65	112	172	176	254	320
6.0	49	72	107	161	156	228	300
9.5	38	74	94	142	140	195	320

TABLE VII. KINETICS OF Cs SORPTION FROM SOLUTIONS, CONTAINING DETERGENT (SF-2U) AND 0.1 mol/L HCL. SORBENT- CLINOPTILOLITE

pH	K_d						
	Time						
	30 min	1 hr	3 hr	6 hr	16 hr	24 hr	72 hr
[SF-2U] = 0.1 g/L							
1.0	111	173	210	702	782	-	1450
4.0	36	41	75	122	180	391	310
6.0	42	43	68	122	149	152	200
9.5	66	62	129	109	223	349	356
[SF-2U] =1 g/L							
1.0	77	43	252	487	614	850	1100
4.0	37	49	83	97	113	196	297
6.0	39	65	83	76	203	197	260
9.5	57	79	75	77	166	214	290

TABLE VIII. KINETICS OF Cs SORPTION FROM SOLUTIONS, CONTAINING FERROCYANIDE-ANION AND 0.1 mol/L HCL SORBENT-CLINOPTILOLITE

pH	K_d						
	Time						
	30 min	1 hr	3 hr	6 hr	16 hr	24 hr	72 hr
$[Fe(CN)_6]^{4-} = 1.10^{-4}$ mol/L							
1.0	420	1200	1158	1220	2250	919	927
4.0	34	56	232	228	228	482	471
6.0	141	81	191	206	210	330	328
$[Fe(CN)_6]^{4-} = 1.10^{-3}$ mol/L							
1.0	52	62	880	856	999	1121	1125
4.0	27	100	180	400	889	660	661
6.0	51	103	289	242	320	477	478

TABLE IX. KINETICS OF Cs SORPTION FROM SOLUTIONS CONTAINING DETERGENT (SF-2U) AND 0.1 mol/L HCL. SORBENT - KU-2

pH	Kd						
	Time						
	30 min	1 hr	3 hr	6 hr	16 hr	24 hr	72 hr
	[SF-2U]= 0.1 g/L						
				[SF-2U]	0.1 g/L		
1.0	86	182	171	317	238	-	322
4.0	17	42	60	63	55	86	106
6.0	69	54	55	52	66	91	86
9.5	59	42	43	50	54	66	66
	SF-2U]= 1.0 g/L						
1.0	112	120	176	226	242	204	215
4.0	38	62	76	26	66	-	69
6.0	59	58	67	32	81	52	74
9.5	41	39	65	33	84	63	79

TABLE X. KINETICS OF Cs SORPTION FROM SOLUTIONS, CONTAINING EDTA AND 0.1 mol/L HCL. SORBENT - KU-2

pH	Kd						
	Time						
	30 min	1 hr	3 hr	6 hr	16 hr	24 hr	72 hr
	[EDTA] = 1.10 $^{-4}$ or 1.10^{-3} mol/L						
1.0	77	203	210	215	-	336	269
4.0	35	58	65	62	104	133	123
6.0	39	64	61	56	61	58	86
9.5	33	42	61	53	-	79	93
	[EDTA] = 1.10^{-3} or 1.10^{-3} mol/L						
1.0	107	117	210	334	195	335	340
4.0	57	79	92	70	95	59	92
6.0	35	49	91	88	82	83	83
9.5	12	66	104	91	91	83	90

TABLE XI. KINETICS OF Sr SORPTION BY CLINOPTILOLITE AND CELLULOSE POLYPHOSPHATE

Time of sorption, hour	pH	Kind of sorbent	Sorption	
			%	Kd 10^2
24 hr	1.1	clinoptilolite	24.0	0.8
	3.0	-"-	90.0	4.46
	5.0	-"-	88.0	3.16
	7.2	-"-	87.0	2.92
	8.9	-"-	80.0	1.68
0.5 hr	1.1	cellulose	78.0	7.9
	3.0	polyphosphate	82.0	7.2
	5.0	-"-	58.0	3.5
	7.2	-"-	59.0	5.3
	8.9	-"-	4.7	0.1
1 hr	1.1	-"-	80.0	5.8
	3.0	-"-	91.0	2.5
	5.0	-"-	72.0	6.0
	7.2	-"-	82.0	9.3
	8.9	-"-	65.5	3.3

TABLE XII. KINETICS OF Cs SORPTION BY CLINOPTILOLITE

Anion concentration, mol/L	pH	Kd						
		5 min	30 min	1 hr	3 hr	5 hr	24 hr	3 days
$[Cl^-]=1\cdot10^{-1}$	1.0	109	217	370	850	866	1323	1370
	4.0	26	47	60	106	140	216	237
	7.0	18	39	57	109	102	194	209
	10.0	31	42	50	83	103	199	276
$[C_2O_4^{2-}]=1\ 10^{-4}$ $[Cl^-]=1\ 10^{-1}$	1.0	71	212	414	395	518	520	518
	4.0	46	118	160	167	275	237	286
	7.0	21	140	147	152	156	177	315
	10.0	46	140	153	173	169	182	312
$[C_2O_4^{2-}]=1\cdot10^{-3}$ $[Cl^-]=1\cdot10^{-1}$	1.0	73	120	129	194	502	644	1000
	4.0	27	89	121	131	193	261	344
	7.0	31	46	88	141	187	267	344
	10.0	40	58	91	98	132	200	260
$[C_2O_4^{2-}]=1\ 10^{-2}$ $[Cl^-]=1\ 10^{-1}$	1.0	76	140	156	301	428	513	782
	4.0	91	109	114	193	220	218	257
	7.0	78	76	94	126	143	195	217
	10.0	64	114	146	167	211	254	289
$[PO_4^{3-}]=1\ 10^{-4}$ $[Cl^-]=1\ 10^{-1}$	1.0	103	191	206	568	961	1416	
	4.0	27	40	46	112	160	229	
	7.0	18	32	41	78	182	247	
	10.0	23	39	44	107	147	240	
$[PO_4^{3-}]=1\ 10^{-3}$ $[Cl^-]=1\ 10^{-1}$	1.0	78	180	197	234	224	454	
	4.0	53	68	119	113	147	240	
	7.0	37	74	125	123	139	246	
	10.0	26	92	114	136	184	186	

From the sorption data obtained, ^{137}Cs co-precipitation with nickel hexacyanoferrate (NFC) was selected as the treatment method.

Laboratory experiments on NFC precipitation initially used simulated solutions. The efficiency of purification of the solutions from Cs was studied as a function of different factors: pH, time, NFC concentration, correlation of components concentration used for NFC precipitation and concentration of detergents. Phase separation was performed using both inertial and sedimentation methods.

It is known that excess of $Fe(CN)_6$ ions in solution favours formation of NFC sols. This can be explained as due to the highly-charged ferrocyanide ions on the surface of sol particles, which become negatively charged, preventing coagulation of colloidal particles. To increase the efficiency of purification from Cs, generation of NFC precipitates should be performed with an excess amount of Ni^{2+} cations.

TABLE XIII. KINETICS OF Cs SORPTION BY ION-EXCHANGE RESIN KU-2

Anion concentration, mol/L	pH	Kd				
		1 hr	3 hr	5 hr	24 hr	3 days
$[Cl^-]=1\ 10^{-1}$	1.0	231	253	284	331	350
	4.0	84	92	106	95	96
	7.0	70	88	85	100	109
	10.0	90	88	98	103	107
$[C_2O_4^{2-}]=1\ 10^{-4}$ $[Cl^-]=1\ 10^{-1}$	1.0	158	182	204	220	210
	4.0	120	145	166	167	184
	7.0	133	160	182	160	187
	10.0	126	135	158	172	187
$[C_2O_4^{2-}]=1\ 10^{-3}$ $[Cl^-]=1\ 10^{-1}$	1.0	142	145	160	172	184
	4.0	123	131	164	180	179
	7.0	100	87	98	126	156
	10.0	81	106	123	30	169
$[C_2O_4^{2-}]=1\ 10^{-2}$ $[Cl^-]=1\ 10^{-1}$	1.0	160	154	168	179	183
	4.0	106	121	136	137	143
	7.0	87	121	124	129	176
	10.0	121	152	149	162	168
$[PO_4^{3-}]=1\ 10^{-4}$ $[Cl^-]=1\ 10^{-1}$	1.0	182	216	595	729	
	4.0	22	34	41	42	
	7.0	47	53	63	100	
	10.0	31	64	70	63	
$[PO_4^{3-}]=1\ 10^{-3}$ $[Cl^-]=1\ 10^{-1}$	1.0	120	132	189	202	
	4.0	56	65	91	101	
	7.0	70	80	85	107	
	10.0	67	102	108	133	
$[PO_4^{3-}]=1\ 10^{-2}$ $[Cl^-]=1\ 10^{-1}$	1.0	89	119	130	137	
	4.0	75	101	102	118	
	7.0	50	54	103	107	
	10.0	73	82	115	126	

In this work, the influence of detergents on the decontamination of the solutions from both Cs and Sr was studied. Experiments with Cs were conducted by phase separation using gravity and inertial methods. In both cases it was found that addition of SF-2U detergent reduces the decontamination efficiency. In the case of gravity separation, the Kd value levelled off at NFC concentrations above $4\ 10^{-3}$ mol/L instead of $6\ 10^{-4}$ mol/L when there is no detergent in solution. When phase separation is performed by centrifugation addition of SF-2U detergent (under equal conditions) leads to a reduction in Kd for Cs by a factor of three.

The influence of SF-2U on the removal of Sr was also studied. The data showed that a reduction in decontamination efficiency occurs as the detergent concentration increases.

Data collected using model solutions under laboratory conditions was used to select optimal conditions for purification from Cs and Sr, namely pH 9-10.5, concentration of precipitation agent ($K_4[Fe(CN)_6]$- 10^{-3} mol/L, $NiCl_2$ - 2. 10^{-3} mol/L), contact time (~ 24 hr), and these conditions were used to treat real wastes. The spent decontamination solutions used to clean-up equipment contaminated by the Chernobyl accident was used. Quantitative analysis of the liquid waste was carried out using atomic emission spectroscopy with inductively coupled plasma. The results of the analyses are presented in Table XIV.

TABLE XIV. COMPOSITION OF LIQUID WASTES.

Contents, mg/L										
Example	Na	K	Al	Zn	Ni	Mn	Cu	Cr	Ca	Fe
N5, 1993			58.6	650	0.7	0.4	3.3	0.07	5.0	5.8
N8, 1993			3.8	4.1	0.5	0.9	4.6	1.2	24.4	2.6
N10,1993			2640	50		0.2	2.4	0.3	4.0	2.5
1995	41900	300	0	6700	1.0	0.3	2.0	1.0		

The NaOH concentration in the solution was in the range 0.16-1.6 mol/L. The high concentration of Al and Zn in the liquid wastes arise from the nature of the decontaminated surfaces which dissolve in basic solutions with formation of corresponding zincates and aluminates. A high concentration of organic compounds was found in the solutions: oil products in the range 200-400 mg/L, anion-active detergent -sodium dodecabenzenesulphonate 1.1 g/L. These concentrations are much higher that the permitted level for release to the municipal sewerage.

The results show that real decontamination solutions are complicated aqueous systems containing bases, inorganic salts, heavy metals, organic compounds, detergents and oil products. The high concentration of the latter is confirmed by the high chemical oxygen demand (COD) of 40000-50000 mg O_2/L (permitted amount is about 560 mg O_2/L).

The presence in solutions of both heavy metals and organic compounds markedly reduced the efficiency of the sedimentation method for liquid waste treatment, in particular Cs co-precipitation with NFC and Sr with insoluble salts of calcium. The problem is that during neutralisation of the solution, hydroxides of heavy metals do not coagulate in the presence of organic compounds, but form very stable suspensions which can only be separated from the solution by very strong centrifugal forces.

Application of the chemical precipitation method for liquid waste treatment is possible only when the concentration of organic compounds does not exceed the amount corresponding to a COD of 2000 mg O_2/L.

3.4. THE STUDY OF Cs AND Sr SORPTION FOR SOLVING THE PROBLEM OF SOIL DECONTAMINATION

Investigations have shown that since the Chernobyl accident, Cs radionuclides in the soil have concentrated mainly (~90%) in the slime fraction, which comprises 10% of the total volume of the soil. This suggests a method for decontamination of soil by separation of the slime fraction. However, a big drawback to this method is that the main portion of the fertile component of the soil is removed with the slime fraction. Because of this, attempts are being made to extract radionuclides of Cs from the slime fraction of the soil. At first the consistencies of sorption and desorption of Cs and Sr radionuclides was investigated for soils of different compositions.

The following method has been used for desorption of Cs and Sr from the soil. A sample of soil taken from the contaminated zone to the south of Belarus was divided into two approximately equal parts. One part has was used for carrying out the model experiments and the other for real experiments. The soil assigned for model experiments (150-170 g) was flooded with H_2O (pH=7.2-8.2) containing ^{137}Cs or ^{90}Sr for a period of 3-4 days with occasional stirring. The solid phase was removed by filtration through a paper filter and the radionuclide content of the solution and in the soil was determined. The quantity of radionuclides absorbed by the soil was determinated from this data. Later, the model and the real samples of the loaded soils were flooded with desorbents of different compositions and the value of desorption of Cs and Sr radionuclides was determined. It can be seen from the data presented in Tables XV-XVI that the values of ^{137}Cs and ^{90}Sr desorption are different for various soils. The difference between the values of desorption in model and real experiments is marked. In addition, experiments on the dialysis of Cs solutions (Table XVII) used for decontamination of Cs from the soil show that in these solutions (both in model experiments and real) the Cs is mainly in the form of hydrated $Cs(H_2O)^+$-cations. In turn it provides confirmation that in the soils ^{137}Cs is in the ionic form.

It is known that the sorption-desorption behaviour of radionuclides and consequently their speciation is greatly affected by the organic content of the soil represented by components such as humus, lignin, polysaccharides, proteins, aminoacids, etc. They contain the functional groups, hydroxyl, carboxyl, amino-, imino-, etc., which can form coordination bonds with metal ions. Many researchers have shown the effect of humic acids on the accumulation of radionuclides in the soils. Differing extent of mobility of Cs and Sr in the soil has been noted. It is explained by the nature of interaction of radionuclides with various soil components, including the humic acids. The effect of humic acids on Cs and Sr desorption from the soils is shown by the data presented in Tables XVIII-XIX.

TABLE XV. DESORPTION OF ^{90}Sr FROM SOILS

Soils	Value of desorption (%)			
	Model experiments		Real experiments	
	0.01M HCl 0.01M CsCl 0.01M $SrCl_2$	0.01M HCl 0.01M CsCl 0.01$SrCl_2$	0.01M HCl 0.01M CsCl 0.01M $SrCl_2$	0.01M HCl 0.01M CsCl 0.01M $SrCl_2$
Sod-podsol (sandy)	44.5±10.1	38.6±8.0	7.3±4.1	7.0±3.0
Sod-podsol (loam)	41.4±6.2	-	10.3±5.1	-

It is seen from this data, that introduction of humic acids does not exert any significant effect on Cs desorption from the soil. In the case of Sr, the introduction of humic acids result in a decrease of Sr desorption from the soil.

TABLE XVI. DESORPTION OF ^{137}Cs FROM SOILS

Soils	Value of desorption (%)			
	Model experiments		Real experiments	
	0.01M HCl 0.01M CsCl 0.01M SrCl$_2$	0.01M HCl 0.01M CsCl 0.01SrCl$_2$	0.01M HCl 0.01M CsCl 0.01M SrCl$_2$	0.01M HCl 0.01M CsCl 0.01M SrCl$_2$
Peat	5.9±3.4	28.1±5.2	2.3±1.1	8.4.0±3.9
Sod-podsol	21.7±7.3	25.2±6.8	12.0±5.6	15.6±3.2
Gray meadow	32.1±3.1	44.0±3.8	11.8±4.7	17.2±5.2
Sandy loam	31.8±5.6	45.2±4.2	14.2±1.9	15.1±4.2
Sandy	37.5±4.5	-	2.1±1.1	5.0±3.1

TABLE XVII. THE SPECIATION OF ^{137}Cs IN THE DESORPTION SOLUTIONS

Soils	Dialysis, Kd			
	Model experiments		Real experiments	
	0.01M HCl 0.01M CsCl 0.01M SrCl$_2$	0.01M HCl 0.01M CsCl 0.01SrCl$_2$	0.01M HCl 0.01M CsCl 0.01M SrCl$_2$	0.01M HCl 0.01M CsCl 0.01M SrCl$_2$
Peat	0.96±0.02	0.93±0.05	0.84±0.09	0.89±0.06
Sod-podsol	0.98±0.02	0.98±0.02	0.97±0.03	0.95±0.03
Gray meadow	0.98±0.02	0.98±0.02	0.74±0.07	0.72±0.05
Sandy loam	0.95±0.04	0.96±0.04	0.95±0.05	0.91±0.05
Sandy	0.90±0.01	-	0.99±0.02	-

TABLE XVIII. INFLUENCE OF HUMIC ACIDS ON DESORPTION OF ^{137}Cs FROM SOIL Desorption solution: 0.01M HCl + 0.01M CsNO$_3$ + 0.01M SrCl$_2$. pH=7.2

Soils	Value of desorption (%)			
	Model experiments		Real experiments	
	Without HA	With HA	Without HA	With HA
Sod-podsolic	21.7±7.3	15.8±5.1	12.0±5.6	15.6±2.6
Sandy soil	37.5±4.5	94.2±2.8	2.1±1.1	0

HA = humic acid

TABLE XIX. INFLUENCE OF HUMIC ACIDS ON DESORPTION OF ^{90}Sr FROM SOIL

Desorption solution: 0.01M HCl + 0.01M $CsNO_3$ + 0.01M $SrCl_2$. pH=7.5

Soils	Value of desorption (%)			
	Model experiments		Real experiments	
	Without HA	With HA	Without HA	With HA
Sod-podsolic (loamy)	41.6±6.2	15.4±9.3	10.4±5.1	2.6±1.3
Soddy-podsolic	44.5±10.1	0	7.0±4.1	0

HA = humic acid

It can be seen from the data in Table XX that Cs sorption by cationite decreases in the presence of humic acids in solution.

TABLE XX. SORPTION OF ^{137}Cs FROM DESORBING SOLUTIONS BY KU-2 CATIONITE pH=6.5-7.5.

Soils	Sorption coefficient, Kd			
	Model experiments		Real experiments	
	Without HA	With HA	Without HA	With HA
Distilled water	$3.3\ 10^4$	$1\ 010^2$		
The solution from sod-podsol soil	$6.4\ 10^2$	$2.2\ 10^2$	$2.3\ 10^3$	$1.8\ 10^2$
The solution from sandy soil	$0.8\ 10^2$	$0.8\ 10^2$	$0.8\ 10^3$	$0.5\ 10^2$

HA = humic acid.

REFERENCES

[1] STARIK J.E. The basis of radiochemistry. M-L, Science, 1969.

[2] DAVYDOV JU.P. Forms of radionuclides in solutions. Minsk, Science, 1978, p.157.

A STUDY ON RADIOACTIVE WASTE TREATMENT WITH INORGANIC MATERIALS

FAN XIANHUA, SU XIGUANG, LONG HUIZUN, ZENG JISHU
Radiochemistry Department,
China Institute of Atomic Energy,
Beijing, China

Abstract

In this paper we report our studies on many kinds of natural materials for the treatment of alpha-bearing liquid waste streams. One type of apatite showed high potential for the separation of actinides from bulk waste streams. The results obtained show that adsorption ratios (**Rd**) for Pu, Am and Ce were 10^2-10^4 at pH 1-3. The influences of pH value and the concentrations of Na^+, Ca^{++}, $NaAlO_2$ and Na_3cit on **Rd** were also studied. Column tests with simulated solution and actual feed were carried out and the column performance can be improved by pre-treatment of P301 material.

1. INTRODUCTION

A quantity of low level radioactive liquid waste containing alpha emitters with the specific activity more than $5{,}9.10^5$ Bq/L, generated from research laboratories, the isotope production centre and other activities, has been collected and stored over the past 20 years in special tanks in the China Institute of Atomic Energy. The waste mentioned above will require pretreatment prior to treatment by means of vaporization process or cement solidification technology if the α specific activity in the final waste forms to be disposed of is more than $3{,}7.10^5$ Bq/kg.

The objectives of various processes for treating liquid alpha-bearing waste are to remove alpha contamination and/or to concentrate the radioactivity into a small volume for subsequent conditioning and disposal. The main alpha emitting radionuclides that need to be considered are plutonium and americium.

In selecting processing options for actinide removal from liquid streams, the following factors should be considered:

- the characteristics of the liquid waste, including arisings, physical, chemical and radiological composition
- the volume reduction factor
- the availability of the treatment processes and their costs
- the reliability and ease of operation

There are various approaches for removal of Pu and Am, such as chemical precipitation, solvent extraction and ion exchange. The application of ion exchange processes to alpha-bearing liquids is more limited. Organic ion exchange resins are frequently applied for concentrating U and Pu from dilute product streams, sometimes achieving a simultaneous purification. However, their application in the treatment of waste steams is still at an early stage of development.

Inorganic ion exchangers have a high potential to separate actinides with efficiency from the bulk waste into a small volume. In the 1970's, a study and application of inorganic sorbents such as bone char and sodium titanate for the removal of radionuclides from waste water [1,2,3,4] was carried out. More promising inorganic ion exchangers for separation of TRU elements from liquid waste streams, with distribution factors (Kd) of 10^2 to 10^4, such as titanium phosphate, zirconium phosphate, hydrous titanium oxide, manganese dioxide and polyantimonic acid etc. have been reported [5] .

The inorganic materials are generally resistant to radiation and stable under oxidizing conditions. Many of these products are commercially available and of low cost. After exhaustion they can be immobilized in cement or by hot pressing for final disposal.

A natural material named P301 sorbent which is one kind of apatite, was used for treatment of waste water containing Pu, Am and Ce with high **Rd** and is described in this paper. The results indicate that P301 sorbent seems much better than those listed above.

2. EXPERIMENTAL

2.1. PREPARATION OF SORBENTS

The various kinds of the natural materials collected from different locations in China were crushed, sieved and the particles ranging from 100 to 140 mesh were collected for use in this experiment.

2.2. PREPARATION OF SIMULATED WASTE SOLUTION

In this study, simulated waste solution containing 2M $NaNO_3$ and 0.1 M $Ca(NO_3)_2$, and adjusted to pH 1-3 were prepared and spiked with ^{239}Pu, ^{241}Am, ^{141}Ce, ^{137}Cs and $^{85+89}Sr$.

2.3. ANALYTICAL EQUIPMENT

HPGe gamma- spectroscopy and liquid scintillation techniques were used to count γ and α-emitters respectively.

2.4. DETERMINATION OF ADSORPTION RATIO

Batch tests were conducted in this experiment. An appropriate amount of sorbent was added to 10.0ml simulated waste solution in a polyethylene vial or centrifuge tube and mixed by stirring or shaking.

After a certain contact time, supernatant liquid was separated by centrifugation and then analyzed. The adsorption ratio (**Rd**) is calculated by the following formula:

$$Rd=\frac{Ao-At}{At}\cdot\frac{v}{w}(mL/g)$$

where:

A_0 is the initial specific activity of the waste solution,

A_t is the specific activity of the supernatant liquid after contact time t,

v is the volume of the radwaste solution to be treated, (ml)

w is the mass of sorbent used (g)

3. RESULTS AND DISCUSSION

3.1. DETERMINATION OF TIME TO SORPTION EQUILIBRIUM

In order to determine the time to reach equilibrium, various kinds of natural materials from different areas in China, coded Y-312, Cs-337, Y-337, Y-300, SSE-24, D-3 and Q-52 etc. have been tested and the results obtained are shown in Fig. 1, 2, 3 and 4. It is obvious that the equilibrium of reaction between sorbents and waste solution is generally reached after 15 hours contact. This shows that the sorption kinetics of natural materials are slow. In the subsequent experiments a contact time of 24 hours was adopted.

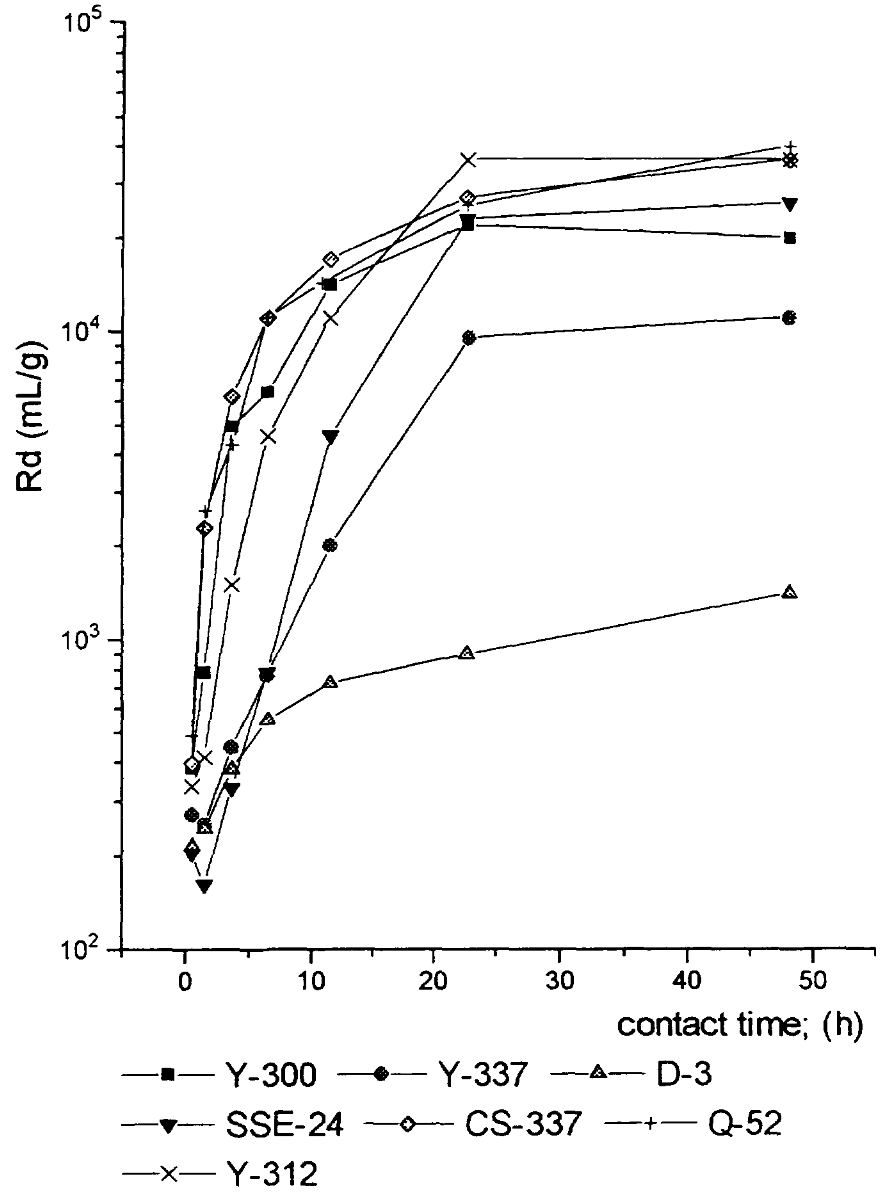

FIG. 1. Effect of contact time on Rd of Pu for P301 materials

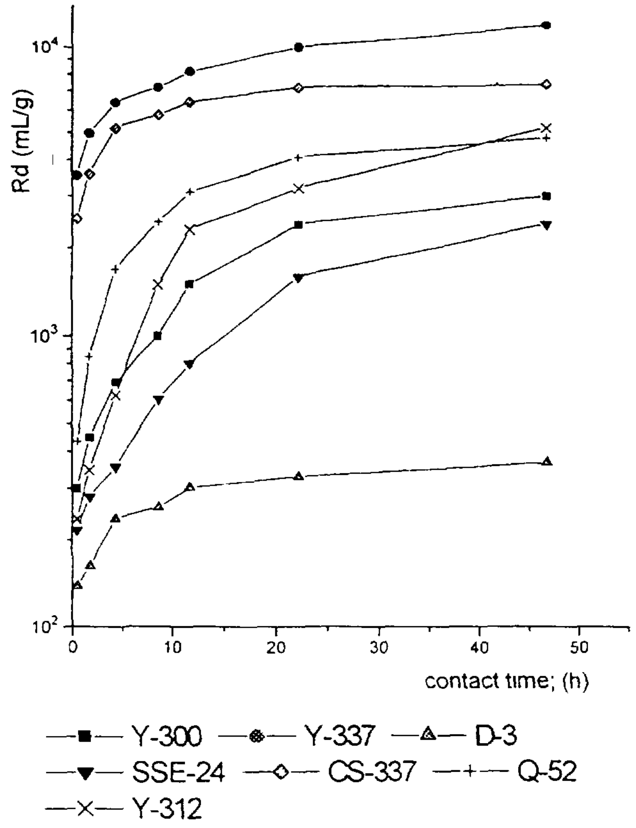

FIG. 2. *Effect of contact time on Rd of Am for P301 materials*

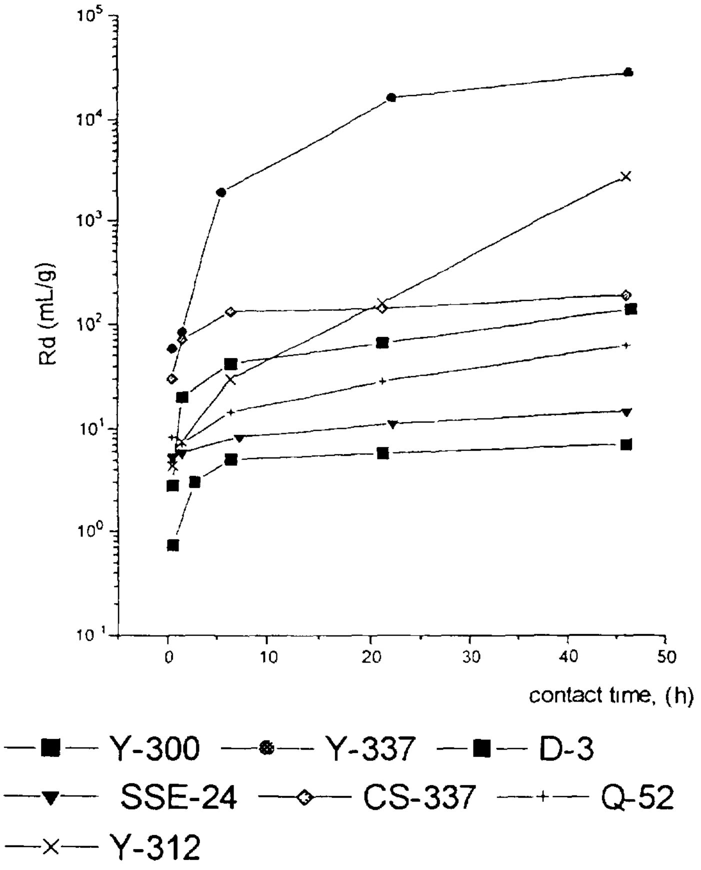

FIG. 3. *Effect of contact time on Rd of Ce for P301 materials*

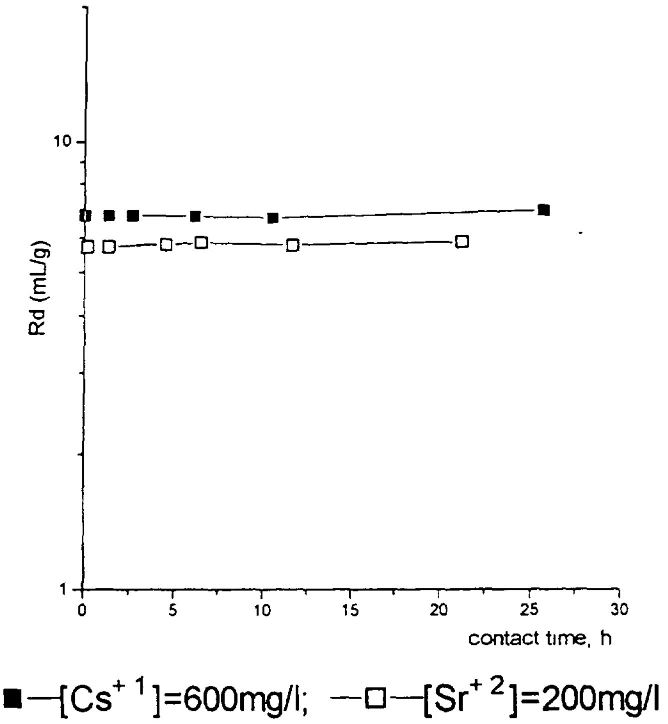

FIG. 4. Effect of contact time on Rd of Cs and Sr for Y-337

3.2. SELECTION OF SORBENT MATERIALS

The adsorption ratios of nuclides, such as Pu, Am, Ce, Sr and Cs between the liquid waste and eight selected inorganic materials selected are shown in Table I.

TABLE I. ADSORPTION RATIOS OF Pu, Am, Ce, Sr AND Cs ON NATURAL MATERIALS FROM DIFFERENT AREAS IN SIMULATED SOLUTION*:

Nuclides	Y 300	Y 337	D-3	SSE 24	Cs 337	Q 52	Y 312	PY**
Pu	2.2E4	1.3	1.0E	2.3E4	1.4E4	8.0E3	3.6E4	1.2E4
Am	2.4E3	6.4	3.2E2	1.6E3	7.2E3	4.1E3	3.2E3	3.9E4
Ce	65	2.6E4	7.0	4.1	1.4E2	28	1.6E2	1.0E5
Sr	1.2	4.9	1.3	7.4	5.0	4.1	28	-
Cs	-	0.32	-	2.8	5.5	10.0	3.4	-

* in the solution:

^{239}Pu: 3.7E5 Bq/L,
^{241}Am: 3.7E4 Bq/L,
Ce : 400mg/L spiked by Ce-141,
Sr : 200mg/L spiked by Sr-85+89,
Cs : 600mg/L spiked by Cs-137,
pH: 1-3.

** PY: Synthetic product, powder.

From Table I, it can be seen that all samples have high adsorption capacity for Pu and Am, but only a few samples, such as Y-337, Cs- 337 and Y-312, are effective for removal of Ce from liquid waste. As the high adsorption capacity and availability of the materials to be used should be considered, Y-337 material (hereinafter P301) was selected for further study.

3.3. EFFECT OF SORBENT DOSAGE ON REMOVAL OF NUCLIDES

The influence of sorbent dosage on removal of Pu, Am is shown in Table II.

TABLE II. EFFECT OF SORBENT DOSAGE ON REMOVAL OF NUCLIDES.

Sample amount added (g)	0.05	0.15	0.25	0.35	0.5
Removal of Pu(%)	95.80	99.95	99.85	99.60	99.98
Removal of Am(%)	99.59	99.76	99.82	99.77	99.75

The results indicate that removal of more than 99.8% of Pu and Am can be obtained when the addition of the inorganic material exceeds 0.15g in 10.0ml waste solution. Therefore addition of 2 weight % P301 material is recommended for the treatment process.

3.4. EFFECT OF HEATING ON THE **Rd** OF Pu AND Am

The adsorption ratios of P301 material activated at 200, 400, 600, 800 and 1000°C for 6 hours were determined. The results are shown in Fig. 5 and indicate that P301 material is thermally stable and retains a high capacity for Pu up to 400°C and for Am up to 600°C. Based on the data obtained from DTA (Fig. 6) it is obvious that P301 material does not begin to decompose until 600°C.

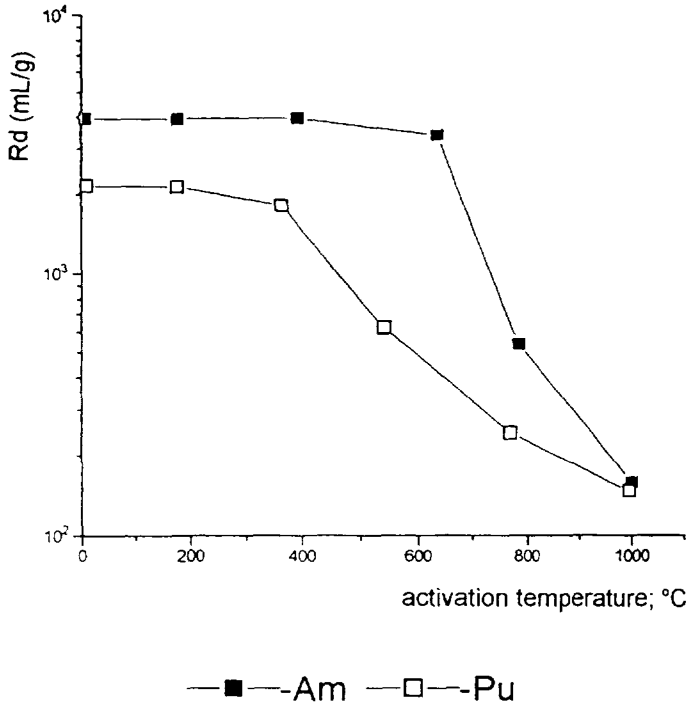

FIG. 5. Effect of activation temperature on Rd of Am and Pu

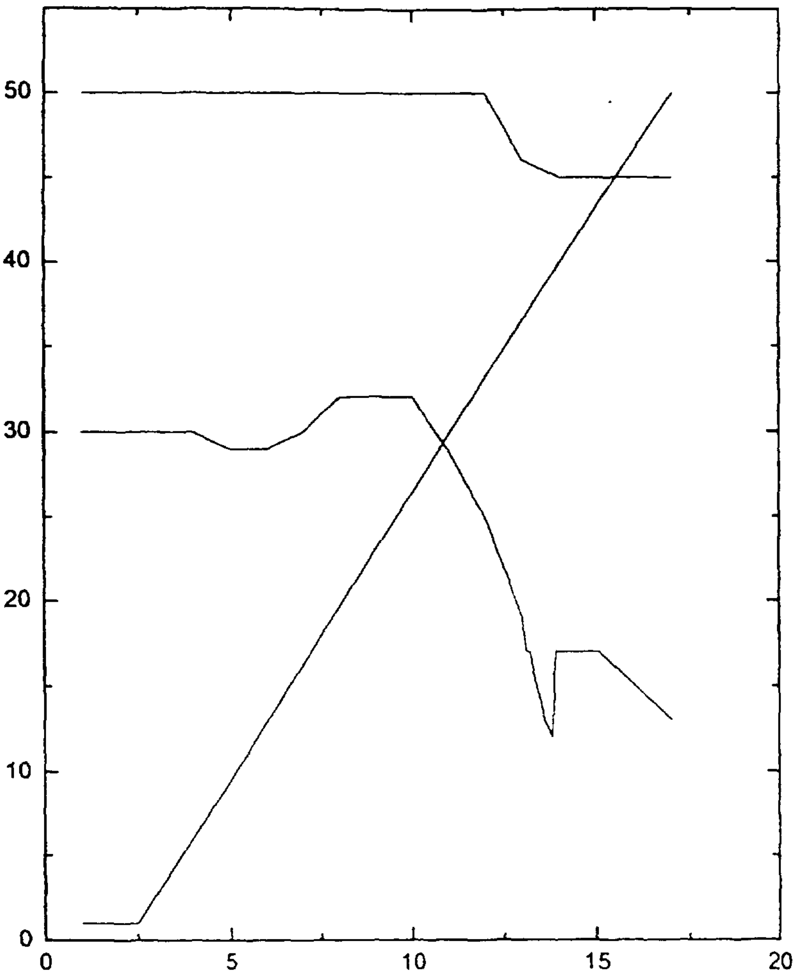

FIG. 6. The result of differential thermal analysis of Pu301 sorbent

3.5. EFFECT OF ACIDITY AND ALKALINITY ON **Rd**

Generally, work on natural inorganic sorbents reported in the literature covers only conditions of very low acidity or alkalinity, for instance pH 5-9. In this study a pH range of 1-12 has been investigated; the results are shown in Fig. 7. Higher acidities such as 0.5, 1.0M and alkalinity such as 1.0, 2.0, 4.0, 6.0M in the waste solution were obtained by addition of strong nitric acid or solid sodium hydroxide into the solution respectively. The adsorption ratios for Pu and Am on P301 material were still greater than 10^2 at 1.0M acidity and 6.0M alkalinity. The results indicate that the P301 sorbent selected for this work has a very high potential for use in waste treatment processes.

3.6. EFFECTS OF CONCENTRATION OF $NaNO_3$ AND $Ca(NO_3)_2$ ON **Rd**

The influence of the $NaNO_3$ and $Ca(NO_3)_2$ concentration on **Rds** were tested and the data are shown in Fig. 8 and Fig. 9. When the concentration of $NaNO_3$ is less than 4M, no effect on **Rd** was observed and adsorption ratios of Pu and Am on the P301 sorbent were constant. However, **Rd** of Ce decreased rapidly with increase of the concentration of $NaNO_3$. The concentration of $Ca(NO_3)_2$ significantly affects the **Rds** of Pu and Am.

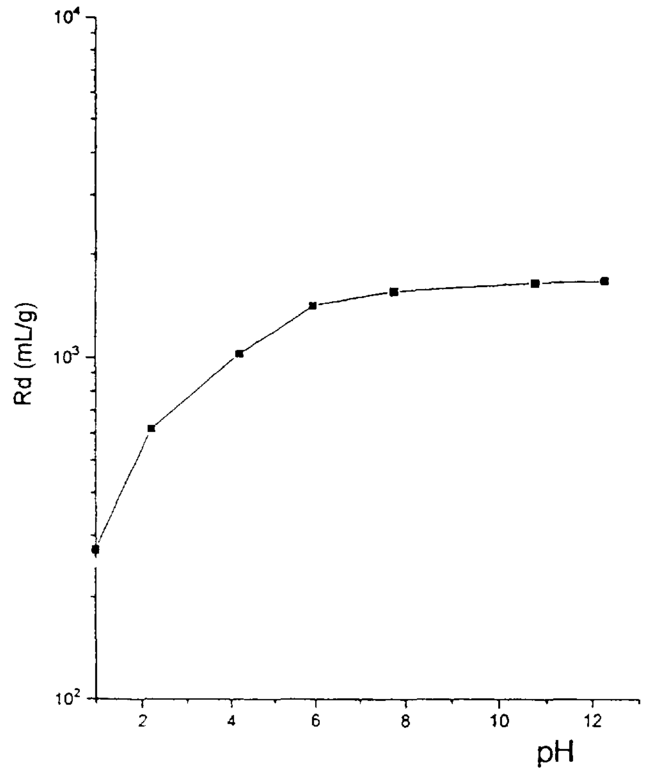

FIG. 7. Effect of pH on Rd of Pu

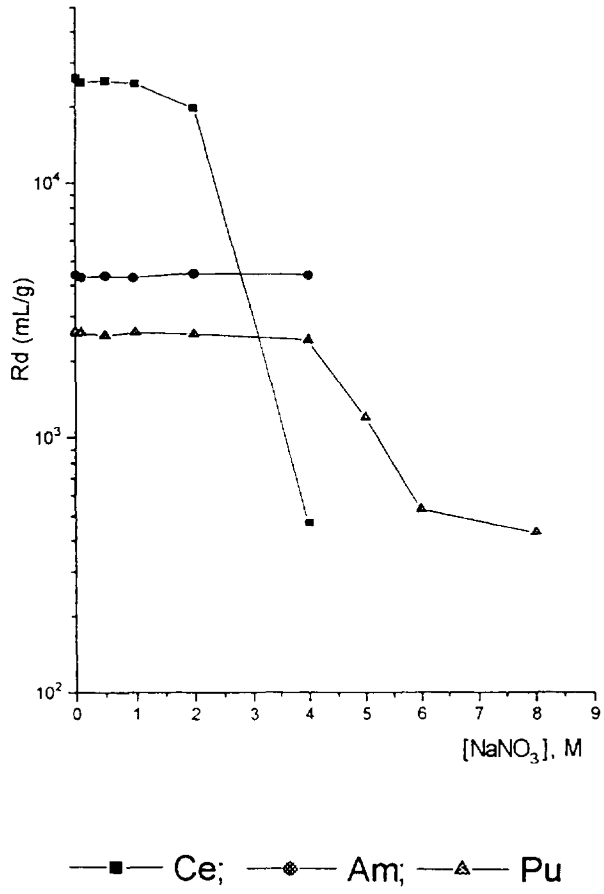

FIG. 8. Effect of concentration of NaNO$_3$ on Rd of Am, Pu and Ce

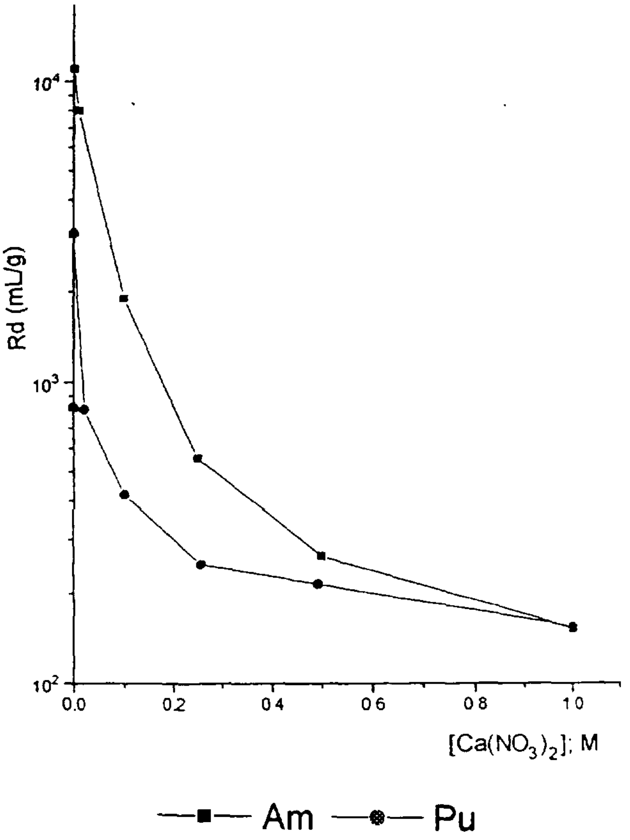

FIG. 9. *Effect of concentration of $Ca(NO_3)_2$ on Rd of Am, Pu*

3.7. EFFECTS OF $NaAlO_2$ AND Na_3cit CONCENTRATIONS ON **Rd** OF Pu

The effect of $NaAlO_2$ and Na_3cit concentrations on adsorption ratios of Pu have been determined. The results are shown in Fig.10 and Fig.11 respectively. The data obtained indicate that only a small effect of $NaAlO_2$ concentration on **Rd** of Pu was observed. When the concentration of $NaAlO_2$ in the waste stream is as high as 0.87M, the **Rd** of Pu in P301 material is still as high as 1×10^3. From Fig. 11, it is seen that when the concentration of Na_3cit reached 0.006M, the **Rd** of Pu on P301 material is nearly zero. The fact that the **Rd** value of Pu is greatly affected by the concentration of Na_3cit indicates complex formation in the waste stream which has a significant influence on the adsorption of Pu by the inorganic material selected for this study.

3.8. BATCH TESTS WITH ACTUAL WASTE STREAM

The chemical composition and concentration of radioactive nuclides in the actual waste stream are listed in Tables III and IV respectively.

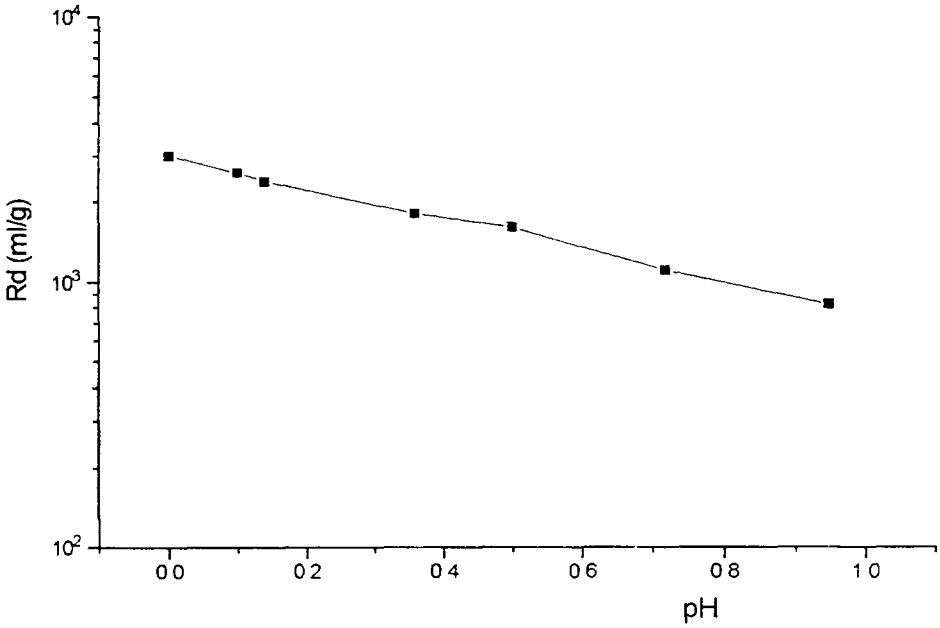

FIG 10 Effect of [NaAlO$_2$] on Rd of Pu

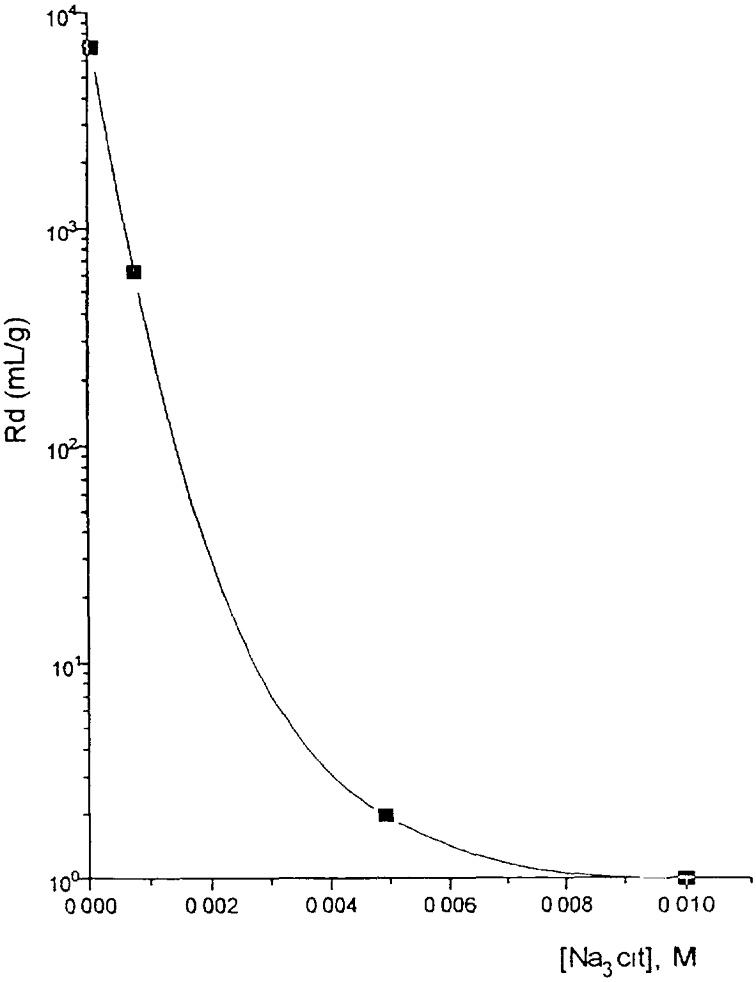

FIG 11 Effect of [Na$_3$cit] on Rd of Pu

TABLE III. CHEMICAL COMPOSITION OF THE REAL WASTE STREAM

Constituent concentration ($mg.L^{-1}$)			
K	20	Mg	16
Na	980	Mn	140
Al	280	Ni	0.82
Ca	250	Sr	0.1
Ce	<0.03	Ti	0.15
Cr	2100	Acidity	0.266
Fe	250	Specific Density	1.02

TABLE IV. CONCENTRATION OF RADIOACTIVE NUCLIDES IN THE REAL WASTE STREAM

Radionuclide concentration ($Bq.L^{-1}$)			
^{137}Cs	2.3E+8	^{90}Sr-^{90}Y	3.7E+8
^{155}Eu	2.4E+5	^{241}Am	2.3E+5
^{154}Eu	4.0E+4	$^{239+240}Pu$	3.6E+5
^{60}Co	2.5E+5	^{241}Pu	3.6E+5

To measure the effect of P301 sorbent dosage added on removal of Pu, batch tests with real waste have been carried out. Firstly, the waste is adjusted to pH2 by addition of NaOH solution and P301 sorbent is then added. After 24 hours contact, the supernatant liquid is separated from the sorbent by high speed centrifugation at 18000rpm for 30 minutes and then analyzed for gross activity. The results are shown in Table V.

TABLE V. EFFECT OF SORBENT AMOUNT ADDED ON REMOVAL OF Pu IN ACTUAL TEST

No:	Volume of waste stream (mL)	Sorbent amount (g)	pH after contact	Removal of Pu+Am (%)
1	50	0.5	2.1	68.2
2	50	1.0	2.2	93.6
3	50	1.5	2.3	98.7
4	50	2.0	2.5	99.6
5	50	2.5	2.5	99.8

From Table V, it can be seen that more than 98% of Pu and Am can be removed from the liquid waste stream when the addition of P301 sorbent is 1.5g in 50mL of waste stream, i.e. about 3 weight percent of sorbent will be needed in a waste stream treatment process. The result is in general agreement with the data obtained in the simulated test (Table II).

3.9. COLUMN TEST

As simulated solution was prepared by dissolving $NaNO_3$ and $Ca(NO_3)_2$ in distilled water at concentrations of 2M and 0.01M respectively. The solution was adjusted to pH2 and then spiked with ^{239}Pu and ^{241}Am. The flow rate of the simulated solution through the column was about 3-4BV/h. The results are shown in Table VI and Fig. 12.

TABLE VI. THE REMOVAL OF Pu AND Am IN THE COLUMN TESTS WITH SIMULATED SOLUTION

Tracer	specific activity of feed (Bq.L^{-1})	specific activity of effluent (Bq.L^{-1})	D.F.
^{239}Pu	1.92x10^6	1.48x10^2	1.3x10^4
^{241}Am	3.07x10^5	1.70x10^1	1.8x10^4

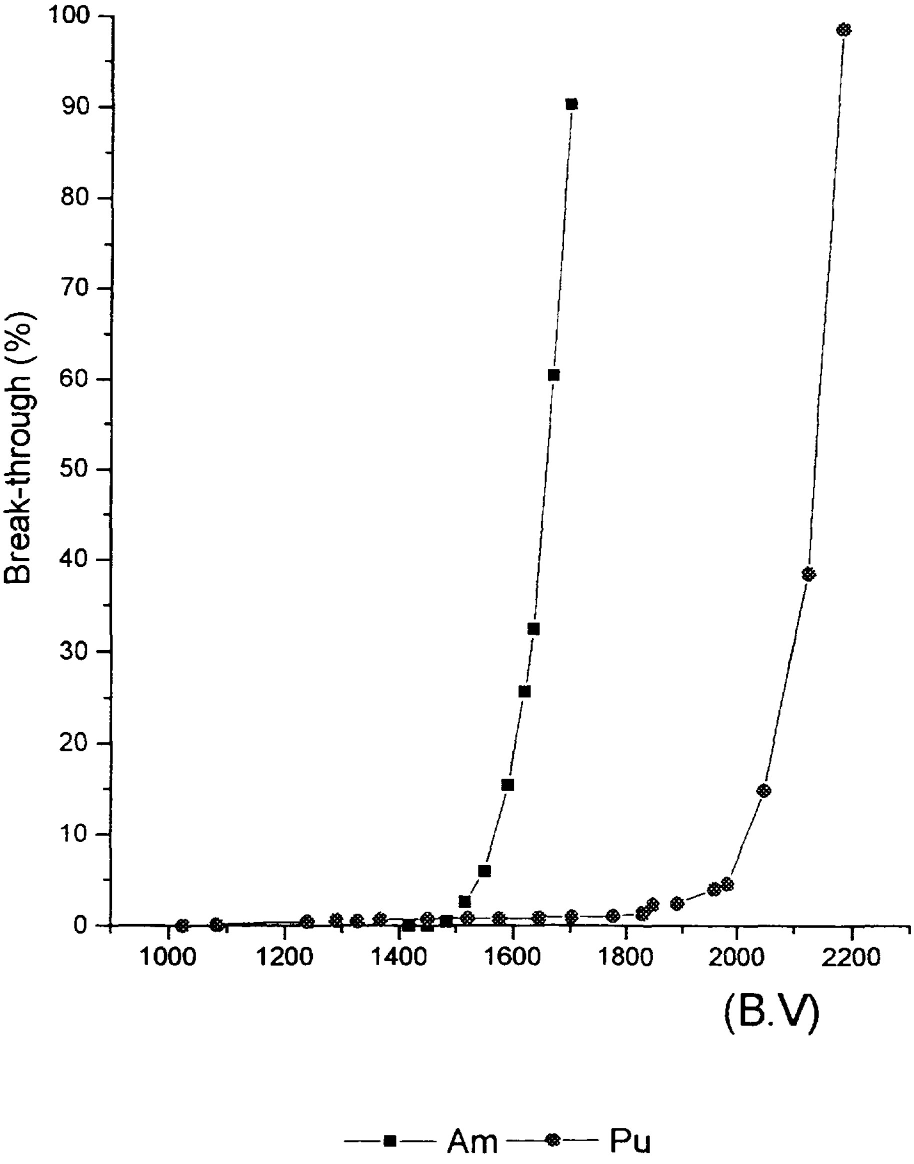

FIG. 12. The result of column test with simulated solution

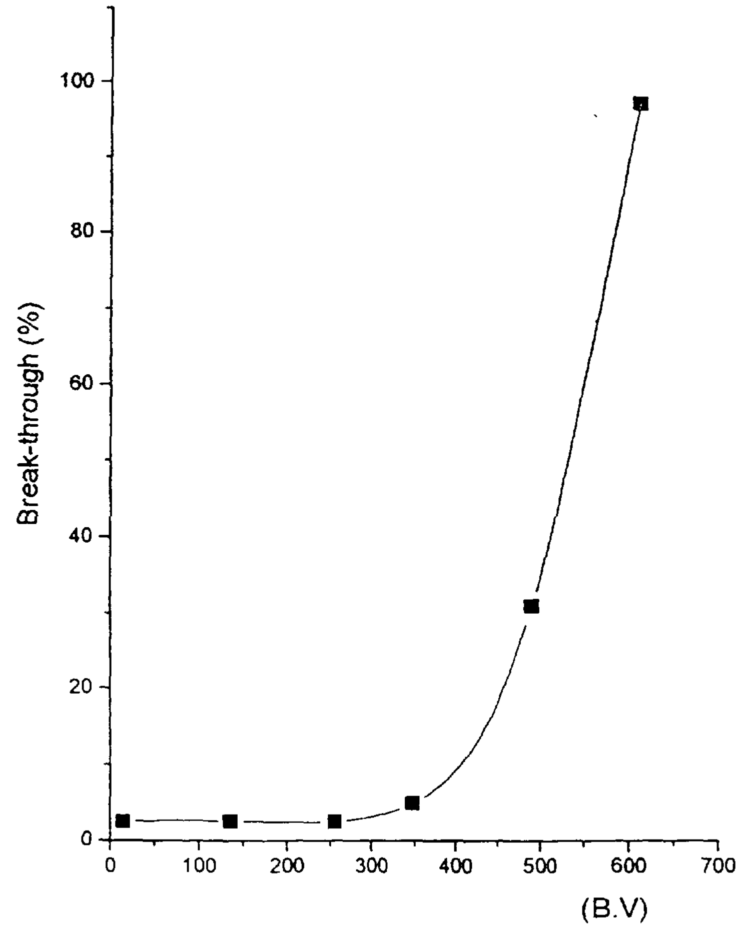

FIG. 13. The result of column test with actual stream

The column test with real waste was also carried out and the results are sho Fig. 13.

From the result of the column test with real waste, it can be seen that the column performance is rather poor. When alpha removal is more than 99.5%, breakthrough occurs at 23 BV which is much less than that obtained in the simulated test. During the test it was found that the flow rate became slower and slower until the test was terminated. In the mean while, some brown deposits on the top surface of the P301 material column and small bubbles between the P301 sorbent and the inner wall of the column were observed. This may be due to the higher concentrations of hydrogen ions and iron ions in the real waste than in the simulated solution. The performance can be improved by pre-treatment of the P301 material prior to column filling.

4. CONCLUSIONS

The test results show that the P301 inorganic material selected in this study possesses high adsorption capacity for Pu, Am and Ce, **Rds** of more than 10^3 for Pu and Am can be still obtained at high concentration of $NaNO_3$. It is evident that the **Rd** of Pu and Am is affected by the concentration of $Ca(NO_3)_2$ and also complexing agents in the waste streams to be treated. There is no obvious effect of $NaAlO_2$ concentration on the adsorption ratio of Pu. The data obtained also indicate that P301 material is very resistant to elevated temperature up to 400°C. The column tests show that the column performance is quite good after pretreatment of the selected materials prior to use.

REFERENCES

[1] SILVER G.I., Study of the Reaction of Uranium and Plutonium with Bone Char, MLM-2384, 1977.

[2] BLANE, D.E., et al., Mound Laboratory Activities on the Removal of Radionuclides from Waste Water Using Bone Char, MLM-2244, 1975.

[3] SCHULZ, W.W., et al., Application of Inorganic Sorbents in Actinide Separation Processes, Actinide Separation, P. 17, 1979.

[4] DOSCH, R.G., The use of Titanates in Decontamination of Defense Waste, SAND 78-0710

[5] INTERNATIONAL ATOMIC ENERGY AGENCY, Treatment of Alpha-bearing Waste, Technical Report Series No.287, IAEA, Vienna (1988)

IMMOBILIZATION OF RADIOACTIVE WASTES THROUGH CEMENTATION USING CUBAN ZEOLITIC ROCK AS ADDITIVE

G. CHALES SUÁREZ, R.CASTILLO GÓMEZ
Nuclear Technology Center,
Nuclear Agency,
La Habana, Cuba

Abstract

The cementation of both simulated and real low level aqueous wastes using Cuban zeolite as additive is described. Mechanical characteristics and leach testing of the cemented waste forms has been studied. The results obtained have shown that the presence of zeolite in the cemented waste form reduces considerably the leach rates of Cs and Co and moreover, mechanical characteristics (set time and compressive strength) are better when compared with direct cementation of aqueous wastes.

1. INTRODUCTION

Cementation, because of its low cost, simplicity and non-combustibility has great application in the solidification of liquid radioactive wastes [1]. In different countries this method is satisfactorily used in the immobilization of radioactive waste using different pozzolanic additives to increase the stability of the radionuclides in the cemented matrix [2,3]. Zeolite is one of them [4].

Cuba has many zeolite deposits with good opportunity for application in management of radioactive wastes. This paper describes the selection of zeolite samples, their characterization as a sorbent; the mixtures used in the cementation studies, the techniques used, the experimental results and their analyses. Mechanical characteristics of some cemented samples and leach testing of ^{137}Cs and ^{60}Co are also reported.

2. MATERIALS AND METHODS

The behaviour as sorbent of ^{137}Cs and ^{60}Co of 10 samples of different local rocks and minerals was examined. The main sorptive characteristics for these radionuclides in these materials depend on mineralogical composition. The zeolitic rocks were better for these purposes.

Zeolites from three areas around the country were selected:

(i) Orozco, from Bahia Honda area, composed of clinoptilotite;
(ii) The Piojillo, from Villa Clara, consisting of clinoptilolite and mordenite and
(iii) Palmarito, in Santiago de Cuba, mainly mordenite. Table I shows some of the characteristics of the selected samples.

The sorptive behaviour for ^{137}Cs and ^{60}Co of the samples was studied.

Most of the results were obtained by using the radioactive indicator method with a 95% reliability. The level of activity of the labeled solution was 10^3-10^5 Bq/L.

TABLE I: CHARACTERISTICS OF ZEOLITE SAMPLES.

	SAMPLE		
Component (%)	PIOJILLO	PALMARITO	OROZCO
SiO_2	64.17	65.78	58.87
Al_2O_3	10.89	10.81	11.87
Fe_2O_3	2.47	1.71	2.65
CaO	4.04	3.86	5.14
MgO	1.23	0.96	2.18
Na_2O	1.28	2.02	1.10
K_2O	0.90	0.79	0.99
TiO_2	0.36	0.25	0.19
*LBI (H_2O)	14.77	13.97	17.12
Volume height (g/cm^3)	1.5	1.37	1.45
Effective porosity	31.67	40.08	38.02
Density (g/cm^3)	2.10	2.11	2.08
Si/Al	5.19	5.38	4.37

*Loss by incineration.

3. CHARACTERIZATION OF THE ZEOLITES

3.1. DETERMINATION OF CHEMICAL STABILITY

The chemical stability of zeolites was determined by means of standard methods. For that purpose, 10 g of 0.250-0.315 mm grain sized sorbent were flushed for 10 minutes with 250 mL of an aqueous solution of Hcl, HNO_3, H_3PO_4, H_2SO_4 or Na_3PO_4. The samples were then dried for 3 hours at 80°C to constant weight to determine the percentage of weight loss in each case.

3.2. DETERMINATION OF THE STATIC SORPTION CAPACITY.

For the purpose of this study, solutions of CsCl and $CoCl_2$ were used at concentrations within the range of 0.01 and 0.2 M, labeled with ^{137}Cs and ^{60}Co. The pH was adjusted with HCl or NaOH solutions to values in the range of 6.5 and 7.0.

0.1 g of the sorbent with a 0.250-0.315 mm grain size was in constant agitation with 10 mL solution during 30 hours at room temperature. The measurements were performed after 24 hours standing. Table II shows the static sorption capacity, which expresses the maximum concentration of the ion in the sorbent.

TABLE II. DISTRIBUTION COEFFICIENT (Kd), DYNAMIC AND STATIC SORPTION CAPACITY FOR $^{60}Co^{2+}$ AND $^{137}Cs^{+}$ IN ZEOLITE SAMPLES

Zeolite	Radionuclide	Sorption Static (meq/g)	Capacity Dynamic (meq/g)	Distribution Coefficient (mL/g)
Piojillo	^{60}Co	0.35	0.25±0.04	667
	^{137}Cs	1.66	1.55±0.06	15009
Orozco	^{60}Co	0.29	0.21±0.03	456
	^{137}Cs	1.64	1.48±0.06	7762
Palmarito	^{60}Co	0.25	0.18±0.03	609
	^{137}Cs	1.05	1.43±0.05	13914

3.3. DETERMINATION OF THE DYNAMIC SORPTION CAPACITY.

1 or 2 grams of the sample were used depending on the ion to be absorbed and 0.01N solutions of Cs^{+} and 0.005N of Co^{2+} labeled with the corresponding radionuclides. The pH was kept between 6.0 and 6.5, a particular size between 0.250-0.315 mm and a flow rate of 2.6 mL/sec. 10 mL fractions were collected up to saturation which was determined radiometrically.

The number of absorbed milliequivalent (meq) of radioelements was determined for each fraction according to equation 1 and 2. The result of the sorbent given in grams expresses the of dynamic sorption capacity (equation 3):

$$Csoln = \frac{I\,soln \cdot Co}{Io} \qquad (1)$$

$$q = CoVo - Csoln \,.\, Vsoln \qquad (2)$$

where

Csoln is the concentration of the solution after sorption (meq/mL),
Co is the concentration of the solution before sorption (meq/mL),
q is the number of sorbed quantity meq,
Io is the counting rate of the solution before sorption (counts/sec.mL),
Isoln is the counting rate of the solution after sorption (counts/sec.mL), and
V is the volume (mL)

$$Cd = \frac{q}{m} \qquad (3)$$

where

Cd is dynamic sorption capacity (meq/g)
m is sorbent mass

3.4. DETERMINATION OF THE DISTRIBUTION COEFFICIENTS (K_d).

A 0.01N solution of $Ca(NO_3)_2$ + $NaNO_3$ in the ratio 3:7 and pH =6.5-7.0 labeled with the radionuclides was used.

0.1 g of the sorbent of a 0.250-0.315 mm grain size was contacted with constant agitation with 10 mL of solution for 30 hours at room temperature. The measurements were performed after 24 hours standing. The Kd was determined according to equation 4:

$$Kd = \frac{(Io - Im)}{Im} \cdot \frac{V}{m} \qquad (4)$$

where:

Io	is counting rate of the solution before sorption (counts/sec.mL),
Im	is counting rate of the solution after the sorption (counts/sec.mL),
V	is volume (mL), and
m	is sorbent mass.

The calculated distribution coefficients and dynamic sorption capacities are given in Table II.

3.5. DETERMINATION OF THE INFLUENCE OF THERMAL AND RADIATION TREATMENT OF THE SORBENT DURING ^{137}Cs SORPTION.

This study was carried out for the zeolitic rocks from Piojillo, Orozco and Palmarito deposits in their natural forms.

The samples were heated for 2, 4 and 6 hours at 200°C, 300°C, 400°C, 500°C and 600°C in a muffle furnace and given radiation doses of $2 \cdot 10^5$ and $2 \cdot 10^7$ rad at 25 +/- 1°C temperature using a MRX 25M ^{60}Co source with a dose rate of 27 rad/sec.

The effect of these treatments on Cs^+ sorption was assessed by the calculated Kd according to equation (4). For this purpose, 0.1 g of the sorbent was contacted with 10 mL of 0.01N solution of CsCl labeled with ^{137}Cs, at pH= 6.9, for 30 hours at room temperature. At the same time, an experiment with samples of the non-treated sorbents was carried out.

The results are shown in Tables III-VI.

4. CEMENTATION

From the results obtained, the zeolite from Piojillo deposit was selected for the immobilization of radioactive wastes.

Initially, the solidification of a solution of $NaNO_3$ + $Ca(CO_3)_2$ in the ratio 7:3, of total concentration 50 g/L, with zeolite, cement and $Ca(OH)_2$, was performed. In Table VII, the composition of the mixtures are shown.

TABLE III. EFFECT OF THERMAL TREATMENT OF SAMPLES FROM PALMARITO-ECCECT ON ^{137}Cs SORPTION

Temp (°C)	Distribution Coefficient (mL/g)			
	Time (h) 0	2	4	6
0	865 +/- 20	--	--	--
200		618 +/- 14	633 +/- 13	607 +/- 23
300		394 +/- 9	336 +/- 7	296 +/- 6
400		160 +/- 3	140 +/- 3	136 +/- 3
500		100 +/- 2	99 +/- 2	99 +/- 2
600		96 +/- 2	99 +/- 2	96 +/- 2

TABLE IV. EFFECT OF THERMAL TREATMENT OF SAMPLES FROM El PIOJILLO EFFECT ON ^{137}Cs SORPTION

Temp (°C)	Distribution Coefficient (mL/g)			
	Time (h) 0	2	4	6
0	896 +/- 22	--	--	--
200		549 +/- 15	575 +/- 14	574 +/- 11
300		532 +/- 19	541 +/- 18	558 +/- 13
400		502 +/- 11	291 +/- 6	302 +/- 7
500		184 +/- 4	186 +/- 4	185 +/- 6
600		106 +/- 2	107 +/- 2	109 +/- 2

TABLE V. EFFECT OF THERMAL TREATMENT OF SAMPLES FROM OROZCO-EFFECT ON ^{137}Cs SORPTION

Temp (°C)	Distribution Coefficient (mL/g)			
	Time (h) 0	2	4	6
0	414 +/- 9	--	--	--
200		202 +/- 4	205 +/- 5	200 +/- 4
300		172 +/- 3	107 /- 2	33 +/- 3
400		54 +/- 2	27 +/- 1	23 +/- 1
500		14 +/- 1	14 +/- 1	13 +/- 1
600		9 +/- 1	8 +/- 1	8 +/- 1

TABLE VI. EFFECT OF RADIATION TREATMENT EFFECT ON ^{137}Cs SORPTION OF NATURAL ZEOLITES ROCKS

Distribution Coefficient (mL/g)			
Zeolite	Dose (Rad)	2x10^5	2x10^7
Nat. Piojillo	574 +/- 14	553 +/- 14	561 +/- 14
Nat. Orozco	280 +/- 8	289 +/- 7	294 +/- 6
Nat. Palmarito	538 +/- 13	522 +/- 12	522 +/- 14

TABLE VII. MIXTURES USED IN THE CEMENTATION STUDIES

No.	Solution %	Zeolite %	Cement %	$Ca(OH)_2$ %
1	27	28	43	2
2	31	29	38	2
3	36	35	27	2
4	36	27	35	2
5	36	29	33	2
6	44	21	33	2
7	46	21	31	2
8	50	19	29	2
9	53	25	20	2
10	60	13	25	2
11	60	9	29	2
12	60	16	22	2

According to set time, homogeneity and compressive strength of the matrix obtained, the mixture of similar composition to number 5 was selected to study the leaching of ^{137}Cs and ^{60}Co from the cemented waste forms using some samples produced from both simulated and real low level aqueous wastes as follows:

System 1: Solutions of $NaNO_3$ + $Ca(NO_3)_2$ of 7:3 ratio with a total concentration of 5 g/L and $^{60}CoCl_2$ with an activity of 1.2 x 10^6 Bq/L.

System 2: Similar to system 1, but without zeolite in the mixture used for cementation.

System 3: Concentrate radioactive solution with ^{137}Cs and activity of $3.2 \cdot 10^6$ Bq/L. The composition of this solution was Na_2CO_3 -- 40g/L, Na_3PO_4 -- 40g/L, $KMnO_4$ -- 40g/L, oxalic acid -- 40 g/L, citric acid --40 g/L and boric acid -- 40 g/L.

System 4: Real aqueous wastes containing ^{60}Co and ^{137}Cs of unknown chemical composition and between 24-52 g/L of total solids content.

System 5: Simulated evaporator concentrates (200 g/L) of composition: $NaNO_3$ -- 100 g/L, $Na_2C_2O_4$ -- 12 g/L, H_3BO_3 -- 24 g/L NaOH -- 12 g/L and $Ca(NO_3)_2$ - 52 g/L, with ^{60}Co at $2.65x10^6$ Bq/L.

In this case, 9 different mixtures with constant content of radioactive solutions and variable zeolite/cement ratio were prepared and mechanical characteristics (compressive strength, set time and absorption by immersion) and leaching of ^{60}Co were determined.

Mechanical characteristics were determined by the classical methods, which are applied in civil engineering.

Leach testing was performed according to the IAEA standard procedure defined by E.Herpe [5] and to the long-term leach testing procedures for solidified radioactive waste forms defined by the International Standardization [6].

The leachant was deionized water with a conductivity 0.8 μmho/cm. The pH of the leaching solution was between 11.39 and 12.43. The temperature of the test was 25 ± 2°C.

The radiometric measurements were performed using a 40x60 mm NaI(Tl) scintillation detector coupled to a radiometer and the minimum detectable rate counting for 1 hour was 15 counts/100 sec value according to the Dementiev method [7]. For samples of system 5, the measurements for leach testing, we used a NaI(Tl) detector of 110x110 mm, BNIF and energetic res. 9%, with ± 25% relative error. In this case, the minimum detectable activity (Amd) was:

Time (Sec)	1000	2000	3000	4000	5000	7000	1000
Amd (Bq/L)	$7.0 \cdot 10^2$	$2.9 \cdot 10^2$	$2.3 \cdot 10^2$	$1.9 \cdot 10^2$	$1.7 \cdot 10^2$	$1.4 \cdot 10^2$	$1.2 \cdot 10^2$

The leaching was determined according to the equation:

$$Rn = \frac{Am \cdot Vt/Vm \cdot m}{Ao \cdot F \cdot tn} \quad (5)$$

where

Rn	is leach rate in g per m^2 per day for the time tn,
Am	is counting rate, per sec, of leachant,
Vt	is total volume of leachant (mL),
Vm	is volume of leachant aliquot (mL),
m	is mass of specimen (g),
Ao	is counting rate per sec of cemented solution,
F	is area of the specimen in m^2 and
tn	is leaching time in days.

The minimum rate for each radionuclide in the experimental condition, according to the detection limit of the installation, was determined.

5. RESULTS AND DISCUSSIONS

The results of chemical stability tests obtained for all zeolite samples can be considered satisfactory considering that they are greater than 95% in both acid and alkaline environments. The high Si/Al ratio of the studied sorbents is the reason for the values of chemical stability obtained [8,9].

On the other hand, studies made with Soviet mordenites and clinoptilolites show that the crystal structure of zeolites is kept even after a high degree of dealuminisation [8].

From the values, reported in Table II we can conclude that Cs^+ sorption is greater than Co^{2+} sorption. This behavior is attributed to the higher ionic radius, lower hydration energy and to the easy polarizability of Cs [10,11].

These studies demonstrate the good selectivity for ^{137}Cs and ^{60}Co of the natural zeolitic rock from "El Piojillo" deposit. As was mentioned earlier, this zeolite is a mixture of clinoptilolite and mordenite in similar proportions.

The results obtained in the study of the influence of the thermal treatment of zeolites, with reference to Cs^+ sorption (Tables III-VI), show that Cs^+ sorption decreases with increase in the treatment temperature.

The results show that only the samples from Orozco treated at 300 and 400°C, and the ones from Palmarito treated at 300°C, have not reached the final value of their sorptive properties in the time interval studied.

X-ray diffraction pattern of samples from the three deposits heated for 4 hours at temperatures ranging from 400°C to 600°C, show that in samples from "El Piojillo" deposit, which are composed mainly of clinoptilolite and mordenite, the intensity of the reflections of the clinoptilolite is reduced from 400°C and its crystallinity gets worse. At 600°C the reflections of the mordenite phase can be seen. This corresponds to the diffractograms of the zeolites from Palmarito which are mainly due to mordenite, where no significant changes take place on being heated to 600°C.

The behavior of the samples from Orozco is similar to the clinoptilolite phase of El Piojillo. At 400°C the intensity of the reflections is reduced with respect to the untreated samples. Taking into account that the percentage of zeolite in the studied rocks is high (80%) and therefore its contribution to the sorptive properties of the rock is incomparably higher than the rest of the components, we can conclude from the X-ray diffraction analysis that the reduction of the sorptive properties of the zeolite due to thermal treatment is not the only consequence of severe changes in the crystal structure. This would explain why the zeolite from Palmarito, though it does not have significant structural changes after being treated at 600°C, has sorptive levels lower than this rock with any treatment at all.

The thermal stability of the zeolitic structure depends on the chemical composition of the samples [12] and on the Si/Al ratio, which conditions the difference in the behavior of zeolites from different deposits.

The zeolite structure is thermally more stable the higher the Si/Al ratio. This agrees with the results reported in Tables III-VI.

During the dehydration process of zeolite, the tetrahedral Al^{3+} is displaced towards the channels, making the access to them possible and therefore the vacancy created by the loss of Al^{3+} is initially filled by H^+.

The loss of the tetrahedral Al^{3+} causes the reduction of the total exchange capacity due to the fact that the deficit of positive charge in the zeolite framework is reduced.

Kd values reported in Table VII show that the sorptive properties of the zeolitic rocks from Orozco, Piojillo and Palmarito do not change with respect to cesium after being exposed to radiation doses of 10^5 and 10^7 rad. The behavior reported elsewhere for zeolites [13] is corroborated by these results.

In all case, the values of the leach rate are small and they are similar to those reported in the literature for low-level radioactive wastes solidified by this method [9]. In the systems 1 and 5 the leaching of ^{60}Co is very low. This positive effect is due to the presence of zeolite as additive. The absence of zeolite in system 2 corroborates this result.

In system 3, although the salt content is higher, the leach rate for ^{137}Cs is low. We can infer this behavior due to the presence of zeolite.

In the case of real wastes the leaching rate obtained for ^{137}Cs is similar to that for system 3 and also similar to the values reported in the literature.

The studied demonstrate, that the matrix in which, the wastes are immobilized have good resistance to the leaching process.

The results for the mechanical characteristics studies in system 5 reported in Table VIII, demonstrate that addition of zeolite to cement/concentrate solution mixtures decrease the set time, but when this addition is in excess (zeolite/cement≥1), the set time does not decrease, though the zeolite is an accelerator in the range studied. A better zeolite/cement ratio corresponds to a mixture number 8 (0.668). These studies demonstrate also, that zeolite as additive in the mixture improve the compressive strength, value for mixture number 9, where zeolite is absent corroborates these results.

Similar behavior was observed in the studies of absorption by immersion, which infer a greater volume of liquid incorporated and better permeability properties for the specimen. In this case, the advantage of zeolite additive in the waste/cement mixture is also found. As with compressive strength, a significant difference was obtained between samples with or without zeolite additives. Studies of the leachability of ^{60}Co for this system, showed that the release of ^{60}Co was below the limit of detection under the conditions of test.

The presence of zeolite in cemented boric acid and borate containing waste provides a much shorter set time and higher compressive strength product when compared with product containing no zeolite.

We can conclude that the presence of zeolite in the waste/cement mixture is advantageous for immobilization of concentrated radioactive waste.

TABLE VIII. COMPRESSIVE STRENGTH, SET TIME, ABSORPTION BY IMMERSION AND LEACHABILITY FOR SPECIMEN CORRESPONDING TO SYSTEM 5

Waste/ Cement+ Zeolite	Zeolite/ Cement	Set Time (hours)	Compressive Strength (MPa)	Absorption by Immersion	Leaching for 28 d (g/cm^2.d)
0.430	1.027	--	41.24	37.3	2.4E-6
0.415	0.956	9.83	41.09	38.3	2.3E-6
0.400	0.889	9.25	41.25	37.5	1.1E-6
0.386	0.832	8.20	43.85	36.1	2.6E-6
0.373	0.785	7.01	46.66	34.1	2.6E-6
0.372	0.743	6.80	42.24	33.8	2.7E-6
0.350	0.702	6.80	44.48	32.3	2.8E-6
0.340	0.668	6.26	46.98	30.7	<2.8E-6
0.362	0.000	10.01	28.28	23.4	<3.2E-6

6. CONCLUSIONS

1. In Cuba there are zeolite deposits with good absorption properties that can be applied in the treatment of radioactive wastes. The sample from El Piojillo deposit is the most important one, because of high selectivity for ^{137}Cs and ^{60}Co.

2. The procedure for the immobilization of low-level radioactive wastes with cementation using zeolite as additive was established. The presence of this material in the cemented waste form reduces the leach rates of Cs and Co and improves the mechanical characteristics.

REFERENCES

[1] GILLIAM, T.M AND DOLE, L.R. Determining leach rates of monolithic waste forms OAK Ridge National Lab. Tennessee, USA (1986).

[2] STONE J.A. Measurement and Control of Cement Set Times in Waste Solidification, South River Lab, South Carolina, USA. (1976).

[3] COLOMBO, P. Some techniques for the solidification of radioactive wastes in concrete. American Nuclear Society, Annual Meeting (1976).

[4] VANCE, E.R. A possible host for ^{137}Cs. Immobilization Material Research. Lab. Pennsylvannia. State University, USA. (1982).

[5] E.D.HESPE. "Leach Testing of Immobilized Radioactive Waste Solid", Atomic Energy Review, Vol 9 (1971) pp 195.

[6] Long-Term leach testing of solidified radioactive waste forms. International Organization for Standardization. ISO 6961-1982 (E).
[7] DEMENTIEV, V.A. Izmerienie malikh aktivnosatiej radioactivinykh preparatov, Atomizdat, Moscú. (1967).
[8] CHELISHEV, N.F, BERINSTEJN B.G, et. al Tseolity-novyj tip mineralnogo Syrya. Moscú Necha, 1987.
[9] American Chemical Society. Catalytic Materials, 1987.
[10] COWSER, K,E, LISHER, L.C. STI/PUB/116. IAEA. 1986.
[11] GOMPER, K. INIS inf- 8520, 1982.
[12] BREK, D. Tseolitovye molekylyarnye. Sita M.Mir. 1976.
[13] TSITSISHVIH, G.V, ANDRONIKASHVILI, T.G. et al Prirodnye Tseolity. Moscú Khimiya, 1985.

RADIOMETRIC EMANATION METHOD IN CHARACTERIZATION OF INORGANIC SORBENTS USED FOR TREATMENT OF GASEOUS AND LIQUID RADIOACTIVE WASTE

V. BALEK, P. FRANTA, F. KEPÁK, Z. MÁLEK, E. KLOSOVÁ
Nuclear Research Institute Řež plc,
Řež, Czech Republic

Abstract

At the Nuclear Research Institute, Řež (Czech Republic) a non-traditional method called Emanation Thermal Analysis has been developed which can be used for characterization of the thermal stability and radiation stability of sorbents as well as for characterization of the stability of solids during interactions with liquid and gaseous components. The method is based on the measurements of radon release rate from samples that have been previously labeled with the parent radionuclides of radon i.e. ^{228}Th, ^{224}Ra. This report presents the results of characterization studies on inorganic sorbents used for the removal of RuO_4 from a gaseous effluent and Cs and Sr from liquid NPP wastes.The Radiometric Emanation Method has also been used to characterize sorbents supplied by other participants in the Co-ordinated Research Programme.

1. INTRODUCTION

The experimental work was carried out in the following directions, the results of which are described in this final report:

1. Use of natural clinoptilolite and synthetic mordenite for removal of RuO_4 vapors from effluent gases.
2. Characterization of thermal behavior of clinoptilolite and mordenite sorbents used for the removal of RuO_4.
3. Use of mordenite for removal of Cs and Sr from liquid NPP wastes.
4. Vitrification of spent mordenite sorbents.
5. Characterization of thermal behavior of spent mordenite containing Cs.
6. Characterization of other materials for inorganic sorbents using radiometric emanation method.

2. USE OF NATURAL CLINOPTILOLITE AND SYNTHETIC MORDENITE FOR REMOVAL OF RuO_4 VAPORS FROM EFFLUENT GASES

In the Nuclear Research Institute, Řež, natural clinoptilolite and synthetic mordenite have been studied as sorbents for removal of $^{106}RuO_4$ vapors which are produced during the vitrification of high level radioactive waste.

The apparatus used for the measurement of RuO_4 breakthrough curves on solid beds of the sorbents is described in Ref. [1]

Natural clinoptilolite from the locality Nižný Hrabovec, East Slovakia has been used, has the following chemical composition (in mass %):

SiO_2-67.0, Al_2O_3- 0.85, CaO-3.6, MgO-0.90, Fe_2O_3 -0.85, Na_2O-0.52, K_2O-3.20.

As regards the phase composition, according to published information the tuff contains 50 - 60 % of crystalline clinoptilolite. The bulk density of non-dried clinoptilolite sample was 1.0 g/cm^3. It ranged from 1.0 to 1.2 g/cm^3 in the reactors. The mercury densities are as follows: (pHg)w = 1.67 g/cm^3 for the non-dried sample and (pHg)d = 1.59 g/cm^3 for a dried sample (200 °C, 6 hours in N_2). Synthetic mordenite was supplied by Slovchémia, Bratislava (Slovak Republic)

The declared composition of the synthetic mordenite type M 315 was (in mass %): SiO_2 86.87, Al_2O_3 - 6.79, CaO - 1.00, Na_2O - 5.34.

The ratio SiO_2: Al_2O_3 of the synthetic mordenite was 12.8, the bulk density: 0.92 g/cm^3. The mordenite sorbent used was granulated, 30 % of haloysite as binder being present in the sample. The bead size was 0.8 - 1.0 mm.

1.1. INVESTIGATION OF RuO_4 SORPTION ON CLINOPTILOLITE

The dependence of the clinoptilolite sorption capacity and of the time to 1 % breakthrough on the reactor length are given in Table I.

TABLE I. DEPENDENCE OF THE CLINOPTILOLITE SORPTION CAPACITY AND OF THE TIME TO 1% BREAKTHROUGH ON THE REACTOR LENGTH

Reactor length, cm	3.0	5.0	7.5	15.0
Sorption capacity, μg Ru/g	58	62	111	151
Time to the 1% breakthrough, min	92	162	400	965

The conditions used for the sorption experiments were: ambient temperature, flow-rate of 250 mL/min used.

The dependence of the clinoptilolite sorption capacity and of the time to 1 % breakthrough on the sorption temperature is given in Table II.

TABLE II. DEPENDENCE OF THE CLINIPTILOLITE SORPTION CAPACITY AND OF THE TIME TO 1 % BREAKTHROUGH ON THE SORPTION TEMPERATURE

Temperature, °C	ambient	50
Sorption capacity, μg Ru/g	58	77
Time to the 1 % breakthrough, min	92	122

Reactor length 3 cm, flow-rate of 250 mL/min.

Some authors [2,3] explain the sorption behavior as the catalytic transformation of RuO_4 according to the following mechanisms:

$$RuO_4 \xrightarrow{Fe_2O_3} RuO_2 + O_2 \tag{1}$$

$$RuO_4 \xrightarrow{RuO_2} RuO_2 + O_2 \tag{2}$$

In the first case this means RuO_4 dissociation catalyzed by Fe_2O_3, or by other oxides, with which the sorbent is either impregnated or that are already present in the sorbent. The second scheme expresses the autocatalytic effect of RuO_2 formed during the first stage of decomposition. These transformations can be followed, in principle, visually by the change of the yellow-brown color of RuO_4 into the black color of RuO_2, that proceeds, e.g., on the apparatus surface [4].

The same behavior was observed also for other types of sorbents, e.g., in the case of silica gel [5]. However, in the case of clinoptilolite, from the very beginning of the sorption only the black color was observed, indicating the practically instantaneous dissociation of the sorbed RuO_4 to RuO_2 and O_2. The dissociation of RuO_2 in the gas phase and on the formation of solid RuO_2 aerosol particles has already been reported [6].

2.2. INVESTIGATION OF RuO_4 SORPTION ON MORDENITE

The experiments were performed in the apparatus schematically shown in Fig. 1 [1].

The size of the reactor used was: diameter 1.61 cm, length 3 cm. The rate of nitrogen flow during both sorption and desorption experiments was 500 mL/min.

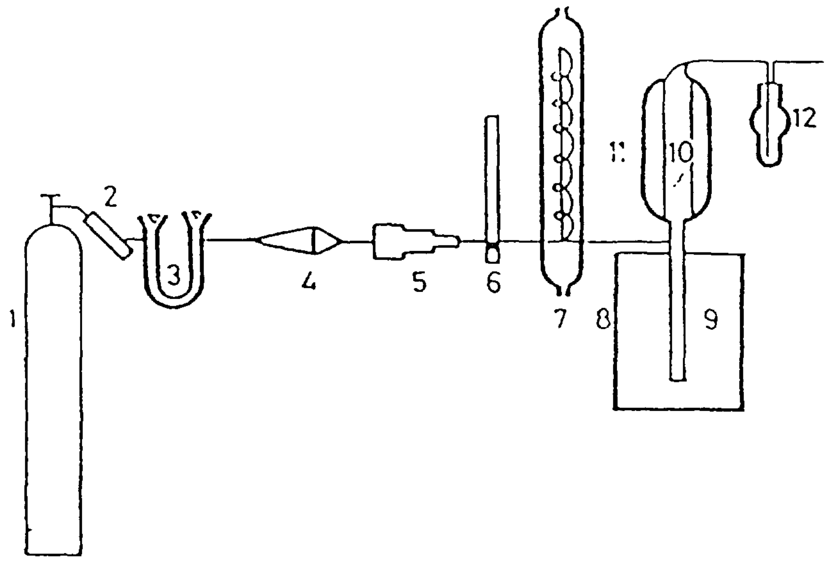

Fig. 1. Scheme of the apparatus for the RuO_4 retention experiments:
1. nitrogen pressure flask; 2. needle valve; 3. U-tube with molecular sieve DUSIMO S 3 A; 4. holder of filter paper AEROS-C; 5. flow rate stabilizer; 6. flow rate meter; 7. heat exchanger; 8. thermosta; 9. Stefan's tube for RuO_4 generastion; 10. reactor; 11. heating system (an ethylene glycol bath for t = 50 and 100°C; 12. washing microbottle with o-tolidine

The sorption capacity to the 1% breakthrough, as determined by the sorption measurement in dynamic condition, was 50 μgRu/g of sorbent. The temperatures used for sorption were 50 and 100 °C. After the sorption of RuO_4, the desorption of RuO_4 was carried out at the same temperature as used for the sorption. The results are presented in Table III.

The results obtained were used in the optimization of conditions for sorption of RuO_4 vapors from the effluent gases of the radioactive waste vitrification unit.

TABLE III. CHARACTERISTICS OF RuO_4 VAPOR SORPTION ON MORDENITE SORBENT

Temperature	50°C	100°C
Sorption capacity (μg Ru/g of sorbent) before the 1% breakthrough	53	51
Time (min) at which the 1% breakthrough was reached	61	66
Percentage of RuO_4 desorbed from the mordenite in the desorption cycle (210 min)	57	2.7
Notation of the sorbent sample used	No. 22	No. 23

3. CHARACTERIZATION OF THERMAL BEHAVIOR OF CLINOPTILOLITE AND MORDENITE SORBENTS USED FOR REMOVAL OF RuO_4 VAPORS

In the design of the technology for the immobilization of spent inorganic sorbents it is necessary to have information about their thermal behavior, such as the stability of the porous system during heating of the sorbent and loss of mass due to the release of volatiles from the sorbent. For the characterization of both virgin and spent mordenite, methods of thermal analysis (thermogravimetry, differential thermal analysis) and radiometric emanation method, developed at Nuclear Research Institute Řež plc, have been used.

3.1. PRINCIPLE OF THE RADIOMETRIC EMANATION METHOD (REM)

The REM [7,8] is based on the measurement of radon release rate from samples previously labeled with the radon parent nuclides, ^{228}Th and ^{224}Ra.

Radon atoms are formed by spontaneous decay of the parent nuclides according to the scheme

$$^{228}\mathrm{Th} \xrightarrow[1{,}9\ \text{year}]{\alpha} {}^{224}\mathrm{Ra} \xrightarrow[3.8\ \text{days}]{\alpha} {}^{220}\mathrm{Rn} \xrightarrow[58\ \text{sec}]{\alpha} \qquad (3)$$

Radon atoms formed during the spontaneous decay in a solid can, in principle, be released from the sample in two ways: (I) by the recoil energy (of the order of 100 keV per atom) which the radon atoms gain during the decay of the radium. This is valid for inert gas atoms being formed close to the surface; the recoil process is temperature independent, or (ii) by diffusion, which is temperature dependent.

The rate of radon release from the sample (called emanation rate E) can be expressed in a simplified way as follows:

$$E = E_{recoil} + E_{diffusion} = K1 \cdot S + (D/\lambda)^{1/2} . K_2 \qquad (4)$$

where

E_{recoil}	is the part of the radon release due to recoil,
$E_{diffusion}$	is the diffusion part of the released radon,
K1	is a temperature independent constant proportional to the external (geometrical) surface area and penetration depth of Rn atoms,
D	is the coefficient of radon diffusion in the sample,
λ	is the decay constant of Rn and
K_2	is a temperature dependent constant depending on the internal surface area (i.e. that obtained by gas adsorption measurements).

The temperature dependence of the radon diffusion coefficient can be expressed by the Arrhenius Law:

$$D = D_o \exp(- Q/RT) \qquad (5)$$

where

D_o	is the pre-exponential term,
Q	is the effective activation energy of radon diffusion of the solid,
R	is the gas constant and
T	is the absolute temperature.

The samples are labeled by impregnation using an acetone solution of radionuclides of ^{228}Th and ^{224}Ra which give rise to ^{220}Rn by α-decay. The sample labeling method is described in detail in [7,8].

The emanation release rate E is expressed in the relative units representing the ratio of the radon release rate normalized to the radioactivity of its ancestors ^{228}Th and ^{224}Ra.

It follows from Eq. (4) that any process in the solid or on its surface accompanied by a change of surface area or radon diffusion properties in the pores or the bulk of solid sample becomes indirectly observable by the REM. Taking into account the size of radon atoms (0.38 nm), it is obvious that changes in nanometer-scale porosity can be revealed in a very sensitive way.

The apparatus for the radiometric emanation method is given in Fig. 2. It ensures the continuous measurement of the inert gas (radon) released from the sample during heating or cooling. The carrier gas (air, nitrogen), is led over the sample taking off the radon atoms released; the radon atoms are carried into the gas detection chamber (alpha-radioactivity semiconductor or scintillation detectors are used).

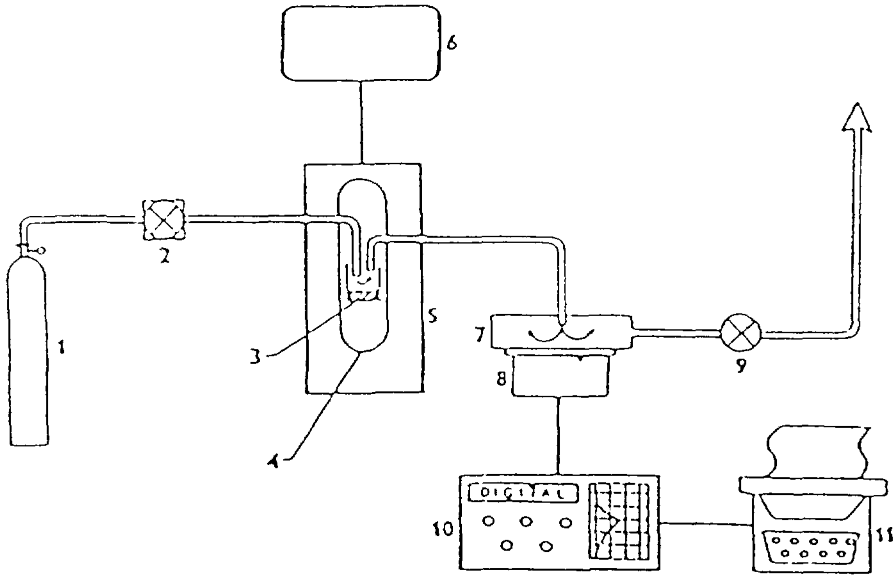

Fig. 2. Schematic of the apparatus for radiometric emanation method:
1 - gas supply; 2 - gas flow stabilizer and flow rate meter; 3 - labelled sample; 4 - sample holder;
5 - furnace; 6 - temperature controller; 7 - measuring chamber; 8 - radioactivity detector;
9 - flow rate meter; 10 - counts meters; 11 - data processors and printer (plotter)

3.2. THERMAL BEHAVIOR OF SPENT CLINOPTILOLITE

Figure 3a demonstrates the REM curves measured during heating and subsequent cooling in the air of spent natural clinoptilolite, containing 15μg of Ru per 1 g of the sorbent. For comparison, the thermogravimetric curve measured during heating in air is demonstrated in Figure 3b. The decrease in mass observed during sample heating, corresponds to the release of water (and other present volatiles, including ruthenium compounds).

The changes in the nanoporosity and morphology of the clinoptilolite are monitored in the REM curve (Fig. 3a). At temperatures above 500°C a decrease of radon release rate E was observed, indicating the decrease of porosity as a result of sintering and pore closure.

In Figure 4 we compare the thermal behavior of spent clinoptilolite containing 15 μg of Ru/g of sorbent (curve 2) and the virgin natural clinoptilolite (curve 1).

The differences are remarkable in the temperature ranges both below 600 °C and above 900°C. It can be stated that the thermal behavior is strongly influenced by the RuO_2 presence on the sorbent: the intensity of densification differs and the quality of the heat treated product is expected to be different. It is obvious that, after the heat treatment to 1200°C, the clinoptilolite is not sufficiently densified, and consequently the conditions for immobilization of hazardous Ru are not fulfilled.

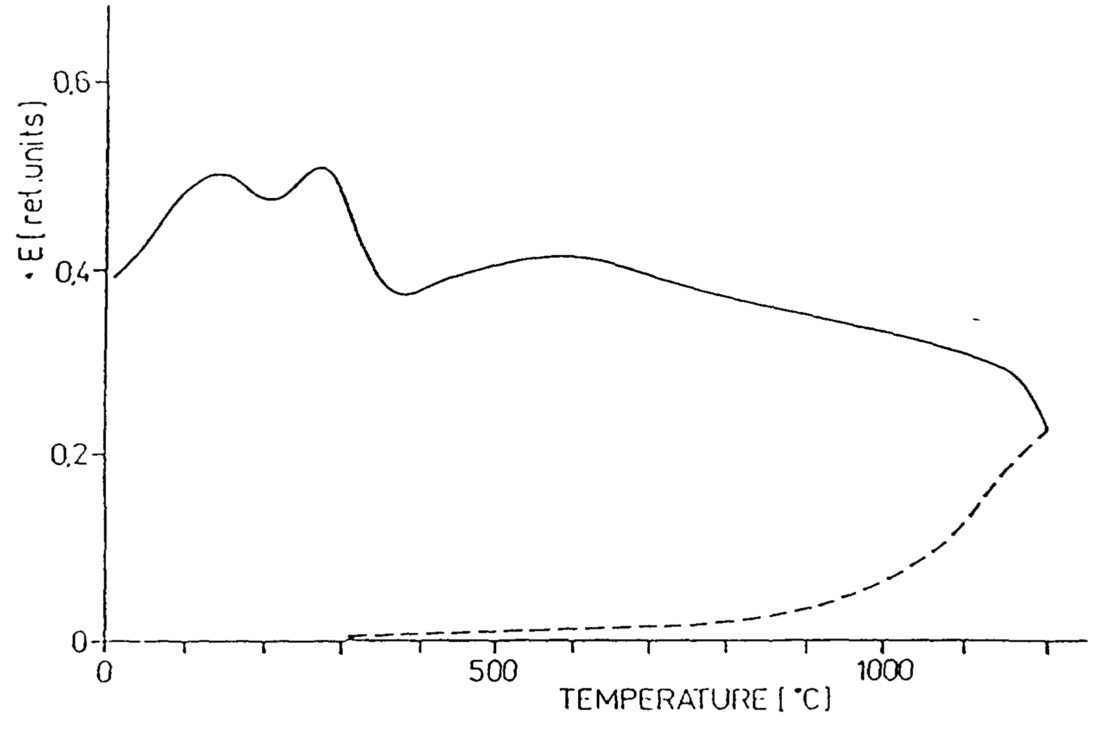

Fig. 3a. The REM curve of spent clinoptilolite (containing 15 μg of Ru (1 g of the sorbent) measured during heating in air, heating rate 5 K/min.

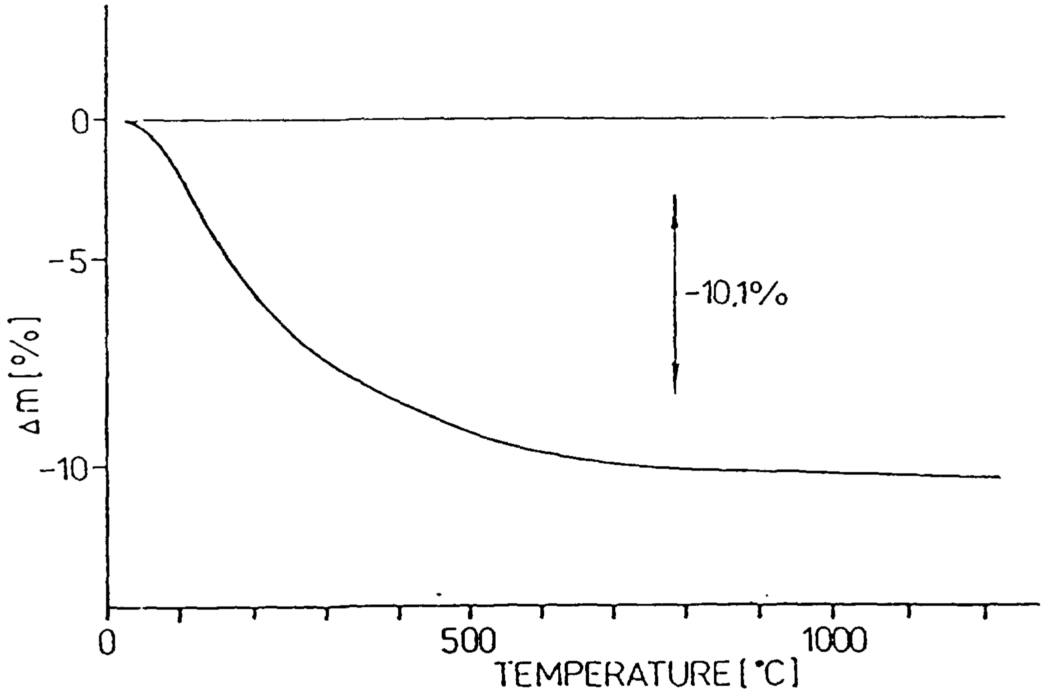

Fig. 3b. The temperature dependence of mass changes (TG curve) of spent clinoptilolite measured during heating in air, heating rate 5 K/min. (For the corresponding REM curve see Fig. 3a.)

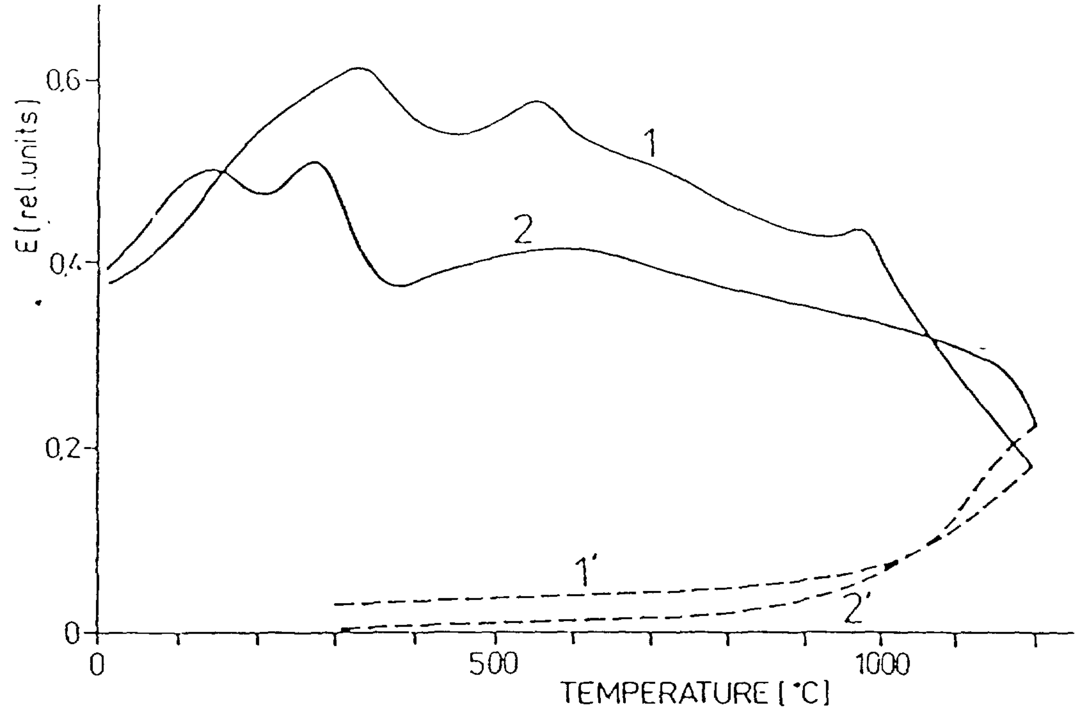

Fig. 4 *The REM curves used for the comparison of thermal behaviour in air of spent and virgin clinoptilolite samples.*
Curves 1 and 1' correspond to the spent clinoptilolite sorbent containing RuO_2, *curves 2 and 2' correspond to the virgin sorbent. The heating and cooling rate was 5 K/min.*
Full lines correspond to the heating runs up to 1200 °C, the dotted lines correspond to the cooling of samples previously heated to 1200 °C.

For the characterization of the diffusion properties and compactness of the heat-treated clinoptilolite samples, the REM cooling curves were used. In Fig. 5 the dependence of log (E $-E_0$) versus 1/T measured by the REM during cooling of the heat treated clinoptilolite samples are compared. The activation energy values Q for radon diffusion in the heat treated samples were determined from the slopes of the curves in Fig. 5 (viz Eq. (4) and (5)) in the temperature interval 1200 - 900°C. The values of Q=193 kJ/mol.. and 129 kJ/mol. were found for spent and virgin clinoptilolite respectively. A higher activation energy of radon diffusion was found in the heat treated spent sorbent compared to the heated virgin sorbent. The differences in the radon mobility can be used for prediction of the diffusion migration of other heavy elements to be sorbed and immobilized by clinoptilolite.

3.3. THERMAL BEHAVIOR OF SPENT MORDENITE CONTAINING RuO_2

From the results of TG shown in Fig. 6, during heating of spent mordenite containing RuO_2 the main loss of the sample mass occurs over the temperature interval 20-400°C. In this interval water is released from the surface and the porous system of the sorbent. The amount

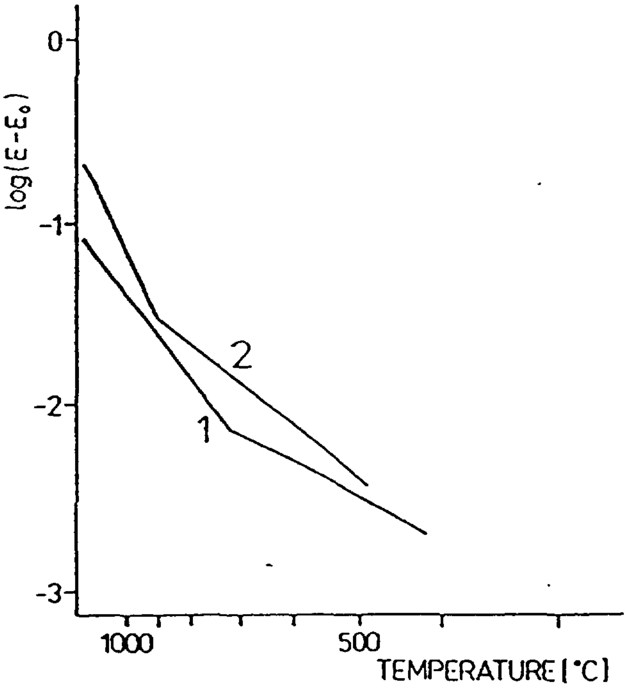

Fig. 5 *The dependence of log(E-Eo) versus 1/T plotted from the values of radon release rate measured during cooling of heat-treated spent clinoptilolite (curve 2) and virgin clinoptilolite sorbent (curve 1). (For the corresponding REM curves see Fig. 4, curves 1' and 2'.)*

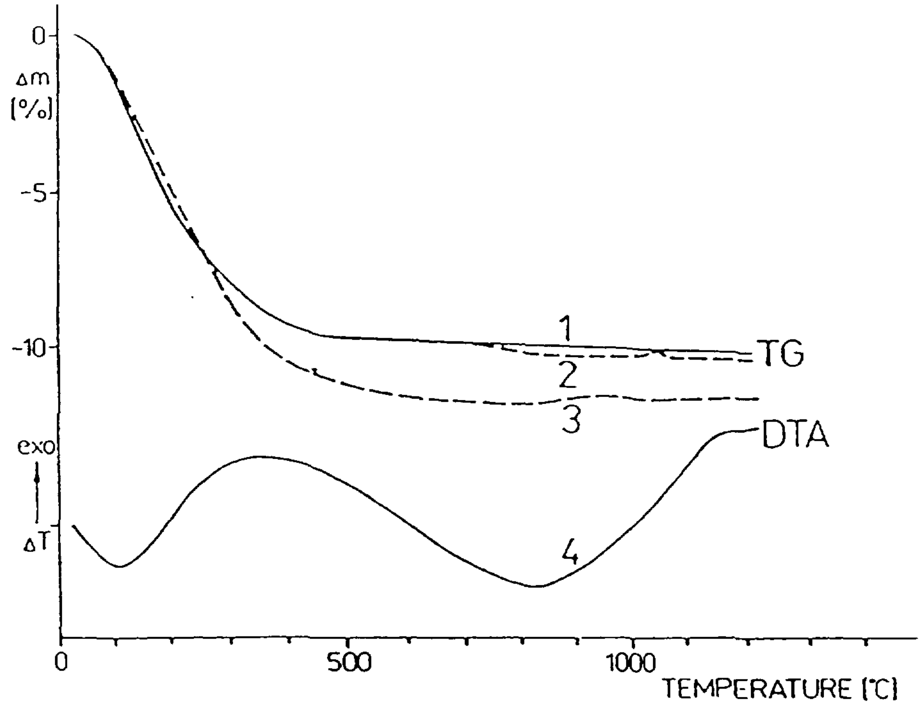

Fig. 6 *Temperature dependences of the mass loss of spent mordenite sorbent containing* RuO_2 *samples Nos. 22 and 23 (curves 1 and 2, resp.) and of virgin mordenite (curve 3). The DTA curve of virgin mordenite is given as curve 4 for comparison. (Heating rate 5 K/min, gas medium: air.)*

of the released volatiles is approx. 10% of the total mass of the mordenite used (containing RuO_2) (see curves 1 and 2, Fig. 7) and approx 12% of the mass of the virgin mordenite sorbent (see curve 3, Fig. 6). This difference can be explained by the fact that a part of the water was desorbed from the sorbent during the sorption - desorption experiments carried out at 50 and 100°C, respectively.

In the temperature range above 600°C, a slight decrease of mass was observed with the samples of the spent mordenite. A higher decrease of mass was observed with sample No.23 where a greater amount of RuO_2 remained sorbed (49.6 μg/g of sorbent) in comparison with sample no.22 (22.8 μg/g of the sorbent remained). The chemical form of the ruthenium sorbed on the mordenite surface is RuO_2 similarly as for the sorption of RuO_4 vapors on clinoptilolite [2].

Above 600 °C the RuO_2 partially decomposes giving Ru and O_2

$$RuO_2 \longrightarrow Ru\ (solid) + O_2\ (gas) \qquad (6)$$

which is reflected by the mass decrease.

At even higher temperatures (above 1 000°C), the oxidation of the remaining RuO_2 takes place, which is indicated by a mass increase.

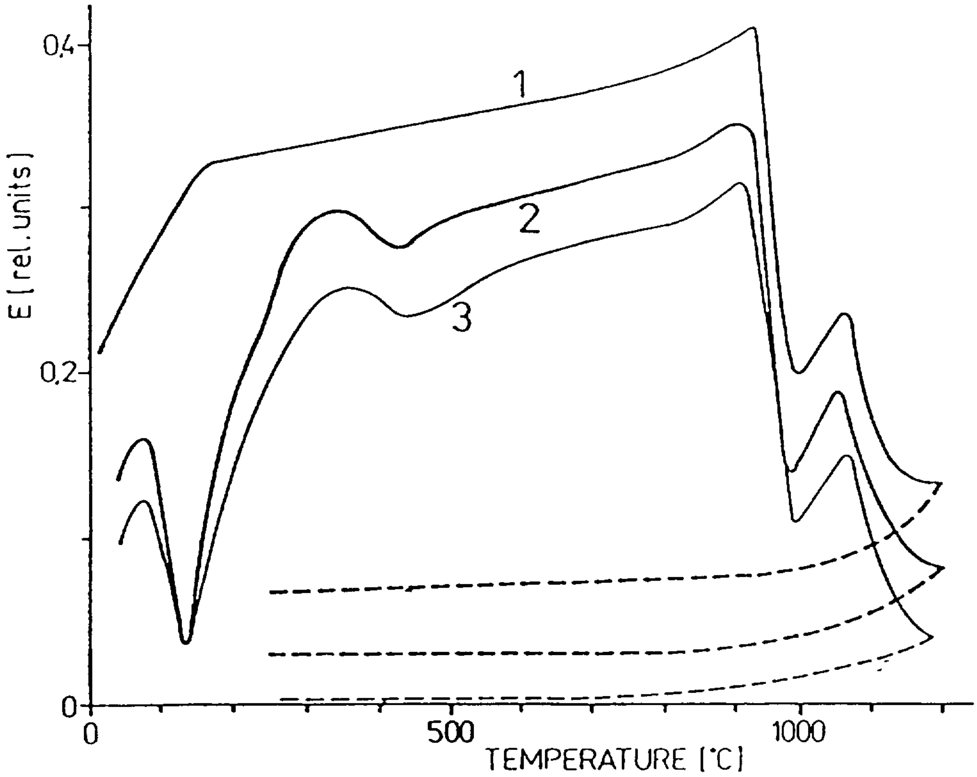

Fig. 7 Results of radiometric emanation method obtained during heating of virgin mordenite (curve 1) and spent mordenite samples containing RuO_2 Nos. 22 and 23 (curves 2 and 3, resp.). (Heating rate: 5 K/min, gas medium: air.)

The REM was used for characterization of the morphology changes of the mordenite sorbents (both virgin and used for RuO_4 vapors sorption) The release of radon was measured continuously under "in-situ" conditions of the sample heating and cooling (heating rate 5 K/min, cooling rate 2 5 K/min were used)

In the temperature interval 20-300°C the thermal behavior of the virgin mordenite and spent mordenite sorbents No 22 and 23 differ (see curve 1 and curves 2 - 3, Fig 6, resp) In this way the influence of the sorbed RuO_2 on the surface of mordenite was characterized

From the differences in the electron microprobe spectra is was concluded that ruthenium was sorbed on the external surface of the whole grain

In the temperature range 900-1000°C a sharp decrease of E was observed with both virgin and spent sorbent This effect reflects the breakdown of the porous system, resulting in the closure of pores and compaction of the initially porous zeolite

It should be mentioned that another effect was observed on the REM curves on heating above 1050°C, which can be ascribed to a structure transition in the haloysite used as binder (30% of haloysite was declared by the supplier) As it follows from the decrease of the REM curve on sample heating above 1050°C, this structure transition can enhance the compaction of the mordenite sorbent In fact, this will be in favor of the encapsulation of the hazardous species present in the spent sorbent

3.4 VITRIFICATION OF THE SPENT MORDENITE CONTAINING RuO_2

At the Nuclear Research Institute, Řež, a low temperature melted glass frit was designed for use as a complementary component with mordenite sorbent to form a glassy product on heating above 1000°C

The chemical composition of the glass frit - mordenite sorbent mixture was as follows (in mass %)

Glass frit component (60 mass %):

SiO_2- 19,2, Al_2O_3- 6 0, ZnO- 4 8, B_2O_3- 7 2, MgO- 3 4,
CaO- 3 4, MnO- 7 4, H_2O- 8 6

Mordenite component (40 mass %).

SiO_2- 27 3, Al_2O_3- 7 7, Na_2O- 0 86, CaO- 0 13, H_2O- 11 0

It was of interest to characterize the thermal behavior of the spent mordenite mixed with the glass frit (in the ratio 2 3) both from the view point of mass loss and the morphology changes during heating up to 1100°C

Thermogravimetry (TG) results of the spent mordenite containing RuO_2 (sample No 22) and its mixture with the glass frit are given in Fig.8, curves 2 and 3, resp For comparison, the TG curve of the glass frit is shown in Fig. 8 as curve 1 It follows from the curves 1 and 2 in Fig 7 that mass loss observed on heating above 800°C is connected with the release of volatile

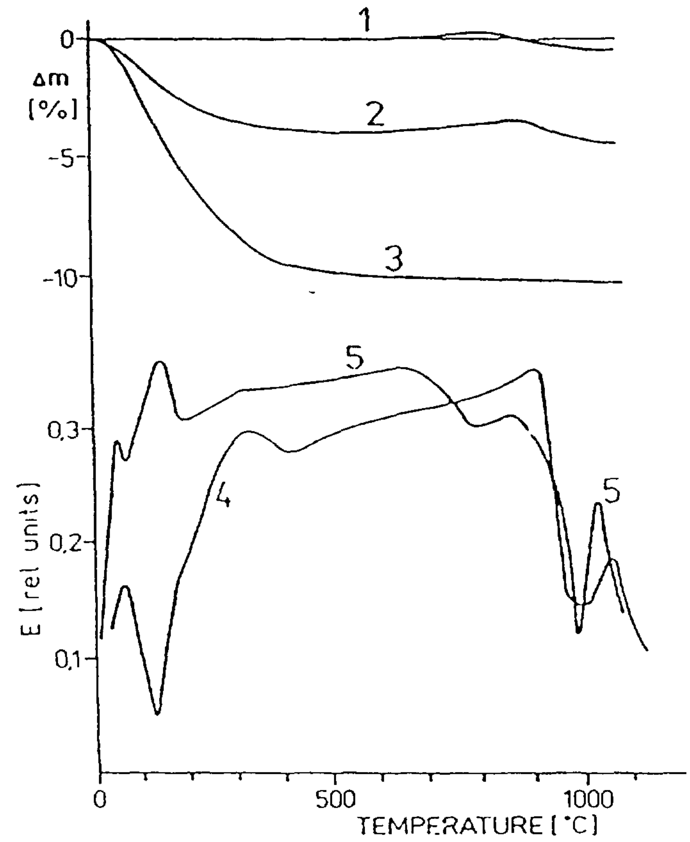

Fig. 8 *Results of thermogravimetry (TG) and REM characterizing thermal behaviour of the spent mordenite sorbent No. 22 containing* RuO_2 *and in the spent mordenite the mixture with glass frit (2:3): Curves 1 - 3 represent TG curves measured during heating of the following samples: glass frit only (curve 1), mixture of the spent mordenite No. 22 glass frit (curve 2), spent mordenite sample No. 22 only (curve 3).*

Curves 4 - 5 represent REM curves measured during heating of following samples: spent mordenite sample No. 22 (curve 4) and the mixture of the spent moraenite No. 22 - glass frit (2:3) (curve 5). (Heating rate 5 K/min, gas medium: air.)

components from the glass frit The REM results (curves 4 and 5 in Fig. 8) characterize early interaction of the glass frit with the surface of spent mordenite sorbent above the glass softening temperature The glass melting enhances the encapsulation of the spent sorbent

It was of interest to compare the thermal behavior of the mixtures glass frit - used mordenite samples No 22 and 23, resp and the mixture of the glass frit - virgin mordenite sorbent The REM was used to characterize the morphology changes taking place in the mixture during heating.

The REM curves of these mixtures are presented in Fig. 9

From the mass loss values measured by thermogravimetry the thermal stability of the mordenite sorbents used for RuO_4 vapors sorption was assessed. Two characteristic temperature intervals 20 - 800 and 800 - 1 200°C are considered in Table IV when reporting the mass loss data

TABLE IV CHARACTERIZATION OF THERMAL STABILITY (MASS LOSS) OF SPENT MORDENITE USED FOR RuO_4 SORPTION

Sorbent	Temperature interval	
	20-800°C	800-1200°C
Spent mordenite No 22	-9 9%	-0 4%
Spent mordenite No 23	-10 0%	-0 5%
Spent mordenite No 22 mixed with glass frit (2 3)	-3 5%	-0 6%
Spent mordenite No 23 mixed with glass frit (2 3)	-4 1%	-0 7%
Glass frit only	0%	-1 0%
Virgin-mordenite	-12 0%	0%
Virgin-mordenite mixed with glass frit (2 3)	-3.9%	-0 6%

The REM curves shown in Figs 8 and 9 enabled us to characterize early interactions of glass frit with mordenite samples and to see the differences in the behavior between the virgin mordenite and used sorbents With the virgin mordenite the first interaction occurs at 600°C, whereas in the temperature interval of 800-1000°C the collapse of the porous system of the mordenite takes place The temperature of the structure transition observed above 1000°C was lowered by the increasing amount of RuO_2 sorbed on the surface

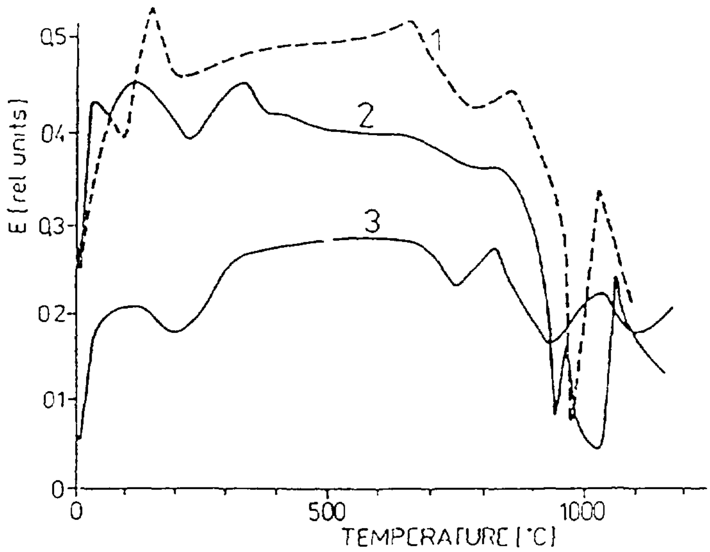

Fig. 9 *Results of REM characterizing thermal behaviour of the following samples:*
Curve 1 - mixture of the spent mordenite No. 22 and glass frit (2:3)
Curve 2 - mixture of the spent mordenite No. 23 and glass frit (2:3)
Curve 3 - mixture of virgin mordenite and glass frit (2:3)
(Heating rate: 5 K/min, gas medium: air.)

We have found that heat treatment up to 1100°C of both the spent mordenite and the spent mordenite with glass frit led to encapsulation of the hazardous species Taking into account that Ru can be released from the surface on heating above 800°C, the use of the glass frit can be recommended The volatilization of Ru is lower at the softening temperature of the glass frit Its interaction with the surface of the spent mordenite reduces the mobility of Ru

4. USE OF MORDENITE FOR REMOVAL OF Cs AND Sr FROM LIQUID NPP WASTES

4 1 SORPTION TESTS

The sorption of cesium both in macroconcentrations and as a carrier-free ^{137}Cs nuclide was determined using synthetic mordenite as a sorbent under dynamic conditions Mordenite was granulated into spherical particles of 0 8 - 1 0 mm diameter Natural haloysite (30%) was used as a binding agent In order to avoid unnecessary handling of the highly active spent sorbent the sorbent was mixed with glass frit before packing the column The spent column packing can be readily vitrified yielding a homogeneous glass containing the sorbent and the capsulated elements

The column packing was simulated by a mixture composed of mordenite and glass frit The granular size of both components was 0 8 - 1 0 mm

Cs was labelled with ^{137}Cs, its radioactivity was measured by a scintillation detector with a NaI(Tl) well crystal and a single-channel analyzer JLK 202

4 2 SORPTION OF WEIGHABLE AMOUNTS OF Cesium

Results of cesium sorption by synthetic mordenite from a solution containing 18 g/L H_3BO_3, 3 3 g/L KOH and 3 mg/L Cs labelled by ^{137}Cs are given in Table V

The column of 5 mL volume was packed with mordenite and glass frit mixture (1 1 wt ratio) The column was fed from the bottom at a flow rate of 100 mL/hr

8 7 mg Cs were entrapped in the column

4 3 SORPTION OF CARRIER-FREE CESIUM

The nuclide ^{137}Cs was sorbed from a solution containing 10 g/L H_3BO_3, 0 3 g/L KOH and 1 4x104 cpm/mL ^{137}Cs The column packing consisted of a mixture of mordenite and the glass frit in 1 1 wt ratio Sorbent bed volume was 10 mL, its height was 10 cm Pumping rate of the feed was 92 mL/hr Results of the sorption are given in Table VI

Sorption efficiency is expressed both by the percentage of Cs removed from the feed and by the decontamination factor DF (calculated from the formula DF = Ao/Ae, where Ao and Ae are the activities of the column feed and the eluate, respectively)

TABLE V. SORPTION OF WEIGHABLE AMOUNTS OF CESIUM BY THE MIXTURE MORDENITE AND GLASS FRIT

Run no.	Volume passed, mL	Cs sorbed %
1	100	100
2	200	100
3	300	99 99
4	400	99 99
5	500	99.99
6	600	99.98
7	700	99 98
8	800	99 95
9	900	99.93
10	1000	99 90
11	1200	99.87
12	1400	99.61
13	1600	99 41
14	1800	99 04
15	2000	98 75
16	2200	98 52
17	2400	97 74
18	2600	97.10
19	2800	96 61
20	2900	95 62

The sorption of cesium and strontium from solutions containing boric acid in acidic neutral, and alkaline media were tested

The sorption of carrier-free ^{137}Cs and ^{85}Sr was measured in static conditions [7] The distribution coefficient K_D was calculated from the formula

$$K_D = A_s \cdot V_a/V_a \cdot m_s \qquad (7)$$

where

A_s is the activity of solid phase $A_s = A_o - A_a$,
A_o is the initial aqueous phase activity,

TABLE VI SORPTION OF CARRIER-FREE ^{137}Cs BY THE MIXTURE OF MORDENITE AND GLASS FRIT

No	Volume passed, mL	decontamination factor DF	Cs sorbed %
1	10	>1000	>99.9
2	333	>1000	>99.9
3	660	>1000	>99.9
4	1000	450	99 7
5	1583	153	99.3
6	3300	121	99 1

A_a is the equilibrium aqueous phase activity,
V_a is the aqueous phase volume (in mL) and
m_s is the weight of sorbent (in g).

The values of K_D found for Cs and Sr sorption on mordenite, in the presence of selected ions are listed in Table VII. From this table the effect of competing ions on the sorption of cesium and strontium on mordenite from the solutions containing 1% H_3BO_3 can be seen.

TABLE VII. VALUES OF K_D FOR Cs AND Sr SORPTION ON MORDENITE

Sorbed element	competing ions in concentration [mol/L]	K_D [mL/g]
Cs	-	$1.0 \cdot 10^5$
Sr	-	$9.2 \cdot 10^4$
Cs	$4 \cdot 10^{-2}$ H+	$1.0 \cdot 10^5$
Sr	$4 \cdot 10^{-2}$ H+	25
Cs	$2 \cdot 10^{-3}$ H+	$1.0 \cdot 10^5$
Sr	$2 \cdot 10^{-3}$ H+	$2.4 \cdot 10^4$
Cs	$2 \cdot 10^{-1}$ Na+	$7.9 \cdot 10^3$
Sr	$2 \cdot 10^{-1}$ Na+	180
Cs	$2 \cdot 10^{-1}$ K+	$3.0 \cdot 10^3$
Sr	$2 \cdot 10^{-1}$ K+	30

5. VITRIFICATION OF SPENT MORDENITE CONTAINING Cesium

Mordenite has been proposed as a sorbent for Cs and can be used, due to its chemical composition, as a glass-forming component. When melted with alkali metal compounds (NaOH, KOH, Na_2CO_3, K_2CO_3 or Li_2CO_3) a glass of required properties can result.

The vitrification of mordenite can be also carried out by melting the mixture of mordenite with a suitable glass frit. This mixture can be used as a sorption column packing, making the handling of high active sorbent considerably easier. Both the vitrification methods mentioned were tested.

In principle, the mordenite could be melted alone, but the temperature required (1300-1600°C) is too high with respect both to the corrosion damage of crucible material and to the volatility of cesium. The glass frit used in the mixture with mordenite melts at 1050°C (the composition of the glass frit was given earlier in the report). For testing the hydrolytic corrosion durability samples were prepared as follows: The mordenite-glass frit mixture (2:3 wt. ratio) was impregnated with the simulated waste solution and melted at 1050°C for 2.5 hours.

The hydrolytic resistance was determined. The electric conductivity of the leachate was 85 μS. Leaching rate of the specimen after 149 days was 8.6×10^{-8} g/cm^2 day.

6. CHARACTERIZATION OF THERMAL BEHAVIOUR OF SPENT MORDENITE CONTAINING Cs

We have investigated the thermal behaviour of the mordenite sorbent used for the sorption of cesium from the water solution containing 1% boric acid (simulating the NPP radioactive waste). The methods of thermogravimetry, differential thermal analysis and radiometric emanation were used.

The model mordenite and glass frit mixture (2 : 3 wt. ratio) was used for the sorption of cesium from the aqueous solution. 276 mg of stable cesium per gram of the sorbent (i.e. 2.08 milligram equivalent of Cs/gram of sorbent) was achieved. The spent sorbent was washed three times and then dried at room temperature.

In Fig. 10 the TG curves of the glass frit (curve 1), the spent mixture of mordenite - glass frit (curve 2), the spent mordenite without frit (curve 3) and virgin, Na-mordenite before cesium sorption (curve 4) are presented.

It can be seen from Fig. 10, that the decrease of the mass of the spent sorbent sample occurs in the temperature interval 50 - 350°C (400°C), whereas for the virgin Na-mordenite sample the decrease of mass continued up to 800°C. The decrease of mass corresponds to the release of water from the sorbent; we can say that the presence of cesium influences the dehydration of the spent sorbent in the above temperature interval.

When the sorbent is heated to higher temperatures, another decrease of mass takes place above 800°C, probably due to the release of volatile components from the glass frit. In Table VIII the TG data for the two temperature regions 20 - 800°C and 800 - 1200°C are listed.

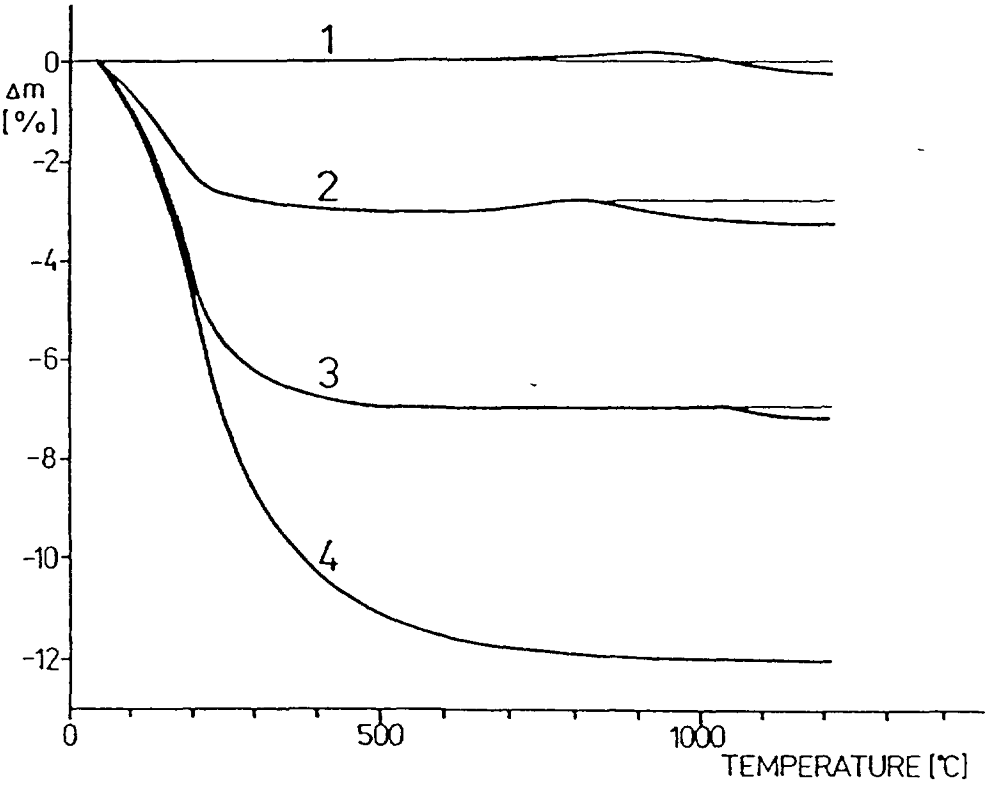

Fig. 10 *Temperature dependence of the mass loss measured during heat treatment of mordenite sorbent, glass frit and their mixture used for the vitrification of the spent sorbent containing caesium.*
Curve 1 - glass frit
Curve 2 - mixture of mordenite and glass frite (2:3 wt. ratio) after treatment with caesium solution
Curve 3 - mordenite sorbent without glass frit after treatment with caesium solution
Curve 4 - virgin mordenite sorbent in the Na-form

TABLE VIII. CHARACTERIZATION OF THERMAL STABILITY (MASS LOSS) OF COMPONENTS OF MORDENITE SORBENT AND THEIR MIXTURE WITH GLASS FRITE USED FOR THE SORPTION OF Cs

Sorbent	Temperature interval		see in Fig. 10
	20-800°C	800-1200°C	
Mordenite with glass frit (2:3) containing Cs	-3.1%	-0.8%	curve 2
Mordenite without glass frit containing Cs	-6.6%	-0.3%	curve 3
Na-mordenite virgin sample	-12.0%	0.9%	curve 4
Glass frit only	0.0%	-1.0%	curve 1

The glass frit used contained lithium and zinc i.e. rather volatile elements. It was of interest to characterize the thermal stability of the glass frit component separately. For this reason we have used the thermogravimetry, DTA and radiometric emanation method and mass spectrometry.

The results of TG, DTA and REM for the glass frit are given in Fig. 11. It can be seen from the TG results (curve 2) that the glass transition temperature, Tg, is in the region of 585 - 590°C. From the REM curve we can say that the annealing of the surface of the glass frit powder takes place from 350 - 600°C. The Tg is indicated by the increase of E at 590°C. The softening point is indicated at 770°C by the decrease of E, the melting is reflected by the increase of E after reaching 950°C. In this temperature interval the decrease of the sample mass was observed on the curve 1, Fig. 11.

Mass spectrometry curves characterized the volatiles released from the glass frit during heating in air in the temperature interval 20 - 1 400°C. A release of the fragment of the mass M/Z = 64 was observed in the temperature interval 870 - 1015°C, which can be ascribed to the release of zinc. No effect corresponding to the lithium containing fragment was observed, which reflects the high thermal stability of lithium silicate compounds formed in the glass frit.

The information about the glass frit thermal behaviour was used in the characterization of the interactions between the mordenite sorbent and the glass frit mixture on heating. In

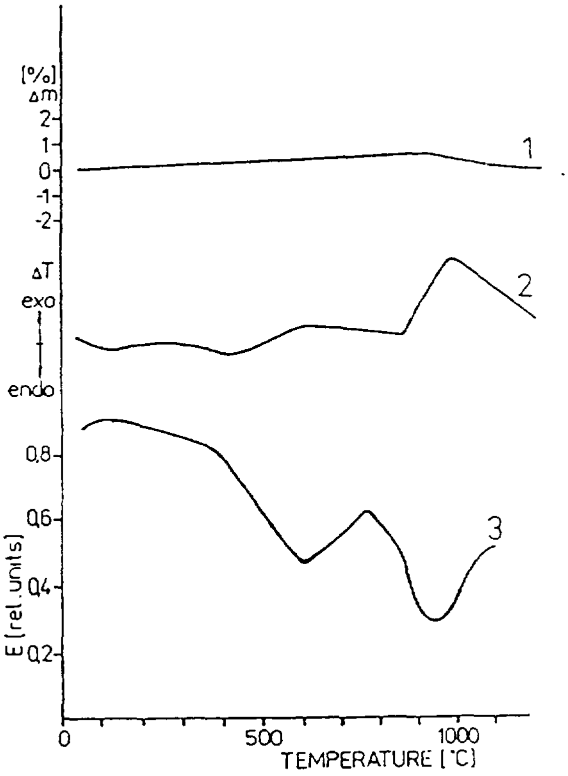

Fig. 11 *Characterization of thermal behaviour of the glass frit designed for the vitrification of spent mordenite.*
Curve 1 - thermogravimetry (mass loss) curve
Curve 2 - DTA curve
Curve 3 - REM curve
(Heating in air at the rate of 5 K/min was used.)

order to understand the processes taking place during heating of the spent mordenite sorbent and its mixture with the glass frit we have used thermogravimetry, DTA and REM. Each of the methods made it possible to obtain independent characteristics about the thermal behaviour of the sorbents.

The TG, DTA and REM curves of the mixture of spent mordenite sorbent with and without glass frit are given in Figs. 12 and 13. It follows from Figs. 12 and 13 that in the temperature interval 20 - 300 °C the release of water from the mordenite takes place, as indicated by the TG curve 1. The water released is accompanied by changes in the sorption properties of the mordenite, as indicated by the release of radon in this interval of temperature. The early interactions of the glass frit with the surface of mordenite takes place from 600°C. The decrease of the mass of the sample observed on the TG curves at temperatures above 800°C corresponds to the release of volatiles from the glass frit.

The effects observed on the REM above 800°C reflect a series of steps of interactions between the mordenite and glass frit.

In both cases the interactions should lead to the enhanced encapsulation of the sorbed species.

7. CHARACTERIZATION OF OTHER INORGANIC SORBENTS USING RADIOMETRIC EMANATION METHOD

It was demonstrated in a number of papers and a monograph [8] that the application of radiometric emanation thermal analysis makes it possible to characterize changes in surface area, morphology, micro- and nanoporosity resulting from processes which take place during structure transitions, phase transformations, sintering and chemical interactions of the solid materials.

The REM has been advantageously applied to assist in the design of new sorbents, especially in the determination of the temperature intervals where the morphology changes take place, determining sorption properties of materials.

The REM enabled us to determine the kinetics of the annealing of surface irregularities, sintering of finely dispersed solids, opening or closure of pores in the porous solids, etc. In this way the results of the REM can serve for optimization of the preparation conditions of sorbents with tailored properties.

The encapsulation of sorbed radionuclides can require the thermal treatment of the spent sorbents (ceramization or vitrification process). The REM has been used in the characterization of these processes. Moreover, the determination of radon diffusion parameters of the heat-treated sorbents before and after radionuclide encapsulation can be used in the evaluation of their transport properties.

A number of materials have been characterized by means of REM in the frame of the IAEA CRP. Some of the materials were prepared at the Nuclear Research Institute Řež plc or in collaboration with other laboratories in the Czech and Slovak Republics.

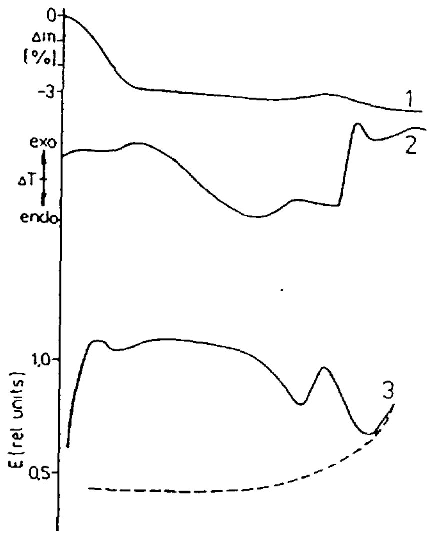

Fig. 12 *Characterization of thermal behaviour of the mixture of mordenite and glass frit (2 : 3 wt. ratio) after treatment with caesium solution.*
Curve 1 - thermogravimetry (mass loss) curve
Curve 2 - DTA curve
Curve 3 - REM curves (the full line corresponds to the heating run, the dotted line corresponds to the cooling run)
(Heating in air, heating/cooling rate of 5 K/min was used.)

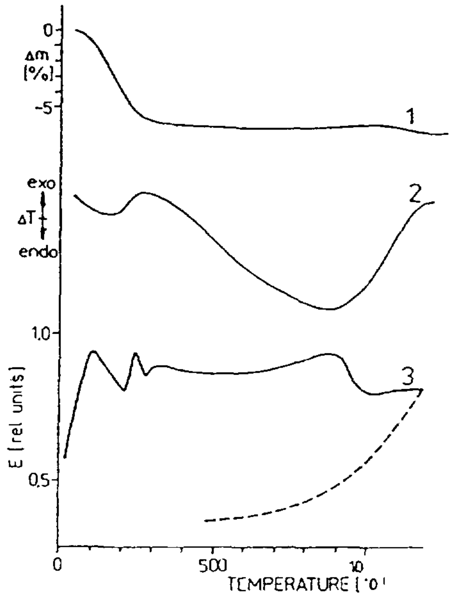

Fig. 13 *Characterization of thermal behaviour of the mordenite sorbent (without the glass frit) such after treatment with caesium solution.*
Curve 1 - thermogravimetry (mass loss) curve
Curve 2 - DTA curve
Curve 3 - REM curves (the full line corresponds to the heating run, the dotted line corresponds to the cooling run)
(Heating in air, heating/cooling rate of 5 K/min was used.)

7.1. COMPARISON OF SORPTION AND MORPHOLOGICAL CHARACTERISTICS OF NATURAL AND CHEMICALLY TREATED CLINOPTILOLITE

Lukáč and Földesová [9] pointed out that the treatment of natural clinoptilolite with NaOH solution affects its ion exchange ability for cesium and cobalt ions. Both Cs$^+$ and Co^{2+} are dominant constituents of nuclear waste. Natural clinoptilolite is a very poor sorbent for cobalt. The possibility of increasing the exchange ability for cobalt by chemically treating clinoptilolite for cobalt was experimentally demonstrated by the authors [9].

The clinoptilolite samples were treated with NaOH solutions of varying concentration (from 0.3M to 5M). The temperature of treatment was 80°C, the treatment time was 4 hours. After decantation the samples were dried at 105°C.

The values of the sorption coefficients determined for Cs$^+$ and Co^{3+} for natural and chemically treated clinoptilolite samples are demonstrated in Fig. 14. It follows from Fig. 14 that the highest exchange ability for Co^{3+} corresponds to the chemically modified clinoptilolite treated by 5M NaOH. The formation of a new zeolite (sodalite) was indicated by X-ray diffraction patterns.

The characteristics of surface area and open porosity demonstrate that the morphology of the samples has changed considerably. It was of interest to characterize, by means of REM, the thermal behaviour of the chemically modified clinoptilolite samples and to mutually compare the respective REM curves. In Fig. 14 the REM curves of natural clinoptilolite and those chemically treated by 1.0 NaOH and 4.0 NaOH are compared.

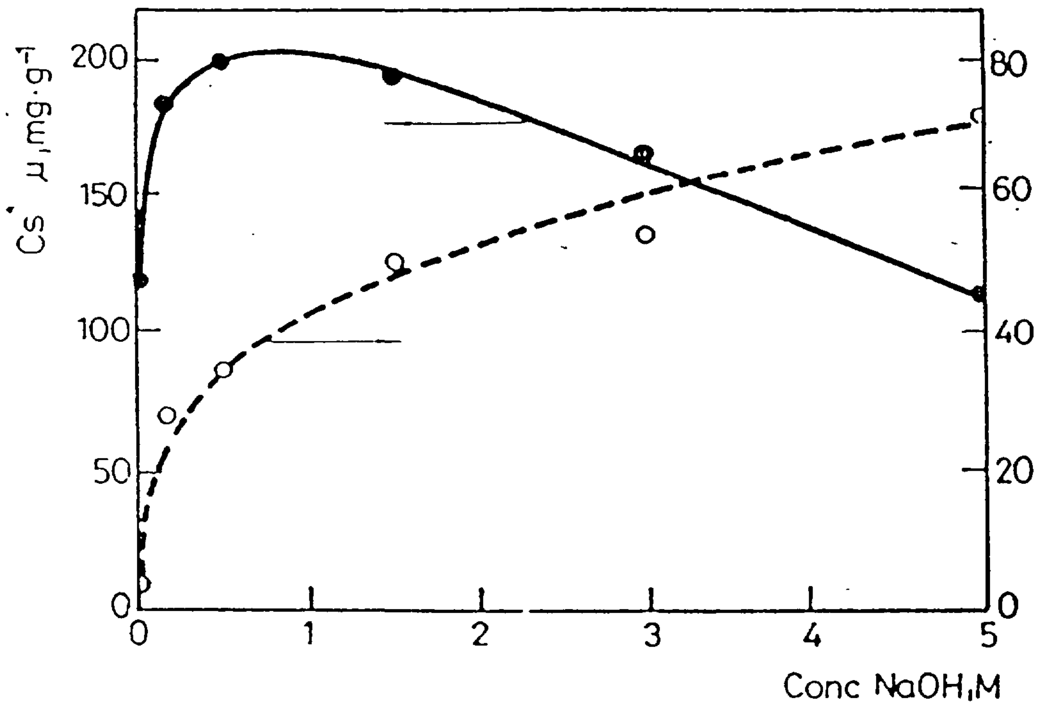

Fig. 14 *Dependence of the sorption coefficients for caesium and cobalt on the concentration of NaOH solution used for the chemical treatment of natural clinoptilolite (locality Nižný Hrabovec, Slovak Republic).*

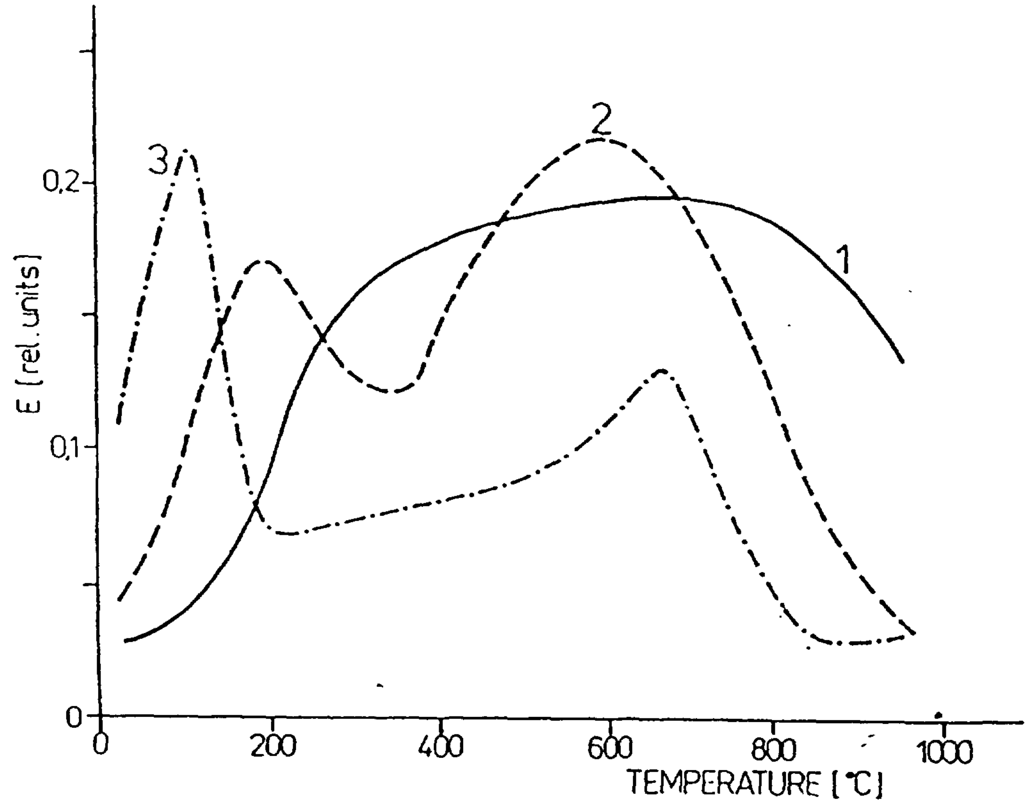

Fig. 15 *REM curves used for the characterization of natural clinoptilolite (curve 1), clinoptilolite treated in 1M NaOH solution (curve 2) and clinoptilolite treated in 4M NaOH solution*
(Heating in air at the rate of 5 K/min was used).

The REM curves reflect deep changes in the character of the morphology of the samples on the heating in air. These changes correspond to changes in the chemical composition [9] of the altered minerals given in Table IX.

TABLE IX. COMPOSITION OF NATURAL AND TREATED CLINOPTILOLITE [IN WT.%]

Component	Natural Clin.	Clin. Treated by 1M NaOH	Clin. Treated by 4M NaOH
SiO_2+I.R*	68.25	62.83	43.75
Al_2O_3	11.66	12.47	14.44
CaO	3.62	3.92	5.05
Fe_2O_3	1.17	1.30	1.76
MgO	1.30	1.77	1.91
L.O.I.**	11.45	12.32	23.51

* - I.R. insoluble residue
**-L.O.I. - loss on ignition

The comparison of the results of different method enabled us to more fully understand the formation of the sorbents with tailored properties. This procedure can be used in the design of other sorbents for radionuclides by chemical treatment of minerals, glasses, fly ashes etc.

According to the interest of the CRP participants expressed during the IAEA CRP Meetings, the thermal behaviour of materials of selected inorganic sorbents was characterized by means of REM at the Nuclear Research Institute Řež. Materials were sent to the NRI Řež by the participants of the CRP.

The materials characterized by the REM supplied by the participants of the IAEA Coordinated Research Programme are listed in Table X.

In this part of the final report the characterization of natural and chemically treated clinoptilolite (Nižný Hrabovec, Slovak Republic) is presented.

Characteristics of other materials for sorbents, supplied by other participants of the IAEA CRP, will be published later in the form of joint reports or publications in international journals.

The conditions used for the thermal treatment of the samples were chosen in accordance with the technological conditions to be used in the treatment of sorbents.

ACKNOWLEDGMENT

The authors wish to express their gratitude to the participants of the IAEA CRP for the fruitful co-operation.

TABLE X.

Materials of the sorbent	**Supplying institute**
Natural and modified clinoptilolite	Slovak Technical University
CZK sorbent Fe based cyanide	Instititute of physical chemistry Moscow (Russia)
Natural zeolite Cuba	National Technical Center, Atomic Energy Agency Havana
Sorbent P-301 China	China Atomic Energy Inst. Beijing
$K_2Ti_6O_{13}$ sorbent	Yonsei University, Seoul, Rep. of Korea
Zeolite Indonesia	National Atomic Energy Agency, Indonesia
Bentonite Indonesia	as above
MnO_2 sorbent	Inst. of Nuclear Chemical and Technical Warszawa, Poland
ZrO_2 hydroxide	BNFL Sellafield U.K.
Al-pillared montmorillonite	BNFL Sellafield U.K.

REFERENCES

[1] KEPÁK, F. et al.: J. Radioanal. Nucl. Chem. 159 (1992) 317.

[2] DONATO, A., BOCOLA, W. Energia Nucl. 18 (1981) 353.

[3] NIKUTIN, I.E. et al., At. energia 45 (1978) 116.

[4] KLEIN, K. et al., Seminar on the testing and operation of off-gas cleaning Systems at Nuclear Facilities, Karlsruhe 1982, p. 639.

[5] Control of semivolatile radionuclides in gaseous effluents at nuclear facilities, Tech. Rep. ser. No. 110, IAEA Vienna 1982.

[6] RIMSHA, S.J.W, CASE, F.N. Proc. 16th DOE Nuclear Air Cleaning Conference, Vol. 2, M.W. First, (Ed.), San Diego 1982, p. 838.

[7] FRANTA, P. et al., Sorption properties of synthetic zeolites from the point of view of their utilization in purification plants in NPP with WWER reactor type (in Czech), Report ÚJV 8114 CH, Nuclear Research Institute Řež.

[8] BALEK, V., TÖLGYESSY, J. Emanation Thermal Analysis and other radiometric emanation methods, in: Comprehensive Analytical Chemistry, Part XII C, Elsevier Science Publishers 1984, 304 pp.

[9] LUKÁČ, P., FÖLDESOVÁ, M. J. Radioanal. Nucl. Chem. Letters 188 (1994) 42.

XA9744278

DEVELOPMENT OF COMPOSITE ION EXCHANGERS AND THEIR USE IN TREATMENT OF LIQUID RADIOACTIVE WASTES

F. ŠEBESTA, J. JOHN, A. MOTL
Czech Technical University,
Prague, Czech Republic

Abstract

Composite inorganic-organic absorbers represent a group of inorganic ion exchangers modified by using binding organic material for preparation of larger size particles having higher granular strength. Such modification of originally powdered or microcrystalline inorganic ion exchangers makes their application in packed beds possible.Modified polyacrylonitrile (PAN) has been used as a universal binding polymer for a number of inorganic ion exchangers. The kinetics of ion exchange and sorption capacity of such composite absorbers is not influenced by the binding polymer mentioned above. The contents of active component in composite absorber can be varied over a very broad range (5-95% of the dry weight of the composite absorber). These composite absorbers have been tested for separation and concentration of various contaminants from aqueous solutions. Their high selectivity and sorption efficiency are advantageous for treatment of various radioactive and/or industrial waste waters, removal of natural and/or artificial radionuclides and heavy or toxic metals from underground water, determination of radionuclides (^{137}Cs, ^{60}Co, U, Ra) in the environment, etc. Examples of some of these applications are presented in this report.

1. INTRODUCTION

The use of inorganic ion exchangers is being considered for many special problems encountered e.g. in treatment of liquid radioactive waste or for decontamination of various types of contaminated water. These exchangers exhibit a number of advantageous properties when compared with synthetic organic ion-exchangers; high selectivity for the capture of certain ions, higher thermal and radiation stability, often good chemical stability even in strongly acid media and good compatibility with matrices used for their immobilization. The major disadvantage of synthetic inorganic ion exchangers is the difficulty in preparing granulated material with sufficient strength for applications. A number of different methods of preparation of granules of inorganic ion exchangers as well as of methods for improvement of granular strength of these materials has been proposed. A detailed review of these methods was published recently [1].

Our studies have been concentrated on the preparation and characterization of "composite ion exchangers". This type of ion exchanger describes the group of inorganic ion exchangers modified by using some binding material for the preparation of larger size particles with higher granular strength. Both inorganic and organic materials may be used as binding materials. Composite absorbers with inorganic binding matrices are based on the following binders, namely: clay minerals, cement, silica-gel and alumina. Procedures for preparation of cement or clays-based exchangers involve preparation of a binder-exchanger paste of suitable consistency, curing and/or drying, followed by grinding and sieving. Various methods of silica-gel application have been designed. Among them a modified sol-gel procedure using a mixture of urea, silicic acid, hexamethylenetetramine, and exchanger as the initial sol is worth mentioning as a high content of exchanger (up to 70 wt.% in some cases) can be obtained. Mixtures of alumina with an exchanger are usually pelletised and calcined. Preparation of composite absorbers with organic binding matrices involves dispersing an exchanger in a solution of a matrix/matrix-monomer/matrix-component, followed by coagulation/polymerisation/polycondensation of the dispersion and separation of a product. By use of appropriate techniques the form of the product can be varied (grains, fibres, etc.). A large number of organic matrices have been examined, some can only be used with certain inorganic ion-exchangers. The presence of a binder can slow down the ion-exchange kinetics and decrease the sorption capacity of the inorganic ion-exchanger by hindering the access of the solution to the surface of the exchanger.

Modified polyacrylonitrile was proposed as an universal binding polymer for practically any inorganic ion exchanger (active component) [2,3]. The method developed enables preparation of granular absorbers even from such inorganic ion exchangers which are impossible or very difficult to synthesize in granular form. The principle scheme for the preparation of composite ion exchangers containing modified polyacrylonitrile (PAN) was presented by Šebesta et al. [4]. There exists several modifications of the preparation procedure. Usually, finely divided inorganic ion-exchanger is mixed with a solution of binding polymer. The composite absorber is produced by coagulating the dispersed mixture in a water bath. In some cases reagents (or their solutions) for the preparation of inorganic ion exchanger can be mixed directly with the solution of the binding polymer instead of using the ready made dried and powdered exchanger. The active component of the composite ion exchanger is then set during (or after) the coagulation of the binding polymer. Another possibility is to mix one of the components of the inorganic ion exchanger with the solution of binding polymer while the other is dissolved in the coagulation bath. These methods enable incorporation of very fine to colloidal particles of active component in the binding polymer which increases the capacity and improves the kinetics of ion exchange of the resulting absorber. The final product can be produced in different forms as desired.

2. COMPOSITE ABSORBERS WITH POLYACRYLONITRILE (PAN) BINDING MATRIX

The use of PAN-based organic binding polymer has a number of advantages given by the relatively easy modification of its physico-chemical properties (hydrophilicity, porosity, mechanical strength). These properties can be modified by the degree of cross-linking of the polymer, the use of suitable co-polymers or by changing the composition and temperature of the coagulation bath. Another advantage is the possibility of preparing the composite ion exchangers directly in the aqueous solution thus eliminating the necessity to wash out the organic water immiscible solvents and oils used in some other processes.

The kinetics of ion exchange on such composite ion exchangers are not influenced by the binding polymer. The contents of active component in the composite exchanger can be varied over a very broad range (5-90 % of the dry weight of the composite ion exchanger) depending on requirements.

A list of composite ion exchangers that have been produced in our laboratory is shown in Table I. These composite absorbers have been developed and most of them tested for removal of radionuclides from liquid radioactive waste produced in the operation and decommissioning of nuclear power plants and for selective separation and concentrating of radionuclides from environmental samples. Their properties depend mainly on the properties of the active component used. Some of the absorbers can be regenerated (e.g. AMP-PAN, TiO-PAN, NaTiO-PAN) some cannot (e.g. ferrocyanides - NiFC-PAN, CoFC-PAN). The possibility of regeneration of composite absorbers is determined solely by the nature and properties of their active components. The procedure enables preparation of absorbers containing mixtures of

TABLE I. PAN-BASED COMPOSITE ABSORBERS

CODE	INORGANIC ION-EXCHANGER
AMP-PAN	Ammonium molybdophosphate
NiFC-PAN	Nickel hexacyanoferrate
KNiFC-PAN	Potassium-nickel hexacyanoferrate
CoFC-PAN	Cobalt hexacyanoferrate
KCoFC-PAN	Potassium-cobalt hexacyanoferrate
ZrP-PAN	Zirconium phosphate
TiP-PAN	Titanium phosphate
MnO-PAN	Manganese dioxide
TiO-PAN	Titanium oxide
ZrO-PAN	Zirconium oxide
MgO-PAN	Magnesium oxide
NM-PAN	Manganese dioxide and nickel hexacyanoferrate
ZrOP-PAN	Zirconium oxide and zirconium phosphate
NaTiO-PAN	Sodium titanate
CSbA-PAN	Crystalline antimonic acid
SnSbA-PAN	Tin(IV) antimonate
TiSbA-PAN	Titanium(IV) antimonate
Ba[Ca]SO_4-PAN	Barium sulphate activated by calcium
CuS-PAN	Copper sulphide
Na-Y-PAN	Synthetic zeolite Na-Y
M315-PAN	Synthetic mordenite M315
CLIN-PAN	Natural clinoptilolite
HPM-PAN CAPM-PAN	Sr- and Ra-selective ternary ion-exchangers the most

various active components in desired ratios. Properties of such a composite absorber can thus be exactly "tailored" to a particular waste stream.

The binding polymer is stable in aqueous solutions of most common electrolytes, apart from concentrated solutions of $ZnCl_2$, LiBr, $CaCl_2$ and NaCNS which are known to dissolve polyacrylonitrile. The polymer also dissolves in acids with concentration higher than 8M HNO_3, 5M H_3PO_4, 5M H_2SO_4. It hydrolyses to gel when in contact with concentrated acids or alkalis for prolonged periods, in alkalis the hydrolysis is faster than in acids. High salinity influences neither the stability nor sorption properties of composite absorbers. The results of a study of chemical and radiation stability of the PAN binder and PAN-based composite absorbers under extreme conditions, that can be expected in treatment of liquid radioactive wastes, are discussed below [5,6].

2.1. CHEMICAL STABILITY

The chemical stability of PAN in the form of beads (B-PAN) similar to the beads of composite absorbers and AMP-PAN composite absorber was studied for contact times up to one month [5,6]. 1M HNO_3 + 1M $NaNO_3$, 1M NaOH + 1M $NaNO_3$, and 1M NaOH were chosen as simulants of USDOE acidic and alkaline wastes.

The methods selected for following the chemical stability included total beads volume measurement and swelling determination complemented by microscopic examination and sieving analysis of the beads. For AMP-PAN, changes in sorption capacity, distribution coefficient (K_d) values, and kinetics of sorption of ^{137}Cs were determined.

The results of testing the chemical stability of PAN beads and AMP-PAN composite absorber are summarized in Table II. These results demonstrate excellent stability of both B-PAN and AMP-PAN in the acidic simulant solution. No changes of either swelling or total beads volume were observed during one month of contact of the beads with the solution. Microscopic examination revealed no cracking or any other mechanical damage for either materials. This finding not only validates the stability of PAN in this conditions, but also proves the absence of any possible negative influence (decomposition catalysis) of the ammonium molybdophosphate active component on the polyacrylonitrile binder.

The results of sorption properties testing corroborated the finding that neither the properties of PAN binder, nor those of the AMP active component are deteriorating in contact with acid simulant solution. No changes in K_d-values, sorption capacity (or their swelling-corrected values), or kinetics of uptake of ^{137}Cs by the AMP-PAN composite absorber could be observed within the testing period. The results obtained also demonstrate one of the main advantages of PAN-based absorbers - rapid kinetics of uptake of ions; the equilibrium sorption value is reached within less than 10 minutes.

In alkaline solutions the stability of PAN beads was found to be limited. An adverse influence of the presence of $NaNO_3$ in NaOH on PAN stability was found. The measured changes of swelling are much more dramatic than the changes of the total beads volume. Microscopic examination showed that the beads suffer mechanical damage during the reconditioning cycle when transferred back to distilled water for swelling determination. The total beads volume is therefore a better quantity for judging the stability of the beads.

TABLE II. CHEMICAL STABILITY OF PAN BEADS (B-PAN) AND AMP-PAN COMPOSITE ABSORBER IN VARIOUS MEDIA [6]

Time of contact [days]	B-PAN		B-PAN		B-PAN		AMP-PAN					
	1M HNO + 1M $NaNO_3$		1M NaOH		1M NaOH + 1M $NaNO_3$		1M HNO_3+1M $NaNO_3$					
	S[%]	V_Y	S[%]	V_Y	S[%]	V_Y	S[%]	V_Y	K_D [mL.g^{-1}]	q [mmole g^{-1}]	K'_D	q' [mmole g^{-1}]
0	89.6	1.00	89.7	1.00	89.5	1.00	59.0	1.00	14100	0.16	34400	0.39
1	88.7	1.00	89.8	0.97	90.0	0.97	58.6	1.02	14500	0.17	34900	0.41
3	88.7	0.99	89.1	0.96	88.5	0.96	56.5	1.02	14100	0.16	32500	0.38
7	89.0	0.99	89.2	1.01	91.0	1.04	57.4	1.00	14300	0.17	33500	0.41
14	88.6	1.00	95.8	1.47	~99	2.31	57.9	0.98	15000	0.17	35600	0.41
30	89.6	0.98	NM^a	2,36^a	NM^a	NM*	56.6	0.98	15800	0.18	36400	0.41

S - *swelling (contents of water) [%]*
K_D, K'_D - *distribution coefficients of ^{137}Cs [mL per gram of swollen or dry absorber, respectively*
q, q' - *practical sorption capacity for caesium [mmole per gram of swollen or dry absorber, respectively]*
Vr - *relative volume of the absorber (relatively to its initial volume), precision Ñ 0.02*
NM - *non-measurable because of decomposition of PAN*
a - *22 days of contact only*

Under the test conditions, PAN was reasonably stable for a period of at least 7 to 10 days. Better stability may be expected in dynamic conditions where the degradation products of PAN will be continuously washed out. Such degradation hydrolysis products may further catalyze and accelerate the hydrolysis of PAN [6].

Because of the high sorption rate achievable with PAN-based composite absorbers, packed beds of these absorbers are usually operated at flow rates of 50 - 100 BV.hr^{-1}. At such flow rates some 10,000 to 20,000 BV of waste could be treated within the 7-10 days of sufficient stability of the absorber. The sorption capacity of most active components (inorganic ion-exchangers) would be exhausted much earlier. Thus the stability of PAN binder in alkaline simulant solutions, even though limited, is sufficient for most applications.

The study of the chemical stability of B-PAN showed that in 0.1M NaOH + 1M $NaNO_3$, B-PAN is stable for 1 month. The chemical stability of B-PAN beads is thus strongly influenced by sodium hydroxide concentration in the concentration range 0.1M - 1M NaOH. It can be concluded that the dependence of PAN stability on the concentration of NaOH displays probably a threshold, above which the acceleration of PAN hydrolysis increases.

2.2. RADIATION STABILITY

The radiation stability of PAN in the form of beads (B-PAN) similar to the beads of composite absorbers and of AMP-PAN composite absorber was studied [5,6] using the same simulant solutions as those used for the study of chemical stability. In addition, radiation stability was determined in distilled water. A radiation dose range of 10^3 to 10^6 Gy was examined. The methods selected for following the radiation stability were the same as used for the study of chemical stability.

The results of the tests are summarized in Table III. No effect of radiation on the stability of PAN was observed up to the total absorbed dose of 10^6Gy for B-PAN irradiated in distilled water.

The radiation stability of AMP-PAN in acidic simulant solution was found to be as good as that of B-PAN in distilled water. Sorption properties of AMP-PAN (K_D-value and/or sorption capacity for ^{137}Cs) were not influenced by radiation.

During determination of kinetics of uptake of ^{137}Cs by the irradiated absorber, a reduced mechanical strength of the beads was found. This effect may be ascribed to an increase in cross-linking during irradiation hardening producing embrittlement of the polymer.

In alkaline simulant solutions two effects combine. In addition to the influence of radiation, the chemical stability in alkaline media has to be considered. When comparing the results presented in Table III (irradiated samples) with the results in Table II (unirradiated samples, 22 days of contact), clear positive influence of these combined effects on the stability of the binding polymer can be observed. While the unirradiated samples decomposed after 22 days either during recycling into distilled water (for 1M NaOH solution) or directly in the solution (in the presence of $NaNO_3$), the irradiated samples remained compact and exhibited finite swelling. This effect is another (positive) consequence of the cross-linking of the polymer discussed previously.

TABLE III. RADIATION STABILITY OF PAN BEADS (B-PAN) AND AMP-PAN COMPOSITE ABSORBERS IN VARIOUS MEDIA [6]

Time of contact [days]	B-PAN		B-PAN		B-PAN		AMP-PAN					
	H_2O		1M NaOH		1M NaOH + 1M $NaNO_3$		1M HNO_3+1M $NaNO_3$					
	S[%]	V_γ	S[%]	V_γ	S[%]	V_γ	S[%]	V_γ	K_D [mL.g^{-1}]	q [mmole g^{-1}]	K'_D	q^1 [mmole g^{-1}]
0	89.8	1.00	89.9	1.00	89.7	1.00	59.0	1.00	14100	0.16	34400	0.39
10^3	89.6	1.00	89.5	0.98	89.8	0.97	59.2	1.05	13800	0.17	33800	0.41
10^4	89.4	1.01	89.4	0.96	89.3	0.97	58.9	1.03	14400	0.17	35000	0.41
10^5	89.0	1.00	89.3	0.96	88.5	0.97	57.4	1.01	14200	0.18	33400	0.41
10^6	88.5	1.00	95.3	2.28	97.8	3.54	56.5	0.99	14000	0.18	32300	0.41

For the explanation of the symbols, see Tab. 2.

3. TECHNOLOGICAL APPLICATIONS

The possibility of preparing composite absorbers with varying selectivity enables development of flow sheets for waste treatment tailored to the specific application. One such flow sheet is shown in Fig. 1. This flow sheet shows a possible treatment of Intermediate/High Level Liquid Waste (ILW/HLW) with selective separation of ^{137}Cs, ^{90}Sr and transuranium elements (TRU). Separated concentrated radionuclides may then be treated for final disposal and the effluent (LLW) may be treated e.g. by cementation. Such approach can result in a large cost saving because of dramatic reduction of the volume of waste.

For other applications, where non-selective removal of all radionuclides is required, special composite absorbers may be prepared. They contain a mixture of active components each selective to one or more radionuclides present in the waste.

Many potential technological applications of composite absorbers have been tested in the recent years, some of them have been reported [7,8]. A few examples of these applications are given in the following paragraphs.

3.1. TREATMENT OF LIQUID RADIOACTIVE WASTES AT A-1 NPP, JASLOVSKÉ BOHUNICE

3.1.1. Long Term Fuel Storage Pond Water

Water in the Long Term Fuel Storage Pond (LTFSP) at the currently decommissioned NPP A-1 at Jaslovské Bohunice (Slovak Republic) is contaminated by the leaks of "chrompik" (K_2CrO_4 solution) from the fuel cans. The main radioactive contaminants of this water are radiocaesium isotopes - some 200 GBq/m^3 of ^{137}Cs and some 50 MBq/m^3 of ^{134}Cs. There are still a few cassettes with damaged spent fuel in the pond and therefore the water cannot be removed from the pond.

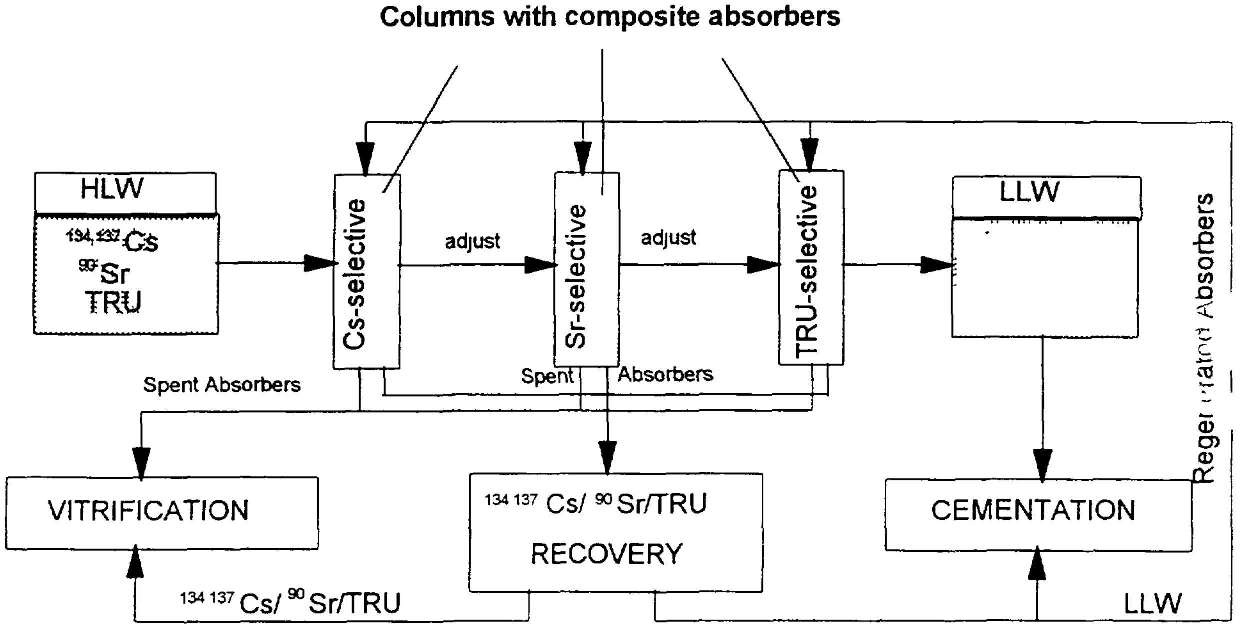

FIG. 1. Possible flow-sheet of ILW/HLW treatment with composite absorbers [7]

Extensive research activities have been carried out by our group in present years using real waste. The use of fluidized bed of NiFC-PAN composite absorber in a small compact column at a flow rate of 500 BV.hr^{-1} has been proposed for decreasing the pond water activity [4, 9]. The treated water is returned to the pond. Pilot plant experiments [9] revealed that as much as 50.000 BV of pond water can be treated by NiFC-PAN composite ion exchanger with a decontamination factor Df > 5. The break-through curve measured in this experiment is shown in Fig. 2.

A mathematical model of circulation treatment of LTFSP water predicts that 8.6 times the total volume of the pond water has to be treated to decrease the ^{137}Cs activity by three orders of magnitude under the above given conditions. 90 litres of NiFC-PAN composite ion exchanger and 3 155 hours of operational time would be needed for the treatment of pond water using a single column with a bed volume equal to 3 litres.

AEA Technology (U.K.) will be responsible for the treatment. The technology proposed by AEA Technology is to use NiFC-PAN absorber, too; 100 L of this absorber was produced at our laboratory and supplied to AEA Technology during 1995.

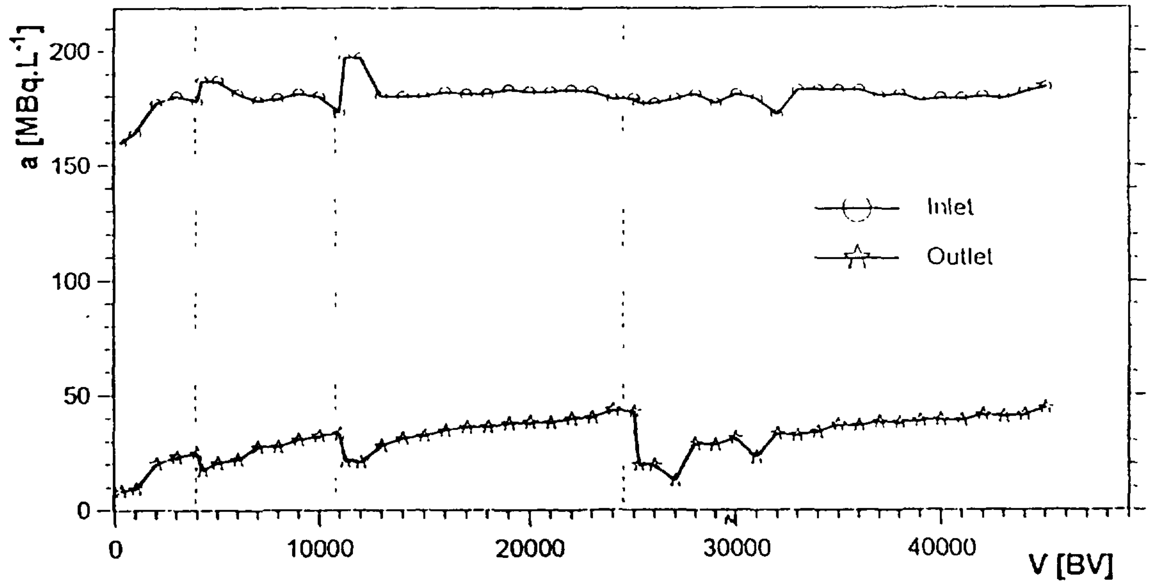

FIG. 2 Dependence of ^{137}Cs specific activity a at the inlet and outlet of the column on the volume V of treated LTFSP water [4]. (-------------- night or weekend interruptions of the experiment)

3.1.2. Biological Shield (BS) Water

Biological shield water represents a low level liquid radioactive waste (V = 350 m^3). The pH of the water is ~8.5, its hardness is relatively low (~1.4 mmole/L). Except for tritium, the water is contaminated mainly by radiocesium. Its concentration varies with the sampling place but does not exceed 20 kBq/m^3 of ^{137}Cs and ~ 150 kBq/m^3 of ^{134}Cs). Other radionuclides (^{60}Co or ^{90}Sr) may be present, their total activity being < 100 kBq/m^3. For the final disposal of the water by regulated discharge into the environment from the NPP site, it would be necessary to decrease the total activity of all the radionuclides (except for tritium) to below 37 kBq/m^3.

To reach this goal, the required minimum value of ^{137}Cs decontamination factor is Df ~ 600. "In situ" dialysis revealed that non-ionic forms of cesium are practically not present [10].

A bench-scale experiment was performed [4] using the same composite NiFC-PAN ion exchanger as described for treatment of LTFSP water. 10000 BV of the water, containing 12 kBq/m^3 of ^{137}Cs was treated, with total cumulative break-through of 0.5 %, i.e. 60 kBq/m^3 or Df = 200 on average. A flow rate of 66 BV/hr was used. The break-through of ^{137}Cs did not significantly increase during the course of the experiment. A Df ~ 103 can be achieved by using two columns in series or by using lower flow-rates.

Composite ion exchangers containing manganese dioxide (MnO-PAN) or sodium titanate (NaTiO-PAN) have been tested for sorption of ^{60}Co. NaTiO-PAN composite ion exchanger has been chosen for detailed testing because of its substantially higher capacity for cobalt (0.57 mmole/L in 0.1M $CoCl_2$ solution in water) and the fact that it can be regenerated [11]. For the model experiment tap water was labelled with ^{58}Co, the break-through of cobalt was 1 - 2 % (Df > 50) at flow rate of 40 BV/hr for treatment of 2000 BV of model water. These parameters are fully sufficient for biological shield water treatment. The same absorber can be used for the separation of ^{90}Sr from biological shield water, thus allowing removal of ^{60}Co and ^{90}Sr in one-stage process.

For treatment of all the 350 m^3 of biological shield water (purification and discharge into the environment) by the proposed technology some 35 litres of NiFC-PAN and 10 - 15 litres of NaTiO-PAN composite ion exchanger would be needed. Some 35 litres of spent NiFC-PAN absorber (approx. 9 kg dry weight) containing ~ 7 GBq of ^{137}Cs and 1 - 2 m^3 of solution from regeneration of NaTiO-PAN composite ion exchanger with total activity of not more than 70 MBq should result from the procedure.

3.2. TREATMENT OF STANDARD LIQUID WASTES FROM NPP KRSKO

PAN-based composite ion exchangers were tested for removal of radiocesium, radiocobalt and radiomanganese from liquid radioactive wastes and concentrates from NPP Krsko, Slovenia [4,12]. The experiments were directed towards testing the applicability of the composite ion exchangers for treatment of wastes from a standard "Westinghouse-type" NPP. Nickel hexacyanoferrate (NiFC-PAN), sodium titanate (NaTiO-PAN), manganese dioxide (MnO-PAN), synthetical mordenite (M315-PAN) and synthetical zeolite (Na-Y-PAN) composite ion exchangers were tested.

Liquid waste from the Boron Recycle Hold-up Tank (BRHT) was a solution of boric acid containing lithium hydroxide for the pH adjustments. The solution was slightly acidic (pH ~ 5.1). In addition to ^{3}H and ^{133}Xe the solution was contaminated mainly by ^{58}Co, ^{60}Co, ^{137}Cs and ^{134}Cs. Lower activities of ^{54}Mn and ^{125}Sb were present. Three combinations of composite absorbers were tested. Combination of the NiFC-PAN and NaTiO-PAN absorbers yielded very high retention of radiocesium on the NiFC-PAN (Df ~ 103) even after treatment of 3000 BV of the solution. The retention of radiocobalt was rather complicated, unexpectedly the greater part of the radiocobalt (>60 %) was separated on the first column with NiFC-PAN exchanger. The total decontamination factors on both the columns did reach the values of Df ~ 50 (^{58}Co) and Df ~ 7 (^{60}Co) after treatment of ~ 1500 BV of the solution. The break-through of ^{54}Mn through both the columns has not been changing significantly, its total decontamination factor being Df ~ 12 for the same volume of solution. It was predominantly sorbed on the NaTiO-PAN column.

In succeeding part of the experiment NaTiO-PAN absorber was replaced by MnO-PAN. The results obtained indicate that the MnO-PAN composite ion exchanger is more effective for the removal of radiocobalt. The effectiveness of ^{54}Mn removal is similar to that found for NaTiO-PAN absorber.

In the third part of the experiment M315-PAN or Na-Y-PAN (first column) composite ion exchangers in combination with MnO-PAN (second column) have been tested. From the results obtained it follows that the M315-PAN and Na-Y-PAN exchangers could be used for the simultaneous removal of radiocesium, radiocobalt and radiomanganese. Their disadvantages are only the lower efficiency of separation of ^{137}Cs (Df ~ 30 - 50) and, probably, a shorter sorption cycle. Their main advantage is the possibility of their regeneration. Their combination with the MnO-PAN absorber is not very advantageous because the additional separation of cobalt and manganese on this absorber is not very pronounced.

The solution from Waste Condensate Tank (WCT) (condensate from evaporator) was slightly acidic (pH ~ 4.2). Radiochemical analysis has shown that ^{58}Co, ^{60}Co, ^{134}Cs and ^{137}Cs radionuclides are present, all of them at relatively low levels (~ 1 kBq/L). Two combinations of composite ion exchangers were used. In the first experiment combination of NiFC-PAN (first column) and MnO-PAN (second column) ion exchangers was used, for the second experiment MnO-PAN replaced by NaTiO-PAN ion exchanger in the second column. This combination yielded better results - total decontamination factors (Df)Cs ~ 50 and (Df)Co = 10 - 20 have been achieved for cesium and cobalt, respectively, after treatment of ~ 1000 BV of WCT solution.

The solution from Waste Hold-up Tank (WHT) was an opalescent, somewhat bad-smelling, liquid containing boric acid (1903 ppm of boron) and probably also other impurities such as detergents or complexing agents. The pH of the original solution was ~ 7.2. It was contaminated by ^{58}Co, ^{60}Co, ^{137}Cs and ^{134}Cs. A combination of NiFC-PAN (first column) and NaTiO-PAN (second column) ion exchangers has been tested. The efficiency of separation of radiocesium was high. The decontamination factor remained steady at ~ 103 throughout all the experiment (volume of treated water 20000 BV). The separation of radiocobalt was, however, more complicated. It was partially (~ 15 %) removed on the NiFC-PAN ion exchanger but the efficiency of the second column with NaTiO-PAN exchanger was insufficient (break-through of $^{58+60}$Co ~ 65%, i.e. Df ~ 1.5). After decreasing the flow rate to 15.7 BV.hr^{-1}, addition of cobalt carrier, and acidification of the solution to pH ~ 3 the break-through could be decreased to about 5% (Df ~ 20). Substitution of the NaTiO-PAN absorber by MnO-PAN has not resulted in marked and sufficient improvement of the results of the sorption of radiocobalt.

From the laboratory-scale experiments performed the following general conclusions could be drawn:

-The composite inorganic-organic ion exchangers can be used for the removal of ^{137}Cs, ^{134}Cs, ^{60}Co, ^{58}Co, ^{54}Mn from liquid radioactive wastes containing boric acid at NPP Krsko.

-The best results were achieved for radiocesium. The decontamination factors with NiFC-PAN ion exchanger reached the values of Df ~ 103 and Df ~ 20-50 for liquid wastes or condensates, respectively.

-The separation of radiocobalt from the given wastes is more complicated. In general it was found that it is partially removed on NiFC-PAN ion exchanger. The decontamination factor was found to be strongly influenced by the addition of cobalt carrier and a change of pH value for some of the wastes studied. A combination of two successive columns filled with either NiFC-PAN and MnO-PAN or NiFC-PAN and Na-Y-PAN was found to be the most effective one.

-For the separation of ^{54}Mn the combination of two successive columns filled with either M315-PAN and MnO-PAN or Na-Y-PAN and MnO-PAN ion exchangers were found to be the most advantageous ones.

3.3. REMOVAL OF CESIUM FROM STRONGLY ACIDIC AND ALKALINE WASTES

The performance of PAN-based composite absorbers for the treatment of US DOE liquid radioactive wastes was demonstrated in dynamic experiments with acidic and alkaline simulated solutions [13]. AMP-PAN and KCoFC-PAN composite absorbers (with ammonium molybdophosphate and potassium-cobalt hexacyanoferrate active components, respectively) were used for separation of cesium from 1M HNO_3 + 1M $NaNO_3$ + 2.10^{-5}M CsCl acidic simulated solution. KCoFC-PAN and two other hexacyanoferrate-based composite absorbers were tested for separation of cesium from alkaline simulated solutions containing 0.01M to 1M NaOH and 1M $NaNO_3$ + 2.10^{-4}M CsCl. Efficiency of the cesium removal was evaluated at flow-rates ranging from 25 to 100 BV (bed volumes) per hour.

The efficiency of cesium separation on the column of AMP-PAN composite absorber from the acidic simulated solution was adversely affected by dissolution of the AMP active component. Nevertheless, good results could be obtained at higher flow-rates (50 - 100 BV/hr). At flow-rates of ~ 50 BV/hr, a decontamination factor Df ~ 103 could be maintained for treatment of ~ 380 BV of the feed. The break-through curves measured on the KCoFC-PAN composite absorber corroborated the anticipated better efficiency of cesium uptake by the KCoFC-PAN absorber at lower flow-rates (see Fig. 3). At a flow-rate of ~ 50 BV/hr, the decontamination factor Df ~ 103 could be maintained for treatment up to 1800 BV.

With the alkaline simulated solutions, the efficiency of KCoFC-PAN, CoFC-PAN and NiFC-PAN composite absorbers for the separation of cesium from 1M NaOH + 1M $NaNO_3$ + 2.10-4M CsCl was compared at a flow-rate of ~ 30 BV/hr. The best performance was shown by the KCoFC-PAN; significant decomposition of all the active components was

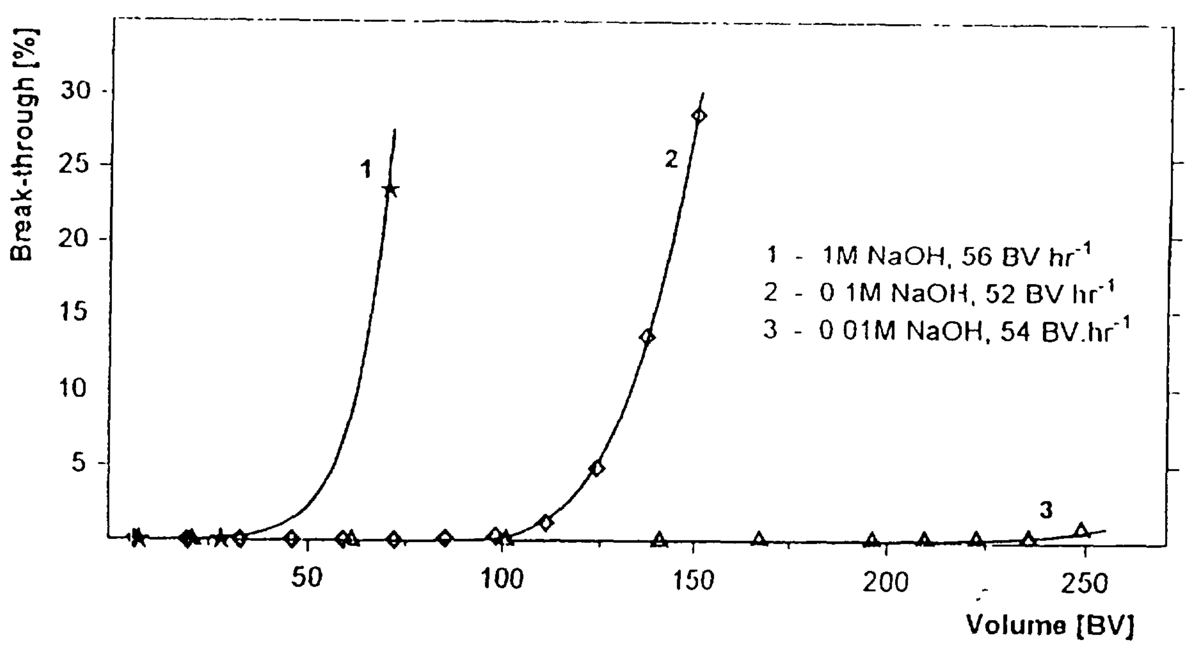

FIG. 3. Break-through curves of ^{137}Cs through a column of KCoFC-PAN absorber from acidic simulant solution at various flow-rates [13].

observed. The study of the influence of flow-rate on cesium uptake by this absorber revealed that the decomposition of the active component cannot be compensated for by applying higher flow-rates.

50 BV/hr was found to be an optimum flow-rate for cesium removal by the KCoFC-PAN absorber at sodium hydroxide concentration equal to 0,1 M. At this flow-rate, the influence of the sodium hydroxide concentration on the uptake of cesium by the KCoFC-PAN absorber from alkaline simulated solutions containing 1 M $NaNO_3$ + 2.10^{-4}M CsCl was studied (see Fig. 4). The efficiency of cesium separation from the solution containing 0.01 M NaOH was found to be comparable to that from acidic simulated solution. At higher sodium hydroxide concentrations, cesium was breaking through significantly earlier due to the decomposition of the active component.

Introductory experiments confirmed that cesium may be washed out of both the AMP-PAN and the KCoFC-PAN cesium-loaded composite absorbers. After the decomposition of the active components of the composite absorbers, cesium can be eluted practically quantitatively from the AMP-PAN in ~ 4 BV of either 1M NH_4OH or 0.1M NaOH; more than 90% of cesium could be washed out from the KCoFC-PAN in ~ 8 BV of 1M $AgNO_3$.

Regeneration of both the AMP-PAN and KCoFC-PAN absorbers for repetitive use was found to be possible. Because of the solubility of the AMP active component, regeneration of this absorber cannot be considered for treatment of large volumes of liquid radioactive wastes. The KCoFC-PAN composite absorber could be regenerated by ~ 50 % in introductory scouting experiments, fully maintaining its sorption capacity.

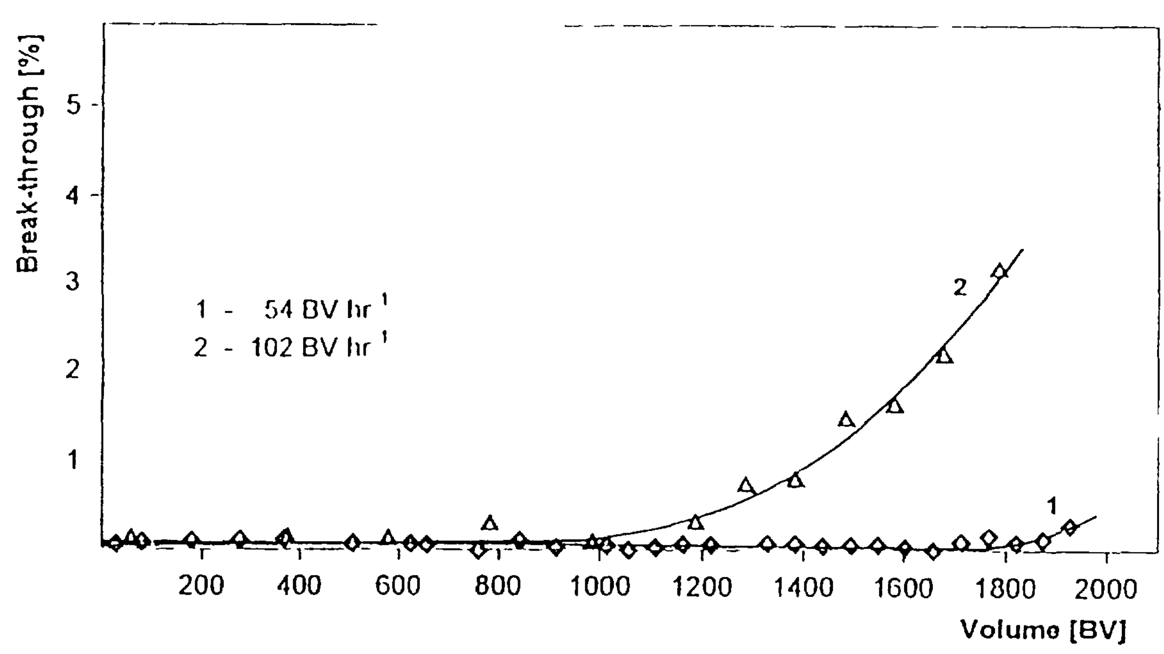

FIG. 4. Influence of NaOH concentration on the break-through of ^{137}Cs through a column of KCoFC-PAN absorber from alkaline simulant solutions (1M $NaNO_3$ + 2.10^{-4}M CsCl) [13].

3 4 REMOVAL OF ^{137}Cs FROM UNDERGROUND WATER

The Swiss National Co-operative for the Storage of Radioactive Waste (NAGRA) has, since May 1984, been operating the Grimsel Test Site (GTS), which is located at a depth of 450 m in the crystalline rock of the Aare Massif of the Central Swiss Alps. Within the framework of the Radionuclide Migration Experiment (MI) a multidisciplinary study aimed at investigating solute transport in fractured media is carried out. The groundwater in the migration fracture is anoxic, has high pH (~ 9.6) and a low ionic strength of 0.0012 M.

At the penultimate stage, migration experiments with chemically more complex nuclides of relevance to repository safety assessment studies were begun.

The aim of our work was to develop a method of decontamination of ^{137}Cs- or ^{134}Cs-contaminated GTS underground water and perform treatment of some 15 m^3 of waste water per migration experiment [14,15]. NiFCPAN composite absorber was selected. Both "off-line" (treatment of water collected in tanks in the course of experiment) and "on-line" (treatment of water directly at the outlet of migration experimental set-up) treatment at pilot-plant scale was tested. The results obtained are summarized in Tables IV, V and Fig. 5.

The results of "off-line" treatment indicated that with NiFC-PAN absorber (grain size > 0.4 mm) some 8 000 BV of waste water can be treated at a flow rate of 60 BV.hr^{-1} with decontamination factor Df > 250. The decontamination factor depended strongly on flow rate of the waste water in the range of flow rates 60 - 120 BV.hr^{-1}. In two successive experiments ~ 9 m^3 and ~ 8 m^3 of waste water contaminated by 200 - 1 000 kBq ^{137}Cs.m^{-3} were treated, respectively.

TABLE IV. RESULTS OF OFF-LINE TREATMENT

Run No.	Column No.	Bed Volume [mL]	Grain Size [mm]	Specific Activity [Bq.L^{-1}] kBq/m^3	Flow rate [BV.hr^{-1}]	Volume Treated [BV/m^3]	Averate Break-through [kBq/m^3]	Average D_f
80	1+2	500	>0.4	235-1050	~60	9000/4.5	<2	>250
85	1	700	0.5-1	205-800	85-100	5700/4	3.5	145
85	2	600	0.5-1	205-800	100-120	6700/4	7.3	70

TABLE V. RESULTS OF ON-LINE TREATMENT

Run No.	Bed Volume [mL]	Grain Size [mm]	Initial Specific Activity [kBq/m^3]	Flow rate [BV.hr^{-1}]	Volume Treated [BV/m^3]	Initial Break-through kBq/m^3	Initial D_f
80	500	>0.4	80	~15	10000	<0.2	>350
85	500	>1	90	~15	12000	<0.2	>450

The results of "on-line" treatment (flow rate 10 BV/hr - 15 BV/hr) have shown that a decontamination factor Df > 102 can be achieved for the first 8 000 BV of treated GTS underground waste water irrespective of whether the ^{137}Cs applied was carrier-free or contained 2.10^{-4} mole of cesium carrier. A decontamination factor as high as 1600 was found at the beginning of the experiment. In three successive experiments ~ 30 m^3 of waste water was treated.

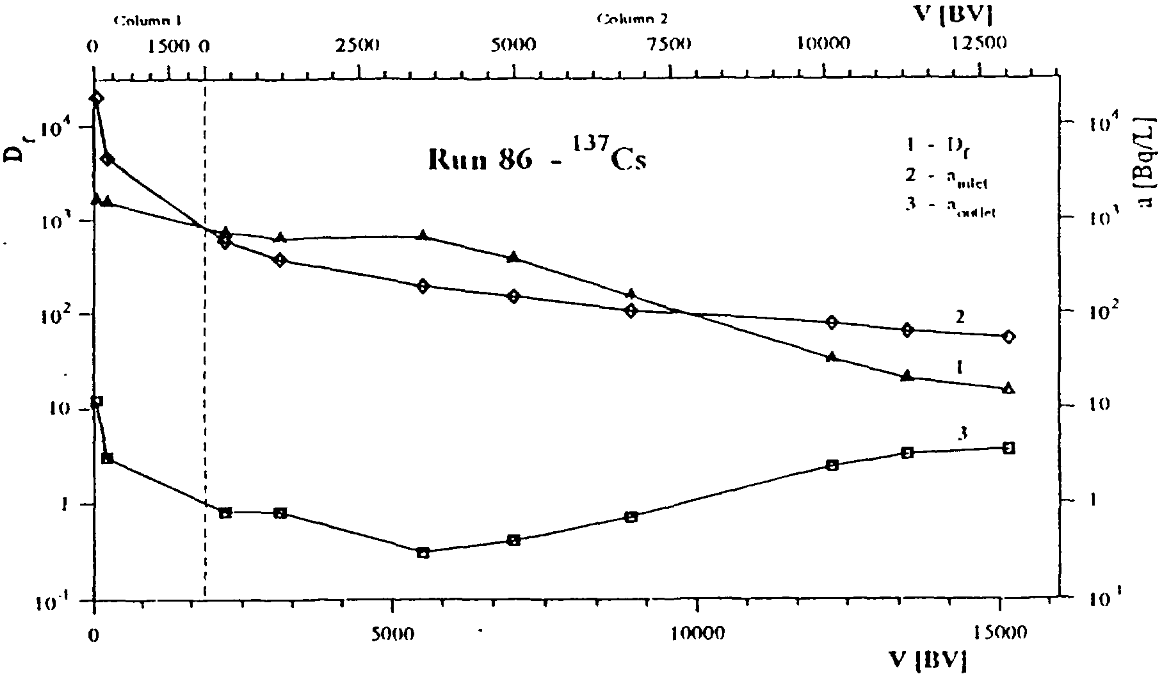

FIG. 5. Results of decontamination of waste water from migration experiment Run No. 86 on NiFC-PAN composite absorber in "on-line" regime [14]. BV = 750 mL, flow rate 10 BV.hr-1, curve 1 = decontamination factor, curves 2 and 3 - activity of water on inlet and outlet of column, respectively.

3.5. CONCENTRATION OF URANIUM FROM WASTE AND SURFACE WATERS

Among the best inorganic ion exchangers for separation and concentration of uranium from surface water, hydrated titanium oxide (TiO) and sodium titanate (NaTiO) can be listed. In an extensive study, methods of preparation of sodium titanate from an industrial intermediate from the pigment industry were examined and the physico-chemical properties of pure TiO and NaTiO ion-exchangers were determined. TiO-PAN and NaTiO-PAN composite absorbers were synthesized and possibilities of application of these composite absorbers for separation of uranium from a model fresh water were examined [8,15].

TiO-PAN and NaTiO-PAN composite absorbers, prepared from hydrated titanium oxide (TiO) and sodium titanate (NaTiO) respectively, were shown to be applicable for extraction of uranium from model solution containing 10^{-3}M $UO_2(NO_3)_2$ in distilled water. Uranium could be easily eluted out from the absorbers using 0.1 M HCl, the possibility of eluting uranium with Na_2CO_3 solution was studied.

Both TiO-PAN and NaTiO-PAN absorbers can be used for repeated extraction of uranium from tap water. Maximum flow rates are 60 BV/hr and 60 - 100 BV/hr for TiO-PAN and NaTiO-PAN absorbers, respectively. Typical break-through curves measured for TiO-PAN composite absorber at various flow rates are shown in Fig. 6. Elution of uranium and regeneration of both absorbers may be accomplished with 0.1M HCl.

The practical sorption capacity (10% break-through) from tap water containing 2.3 mg $U \cdot L^{-1}$ (~ 10^{-5} M) measured at flow rate of 100 BV/hr was ~ 4.6 mg and ~ 1.5 mg of uranium per mL of swollen TiO-PAN and NaTiO-PAN absorber, respectively. TiO-PAN composite absorber is thus, more advantageous.

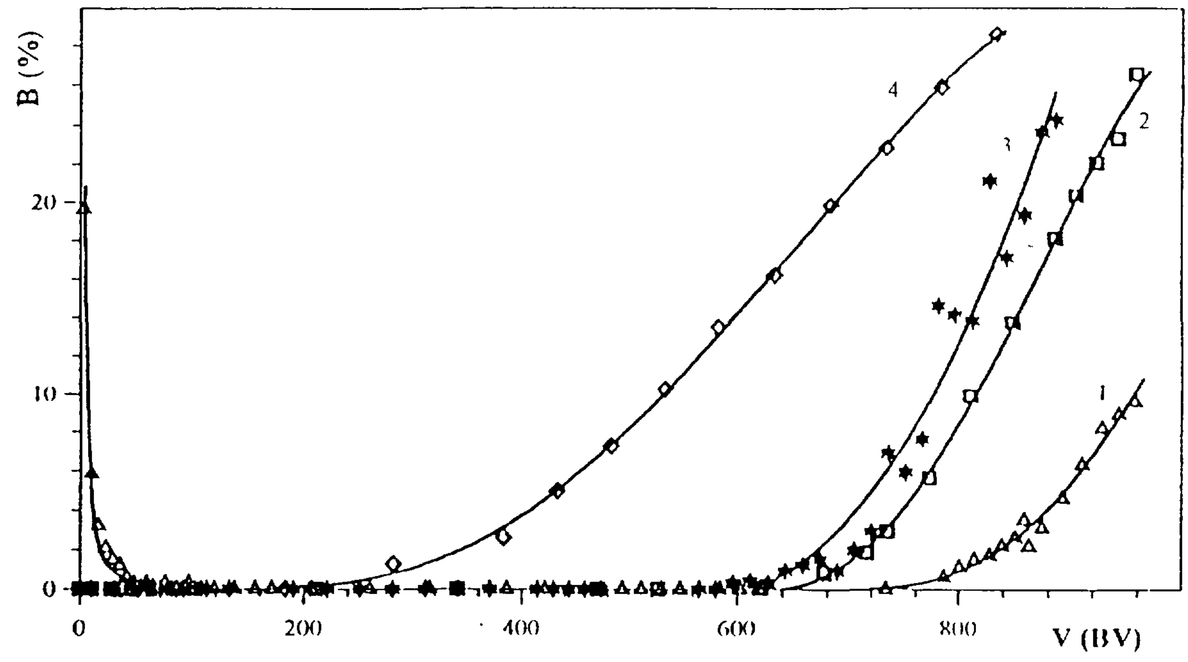

FIG. 6 *Break-through (B) curves of uranium on TiO-PAN composite absorber (BV = 10 mL) from 10^{-4} M $UO_2(NO_3)_2$ (~ 23 mg U/L) in tap water [8].*
Curve 1 - fresh absorber, flow rate 18 BV/hr, curves 2, 3, 4 - regenerated absorber, flow rate 18 BV/hr, 60 BV/hr and 100 BV/hr

3.6. REMOVAL OF RADIUM AND THORIUM FROM WATER AND SALINE SOLUTIONS

This research was conducted in collaboration with the University of Oxford, Particle & Nuclear Physics, Nuclear Physics Laboratory with the prospect of possible application of the absorbers at the Sudbury Neutrino Observatory (SNO) to purify H_2O, D_2O and NaCl used in preparation of 0.25 % solution of NaCl in D_2O, down to 10^{-15} g/g of uranium, thorium, and their daughter radionuclides. Based on the preliminary tests of selected composite absorbers, absorbers containing the following active components have been chosen for testing - barium sulphate activated by calcium, manganese dioxide, titanium dioxide, and sodium titanate. The media tested included distilled water, 3% NaCl, and 10% NaCl solutions.

TABLE VI. K_D [$mL.mL^{-1}$] VALUES FOR ^{226}Ra [17]

Absorber	0% NaCl		3% NaCl		10% NaCl	
	pH	K_d	pH	K_d	pH	K_d
$Ba[Ca]SO_4$-PAN	6.9	2550	6.9	8250	7.2	1180
MnO-PAN	7.1	1430	6.8	13750	7.1	11790
TiO-PAN	6.7	3520	6.8	7200	7	8810
NaTiO-PAN	7.6	290	6.7	11630	6.7	12402

Distribution coefficients of radium found for all the four absorbers studied are given in Table VI together with equilibrium pH values. For ^{234}Th "equilibrium" distribution coefficients were not determined. The values of distribution coefficients after 120 minutes of contact $(K_D)_{120}$ (calculated from kinetics measurement data) are summarized in Table VII.

From the results achieved it could be concluded that for separation of radium from water without NaCl, TiO-PAN absorber was most suitable (Df ~ 300 - 500). From the results of column experiments performed with sodium chloride solutions, MnO-PAN absorber seems to show the best performance (Df ~ 500 - 1000). Typical break-through curves obtained are shown in Fig. 7.

TABLE VII. $(K_D)_{120}$ VALUES FOR ^{234}Th [17]

Absorber	0% NaCl		3% NaCl		10% NaCl	
	pH	K_d	pH	K_d	pH	K_d
$Ba[Ca]SO_4$-PAN	6.7	1100	--	--	--	--
MnO-PAN	6.8	8.5	--	--	--	--
TiO-PAN	5.7	240	5.8	370	6.2	220
NaTiO-PAN	7.4	3.0	--	--	--	--

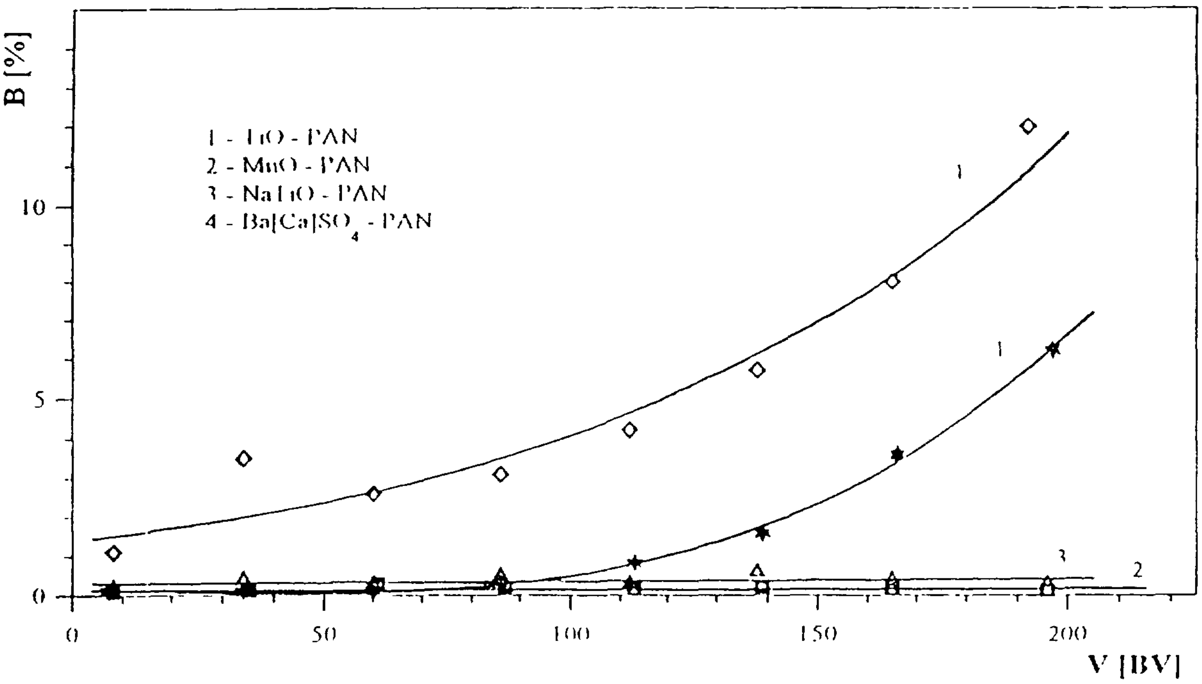

FIG. 7. *^{226}Ra break-through curves on various absorbers from 10 % NaCl solution [8].*
Curve 1 - TiO-PAN, curve 2 - MnO-PAN, curve 3 - NaTiO-PAN and curve 4 Ba[Ca]SO_4-PAN composite absorbers

For separation of thorium from water without sodium chloride only Ba[Ca]SO_4-PAN absorber may be used (Df ~ 20). TiO-PAN absorber is most suitable for separation of thorium from sodium chloride solutions (Df ~ 70 for 3% NaCl and Df ~ 20 for 10% NaCl). Generally, it can be concluded that the separation of thorium is more complicated than separation of radium.

3.7. SEPARATION OF RADIUM IN THE PROCESS FOR TREATMENT OF WASTE WATER FROM UNDERGROUND URANIUM LEACHING

During "in situ"-leaching of uranium in northern Bohemia some 97 million m^3 of technological solutions containing up to 20 g of H_2SO_4 and ~ 70 g of dissolved salts per liter were produced. These underground solutions are contaminated by a range of natural radionuclides. The radionuclides of most concern are those of thorium (^{228}Th, ^{230}Th), radium (^{226}Ra, ^{228}Ra), and ^{227}Ac and ^{210}Pb. As a result of leakage out of the leaching fields, as much as 92 million m^3 and 2-20 million m^3 of water in cenoman and thuron aquifers respectively are contaminated.

As a part of a more general investigation of problems of treating solutions from underground uranium leaching, possibility of application of selected composite absorbers has been studied in trial experiments. These experiments were directed towards separation of radium from the waste solutions.

Separation of radium from waste leaching solutions

Waste leaching solutions are relatively acid (pH = 1.1) and saline (total concentration of sulphate anion 51 kg.m^{-3}) from which most of the uranium was removed using synthetic ion-exchangers. Ba[Ca]SO_4-PAN absorber was tested for radium separation. In the first experiments, quantitative uptake of radium was found for all the flow rates tested (5, 20 and 50 BV/hr) after treating to 60 BV of solution. The capacity of the absorber for radium was tested by treating 10 L of waste with a column with BV=10 mL at a flow rate of 25 BV/hr. The uptake of radium remained quantitative even after the treatment of all of this solution. It was verified that no thorium was concentrated on this absorber.

Separation of radium from products of waste leaching solutions treatment

In the framework of the evaporation technology proposed for liquidation of waste leaching solutions it is anticipated that some of the solid products resulting from evaporation may be commercialized. The main product of interest is ammonium-aluminum sulphate $\{NH_4Al(SO_4)_2.12\ H_2O\}$ that might (after calcination to Al_2O_3) be used as a raw material for aluminum production. Because of this foreseen application, the alum produced should not be contaminated by natural radionuclides contained in the solution treated.

Two processes to separate radium using the Ba[Ca]SO_4-PAN absorber were tested. In the first experiments, it was found that Ba[Ca]SO_4-PAN absorber is not suitable for radium sorption from hot concentrated alum solutions (~ 80°C), because of visible dissolution of the active component of the absorber. In the second series of experiments heavily saturated solution of raw alum was passed through a column of Ba[Ca]SO_4-PAN absorber at a flow rate 10 - 20 BV.hr^{-1}. The treated solution was then concentrated and the alum crystallized. The concentration of both radium isotopes and ^{228}Th in this alum was approaching zero.

From the results achieved, it can be concluded that the application of this absorber is the polishing of evaporator condensates to remove thorium and radium, and polishing of some of the desalination products that might find technical application.

4. OPTIONS FOR TREATMENT OF SPENT COMPOSITE ABSORBERS

Composite absorbers represent a group of absorbers similar both to organic ion-exchange resins and inorganic ion-exchangers. From the point of view of stability and treatment for final disposal their main feature is that the organic binding polymer (PAN) is inert and all the radionuclides are bound to the inorganic active component. Thus in contrast to organic ion-exchange resins even when decomposition of organic binding matrix occurs (radiation, chemical, thermal or biological decomposition) no radionuclides are released.

4.1. CEMENTATION [15,18]

Cement samples were prepared by mixing of appropriate amounts of dewatered (swollen) composite absorbers with Portland Cement PC-400 and water (see Table VIII). Additional cement samples were prepared with admixtures of clinoptilolite (Czech origin, grain size < 0.3 mm), see Table IX. The 4 x 4 x 4 cm cubic samples produced were demoulded after 24 hours, sealed into polyethylene bags and cured for an additional 27 days at ambient temperature: the resulting samples were strength tested. For freeze/thaw cycles the cement composition of cement mix: 15 g wet absorber + 30 g PC-400 + 8 g water + clinoptilolite samples were frozen for 2 days at - 25°C and two days de-frozen at ambient temperature. Visual quality of cement samples during soak/dry cycles was evaluated after soaking the samples for 2 days followed by 2 - 3 days' drying at ambient temperature.

From the results of tests performed (Table VIII) it can be concluded that the loading of cement mix with dry composite absorber up to 5-9% (w/w) is acceptable. Maximum loading depends on type of composite absorber and its grain size. The maximum loadings found are comparable to maximum loading of cement matrix with pure inorganic ion-exchangers [25].

Solidification of radioactive wastes with cement has a disadvantage of relatively high leachability of ^{137}Cs. One possibility how to improve leakage resistance of the resulting concrete is addition of suitable additives. Natural clinoptilolite is one of the possible candidates for such additives. This is why influence of clinoptilolite admixtures on quality of cement samples with encapsulated composite absorbers was studied. From the results shown in Table IX it follows that admixtures of clinoptilolite improve compressive strength of the resulting cement samples. No significant deterioration of the quality of composite absorber - cement product with admixtures of clinoptilolite was observed after repeated freeze/thaw or soak/dry cycles.

TABLE. VIII CHARACTERISTICS OF CEMENT SAMPLES WITH ENCAPSULATED COMPOSITE ABSORBERS [150].

Composite Absorber	Dry Residue of Absorber [%]	Cement Mix					
		Water [g]	PC-400	Wet Absorber [g]			
				15	30	45	60
TiO-PAN	19 4	10	30	HS-WR	HS-WR	USS	USS
MnO-PAN	21 1	8	30	HS-WR	HS-WR	USS	USS
Ba[Ca]SO_4-PAN	19 6	8	30	HS-WR	USS	USS	USS
KNiFC-PAN	17 8	8	30	HS-WR	USS	NT	NT
NiFC-PAN	21 6	8	30	HS-WR	USS	NT	NT

PC-400 - Portland Cement PC-400
HS-WR - Visually Homogenous Samples with no signs of cracking or powdering.
- Stability in Water Resistant after soaking for 1 week.
USS - Unsatisfactory samples
NT - Not tested

4.2. VITRIFICATION

Because of the high efficiency and selectivity of composite absorbers, a volume reduction factor of 10^4 to 10^5 can be obtained in waste treatment. In some cases, spent composite absorbers represent high level waste. Immobilization of such materials in cement may not be acceptable and/or safe enough.

TABLE. IX. INFLUENCE OF ADMIXTURE OF CLINOPTILOLITE ON QUALITY OF CEMENT SAMPLES WITH ENCAPSULATED COMPOSITE ABSORBERS [15].

Composition of cement mix: 15 g wet absorber + 30 g PC-400 + 8 g water + clinoptilolite

Composite Absorber		Cement Mix				
	0	1			3	
	CS	CS	CS-5F	VQ-5SD	CS	CS
TiO-PAN	9.8	28.7	15	GQ	27.3	GQ
MnO-PAN	8.5	23.6	28.4	GQ	34	GQ
Ba[Ca]SO_4-PAN	6.3	NM	NM	NM	25.9	GQ
KNiFC-PAN	~9	10.4	7.5	GQ	17.6	GQ
NiFC-PAN	~13	12.1	11.6	GQ	17.1	GQ

For residue after drying see Tab. 4.1-1

CS - Compressive strength after 28 days of curing [MPa]

CS-5F - Compressive strength after 28 days of curing and five freeze/thaw cycles [MPa]

VQ-5SD- Visual quality of sample after five soak/dry cycles

GQ - Good quality NM - Not measured

The possibility of vitrifying NiFC-PAN absorber was tested in trial experiments [16, 18]. The dried absorber was mixed with a low-melting glass frit in different ratios and melted in porcelain crucibles. Viscosity, visual quality and hydrolytic resistance of samples were examined. Melts produced from mixtures containing 10% (w/w) of absorber were highly viscous, it was hardly possible to pour them from the crucible. When only 5% (w/w) of dried absorber was added to the mixture, the melt could be easily poured from the crucible and the melt was transparent and homogeneous.

Hydrolytic resistance of the product was tested by leaching 1g of crushed glass specimen (0.3 - 0.5 mm, 5% of dried absorber) in 50 mL of distilled water for 24 hours. The electrical conductivity of the leachate ranged from 6 to 8 mS/cm. Following the criteria for fast preliminary evaluation it is assumed that vitrified materials which yield hydrolytic resistance lower than 20 mS/cm in such tests are suitable for long term storage as high level waste.

From the results achieved so far it can be concluded that vitrification may be used for the final treatment of spent composite absorbers for their disposal in radioactive waste repositories. The experiments performed with NiFC-PAN absorber proved that the presence of PAN binding polymer does not disqualify composite absorbers from final treatment by vitrification.

4.3. LEACHING OF CESIUM FROM CEMENTED NIFC-PAN ABSORBER

The most important parameter of cemented waste is its leachability. Two series of dynamic leaching tests (the leachant was exchanged periodically) were carried out [16,20,21]. In the first series, differences between cesium leaching from cemented cesium solution, cesium loaded powdered NiFC absorber, and cesium loaded NiFC-PAN composite absorber were established. In the second series the influence of clinoptilolite additions on cesium leaching from cemented cesium loaded NiFC-PAN composite absorber was determined. Dependences of cumulative fractions leached on the leaching time were measured. Diffusion coefficients were calculated from the slope of the plot of cumulative activity leached vs. square root of leaching time. In addition, incremental leach rates corrected for the surface to volume ratio of the tested species and related to total activity of the species were calculated. The results of comparison of various cemented species are shown in Figs. 9 and 10, the diffusion coefficients found are listed in Table X.

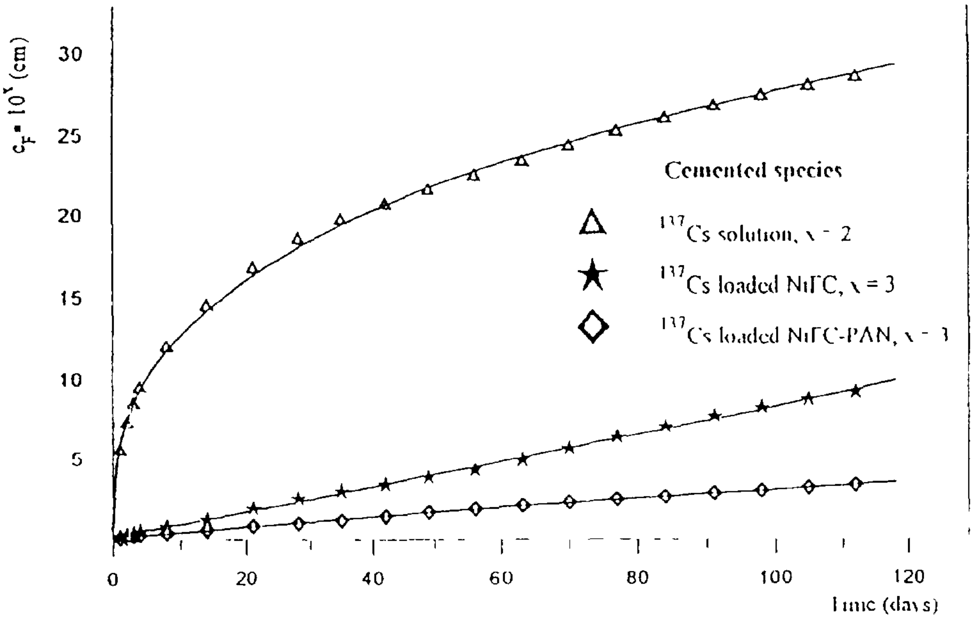

FIG. 8. Influence of specimen type on the cumulative fraction of caesium leached

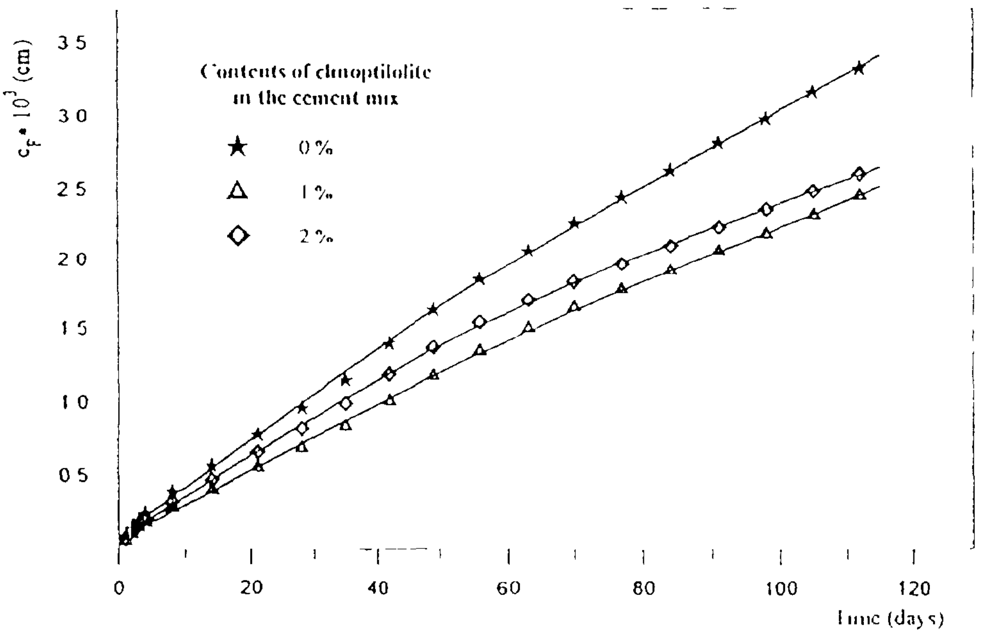

FIG. 9. Influence of clinoptilolite admixtures in the cement mix on the cumulative fraction of caesium leached from cemented NiFC-PAN composite absorber

From the evaluation of the data and from the comparison of the cumulative fractions leached and incremental leach rates found with data obtained by other authors, the following main conclusions could be drawn:

Cumulative fractions leached are ~ 30 and ~ 100 times lower for samples loaded by NiFC or NiFC-PAN, respectively, when compared to cemented ^{137}Cs solution. No more than 0.3 % of ^{137}Cs was leached from the cemented NiFC-PAN absorber in four months.

TABLE X. 10 DIFFUSION COEFFICIENTS OF CESIUM FROM VARIOUS CEMENTED SPECIES

Cement Mix	NiFC-PAN [% dry weight]	NiFC [% dry weight]	Clinoptilolite [%]	Diffusion Coefficient	
				[$cm^2.day^{-1}$]	[$m^2.s^{-1}$]
I.	6.3	-	0	$1.7.10^{-7}$	$2.0.10^{-10}$
II.	6.3	-	1	$9.6.10^{-8}$	$1.1.10^{-10}$
III.	6.2	-	2	$9.1.10^{-8}$	$1.1.10^{-10}$
IV.	-	6.4	-	$1.4.10^{-6}$	$1.6.10^{-9}$
V.	-	-	-	$2.4.10^{-4}$	$2.8.10^{-7}$

- Probable explanation of these results is positive influence of the relatively hydrophobic PAN binder the lowest leach was obtained for samples prepared from grout containing ~ 1% of clinoptilolite.
- The shape of the curves describing the dependence of the incremental leach rate on time suggest a chemical reaction taking place during the 3rd to 6th weeks of the leaching.
- The dependence of c_F on time is linear for leaching periods longer than six weeks and/or during the first two weeks.
- The lowest leach was obtained for samples prepared from grout containing around 1% of clinoptilolite.

The leachabilities found for cemented NiFC-PAN absorber are at least one order of magnitude lower than any results published till now. The most probable explanation of such a low leachability of ^{137}Cs from the samples is its strong association with the active component of NiFC-PAN absorber - nickel hexacyanoferrate and a positive influence of the relatively hydrophobic polyacrylonitrile binder. These experiments are currently complemented by a study of the influence of irradiation on the leaching of cesium; experiments to established the influence of temperature on cesium leaching will be commenced soon. The complete set of results will be presented at the Fourth International Conference on Nuclear and Radiochemistry - NRC4 at Saint-Malo, France, on September 8-13, 1996.

REFERENCES

[1] ŠEBESTA F., JOHN J.: An Overview of Development, Testing, and Application of Composite Absorbers, LA-12875-MS, February 1995, 30 pp.

[2] STOY V., ŠEBESTA F., JIRÁSEK V., STOY A.: Selective Absorber for Radium and the Procedure for its Production. Czech Patent A.O. 181605 (1980).

[3] ŠEBESTA, F. et al., Exchanger Composed from an Active Component and a Binding Organic Matrix and the Way of its Production, Czech Patent AO 273369, 1992.

[4] ŠEBESTA F., MOTL A., JOHN J., PRAZSKY M., BINKA J.: Composite Ion-Exchangers and their Possible Use in Treatment of Low/Intermediate Level Liquid Radioactive Wastes. In: Proc. 1993 Int. Conf. Nucl. Waste Management and Environmental Remediation, September 5-11, 1993, Prague; Vol. 3, pp.871-878, ASME, New York, 1993.

[5] ŠEBESTA F., JOHN J., MOTL A., WATSON J.: Development of PAN-Based Absorbers for Treating Waste Problems at U.S. DOE Facilities, In: SLATE, S. - FEIZOLLAHI, F. - CREER, J., eds.: ICEM'95 Proc. The Fifth International Conference on Radioactive Waste Management and Environmental Remediation, September 3-7, 1995, Berlin, Vol. 1, pp.361-365, ASME, New York, 1995.

[6] ŠEBESTA F., JOHN J., MOTL A., TAMBERG K.: Evaluation of Polyacrylonitrile (PAN) as a Binding Polymer for Absorbers Used to Treat Liquid Radioactive Wastes, Phase I Draft Report of Agreement for Services No. FSU/CTU-1 between the Florida State University and the Czech Technical University in Prague, SAND95-2729, November 1995, 46 pp.

[7] ŠEBESTA F., JOHN J., MOTL A.: Separation and Concentration of Contaminants Using Inorganic-Organic Composite Absorbers, In: Proc. BUDAPEST '94 Second International Symposium and Exhibition on Environmental Contamination in Central and Eastern Europe, Budapest, Hungary, September 20-23, 1994, pp.1052-1055.

[8] ŠEBESTA F., JOHN J., MOTL A.: Inorganic-Organic Composite Absorbers with Polyacrylonitrile Binding Matrix - Possible Applications, In: Proc. SPECTRUM '94 Nuclear and Hazardous Waste Management International Topical Meeting, Atlanta, USA, August 14-18, 1994, ANS, LaGrange Park, Il,1994, Vol. 2, pp.856-861.

[9] ŠEBESTA F., JOHN J., MOTL A.: Verification of Technology of Decreasing the Long Term Fuel Storage Pond Water Activity at NPP A-1 (in Czech), Faculty of Nuclear Sciences and Physical Engineering, CTU Prague, 1992, 43 pp.

[10] ŠEBESTA F., MOTL A.: Decontamination and Treatment of Radioactive Wastes (in Czech), Report of A 01-125-818/03 Research Programme, Faculty of Nuclear Sciences and Physical Engineering, CTU Prague, 1989, 24 pp.

[11] ŠEBESTA F., MOTL A.: Decontamination and Treatment of Radioactive Wastes (in Czech), Report of A 01-125-818/03 Research Programme, Faculty of Nuclear Sciences and Physical Engineering, CTU Prague, 1990, 17 pp.

[12] ŠEBESTA F., MOTL A.: Testing of Composite Inorganic-Organic Ion Exchangers for the Treatment of Liquid Radioactive Wastes from NPP Krτko, Report from the Research Agreement between FJFI and J. Stefan Institute, Ljubljana, Slovenia, Faculty of Nuclear Sciences and Physical Engineering, CTU Prague, 1991, 41 pp.

[13] ŠEBESTA F., JOHN J., MOTL A.: Evaluation of Polyacrylonitrile (PAN) as a Binding Polymer for Absorbers Used to Treat Liquid Radioactive Wastes, Phase II Final Report of Agreement for Services No. FSU/CTU-1 between the Florida State University and the Czech Technical University in Prague, Faculty of Nuclear Sciences and Physical Engineering, Prague, December 1995, 30 pp.

[14] ŠEBESTA F., JOHN J., BÜHLER C., RAZ U.: Treatment of Underground Water Contaminated by ^{137}Cs at NAGRA Grimsel Test Site, Switzerland, In: Proc. SPECTRUM '94 Nuclear and Hazardous Waste Management International Topical Meeting, Atlanta, USA, August 14-18, 1994, ANS, LaGrange Park, Il, 1994, Vol. 2, pp.231-236.

[15] ŠEBESTA F., JOHN J., MOTL A.: Development of Composite Ion-Exchangers and their Use in Treatment of Liquid Radioactive Wastes, Progress Report of the Research Contract No. 7381/RB, Faculty of Nuclear Sciences and Physical Engineering, Prague, January 1994, 67 pp.

[16] ŠEBESTA F., JOHN J., MOTL A.: Development of Composite Ion-Exchangers and their Use in Treatment of Liquid Radioactive Wastes, Progress Report of the Research Contract No. 7381/R1/RB, Faculty of Nuclear Sciences and Physical Engineering, Prague, February 1995, 52 + 14 pp.

[17] ŠEBESTA F., JOHN J., MOTL A., HOOPER E.W.: Removal of Radium and Thorium from Water and Saline Solutions Using Inorganic-Organic Composite Absorbers with Polyacrylonitrile Binding Matrix, In: Proc. IEX '96 Int. Conf. Ion Exchange Developments and Applications, July 14-19, 1996, Cambridge, U.K., in press.

[18] ŠEBESTA F., JOHN J., MOTL A., STEINEROVÁ J.: Treatment of Spent Composite Ion-Exchangers for Final Disposal, In: Workshop'95, Vol. 3, section Nuclear Engineering, Prague, January 23-26, 1995, CTU Prague, 1995, pp.861-862.

[19] BEAVEN G.W., CROSS J.E., HOOPER E.W.: Study of the Behaviour of Inorganic Ion Exchangers in the Treatment of Medium Active Effluents. Part V. The Encapsulation of Inorganic Ion Exchangers in Cement, Report AERE-G 4421, 1988, 13 pp.

[20] ŠEBESTA F., JOHN J., MOTL A.: Development and Testing of Composite Absorbers. Combined Quarterly Reports II/1995 and III/1995 of "Memorandum of Understanding" between the Los Alamos National Laboratory and Czech Technical University, Department of Nuclear Chemistry; Faculty of Nuclear Sciences and Physical Engineering, Prague, September 1995, 49 pp.

[21] JOHN J., ŠEBESTA F., MOTL A.: Studies of Options for Treatment of Spent PAN-Based Composite Absorbers, In: Abstracts of Presentations on the XI. Seminar on Separation Chemistry, Lázn Bohdanef, Czech Republic, November 7-9, 1995 (published in abstract form only).

USE OF INORGANIC ION EXCHANGE MATERIALS FOR THE TREATMENT OF LIQUID WASTE

I.M. EL-NAGGAR, E.S. ZAKARIA, M.A. EL-ABSY,
M.M. ABDEL-HAMID, M.M. ABO-MESALAM,
S.A. SHADY, M.A. ABDELWAHAB, H.F. ALY
Nuclear Fuel Technology Department,
Hot Laboratories Centre,
Atomic Energy Authority,
Cairo, Egypt

Abstract

To examine the ion exchange behaviour of the double salts of polybasic acids with tetravalent metals type such as cerium(IV) and tin(IV) antimonates, different samples were prepared, heated at different temperatures and exposed to γ-irradiation. These samples were subjected to X-ray, infra-red and thermal analysis. The exchange properties of the studied materials improved on increasing the Sb, Ce or Sn molar ratios and the drying temperature. The rate of the isotopic exchange was controlled by particle diffusion for the metal ions studied and was faster as the heating temperature was increased but slower for materials with a higher exchange capacity. The physical thermodynamic parameters have been evaluated which give some information regarding the mechanism of ion exchange on the surface of inorganic materials. The removal of radioactive isotopes of Na^+, Cs^+, Sr^{2+}, Co^{2+} and Eu^{3+} was carried out by in-situ precipitation or by using preformed precipitate of tin(IV) and cerium(IV) antimonates. The products of in-situ precipitations act as ion exchange materials with high chemical and radioactive stabilities. The new materials have relatively high capacity compared with CeSb and SnSb. The irradiated cerium(IV) antimonate has been successfully used for the quantitative separation of cesium which suggests its use in the treatment of active liquid waste.

1. INTRODUCTION

Some of the general methods which are in current use for the treatment of radioactive waste are chemical precipitation, adsorption and ion exchange [1,2]. The choice of a suitable technique is governed by the chemical composition of the waste solution and by economic factors [1]. The potential usefulness of inorganic ion-exchangers has been proven in various areas of nuclear fuel cycle technology, especially in the separation and fixation of fission products and actinides and in the treatment of effluents from nuclear power plants. Inorganic ion-exchangers and adsorbents have been receiving attention for these purposes because of their strong chemical affinity, high retention capacity for cation radionuclides and high resistance to radiation. Inorganic ion-exchangers of high adsorption selectivity can be used as adsorbents and, additives in solidification of liquid wastes. Among several new synthetic ion-exchange materials, the double salts of polybasic acids with tetravalent metal types, tin(IV) antimonate (SnSb) and cerium(IV) antimonate (CeSb) were studied in the present work as adsorbents for decontaminating liquid wastes which contain fission products.

2. EXPERIMENTAL

The methods of preparation of the samples and the various experimental techniques are described elsewhere [3-5]. In summary, most of the samples of CeSb were prepared by addition of antimony(V) chloride or antimony metal dissolved in aqua regia to cerium ammonium nitrate or tin(IV) chloride solutions of different concentrations and molar ratios.

All the samples prepared were initially dried at 50°C and stored at room temperature. Portions of the samples were heated at different temperatures. The equilibrium measurements and the isotopic exchange reactions were carried out as previously reported [1, 2].

The in-situ precipitation of the elements with tin(IV) and cerium(IV) antimonates was carried out as mentioned before [2-7].

Column operation, was also carried out as reported earlier [8-10].

3. RESULTS AND DISCUSSION

The work on cerium(IV) and tin(IV) antimonates is in course of publication in papers and a thesis, some results have been published or accepted for publication [6-15].

Since the detailed results will require a large space and volume, many results will be omitted. However, the omission will not affect the integrity of this report.

Structure Features

X-ray analysis of the various samples has shown that all of them are semi-crystalline and that the crystallinity of the materials slightly increases with increasing the Sb/Ce and Sb/Sn ratios and the heating temperature of the materials in the investigated range, 50-400°C. However, a sharp improvement of crystallinity occurs at 850°C.

The IR spectra for all samples of cerium(IV) antimonates prepared at various Sb/Ce ratios have a similar general appearance but differ in details, probably due to surface structure differences. The same can be said for all tin(IV) antimonate samples. The absorption bands at 2500-3600 and 1640 cm^{-1} for all samples can be assigned to the stretching and deformation vibration of interstitial water with strong hydrogen ion bonding. The decrease in water content of the sample, as demonstrated by the decrease in band intensities of molecular water at about 3900 and 1640 cm^{-1}, follows the increase in heating temperatures.

Thermogravimetric (TG) and differential thermal analysis (DTA) curves for CeSb showed that the first weight loss at 106°C, corresponds to loss of free water. The weight loss continued up to 646°C, showing that CeSb has a good thermal stability compared with other inorganic ion exchange materials [16,17].

The small exothermic peak at 334°C, corresponds to crystallization of CeO_2. No weight loss occurred in the range 646-820°C for CeSb samples.

The TG and DTA curves of SnSb showed that the first weight loss corresponds to loss of the water of hydration at 94°C. The very small endothermic peak accompanied with loss of weight at ~530°C may be associated with further condensation of the antimonate groups.

Apparent Capacity Measurements

The ion-exchange capacities of CeSb and SnSb samples heated at different temperatures are given in Tables I and II. The data in the tables showed that the ion-exchange capacity for

Na^+ and Cs^+ on all samples heated at 200°C are slightly decreased due to the loss of the free water. At 400°C, it seems that the capacities are generally higher. On heating at 600°C, strongly bonded water is removed and the capacity simultaneously decreases. No ion-exchange behaviour can be observed in CeSb and SnSb heated at 700°C [17-18].

TABLE I. CAPACITY FOR Na^+ AND Cs^+ IONS ON VARIOUS CERIUM (IV) ANTIMONATE SAMPLES DRIED AT DIFFERENT TEMPERATURES.

Sb/Ce ratios	Heating temperature (°C)	% of water content (wt)	Capacity (meq/g)	
			Na^+	Cs^+
0.5	50	17.16	0.952	0.74
	200	13.80	0.918	0.71
	400	5.11	1.090	0.87
	600	1.23	0.035	0.012
0.75	50	16.88	1.26	1.06
	200	13.33	1.12	1.02
	400	7.71	1.33	1.24
1.33	50	17.35	1.34	1.12
	200	13.88	1.24	1.06
	400	7.34	1.42	1.16
2.39	50	17.08	1.36	1.18
	200	14.16	1.31	1.13
	400	7.86	1.44	1.21

The capacities of unirradiated and irradiated CeSb and SnSb samples are given in Table III. From this table, it may be deduced that the decrease in capacity for Na^+ and Cs^+ for both samples should be related to both water of crystallization and that the structural water may undergo radiolysis resulting in a loss of exchange capacity or partial decomposition due to redox reactions [8]. In addition there are probably a few relatively strong acidic sites, that decrease with increasing the irradiation dose.

Distribution Studies

The sorption behaviour of ^{22}Na, ^{134}Cs, ^{85}Sr, ^{60}Co and $^{152,154}Eu$ from a mixed solution at $10^{-4}M$ nitric acid media (for each ion), on the different CeSb or SnSb samples from is

TABLE II. CAPACITY FOR Na^+ AND Cs^+ IONS ON VARIOUS TIN(IV) ANTIMONATE SAMPLES DRIED AT DIFFERENT TEMPERATURES

Sb/Sn ratios	Heating temperature, (°C)	% of water content, (wt)	Capacity (meq/g)	
			Na^+	Cs^+
0.5	50	15.45	1.09	0.83
	200	12.72	0.89	0.73
	400	3.44	1.16	0.89
	600	1.22	0.051	0.017
0.59	50	17.70	1.35	1.17
	200	12.23	1.23	1.07
	400	5.61	1.41	1.29
0.67	50	18.83	1.41	1.23
	200	12.24	1.37	1.12
	400	6.55	1.47	1.31
1.43	50	17.48	1.44	1.28
	200	12.32	1.39	1.22
	400	5.61	1.51	1.35

TABLE III. CAPACITY VALUES FOR UNIRRADIATED SAMPLES AT 25±1°C

	Capacity for CeSb (meq/g)			Capacity for SnSb (meq/g)		
Cation	Unirradiated	1 MGy	1.3 MGy	Unirradiated	4.4 MGy	6.4 MGy
Na+	1.261	1.18	1.124	1.09	1.07	0.997
Cs+	1.060	1.01	0.975	0.83	0.77	0.768

described in terms of the distribution coefficient (K_d ml g^{-1}) of the individual cations under comparable experimental conditions (Tables IV & V). These tables showed that the selectivity of the exchanger increased with the Sb/Ce and Sb/Sn ratios. The selectivity decreased in the order, $Eu^{3+} > Co^{2+} > Sr^{2+} > Cs^+$ for SnSb and $Eu^{3+} > Sr^{2+} > Cs^+ > Na^+$ for CeSb.

Tables VI, VII show that the sorption uptake of Eu^{3+} decreases with the heating temperature up to 200°C. At 400°C, it is seen that the sorption generally increases in agreement with the apparent capacity measurements.

Separation factors between Eu^{3+}, Sr^{2+} and Cs^+ have been improved by γ-irradiation of CeSb and SnSb (Tables VIII & IX). The data given in these tables showed that the K_d values decreased with increasing absorbed dose.

TABLE IV. K_D OF Na^+, Cs^+, Sr^{2+}, Eu^{3+} IN HNO_3 MEDIA ON CeSb OF DIFFERENT Sb/Ce MOLAR RATIOS AT 25°C

$[HNO_3]$	Na^+ Sb:Ce				Cs^+ Sb:Ce				Sr^{2+} Sb:Ce				Eu^{3+} Sb:Ce			
M	0.5	0.75	1.33	2.39	0.5	0.75	1.33	2.39	0.5	0.75	1.33	2.39	0.5	0.75	1.33	2.39
0.1	27	53	107	255	190	265	430	511	5030	10100	10500	V.H	V.H	V.H	V.H	V.H
0.25	11.5	23.8	44	100	83	115	165	220	855	1339	2790	6150	V.H	V.H	V.H	V.H
0.5	6.25	12	22	52	44	63	91	116	198	451	625	1470	2800	7000	25000	V.H
1.0	3.5	6	13	17	23	35	49	59.5	52	110	160	360	360	820	3150	5100
2.0	1.8	3.3	5	13.8	13	17.5	25	31	13.5	25	37.5	85	47.5	115	350	590
3.0	1.2	2.4	3.5	9	8.8	12	16.5	21	6	12	15.5	37	15.3	48	105	165
4.0	1.0	1.5	2.85	6.8	6.75	9.8	13.8	16.5	3.4	7	8.5	29.5	6.7	13	48	72
6.0	0.7	1.2	1.9	4.8	4.8	6.5	9	11	1.6	3.4	3.8	9	1.9	3.6	13	20.5

TABLE V. K_d VALUES OF Cs^+, Sr^{2+} AND CO^{2+} IN HNO_3 MEDIA ON SnSb OF DIFFERENT Sb/Sn MOLAR RATIOS AT 25°C

$[HNO_3]$,	Cs^+ Sb:Sn				Sr^{2+} Sb:Sn				Co^{2+} Sb:Sn			
M	0.5	0.59	0.67	1.43	0.5	0.59	0.67	1.43	0.5	0.59	0.67	1.43
0.1	1000	1203	1370	1800	15000	--	--	--	>20000	--	--	--
0.5	181	241	270	342	850	1105	1300	1500	1146.9	1600	1700	2587
1.0	95	116	135	171	220	275	312	375	288.2	400	440	651
3.0	32	3.8	43.7	57	25.8	31	36.5	39.3	32.6	45	50	73
4.0	23	28.7	32.5	43	15.9	16.2	21	23.7	19.5	27	28	43

TABLE VI. K_d VALUES OF Eu^{3+} IN HNO_3 MEDIA ON CeSb AT DIFFERENT Sb/Ce MOLAR RATIOS AND DRYING TEMPERATURES

[HNO_3],	Sb:Ce=0.75 drying tempeature;			Sb:Ce=1.33 drying temperature;			Sb:Ce=239 drying temperature			Sb:Ce=2.39 drying temperature;		
M	50°C	200°C	400°C	50°C	200°C	400°C	50°C	200°C	400°C	50°C	200°C	400°C
0.5	2800	2312	5000	7000	3400	V.H	25000	10023	V.H	V.H	V.H	V.H
1.0	360	291	660	820	425	2650	3150	1220	7500	5100	1915	10200
1.25	195	155	340	520	198	1250	1600	623	3500	2225	977	5600
2.0	47.5	39	88	115	55	280	350	156	725	590	267	1300
3.0	15.3	11.5	28.5	48	17.2	90	5	44	230	165	75	380
4.0	6.7	5.1	12.5	13	7.5	39.5	48	8.5	96	72	32.6	163
6.0	1.9	1.65	4.2	3.6	2.4	11	13	5.5	28	20.5	10.2	45

TABLE VII. K_d VALUES OF Eu^{3+} IN HNO_3 MEDIA ON SnSb AT DIFFERENT Sb/Sn MOLAR RATIOS AND DRYING TEMPERATURES

[HNO_3]	Sb:Sn=0.5 drying temperature;			Sb:Sn=0.59 drying temperature;			Sb:Sn=0.67 drying temperature;			Sb:Sn=1.43 drying temperature;		
M	50°C	200°C	400°C	50°C	200°C	400°C	50°C	200°C	400°C	50°C	200°C	400°C
0.1	≥10000	--	--	--	--	--	--	--	--	--	--	--
0.5	1800	660	2800	2402	777	3305	2600	1110	3951	4800	2800	5989
1.0	263.5	77.5	34.0	390	93	453	340	134	514	590	335	805
3.0	11.1	3.2	15.2	121	3.8	19	14	5.4	21	23	13.5	30.5
4.0	5	1.3	6.67	5.8	1.7	8.3	6	2.3	8.9	10.1	6	13

TABLE VIII K_d VALUES AND SEPARATION FACTOR (a) OF CERTAIN RADIONUCLIDES ON CeSb IN HNO_3 MEDIUM AT 25^0C

γ-doses	Unirradiated				1MGy				1 3MGy			
	K_d mL/g, (a)				K_d mL/g, (a)				K_d mL/g, (a)			
pH	Cs^+	Sr^{2+}	Co^{2+}	Eu^{3+}	Cs^+	Sr^{2+}	Co^{2+}	Eu^{3+}	Cs^+	Sr^{2+}	Co^{2+}	Eu^{3+}
1 02	253	1110	4000	1520	201	930	3570	1400	155	775	3139	630
		(4 4)	(15 8)	(6)		(4 6)	(17 8)	(7)		(5)	(20 3)	(4 1)
		(3 6)	(1 4)			(3 8)	(1 5)				(4 1)	(0 8)
			(0 4)				(0 4)					(0 2)
2 05	580	1503	4330	3600	498	1270	3800	3300	411	950	3300	1379
		(2 6)	(7 5)	(6 2)		(2 6)	(7 6)	(6 6)		(2 3)	(8 0)	(3 4)
			(2 9)	(2 4)			(3)	(2 6)			(3 5)	(1 5)
				(0 8)				(0 9)				(0 4)
2 89	1400	2100	4950	8750	1197	1650	4400	8250	1000	1198	3850	3100
		(1 5)	(3 5)	(6 3)		(1 4)	(3 7)	(6 9)		(1 2)	(3 9)	(3 1)
			(2 4)	(4 2)			(2 7)	(5)			(3 2)	(2 6)
				(1 8)				(1 9)				(0 8)
3 97	2700	2500	5600	19800	2200	2020	4970	18700	1700	1370	4400	6750
		(0 9)	(2 1)	(7 3)		(0 9)	(2 3)	(8 5)		(0 8)	(2 6)	(4)
			(2 2)	(7 9)			(2 5)	(9 3)			(3 2)	(4 9)
				(3 5)				(3 8)				(1 5)
4 93	4450	2820	6500	V H	3400	2400	5850	V H	2880	1500	5300	V H
		(0 6)	(1 5)			(0 7)	(1 7)			(0 5)	(1 8)	
			(2 3)				(2 4)				(3 5)	

TABLE IX K_d VALUES AND SEPARATION FACTOR (a) Cs^+, Sr^{2+}, Co^{2+} and Eu^{3+} in HNO_3 MEDIUM ON SnSb AT DIFFERENT ADSORBED γ-DOSES AT 25 ± 1^0C

γ doses	Unirradiated				4 4 MGy				6 4MGy				99 8MGy			
$[HNO_3]$,M	K_d mL/g, (a)				K_d mL/g, (a)				K_d mL/g, (a)				K_d mL/g, (a)			
	Cs^+	Sr^{2+}	Co^{2+}	Eu^{3+}	Cs^+	Sr^{2+}	Co^{2+}	Eu^{3+}	Cs^+	Sr^{2+}	Co^{2+}	Eu^{3+}	Cs^+	Sr^{2+}	Co^{2+}	Eu^{3+}
0 1	1000	1500 0	=20000	=10000	650	11136	9503	>10000	569	10104	8828	>10000	578	95550	8901	>10000
		(15)	(20)	(4 1)		(17)	(14 6)	(15 4)		(17 8)	(1 5)	(17 6)		(16 5)	(15 4)	(17 3)
			(1 3)	(0 8)			(0 9)	(0 9)			(0 9)	(1)			(0 9)	(1)
				(0 2)				(1 1)				(1 1)				(1 1)
0 5	181	850	1146 9	1800	99 5	380	360 5	110	110	370	379	1070	103	359 6	361	939 5
		(4 7)	(6 3)	(9 9)		(3 8)	(3 6)	(11 1)		(3 4)	(3 4)	(9 7)		(3 5)	(3 5)	(9 1)
			(1 3)	(2 1)			(0 9)	(2 9)			(1)	(2 9)			(1)	(2 6)
				(1 6)				(3 1)				(2 8)				(2 6)
1 0	95	220	288 2	263 5	55 4	92	95	149	54 3	95 3	93 8	160	53 1	95	94 6	159 7
		(2 3)	(3)	(2 6)		(1 7)	(1 7)	(2 7)		(1 8)	(1 7)	(2 9)		(1 8)	(1 8)	(3)
				(0 9)				(1 6)				(1 7)				(1 7)
3 0	32	25 8	32 6	11 1	17 5	10 5	10 5	8 1	17	9 98	11	6 8	18	12 48	10 8	6 1
		(0 8)	(1)	(0 3)		(0 6)	(0 6)	(0 5)		(0 6)	(0 6)	(0 4)		(0 7)	(0 6)	(0 3)
			(2 3)	(0 4)			(1)	(0 8)			(1 1)	(0 7)			(0 9)	(0 5)
				(0 3)				(0 8)				(0 6)				(0 6)
4 0	23	15 9	19 5	5	10 1	6 3	6	3 1	11 3	6	6 1	2 9	10 2	7 39	5 7	3 3
		(0 7)	(0 8)	(0 2)		(0 6)	(6 6)	(0 3)		(0 5)	(0 5)	(0 2)		(0 7)	(0 6)	(0 3)
			(1 2)	(0 3)			(1)	(0 5)			(1)	(0 5)			(0 8)	(0 4)
				(0 3)				(0 5)				(0 5)				(0 6)

Isotopic Exchange

As was mentioned in the previous reports [1,2], the rate of isotopic exchange of Cs^+, Sr^{2+} and Co^{2+} from 0.1M solution of metal ions on cerium (IV) or tin (IV) antimonates was followed by the variation of Qt/Qe with time for its exchange in the different samples. The plots of F and Bt versus t for all metal ions investigated are studied in detail in the previous reports (1,2). Only Co^{2+}/*Co^{2+} exchange on tin(IV) antimonate (Fig. 1) is discussed here for the sake of brevity. The values of D for the metal ions investigated, were calculated from these figures and are given in Tables X & XI. These tables show that D for Cs^+, Sr^{2+} and Co^{2+} increases with increase of heating temperature from 50 to 400°C. This seems to be mainly related to the pore sizes.

Tables X & XI, show that the D value for Cs^+, Sr^{2+} and Co^{2+} decrease with pH values and increasing capacities on CeSb and SnSb. This may be due to the involvement of narrower pores at the high pH values.

The effect of reaction temperature on the rate of isotopic exchange was studied for the samples heated at 50, 200 and 400°C using 0.1M metal ion solutions. The rate of the exchange reactions increased with the reaction temperatures. The self diffusion values of Cs^+, Sr^{2+} and Co^{2+} are summarized in Tables X & XI for both materials. When log D was plotted against

TABLE X SELF DIFFUSION COEFFICIENT, ACTIVATION ENERGY AND ENTROPIES OF ACTIVATION OF Cs^+/*Cs^+, Sr^{2+}/*Sr^{2+} AND Co^{2+}/*Co^{2+} ON CERIC ANTIMONATE (AVERAGE PARTICLE SIZE 0 27±0 02 mm) AT 30°C

Exchange system	pH	Heating Temp (oC)	$D \times 10^9$ cm^2s^{-1}			D_o	E_a	ΔS*
			30°C	45°C	60°C	cm^2s^{-1}	KJ moL^{-1} -	J $moL^{-1}K^{-1}$
Cs^+/*Cs^+	5 6	50	0 76	1.34	1.99	1 21	18 235	-86.25
		200	1 014	1 394	2 02	0 556	15 609	-92 72
		400	1 394	1 902	2 515	0 243	12 764	-99 60
Sr^{2+}/*Sr^{2+}	5 6	50	20 7	29.5	36 5	11 32	15 601	-67 63
		200	23.9	40 7	69 0	374 9	23 930	-38 55
		400	38.8	64 7	85.8	22 737	22.737	-38 54
	3 0	50	22.3	36.2	46 5	50 77	19 147	-55 18
		200	25.91	42 70	69 9	116 81	20.812	-34 72
		400	37 90	69.01	134 5	595.00	23 940	-48 23
Co^{2+}/*Co^{2+}	3 68	50	22 43	36.23	55 21	96 41	20 678	-49 85
		200	21 87	34 51	48 31	29 60	17 37	-59 65
		400	25 90	46 61	86 20	568 0	24 731	-35 10

TABLE XI SELF DIFFUSION COEFFICIENT, ACTIVATION ENERGY AND ENTROPIES OF ACTIVATION OF $Cs^+/{}^*Cs^+$, $Sr^{2+}/{}^*Sr^{2+}$ AND $Co^{2+}/{}^*Co^{2+}$

Exchange system	Heating temperature (°C)	Dx10^9 cm^{2}s^{1}			D_o	E_a	ΔS*
		30°C	45°C	60°C	cm^{2}s^{1}	KJ moL^{1}	J moL^{1}K^{1}
$Cs^+/{}^*Cs^+$	50	12 32	41 20	50 11	1 322x10^{4}	21 70	-47 22
	200	36 90	56 29	84 40	2 30x10^{4}	22 00	-42 26
	400	53 30	82 40	121 6	3 03X10^{4}	22 526	-40 32
SR^{2+}/Sr^{2+}	50	0 92	1 54	2 02	1 17X10^{7}	11 97	-105 7
	200	1 20	1 82	2 47	3 62x10^{7}	13 68	-97 80
	400	1 65	2 47	3 42	5 45x10^{7}	14 36	-92 88
$Co^{2+}/{}^*Co^{2+}$	50	1 13	1 69	2 37	2 26X10^{-6}	19 15	-81 06
	200	2 25	3 76	5 63	1 17x10^{4}	27 35	-48 24
	400	2 91	6 09	2 92	1 28x10^{3}	32 74	-28 35

1/T for $Co^{2+}/{}^*Co^{2+}$ exchange, straight lines were obtained (Figs. 2,3) enabling estimation of the activation energy (E_a) and the pre-exponential constant (D_o). The relatively small activation energy values given in Tables X & XI for the different cations suggest that the rate is particle diffusion controlled The negative values for the entropy of activation suggests that upon exchange of that cations, no significant structure change occurs in cerium and tin (IV) antimonates [20-24]

Chemical In-Situ Precipitation

This investigation was mainly carried out to find the best conditions for the removal of elements through the formation of insoluble salts or their retention by the precipitate, considering that the precipitate itself may act as an ion exchanger.

Several in-situ precipitations of metal cations (M) with SnSb or CeSb were investigated The uptake of each of cations Na, Cs, Sr, Co and Eu is relatively high (Tables XII & XIII) The capacities of the product precipitate itself, acting as ion-exchanger with different selectivities for Na^+ and Cs^+, as given in Tables XIV and XV. The in situ chemical precipitation for each of radwaste or for mixed radwaste with CeSb or SnSb was carried out The uptake and decontamination factor of these elements are given in Tables XII & XIII

When these precipitates are treated with different nitric acid concentrations the metal ions in-situ precipitated with SnSb or CeSb are released to different amounts (Figs 4,5)

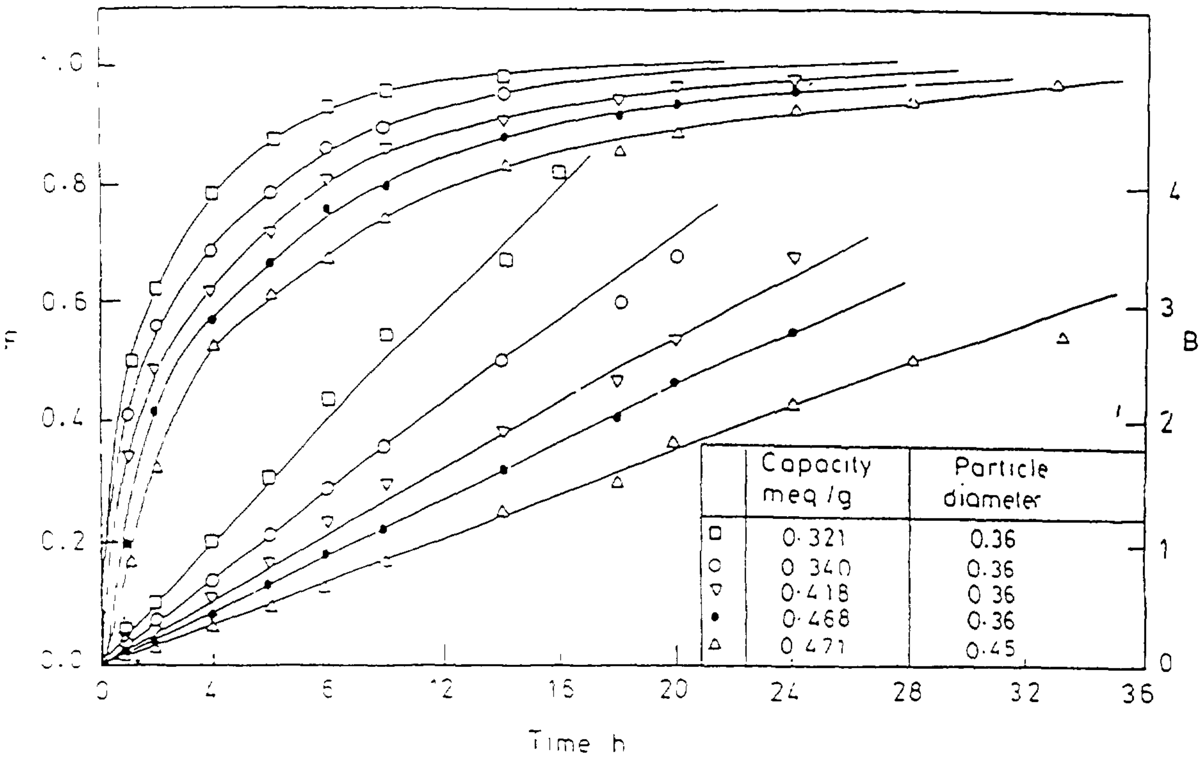

FIG. 1. Variation of F with time for isotopic exchange of cobalt ion on tin (IV) antimonate heated at 50, 200 and 400°C at different particle sizes and capacities

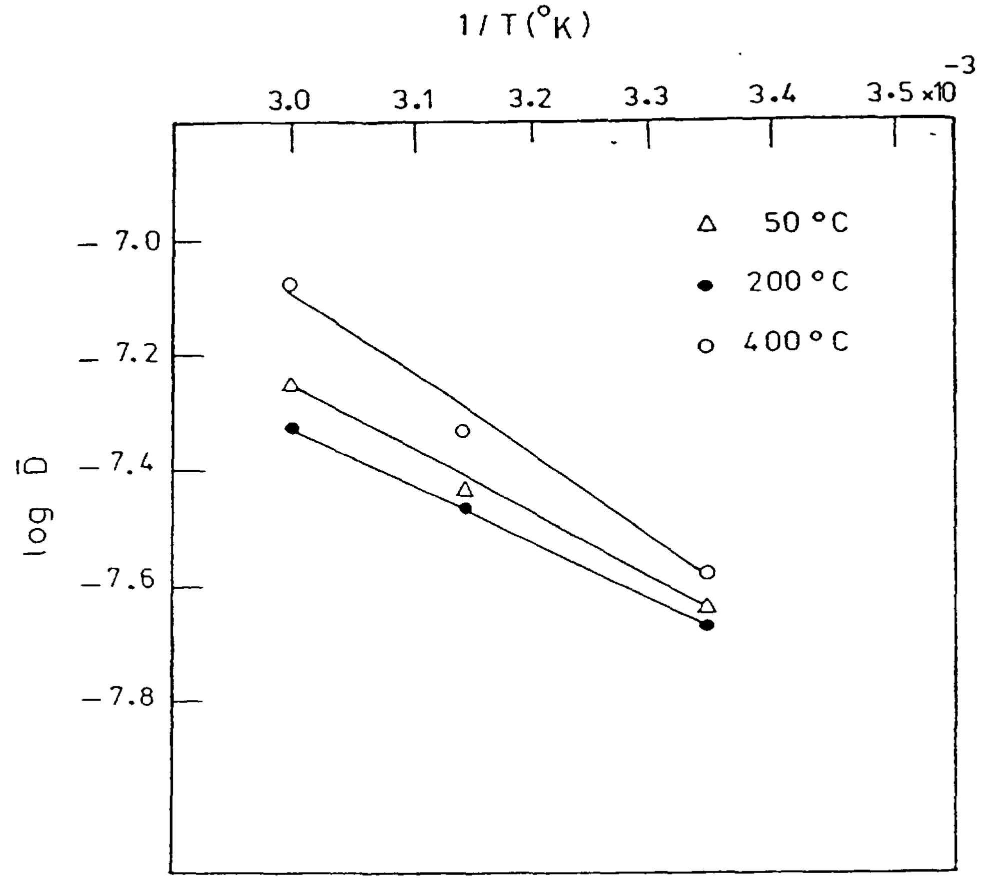

FIG. 2. Dependence of log D on 1/T for isotopic exchange of Co^{2+}oin cerium (IV) antionate dried at 50,200 and 400°C at pH=3.68

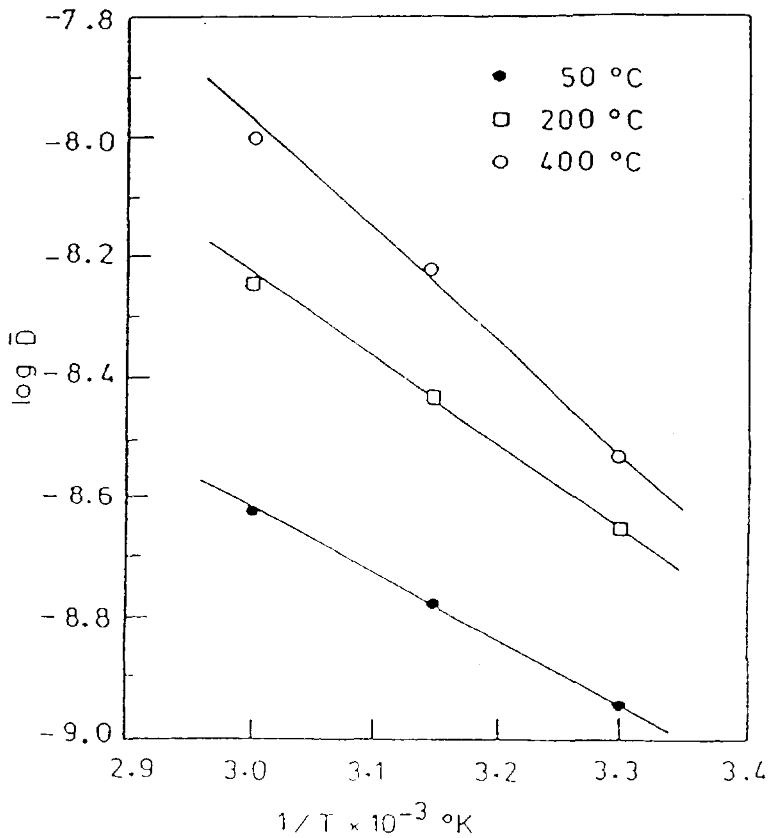

FIG. 3. Dependence of log D on 1/T for isotopic exchange of Co^{2+} antimonate heated at 50, 200 and 400°C

TABLE XII. IN-SITU PRECIPITATION OF ^{60}Co, ^{134}Cs, ^{22}Na, $^{152+154}$Eu AND ^{85}Sr WITH CERIUM (IV) ANTIMONATE

Element	% uptake	D.F.
Co-60	83.5	6.08
Cs-134	81.14	5.3
Na-22	80.43	5.11
Eu-152+154	72.18	3.59
Sr-85	87.79	8.19

TABLE XIII. IN-SITU PRECIPITATION OF ^{60}Co, ^{134}Cs, ^{22}Na, $^{152+154}$Eu AND ^{85}Sr WITH TIN(IV) ANTIMONATE SAMPLES.

Element	% uptake	D.F.
Co-60	75.81	4.14
Cs-134	60.87	2.56
Eu-152+154	89.79	6.53
Sr-85	87.79	8.19

TABLE XIV. WATER CONTENT, Cs^+ AND Na^+ CAPACITIES AND X-RAY DIFFRACTION OF DIFFERENT IN-SITU PRECIPITATES

Exchanger	Water content %	Capacity		X-ray diffraction
		Cs^+	Na^+	
CeSb	13 39	0 47	1 46	amorphous
CoCeSb	15 48	0 48	1 72	,,
CsCeSb	17 23	0 52	1 84	,,
NaCeSb	17 7	0 1038	0 1570	,,
EuCeSb	15 9	0 29	1 68	,,
SrCeSb	15 29	0 47	1 65	,,

TABLE XV WATER CONTENT AND CAPACITIES Cs^+ AND Na^+ AND X-RAY DIFFRACTION OF DIFFERENT IN-SITU PRECIPITATES

Exchanger	Water content %	Capacity		X-ray diffraction
		Cs^+	Na^+	
SnSb	15 42	0 72	0 94	amorphous
CoSnSb	14 62	0 66	0 72	,,
CsSnSb	18 12	0 69	1.34	,,
EuSnSb	18 66	0 72	1 65	,,
SrSnSb	13 98	0 46	0.67	,,

The capacities of the treated precipitate (H-form) were determined and are given in Tables XVI & XVII The capacities are less compared to the capacities of the untreated precipitate (M-form) Figures 4, 5 and Tables XVI, XVII show that some of the metal ions precipitate with SnSb or CeSb and are captured inside the precipitate From the above mentioned, we deduced the possible repeated use of these materials for removal of radioactive nuclides from waste solutions

TABLE XVI CAPACITIES FOR THE UNTREATED AND THE 8M HNO_3 TREATED M-CeSb

Exchanger	Capacities for the untreated samples,meq/g		Capacities for the samples treated by 8M HNO_3,meq/g	
	Cs^+	Na^+	Cs^+	Na^+
Cs*CeSb	0 52	1 84	0 39	0 421
Co*CeSb	0 48	1 72	0 43	0 382
Sr*CeSb	0 47	1 65	0 41	0 401

TABLE XVII CAPACITIES FOR THE UNTREATED AND THE 8M HNO_3 TREATED M-SnSb

Exchanger	Capacities for the untreated samples,meq/g		Capacities for the samples treated by 8M HNO_3,meq/g	
	Cs^+	Na^+	Cs^+	Na^+
Cs*SnSb	0 69	1 34	0 01	0 08
Co*SnSb	0 66	1 62	0 27	0 52
Sr*SnSb	0 46	1 67	0 22	0 41
Eu*SnSb	0 72	1 65	0 35	1 53

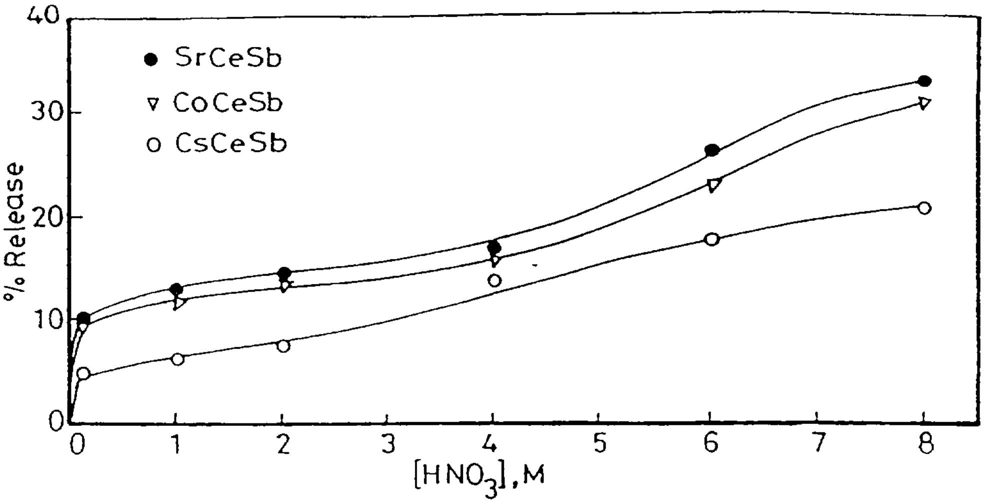

FIG. 4. Elution of different cations (^{134}Cs, ^{60}Co and ^{85}Sr) in-situ precipitated with CeSb at different [HNO_3]

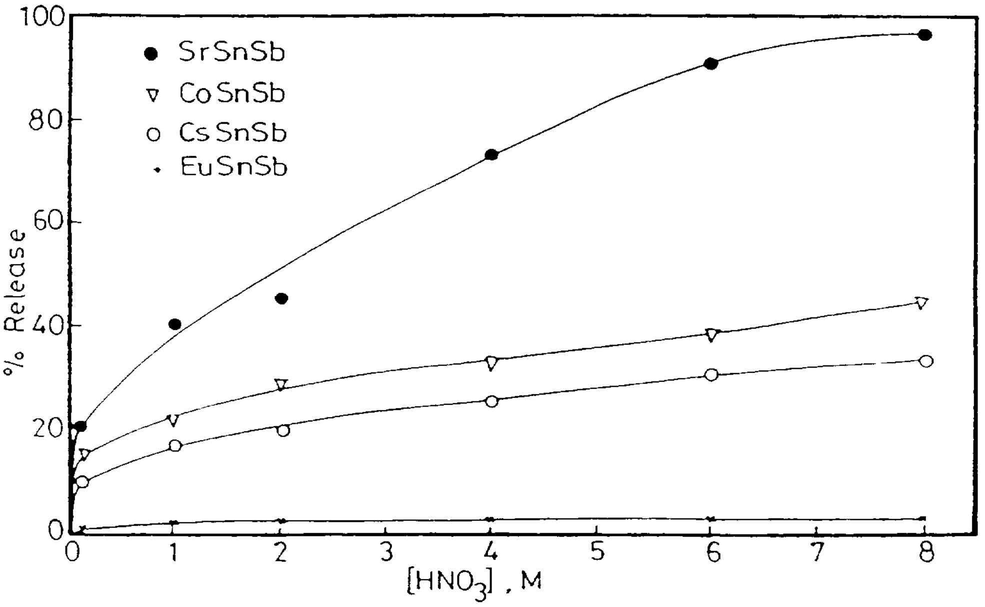

FIG. 5. Elution of different cations (^{134}Cs, ^{60}Co, ^{85}Sr and ^{152,154}Eu) in-situ precipitated with SnSb at different [HNO_3]

Column Operation:

The exploration of the possibilities of use of CeSb and SnSb in separation of some radionuclides from each other and from solutions of high $NaNO_3$ and/or HNO_3 concentrations was investigated.

Amounts of 1g CeSb of the sample that received the highest absorbed dose (1.3MGy) in 10 mL of water were packed into identical chromatographic columns of 0.5 cm diameter forming a bed of 4.50 cm length. 5mL of the tracer solution (Cs-Sr, Cs-Co and Cs-Eu) at a constant metal ion concentration in 10^{-5}M HNO_3 were separately loaded onto the columns at a flow rate of 0.5 mL/min. Column runs were conducted by collecting and counting equal effluent fractions at the same flow rate.

Figure 6 depicts separate breakthrough curves for Cs^+, Sr^{2+} and Eu^{3+} solutions at an initial concentration of 10^{-4}M for each of them and a flow rate of 0.5 mL/min. It is clear that the retention sequence of the individual cations is consistent with that obtained in the batch equilibration experiments ($Eu^{3+} > Sr^{2+} > Cs^+$).

Regeneration of the adsorbent from the retained metal ions was achieved by passing 20 mL of 3M HNO_3 through the exchanger bed at a flow rate of 1 mL/min^{-1}. The exchanger was found to be durable for more than 10 sorption/desorption cycles without measurable changes in its physical and ion exchange properties.

A throrough examination of the results given in Fig. 6 suggests some useful radiochemical separations of the couples Cs^+-Sr^{2+}, Cs^+-Eu^{3+} and Cs^+-Co^{2+}. Using the previously mentioned chromatographic columns, quantitative loading of the specific mixture from 10^{-5}M HNO_3 solutions was obtained. Clean separation of Cs was achieved on passing 10 mL of 1 M HNO_3 through the column. Elution of the other tracer elements was carried out with 3M HNO_3. Examples of the elution profiles produced are given in Figure 7.

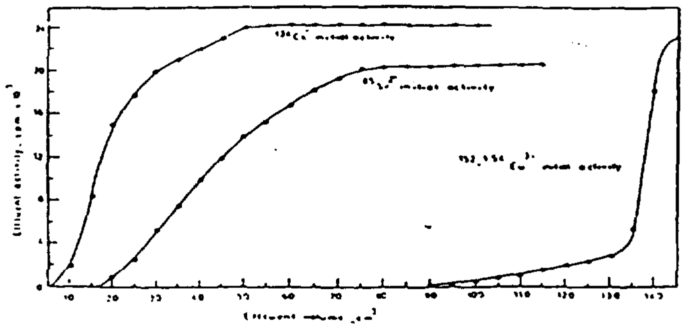

FIG. 6. Breakthrough curves of mixture of CS^+, Sr^{2-} and Eu^{3-} (10^{-4}M for each) in 1 M HNO_3 solutions containing 5 × 10^3

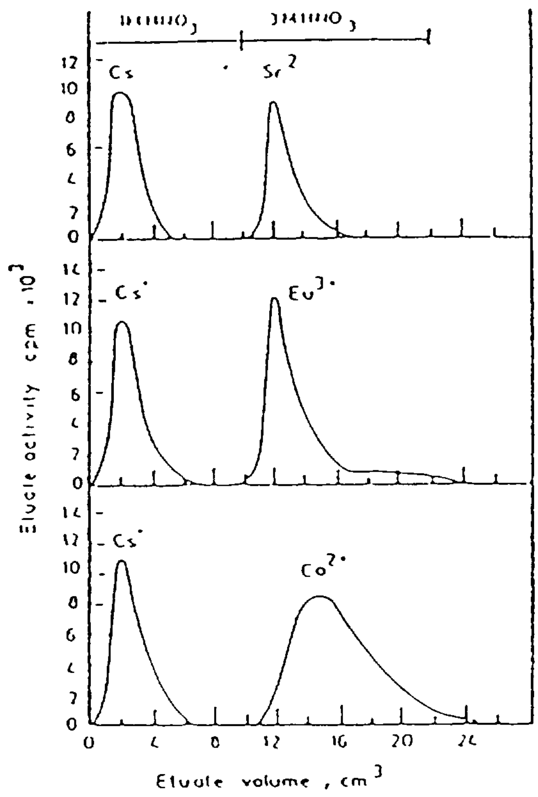

FIG 7 Elution Curves of Cs-Sr, Cs-Eu and Cs-Co Couples with 1M and 3M HNO3 solutions from 1g columns of irradiated cerium (IV) antimonate (1 3 MGy absorbed dose, 0 12-0-24mm mesh size, 0 5 cm diameter, 4 5 cm length and 0 5 cm^3/min flow rate)

ACKNOWLEDGEMENT

This work was performed with partial financial support, under auspices of the International Atomic Energy Agency (IAEA), under contract No 2713/RB The Agency interest and support in this work is gratefully acknowledged

REFERENCES

[1] EL-NAGGAR, I M , EL-ABSY, M A , ABDEL-HAMID, M M , EL-DESSOUKY, M I , ZAKARIA, E S , ALY, H F , 1st Progress report submitted to IAEA, Research Contract No 7213/RB (1993)
[2] EL-NAGGAR, I M , ZAKARIA, E S , EL-ABSY, M A , ABDEL-HAMID, M M , ABO-MESALAM, M M , SHADY, S A , ABDEL-MEGUID, M M , ALY, H F , 2nd progress report submitted to IAEA, Research Contract No 7213/RB (1994-1995)
[3] VESELY, V , PEKAREK, V Talanta, 19, 219 (1972)
[4] PEKAREK, V , VESELY, V , Talanta, 19, 12 (1972)
[5] FULLER, M J , Chromatogr Rev 14, 45 (1971)
[6] EL-NAGGAR, I M , EL-DESSOUKY, M I , ALY, H F , "International Conference on Nuclear Waste Management and Environmental Remediation, Prague, Sept 5-11 (1993)
[7] ABO-MESALAM, M M , m Sc Thesis, Ain Shams Univ , Cairo, Egypt (1993)
[8] ALY, H F , EL-ABSY, M A , ZAKARIA, E S , EL-NAGGAR, I M , International Conference on Radioactive Waste Management and Environmental Remediations, Berlin, Germany, Sept 3-7 (1995) Vol 1, p 371

[9] EL-NAGGAR, I M , ABDEL-HAMID, M M , SHADY, S A , ALY, H F , InternationalConference on Radioactive Waste Management and Environmental Remediation, Berlin, Germany, Sept 3-7 (1995) Vol 1, p 367

[10] EL-NAGGAR, I M , EL-ABSY, M A , SALAMA, H N , EL-WAHAB, M A , SOUKA, N , Radiochim Acta, 6291 (1993)

[11] EL-NAGGAR, I M , ABDEL-HAMID, M M , ALY, H F , "Solv Extr Ion Exch , 12, 651 (1994)

[12] ZAKARIA, E S Ph D Thesis, Ain Shams Univ , Cairo, Egypt (1994)

[13] ABDEL-MEGUID, A M , M Sc Thesis, Cairo Univ , Cairo, Egypt, (1995)

[14] EL-NAGGAR, I M , EL-DESSOUKY, M I , ALY, H F , Reactive Polymer, accepted (1995)

[15] EL-NAGGAR, I M , ZAKARIA, E S , H F , ALY, Reactive Polymer, accepted (1995)

[16] RUVARC, A , "Inorganic Ion Exchange Materials", Editors, A Clearfield, Chap 5, CRC, Florida (1982)

[17] CLEARFIELD, A , PACK, S P , J Inorg Nucl Chem , 42, 137 (1980)

[18] EL-NAGGAR, I M , Ph D Thesis, Ain Shams Univ Cairo, Egypt (1984)

[19] EL-NAGGAR, I M , EL-ABSY, M A , J Radioanal & Nucl Chem Articles, 157, 313 (1992)

[20] RAMAT, J P , THIND, P S , J Phys Chem , 80, 1384 (1976)

[21] EL-NAGGAR, I M , MAGHRAWY, H B , J Radioanal Nucl Chem , Articles, 116, 325 (1987)

[22] MATHEW, J S , Rardon, N , Can J Chem , 55, 3857 (1966)

[23] EL-NAGGAR, I M , EL-DESSOUKY, M I , ALY, H F , Solid State Ionic, 57, 339 (1992)

[24] FREEMAN, D C , STAMIRS, D N , J Chem Phys , 35, 799 (1961)

XA9744280

TESTING AND MODELLING THE PERFORMANCE OF INORGANIC EXCHANGERS FOR RADIONUCLIDE REMOVAL FROM AQUEOUS NUCLEAR WASTE

R. HARJULA, J. LEHTO, A. PAAJANEN, L. SAARINEN
Laboratory of Radiochemistry,
University of Helsinki,
Helsinki, Finland

Abstract

Three different inorganic sorbents/ion exchangers have been tested in this work. Granular hexacyanoferrate-based ion exchanger was developed for Cs removal from radioactive liquid waste at NPPs. It was tested for Cs removal from waste solutions containing different complexing agents an detergents. Radiation stability and thermal stability test has shown, that this sorbent can be used for treatment of medium-active waste treatment. Active carbon materials were tested for Co removal from liquid waste effluents at NPPs. It was found that ^{60}Co cannot be removed from the evaporator concentrates with reasonable efficiency and a combined process with up-stream precipitation step is needed for better Co separation efficiency. Granular modified titanium oxide was tested for ^{90}Sr removal from the waste effluents and showed very high efficiency. A mathematical model was developed to analyse ion exchange performance in feeds of different chemical and radiochemical compositions.

1. TESTING OF Cs TREAT ION EXCHANGER

1.1. INTRODUCTION AND SCOPE OF WORK

CsTreat is a granular hexacyanoferrate-based ion exchanger (supplied by IVO International Ltd.) suitable for fixed-bed column separation of ^{134,137}Cs from radioactive liquid wastes. The CsTreat system is in use at Loviisa NPP, Finland, for removal of ^{137,134}Cs from evaporator concentrates [1,2]. These liquid wastes have high concentrations of $NaNO_3$ (2-3 M), KNO_3 (0.1-0.2 M) and $Na_2B_4O_7$ (0.5 - 1 M). Very high column breakthrough capacities (up to 20 000 bed volumes) have been obtained at Loviisa with high decontamination factor DF (DF > 2000). Two CsTreat systems are being exported by IVO for the treatment of high-salt waste solutions. In addition, a CsTreat system has been used in Paldiski, Estonia, to decontaminate low-salt waste solutions that arose from the operation of training reactors by the former Soviet Navy. In Paldiski, a total of 760 m^3 of waste solution originating from four different storage tanks (^{137}Cs 1.5-200 kBq/L) was treated using a single 12 litre column. This corresponds to a minimum breakthrough capacity of 63 300 bed volumes since at the termination of the purification campaign, when all the waste liquids had been treated, there was no sign of exhaustion of the CsTreat column.

Present industrial scale operating experience demonstrates that CsTreat has a very good performance both in high-and low-salt solutions. The latter case has received additional proof in recent tests at Callaway NPP, USA. Further laboratory testing has been carried out in simulated waste solutions to evaluate the performance of CsTreat for an even wider range of applications, e.g. for the treatment of medium active high-salt solutions and medium salt decontamination solutions. Some of these results are reported in this paper.

Previously, the radiation stability of the ion exchanger has been confirmed up to radiation doses of 5 MGy [3]. This dose arises from ^{137}Cs-loadings of about 1 Ci/kg exchanger, which is the upper limit envisaged for the operation at Loviisa NPP. In order to confirm radiation stability of the material for applications involving higher ^{137}Cs-loadings, further experiments have been carried out up to a dose of 100 MGy.

In order to confirm the safety of hexacyanoferrate in accidental fire or in possible high-temperature vitrification process, the gaseous thermal decomposition products of hexacyanoferrate ion exchanger have been identified [4]. In an earlier study, the solid decomposition products were examined [5].

1.2. TESTING IN SIMULATED WASTE SOLUTIONS

1.2.1 Effect of complexing agents/detergents

The effect of several complexing agents (EDTA, NTA, oxalate) and a detergent builder (Na-polyphosphate) on exchange of ^{134}Cs in hexacyanoferrate has been studied by measuring the distribution coefficients K_D in simulated evaporator concentrate (Table I). The pH of the simulant was adjusted to a range of 6 -12.5. The dose of added complexing agents or detergent builder was 1 g/L and 10 g/L. EDTA and NTA had a strong decreasing effect on the K_D-values of ^{134}Cs above pH of about 10 at a dose of 10 g/L (Fig. 1). Na-polyphosphate seemed to have a slight increasing effect at high pH of 12.5. Oxalate did not have any detectable effect at any pH value covered in the experiments (7-12.6). At a lower dose of 1 g/L no decrease was observed in the K_D for any of the reagents studied.

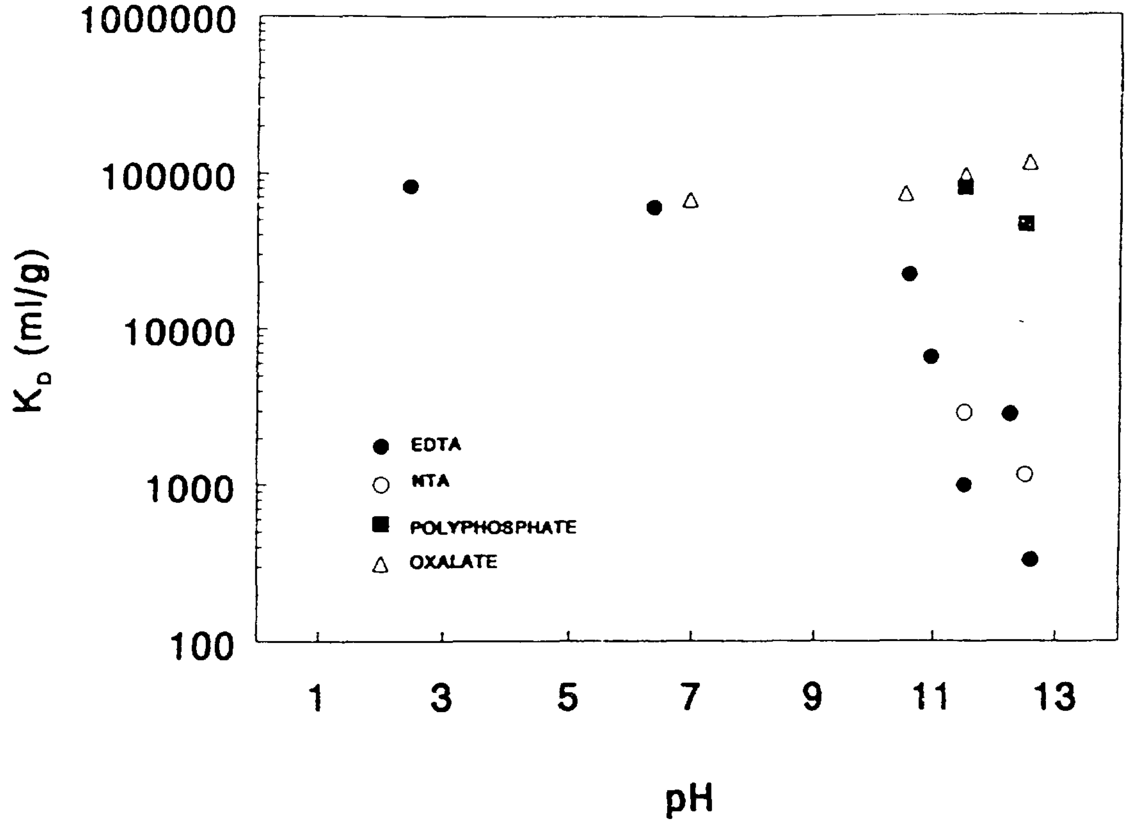

FIG 1. Distribution coefficient K_D of ^{134}Cs as a function of pH for hexacyanoferrate ion exchanger in simulated evaporator concentrates (for composition, see Table I) dosed with 10 g/L of complexing agents and detergent builders.

TABLE I. COMPOSITION OF SIMULATED EVAPORATOR CONCENTRATE

CONSTITUENT	CONCENTRATION
$NaNO_3$	1.75 M
NaOH	0.75 M
$Na_2B_4O_7$	0.25 M
KNO_3	0.2 M
pH	13.4
^{134}Cs	400 kBq/L

TABLE II. CONDITIONS AND RESULTS FOR THE SMALL SCALE COLUMN TESTS.

WASTE TYPE	CONSTITUENTS (g/L)	DF	BREAKTHROUGH CAPACITY
High-salt reprocessing waste	$NaNO_3$ 250 g/L, pH = 10 Cs 0.5 ppm, ^{134}Cs tracer	min. 15 000 max. 30 000	> 4000 BV*
Medium-salt decontamination waste	Na 5.0 g/L, NH_3 0.05 g/L Na-oxalate 0.05 g/L NTA 0.05 g/L, pH = 10 Na-polyphosphate 0.05 g/L, ^{134}Cs tracer	min. 1000 max. 3000	> 4200 BV*
Medium-salt regeneration solution	Na 6.7 g/L, K 3.3 g/L pH = 6 ^{134}Cs tracer	min. 6000 max. 7000	> 2000 BV*
Low-salt NPP waste water	Na 320 ppm, Ca 17 ppm pH = 6 ^{134}Cs tracer	avg. 3000	> 55 000 BV*

BV= bed volumes, *= no breakthrough observed when experiment stopped

1.2.2. Performance in simulated waste solutions

CsTreat has been tested in simulated waste solutions using small scale (bed volume 1-2 cm^3) column experiments. Some of the solution compositions and test results are summarized in Table II.

In all the tests CsTreat showed a very good performance. For practical reasons, most of the experiments were discontinued after a flow of 2000-4000 bed volumes of solutions. Rather high activity concentrations of ^{134}Cs (185 kBq/L) had to be used in the solutions to measure accurately the high decontamination levels. In order to avoid high build-ups of activity in the column, experiments were discontinued even though no breakthrough of ^{134}Cs was observed. However, in certain shielded column experiments as much as 55 000 bed volumes of solution have been treated to date, corresponding to activity loadings of 30 Gbq of ^{134}Cs per kilogram of the CsTreat exchanger.

1.3. RADIATION STABILITY

The radiation stability of hexacyanoferrate exchanger was studied by irradiation with a ^{60}Co-source. The absorbed dose was varied between 5 - 100 MGy by irradiating exchanger samples 8-170 days at a dose rate of 25 kGy/h.

FTIR spectra and XRD patterns of the samples were measured before and after the irradiations and no significant changes could be detected in these experiments even at the highest dose of 100 MGy. In addition, K_D experiments carried out with actual evaporator concentrate from Loviisa NPP showed that the irradiations had no decreasing effect on the ^{134}Cs uptake capacity of the exchanger (Fig. 2).

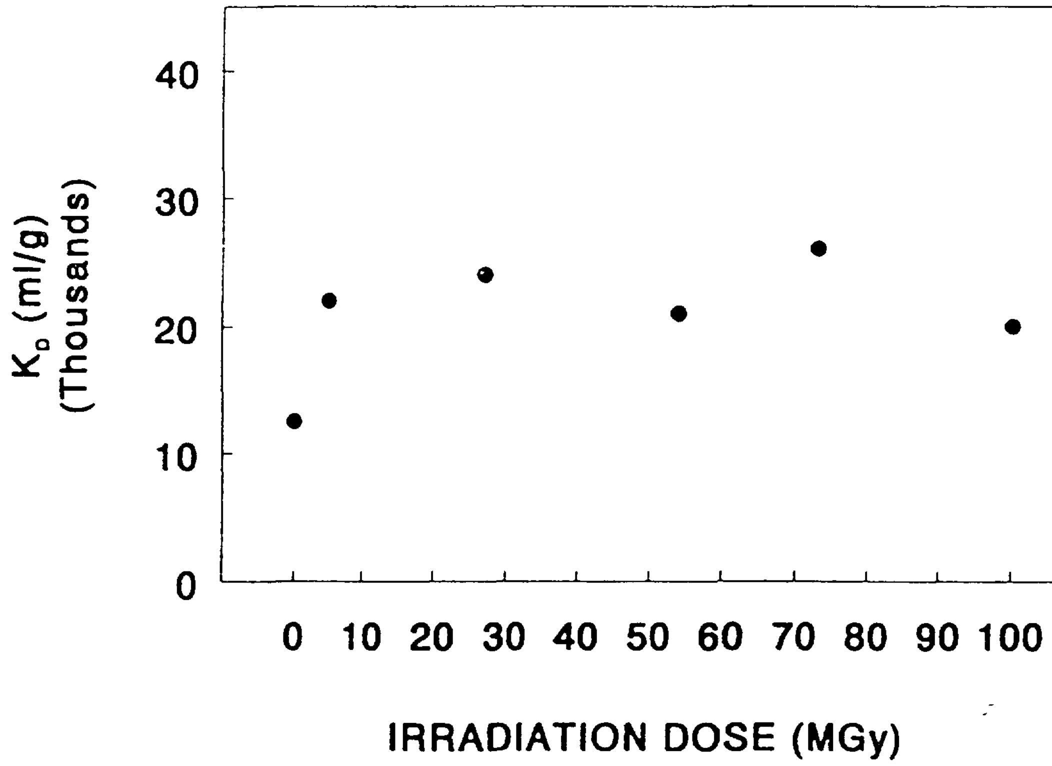

FIG. 2. Distribution coefficient K_D of ^{134}Cs for hexacyanoferrate exchanger in evaporator concentrate solution (Loviisa NPP) after irradiation (^{60}Co-source) with various doses.

These experiments show that at least about 0.75 TBq of ^{137}Cs can be loaded per one kilogram of hexacyanoferrate without detectable loss of uptake capacity for ^{137}Cs or without noticeable structural damage to the material.

1.4. THERMAL DECOMPOSITION

Thermal decomposition of potassium cobalt hexacyanoferrate ($K_2CoFe(CN)_6$), resembling the material in use at Loviisa NPP, was studied by identifying the gaseous decomposition products [4]. $K_2CoFe(CN)_6$ sample was heated through the range of 20-360°C in synthetic air and a FTIR gas detector was used to identify and quantify the evolved gaseous products.

The material lost water in the temperature range of 20-170°C and started to decompose at 240°C. CO_2, N_2O, NO, NH_3 and NO_2 were evolved from the sample above this temperature. The amount of CO_2 released corresponded well to the amount of carbon originally present in the sample. However, the amount of nitrogen containing gases was lower than expected. It is therefore assumed that N_2, which is not IR-active, was released from the material as well.

Highly poisonous HCN gas was not detected. This is important considering accidental fire during storage of material or vitrification of the material in a high temperature process.

1.5. CONCLUSIONS

CsTreat ion exchanger being used at Loviisa NPP for the removal of $^{134,137}Cs$ from high-salt evaporator concentrates is very efficient also for other types of waste solutions. For medium- and low salt solutions the decontamination factors obtainable in column operation are very similar to those obtained for high-salt solutions. In batch tests, common detergent builders, e.g. polyphosphates, interfere slightly with Cs-uptake only when pH is high (pH > 12). The interfering effect of common complexing agents (EDTA, NTA) is large at higher pH's (pH > 10) when the dose is 10 g/L. At lower doses (1 - 0.1 g/L) there seems to be no interfering effect. Column tests carried out at 50 mg/L concentration level did not show any significant effect of these chemicals on the efficiency of the ion exchanger. Radiation stability experiments show that the material is resistant for use in medium-active waste solutions.

2. TESTING OF ACTIVE CARBON MATERIALS FOR ^{60}Co REMOVAL

2.1. INTRODUCTION AND SCOPE OF WORK

In the evaporator concentrates of Loviisa NPP, Finland, the activity concentration of ^{60}Co is usually in the range 1 - 10 kBq/L. However, about 95-98 % of the total radioactivity is usually due to $^{134,137}Cs$ after the liquid has been stored for a few years and thus removal of cesium is sufficient to provide the required decontamination of these liquids for discharge into sea. Occasionally, much higher ^{60}Co levels may be present in the evaporator concentrates. Arising from the primary circuit decontamination campaign in 1995, 250 kBq/L of ^{60}Co is present in the liquid in one of the storage tanks; this is more than the activity concentration of ^{137}Cs in this solution.

2.2. SCREENING TESTS

Previously, a large number of flocculants, precipitants, ion exchangers and adsorbents have been tested for the removal of ^{60}Co from the evaporator concentrates of Loviisa NPP [6]. The composition of the evaporator concentrates are similar to the composition of the simulant in Table I. These static screening tests [6] showed that precipitation with sulphide or adsorption on active carbons were the most efficient methods for removal of ^{60}Co (Table 3). Uptake of ^{60}Co by active carbons varied considerably, being in the range of 7-77 %. This is understandable since the properties of these materials can vary widely depending on the raw material and activation method used. Flocculants and chelating ion exchange resins appeared to be ineffective.

TABLE III. SUMMARY OF SCREENING EXPERIMENTS FOR ^{60}Co REMOVAL.

MATERIAL GROUPS	NUMBER	DOSE	REMOVAL (%)
Flocculants	5	0.1 g/L	0 - 14
Precipitants	5	0.01 mol/L	5 - 90
Ion exchangers	15	10 g/L	0 - 17
Adsorbents	20	10 g/L	7 - 77

2.3. COLUMN EXPERIMENTS

Column experiments with active carbons were carried out with the Loviisa evaporator concentrate both at laboratory scale (bed volume BV = 5.5 cm^3) and at pilot scale at pH = 11.5, which is the target operational pH for the Cs-removal. For the pilot experiments, the Cs-removal plant of Loviisa NPP with its 8 liter columns was used. Laboratory experiments indicated that a very slow flow rate in the order of 1 BV/h would be needed to avoid very early breakthrough of ^{60}Co. Even at such a slow flow rate, the performance of active carbon beds was rather modest (Fig. 3). Instant leakage of ^{60}Co took place from the columns and after 100 bed volumes of liquid had been passed through the column, the breakthrough was 100 % at the laboratory scale and 47 % at pilot scale.

It is obvious that ^{60}Co was present in the evaporator concentrate in some other form than cobalt ions. Calculated from the literature data [7], $Co(OH)_2$ is the dominating Co-species in solution at pH = 11.5. On the other hand, calculations also show that even moderately selective ion exchangers should be able to free the cobalt from this species. Ultrafiltration experiments with a 5 kD membrane have earlier shown 15 % retention of ^{60}Co in the evaporator concentrate. If ^{60}Co is present in the liquid in colloidal form the particle size must thus be very small. It is also possible that evaporator concentrate contained some strong complexing agents for cobalt.

It has proven to be very difficult to remove cobalt efficiently from the Loviisa evaporator concentrate with a single step method. However, by combining several methods, e.g. precipitation and column uptake, it has been possible to remove 95-98 % of ^{60}Co from the solutions.

2.4. CONCLUSIONS

Column adsorption by active carbon alone cannot remove ^{60}Co with reasonable efficiency from the evaporator concentrates. A combined process that includes an up-stream precipitation step would perform with much better separation efficiency but it would require much more complicated process equipment.

3. TESTING OF A MODIFIED TITANIUM OXIDE FOR ^{90}Sr REMOVAL

A method to produce granular modified titanium oxide suitable for column operations has been developed and the material is being produced by IVO International Ltd, Finland, under the trade name SrTreat. This material is highly effective in the removal of ^{90}Sr from concentrated alkaline $NaNO_3$ solutions which are characteristic for nuclear fuel reprocessing plants. In batch experiments, for example, the distribution coefficient was 34,700 ± 8,600 mL/g in 3 M $NaNO_3$ solution at pH of 10.8. The strontium uptake, determined with a batch method equilibrating 1.0 g samples of sodium titanate with 100 mL of 0.03 M $Sr(NO)_2$ solution, was also very high, 5.56 ± 0.20 meq/g.

Column experiments with various nuclear waste simulants have also shown that this titanium oxide product is very efficient in the removal of radioactive strontium and that the granules are sufficiently resistant to be used in packed bed columns (Fig. 4). The optimum operating pH in this sodium ion concentration was 10 and above, at these pH values approximately one thousand bed volumes could be treated with a decontamination factor greater than 1000 (99.9 % removal). Five thousand bed volumes could be treated with a decontamination factor higher than 200 (99.5 % removal).

In more dilute $NaNO_3$ solutions, 0.2 M and 0.002 M, at pH 7, the performance of SrTreat columns was even better (Fig. 5). At least a few thousand bed volumes could be purified with a decontamination factor between 700 and 1000.

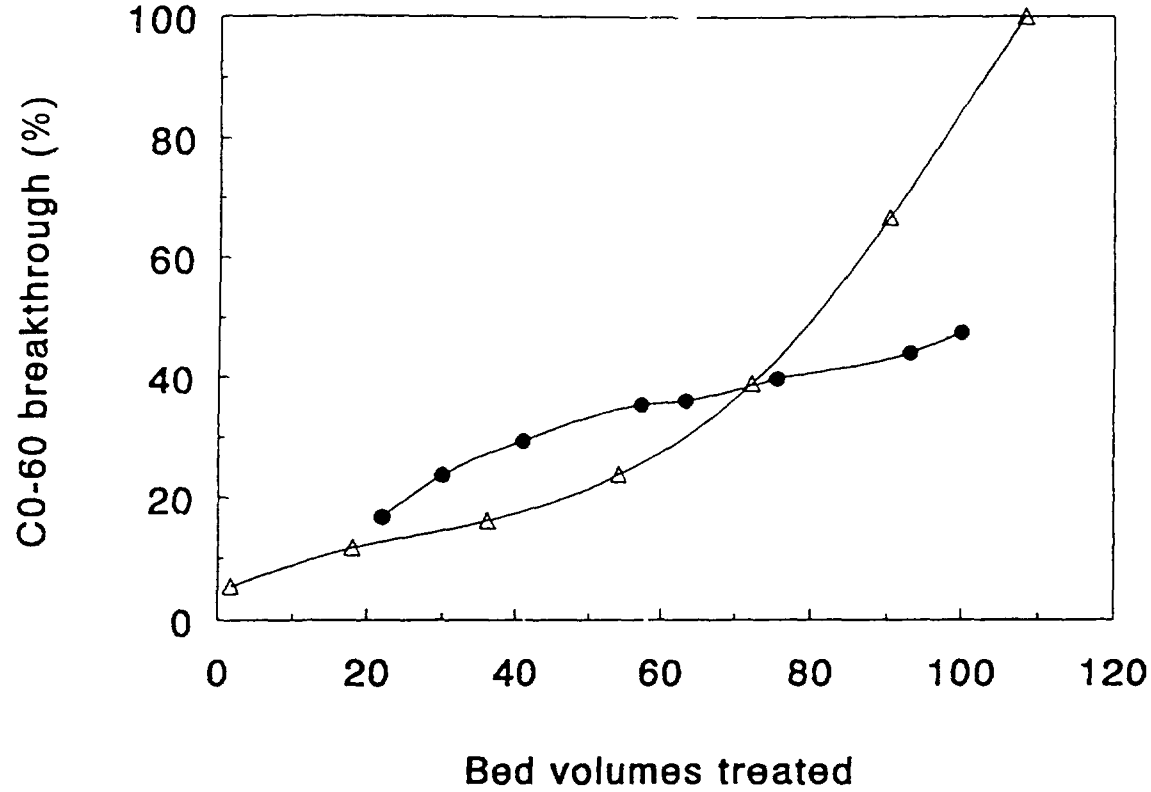

FIG. 3. Breakthrough of ^{60}Co from laboratory scale (Δ, bed volume BV = 5.5 cm^3) and pilot scale (●, BV = 8 L) active carbon columns. Flow rate 1 BV/h.

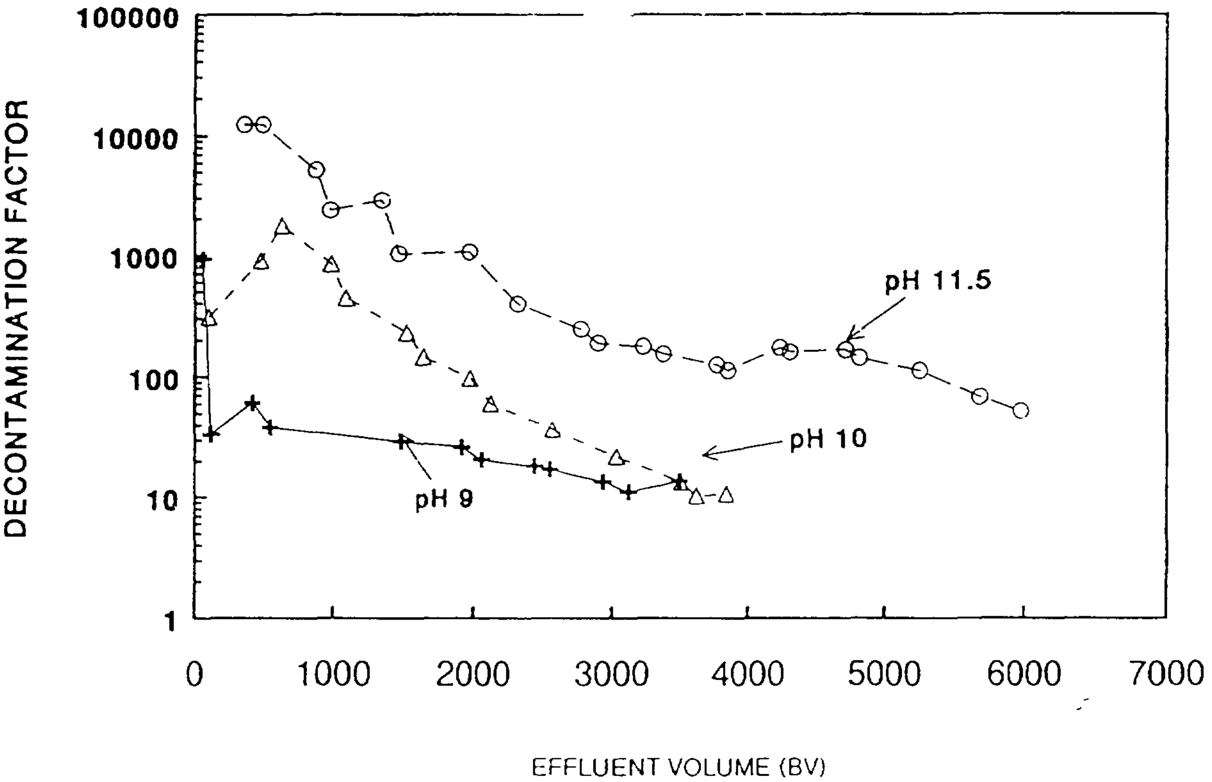

FIG. 4. Decontamination factor for strontium removal by a titanium oxide column as a function of treated 3 M $NaNO_3$ solution volume presented in bed volumes. Initial pH: o = 11.5, Δ = 10, + = 9.

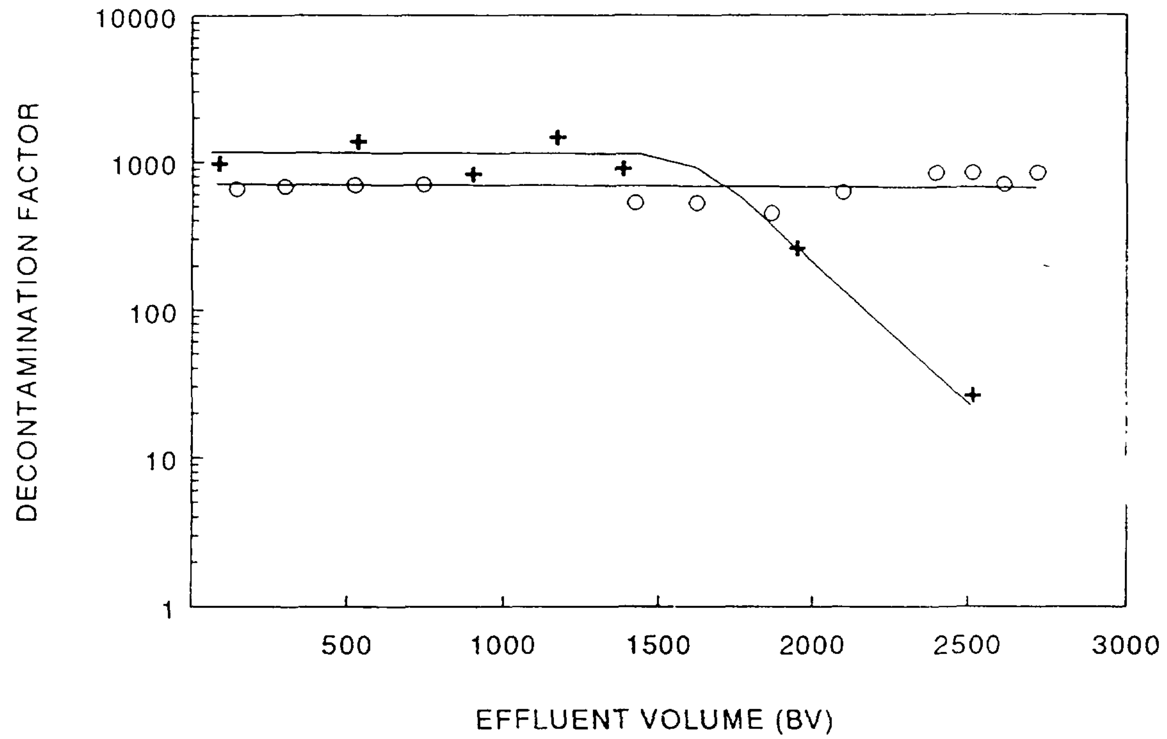

FIG. 5. Decontamination factor for strontium removal by a titanium oxide column as a function of treated $NaNO_3$ solution volume presented in bed volumes. Initial pH 7. o = Na concentration 0.002 mol/L, + = Na concentration 0.2 mol/L.

4. MODELING OF STATIC AND DYNAMIC ION EXCHANGE IN ZEOLITES

4.1. INTRODUCTION AND SCOPE OF WORK

Modeling of ion exchanger performance in feeds of different chemical and radiochemical composition facilitates the application of ion exchangers in industrial processes. In particular in the nuclear field, predictive models are very useful in the design and optimization of ion exchange processes by minimizing the amount of "hot" experiments which can be very expensive and may require considerable time to complete.

Considering ion exchange, nuclear waste solutions contain radioactive ions at very low trace concentrations and a large excess of inactive metal salts (macro-components). Very little data can be found in the literature on the behavior and modeling of such ion exchange systems in which more than two exchanging ions are present.

Zeolites are efficient materials for the removal of many key radionuclides, e.g. ^{137}Cs and ^{90}Sr, from low-salt waste solutions. In addition, zeolites are very suitable materials for the development of ion exchange models, since they have well-known structures and compositions and their ion exchange properties can be adjusted by changing the framework structure and charge density. Modeling studies of several ion exchange systems comprising of several macro- and trace ions are underway in our laboratory. Study of trace ^{134}Cs exchange in mordenite in the presence of macro-concentrations of sodium and potassium has been extended to both static (batch) and dynamic (column) conditions and is given as an example of our modeling work in this report.

4.2. STATIC EXCHANGE CONDITIONS

In the system ^{134}Cs/Na/K it has been found that the distribution coefficient K_D, i.e.

$$K_D = \frac{[Cs]_z}{[Cs]_s} \tag{2}$$

where $[Cs]_z$ and $[Cs]_s$ are the concentrations of ^{134}Cs in the zeolite and in the solution respectively, is a linear function of the mole fraction of exchangeable potassium in the zeolite at a given total ion concentration in solution. In addition, at a given fractional loading of potassium in the zeolite, the K_D shows inverse proportionality to the total ion concentration in the solution (Fig. 6). This equilibrium can be predicted using appropriate pseudobinary selectivity coeffcients [8]. However, from the linear dependence of the K_D, a more simple equation can be derived for the calculation of K_D, i.e.

$$\log K_D = \overline{E}_{Na} \log(k_{Cs/Na} Q/N_T) + \overline{E}_K \log(k_{Cs/K} Q/N_T) \tag{3}$$

where $k_{Cs/Na}$ and $k_{Cs/K}$ are the the binary selectivity coefficients of trace Cs exchange in pure Na- and K-forms of the zeolite. $\bar{E}_{Na}$ and $\bar{E}_K$ are the equivalent fractions of Na and K in the zeolite. In the simple binary systems ^{134}Cs/Na and ^{134}Cs/K the familiar relationship is valid, i.e.

$$\log K_D = \log(k_{Cs/M} Q) - \log[M] \tag{4}$$

where M is Na or K. The numerical values of $k_{Cs/Na}$ and $k_{Cs/K}$ in Equation 2 and Equation 3 are identical.

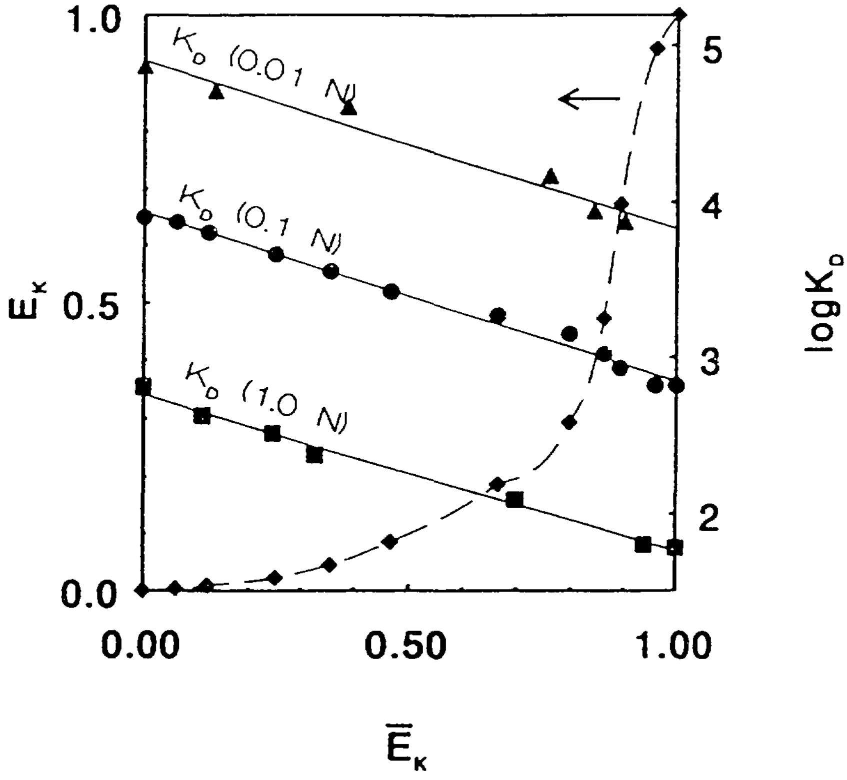

FIG. 6. Ternary ^{134}Cs/Na/K equilibrium in mordenite: distribution coefficient K_D of ^{134}Cs and equivalent fraction of potassium in solution (E_K) as a function of fractional equivalent loading (E_K) of K in the zeolite.

4.3. DYNAMIC EXCHANGE CONDITIONS

Distribution coefficient K_D, which can be calculated from Equation 2 or Equation 3 for a given solution composition, can then be used to calculate the total capacity of the zeolite column for ^{134}Cs, in terms of solution volume V_{tot} (L) that can be treated with a given amount m (kg) of zeolite in the bed. This volume V_{tot} is obtained from

$$V_{tot} = K_D m \tag{5}$$

This volume V_{tot} corresponds to the area above the column breakthrough curve (see e.g. Fig. 7). The shape of the breakthrough curve and the breakthrough capacity (e.g. the solution volume at 1 % breakthrough) depend on operational conditions (zeolite grain size, solution flow rate) and ultimately on the appropriate diffusion coefficients of the exchanging ions in the system. We are developing a PC simulation programme incorporating the common

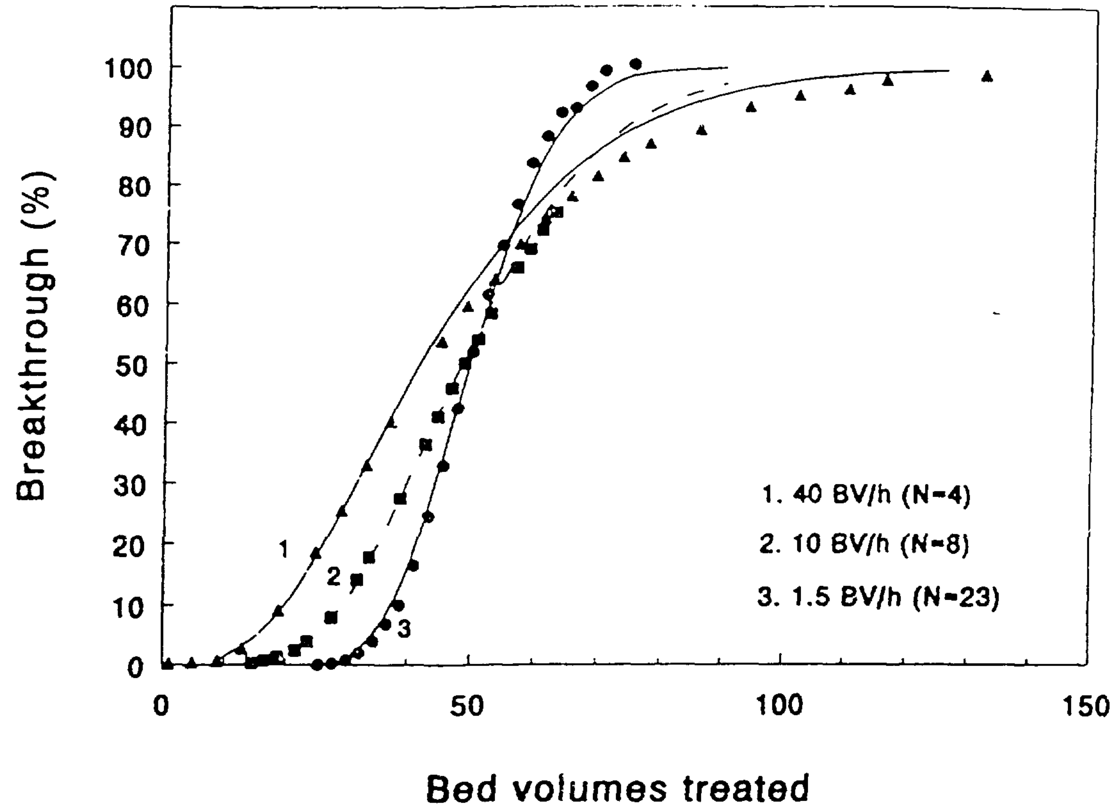

FIG. 7. Simulated (solid and broken curves) and measured breakthrough curves of ^{134}Cs in 1 M KNO_3 solutions at different flow rates.

"transfer unit" approach [8] for the calculation of the column performance. According to this concept, the plate concept, increasing the number of "transfer units" (N) improves the column efficiency: the breakthrough curve becomes steeper and thus the degree of column utilisation is improved (Fig. 7). The number of transfer units is obtained from fundamental data, i.e. for film-diffusion controlled exchange

$$N_f = A(D_f)^{1/2} d^{-3/2} s u_0^{-1/2} \tag{6}$$

where D is the diffusion coefficient, d is the particle diameter, s is the column height and u_0 is the linear flow rate. For particle diffusion controlled exchange:

$$N_p = BK_D D_p s d^{-2} u_0^{-1} \tag{7}$$

Both mechanisms may contribute simultaneously to the kinetics of the exchange and can be taken into account in the model [9].

Figure 7 shows as an example some predicted and observed breakthrough curves of ^{134}Cs in small laboratory-scale (bed volume 1.5 ml) mordenite columns at different flow rates. Equation 4 (film-diffusion controlled exchange) with $D_f = 2.6 \times 10^{-6}$ cm^2/s has been used in the simulations. In general it has been found that concepts described above give good agreement between observed and predicted column performance. Further modelling work is presently being carried out in the mixtures of Na- and K-salt solutions with a special emphasis on the prediction of diffusion coefficients in the three-component systems.

ACKNOWLEDGEMENTS

The research work described in Sections 1, 2 and 3 has been commissioned by IVO International Ltd, Finland.

REFERENCES

[1] R. HARJULA, J. LEHTO, E. TUSA AND A. PAAVOLA, Nuclear Technology, 107(1994)272.

[2] E. TUSA, A. PAAVOLA, R. HARJULA AND J. LEHTO, Nuclear Technology, 107(1994)272.

[3] J. LEHTO AND L. SZIRTES, Radiat. Phys. Chem., 43(1994)261.

[4] J. LEHTO, M. PETTERSSON, J. HINKULA, M. RÄSÄNEN AND M. ELOMAA, Thermochim. Acta, 265(1995)25

[5] J. LEHTO, S. HAUKKA, P. KOSKINEN AND M. BLOMBERG, Thermochim. Acta, 160(1990)343.

[6] A. PAAJANEN, J.LEHTO AND R. HARJULA, Proceedings of Waste Management '94, Tucson, Arizona, Vol. 2, p. 833.

[7] C.F. BAES AND R.E. MESMER, Hydrolysis of Cations, Krieger Publishing Co., Malabar, Florida, 1986.

[8] HIESTER NK, VERMEULEN T, KLEIN G, Adsorption and Ion Exchange. In: Perry JH, Chilton CH (eds) Chemical Engineers' Handbook. McGraw-Hill, New York, 1963, p. 16-1.

[9] G. KLEIN AIChE Symp Ser No. 242, 81(1985)28.

XA9744281

USE OF SYNTHETIC ZEOLITES AND OTHER INORGANIC SORBENTS FOR THE REMOVAL OF RADIONUCLIDES FROM AQUEOUS WASTES

S.K. SAMANTHA, I.J. SINGH, S. JAIN, S. SATHI,
K.VENKATESAN, M. RAMASWAMY,
T.K.THEYYUNNI, H.R. SIDDIQUI
Process Engineering and Systems Development Division,
Bhabha Atomic Research Centre,
Trombay, Mumbai, India

Abstract

Several synthetic zeolites and inorganic sorbents were tested in the laboratory for the sorption of various radionuclides present in radioactive aqueous waste streams originating from nuclear installations. The sorption of the critical radionuclides like ^{137}Cs, ^{90}Sr and ^{60}Co from low level waste solutions was studied using the synthetic zeolites 4A, 13X and AR1 of Indian origin. Granulated forms of ammonium molybdophosphate and $CaSO_4$-$BaSO_4$ eutectoid were tested for the sorption of cesium and strontium respectively, from acidic solutions. The removal of radiostrontium from alkaline salt-loaded intermediate level reprocessing wastes was studied using hydrous ferric oxide-activated carbon composite sorbent, hydrous titania and hydrous manganese dioxide. The results of these investigations are expected to be of value in formulating radioactive waste treatment schemes for achieving high decontamination and volume reduction factors.

1.INTRODUCTION

High-capacity, radionuclide-specific inorganic sorbents are becoming increasingly acceptable for removal and fixation of radionuclides present in various aqueous wastes generated at nuclear installations [1]. Stringent international regulations and growing global concern on the release of radioactivity to the environment have provided the necessary impetus world-wide for development work in this area. Amongst the attractive features of inorganic sorbents are their high thermal and radiation stabilities as well as compatibility with conventional immobilization matrices. As part of a programme on the development of improved treatment and conditioning processes for radwastes of different categories from our nuclear installations [2,3], the present work was undertaken to identify suitable sorbents for efficient removal of various radionuclides present in aqueous effluents. These sorbent based processes are expected to provide alternate treatment schemes and/or supplement existing waste management practices in order to achieve higher decontamination and volume reduction factors.

2.MATERIALS AND METHODS

2.1. SORBENT MATERIALS

Except for the synthetic zeolites which were commercial products, the other inorganic sorbents were prepared in the laboratory from reagent grade chemicals.

2.1.1. Synthetic zeolites

Naturally occurring zeolites are not commercially available in India. However, zeolites of type 4A, 13X and AR1 (mordenite) are synthetically produced by Indian Petrochemicals Corporation Limited (Catad Division) and are commercially available. Samples of these zeolites, procured in the form of 1.5 mm diameter cylindrical pellets, were crushed and sieved to smaller particle sizes (in the range of -20+60 mesh ASTM) for sorption experiments. While all zeolites were used in the Na-form as supplied, in the case of AR1 zeolite the H-form was also prepared by acid treatment of the original Na-form zeolite.

2.1.2. Other inorganic sorbents

2.1.2.1. Granulated ammonium molybdophosphate:

AMP powder was prepared in the laboratory and granulated using polyvinyl butyryl as the binder.

2.1.2.2. Granulated $CaSO_4$-$BaSO_4$ eutectoid

$BaSO_4$ was activated by heat treatment with $CaSO_4$ to form a eutectoid in powder form which was then granulated using acetal based binder.

2.1.2.3. Hydrous ferric oxide-activated carbon composite sorbent

Hydrous ferric oxide was precipitated inside the pores of high surface area coconut shell activated carbon by first soaking in $FeCl_3$/HCl followed by exposure to vapours of concentrated ammonia. The product was used after thorough washing and drying in air. Activated carbon of different particle sizes was used in these preparations.

2.1.2.4. Hydrous titania

Hydrous titania was prepared by hydrolysis of titanium tetrachloride with sodium hydroxide [4, 5]. The white precipitate obtained was repeatedly washed and air-dried for three to four weeks. The glassy gel finally obtained was crushed and sieved to get -30+50 mesh (ASTM) size particles.

2.1.2.5. Hydrous manganese dioxide

Hydrous manganese dioxide having suitable column properties was prepared in the laboratory by reaction between acidic solutions of potassium permanganate and manganous sulphate [6]. Particles in the -30+50 mesh (ASTM) size range were used for sorption tests.

2.2. SORPTION TESTS

Both batch equilibrations and column tests were performed using either synthetic test solutions or real wastes.

2.2.1. Batch equilibration tests

A known weight (0.1 or 0.25 g) of the sorbent was equilibrated with a known volume (10 or 25 mL) of the test solution in stoppered glass or polyethylene vials using a wrist-action shaking machine. The uptake of a radionuclide was calculated from the measured values of its activities before and after equilibration. The results are expressed either as distribution coefficient (K_d) values or as percent (%) activity removed:

$$K_d=\frac{(A_0-A_e)\cdot V}{A_e\cdot W},mL/g \qquad (1)$$

$$\%\ activity\ removed=\frac{A_0-A_e}{A_0}\cdot 100 \qquad (2)$$

where

A_0 and A_e	are the activities before and after equilibration (counts/min/mL),
V	is the volume of test solution (mL), and
W	is the weight of sorbent used in the equilibration (g).

From a knowledge of the moisture content of the sorbents it is also possible to calculate K_d values in terms of their dry weights. All equilibrations were done in duplicate.

2.2.2. Column experiments

Small glass columns (ca. 10 mm dia.) containing 3 to 5 g of sorbents were used in these tests. The waste feed solution was passed through the column from top to bottom using a peristaltic pump. The flow rate, unless otherwise stated, was about 10 bed volumes per hour. Effluent samples were collected periodically and analysed.

2.3. RADIOMETRIC ANALYSIS

The synthetic test solutions were prepared using ^{134}Cs, ^{60}Co or $^{85+89}$Sr radiotracers as desired. A NaI(Tl) scintillation probe coupled to a single-channel analyser was used for radiometric analysis of these gamma emitting radioisotopes. The activity of ^{90}Sr in real wastes was measured using a G.M. counter after radiochemical separation. A HPGe detector coupled to a multichannel analyser was used for analysis of real wastes containing a mixture of gamma emitters.

3. RESULTS AND DISCUSSION

3.1. TESTING OF ZEOLITE 4A WITH LOW LEVEL EFFLUENTS

Batch experiments in the laboratory, using tracer solutions at various pH values, showed that zeolite 4A is the most effective among the three zeolites for sorption of strontium at near neutral pH [7]. It has significant sorption capacity for caesium as well. Based on this information, laboratory scale column runs were conducted using low level effluents of different origins.

3.1.1. Low level effluents from power reactors

The low level wastes generated by the nuclear power stations in India contain tracer quantities of fission products and activation products of which ^{137}Cs, ^{90}Sr and ^{60}Co are the radionuclides of significance. In general, it has been found that radiocaesium makes the highest contribution to gross beta activity. These effluents have low TDS values ranging from a few hundred ppm to a maximum of 2500 ppm, depending upon the source of generation, and a pH range of 8.0 to 9.0. The dissolved solids are mainly due to presence of sodium salts. The results of batch equilibration and column runs conducted using typical waste samples from a BWR station are given in Table I and Table II [8].

TABLE I. BATCH EQUILIBRATION OF ZEOLITE 4A WITH BWR LOW LEVEL EFFLUENTS

A. Waste Composition	Floor drain waste	Regenerant waste
Gross ß, Bq/mL	15	41
^{90}Sr, Bq/mL	0.1	0.6
^{137}Cs, Bq/mL	9.5	333
TDS, mg/L	1045	2400
B. Distribution Coeff.		K_d, mL/g
Floor drain waste	^{137}Cs	3071
	Gross ß	6812
Regenerant waste	^{137}Cs	1598
	Gross ß	1621

TABLE II. COLUMN TESTING OF ZEOLITE 4A WITH BWR LOW LEVEL EFFLUENTS

Decontamination Factors						
Number of bed volumes passed	Floor drain waste			Regenerant waste		
	Cross β	^{137}Cs	^{90}Sr	Cross β	^{137}Cs	^{90}Sr
500	210.3	137.2	-	25.3	16.6	-
1000	99.8	27.4	88.2	6.6	5.5	233.1
1500	32.4	20.3	-	3.7	3.4	-
2000	7.7	10.3	-	3.0	2.4	105.0
2500	5.9	5.7	18.0	1.7	1.5	32.1
3000	2.7	2.2	9.0	-	-	-

Sorbent particle size : 18÷50 mesh (ASTM)
Bed volume : 5 mL
Flow rate : 10-12 bed volumes/hr

3.1.2. Low level waste effluents from other sources

An effluent treatment plant at Trombay treats low level effluents received mostly from research reactors, radiochemical/ isotope laboratories and a reprocessing plant, by a chemical precipitation method. A sample of waste from this facility was used for testing with zeolite 4A [7]. The characteristics of this waste sample are given in Table III.

TABLE III. TYPICAL CHARACTERISTICS OF LOW LEVEL EFFLUENTS FROM AN EFFLUENT TREATMENT PLANT

pH	10.5	^{90}Sr	2Bq/mL
TDS	960 mg/L	^{137}Cs	4.4Bq/mL
Gross β	10.4 MBq/mL	^{106}Ru	0.75Bq/mL
		^{144}Ce	0.5Bq/mL

The results of a laboratory column test on the decontamination of this waste using synthetic zeolite 4A are presented in Table IV. It is seen from the results that zeolite 4A is quite effective in removing ^{90}Sr from this waste.

TABLE IV. COLUMN TESTING OF ZEOLITE 4A WITH LOW LEVEL EFFLUENTS FROM AN EFFLUENT TREATMENT PLANT

Bed volumes passed	Decontamination Factors		
	Gross β	^{90}Sr	^{137}Cs
1000	100	180	71
2000	5	180	3
3000	3	40	1.2
4000	2.5	30	--
5000	2.0	30	--
6000	2.0	30	--

3.2. TESTING OF ZEOLITE AR1 WITH LOW LEVEL EFFLUENTS

From earlier studies carried out for sorption of caesium from low level waste solutions, it was found that zeolite AR1 is a promising sorbent for cesium [7]. Laboratory scale column experiments were conducted using two types of waste solutions as discussed below.

3.2.1. Low level effluents from reprocessing plant

An experiment was conducted using actual waste effluent sample which had the characteristics given in Table V. The results of a column experiment using zeolite AR1 with this waste solution are presented in Table VI.

TABLE V. TYPICAL CHARACTERISTICS OF A REPROCESSING PLANT LOW LEVEL EFFLUENT

pH	8.3	^{90}Sr	5.5 Bq/mL
TDS	1700 mg/L	^{137}Cs	9.6 Bq/mL
Gross β	17 MBq/mL	^{106}Ru	1.0 Bq/mL

As seen in Table VI, zeolite AR1 is effective for removal of caesium from the reprocessing plant low level waste effluents. However, its strontium removal efficiency is not satisfactory.

3.2.2. Low level acidic waste condensates

Amongst the three zeolites under investigation, zeolite AR1, which is of mordenite type with high Si/Al ratio, was found to be stable in moderately acidic solutions. Batch equilibration tests were performed to study the uptake of trace radiocaesium from mildly acidic HNO_3 solutions. The H-form of AR1 (AR1-H) was also included along with the "as received" Na-form. The results are given in Table VII.

TABLE VI. COLUMN TESTING OF ZEOLITE AR1 WITH REPROCESSING PLANT LOW LEVEL EFFLUENT

Bed volumes passed	Decontamination factor	
	^{137}Cs	^{90}Sr
500	200	1.5
1000	200	1.5
2000	120	1.1
3000	100	1.1
4000	70	-
5000	61	-
6000	50	-

TABLE VII. UPTAKE OF RADIOCAESIUM FROM NITRIC ACID SOLUTION BY SYNTHETIC ZEOLITES

Solution: O.1N HNO_3 containing 1 mg/L of Cs with ^{134}Cs tracer

Zeolite	K_d, mL/g
4A-Na	60
13X-Na	140
AR1-Na	5070
AR1-H	11220

As seen in Table VII, zeolite AR1-H shows considerable affinity for caesium in dilute nitric acid solutions. It is also evident that the affinity of zeolite AR1 can be enhanced considerably by converting the Na-form into the H-form. A column experiment was conducted to test the usefulness of AR1-H zeolite in removing tracer radiocaesium from 0.1N HNO_3 solution. Results are given in Table VIII.

TABLE VIII. COLUMN TESTING OF ZEOLITE AR1-H WITH ACIDIC SOLUTION
Feed: 0.1N HNO_3 containing 1 mg/L of Cs with ^{134}Cs tracer

Bed volumes passed	1000,	2000,	4000,	5000,	5500
DF obtained	>1000,	>1000,	>1000,	>1000,	>1000

The laboratory results indicate that zeolite AR1-H is highly promising as a sorbent for decontamination of acidic condensates having caesium activity.

3.3. TESTING OF SYNTHETIC ZEOLITES WITH RADIOACTIVE WASTE SOLUTIONS RESULTING FROM WET OXIDATION OF SPENT ION EXCHANGE RESINS

Catalytic reaction with H_2O_2 is used for the oxidative destruction of spent ion exchange resins generated at nuclear facilities [9]. These spent resins contain ^{60}Co, ^{137}Cs and ^{90}Sr as the major radionuclides. The aqueous waste generated in this process contains all the radionuclides originally present in the spent resin in addition to the ionic constituents derived from the functional groups of the resin and copper sulphate catalyst. Synthetic zeolites were tested by batch equilibration using simulated resin waste solutions spiked with radiotracers. Results obtained in these tests are given in Table IX. From the K_d values it is evident that zeolite 4A, AR1 and 13X could be selected for column studies for removal of ^{90}Sr, ^{137}Cs and ^{60}Co, respectively, from the simulated resin waste solutions. Column experiments using the three resins showed that DFs of 100 and above could be obtained for these radionuclides for hundreds of bed volumes of waste solution. It is concluded that these synthetic zeolites are effective as sorbents for trapping radionuclides released into solution after oxidative destruction of spent ion exchange resins.

TABLE IX. UPTAKE OF RADIONUCLIDES FROM SIMULATED RESIN WASTE SOLUTION BY SYNTHETIC ZEOLITES

Zeolite	Distribution coefficient (K_d, mL/g)		
	^{137}Cs	^{90}Sr	^{60}Co
4A	340	2120	737
13X	-	1900	2171
AR1	1614	1010	8

3.4. GRANULATED AMMONIUM MOLYBDOPHOSPHATE (AMP)

It is known that AMP has high selectivity for caesium in acidic solutions. However because of the microcrystalline nature of AMP, this material is not used for column applications. In the present work, AMP was used in the form of a granulated product prepared using polyvinyl butyryl as binder.

3.4.1. Batch equilibration

The granulated AMP product was tested by batch equilibration for caesium uptake from nitric acid solutions. The results are given in Table X and Table XI. The results indicate that AMP retains the sorption properties for caesium from acidic solutions at all nitric acid concentrations even after granulation. Sorption capacity improves with decrease in particle size of the composite material.

TABLE X. CAESIUM UPTAKE CAPACITY OF GRANULATED AMP
Solution used : O.1 M $CsNO_3$ with ^{134}Cs tracer

Mesh size (ASTM)	10-20	20-40	40-60	60-80	ungranulated powder
Cesium uptake capacity meq/g	0,28	0,37	0,44	0,61	1,0

TABLE XI. SORPTION OF CAESIUM FROM NITRIC ACID SOLUTIONS BY GRANULATED AMP
Sorbent : 0.2 g
Solution : 10 mL of HNO_3 solution containing ^{134}Cs tracer

Mesh size (ASTM)	Percentage sorption from HNO_3 solutions		
	0.5 M	1.0 M	3.0 M
10-20	98.8	98.6	98.3
20-40	99.4	99.2	99.0
40-60	99.6	99.5	99.4
60-80	99.7	99.6	99.5

3.4.2. Column experiments

The granulated product of different particle sizes was tested in column experiments for the removal of radiocaesium from simulated acidic high level waste solution, the chemical and radiochemical composition of which is given in Table XII. A 10mm dia. column containing 3.0 mL of the product was used in these experiments. A flow rate of 15 bed volumes per hour was maintained. Breakthrough curves obtained for three different particle sizes are given in Fig.1. Results indicate that a DF of at least 1000 can be obtained for 250

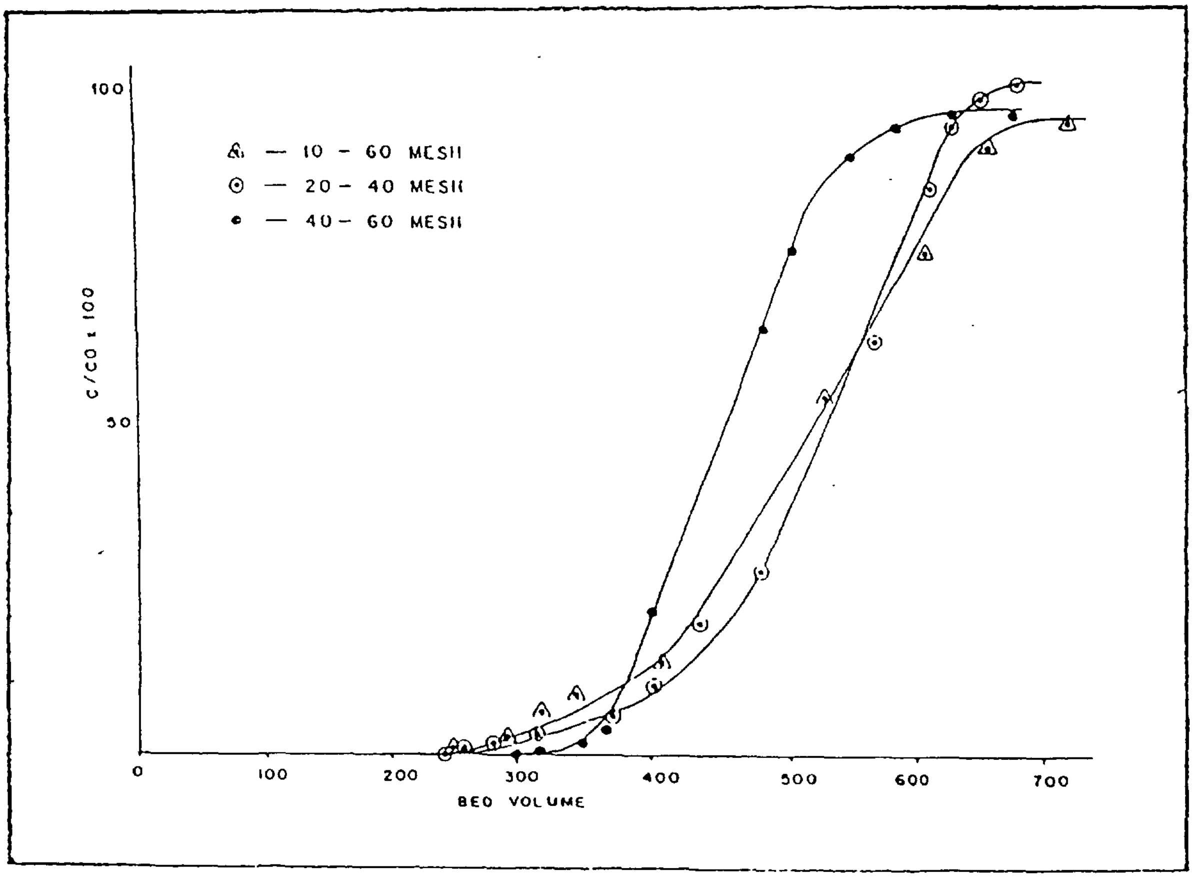

FIG. 1. Caesium removal from simulated water by granulated ammonium molybdophosphate

to 350 bed volumes depending on the particle size of the sorbent. As expected lower particle size gave better results.

TABLE XII. COMPOSITION OF THE SIMULATED HIGH LEVEL WASTE

HNO_3 3 M	^{137}Cs 220 CiBq/L
$NaNO_3$ 50 g/L	^{90}Sr 260 GBq/L
Uranium 35 g/L	^{144}Ce 2200 GBq/L
Fe^{+3} 0.5 g/L	^{106}Ru 370 GBq/L
	^{95}Zr 74 GBq/L

3.5. GRANULATED $CaSO_4$-$BaSO_4$ EUTECTOID

Batch equilibration tests with granulated sorbent of -10+ 60 ASTM mesh size showed that Kd values of the order of 10^4 mL/g were achievable in 10^{-4} to 10^{-1} M HNO_3 solutions containing traces of radiostrontium. The sorption of radiostrontium was found to be affected by HNO_3 concentration with only about 70% removal in 3.0 M HNO_3 solutions. High salt concentration was also found to adversely affect the sorption of strontium. The K_d value decreased from 8000 to 2000 mL/g on increasing the concentration of $NaNO_3$ from 0.01 to 1.50 M.

Column tests were carried out using a 10mm dia. column and 3mL volume of the sorbent. The feed solution used was 5.2 GBq of carrier strontium and a feed rate of 10 bed volumes per hour was maintained.

A decontamination factor of 50 was obtained for 175 bed volumes. Complete breakthrough was achieved when about 200 bed volumes of solution was passed.

It appears from these studies that granulated calcium-barium sulphate eutectoid holds promise as a sorbent for removal of strontium from dilute acidic/alkaline or low salt content solutions.

3.6. REMOVAL OF RADIOSTRONTIUM FROM INTERMEDIATE LEVEL ALKALINE REPROCESSING WASTES

Intermediate level wastes are mainly generated as acidic (2 to 3 M HNO_3) solutions during evaporation of the various raffinates from reprocessing operations. Before storing in underground carbon steel tanks, they are neutralized with sodium hydroxide and sodium carbonate. The major radionuclide found in these wastes is the fission product ^{137}Cs with minor quantities of ^{90}Sr and ^{106}Ru also present. Besides these fission products, the wastes also contain small quantities of uranium and traces of plutonium.

As part of a programme to develop a comprehensive treatment scheme for this type of waste, we have already demonstrated that ^{137}Cs, the major radionuclide, can be very effectively removed using either a resorcinol-formaldehyde polycondensate resin (RFPR) [10, 11] or a granular inorganic sorbent such as potassium cobalt(II) hexacyanoferrate(II) [12] prepared in the laboratory. For the removal of uranium and plutonium, destruction of carbonate by nitric acid followed by addition of alkali has been found to be an effective method. The uranium precipitates as its diuranate in this step and carries down all the plutonium and most of the strontium as well. The present work is concerned with finding suitable sorbents for removing traces of radiostrontium still remaining in these solutions.

3.6.1. Hydrous Ferric Oxide-Activated Carbon Composite Sorbent

The radionuclide scavenging properties of hydrous ferric oxide are well known. The composite sorbent prepared in the present work was tested by batch equilibration for removal of trace radiostrontium from an alkaline salt-loaded synthetic test solution. Tests with unimpregnated activated carbon were also carried out for comparison. The results are given in Table XIII.

It is seen from the results that deposition of hydrous ferric oxide inside the pores of activated carbon considerably enhances the uptake of radiostrontium. The results also show that, in general, the uptake increases with decrease in particle size of the composite sorbent. Longer equilibration periods are also useful, particularly in the case of larger particles. The results of column testing with this composite sorbent were not very encouraging. Premature breakthrough of radiostrontium took place, possibly due to slow kinetics of sorption.

TABLE XIII. UPTAKE OF RADIOSTRONTIUM BY HYDROUS FERRIC OXIDE-ACTIVATED CARBON COMPOSITE SORBENT

Sorbent : 0.1 g

Solution : 50 mL (1.0 M $NaNO_3$ + 0.1 M NaOH + $^{85+89}Sr$ tracer)

Sorbents particle size (ASTM)		Percent sorbed from solution			
		24 hrs	48 hrs	72 hrs	96 hrs
30-40	Basecarbon Composite sorbent	35.06 92.05	30.23 96.33	39.76 96.87	37.50 97.12
50-60	Basecarbon Composite sorbent	41.86 94.31	43.18 96.50	49.49 96.75	47.92 97.40
60-80	Basecarbon Composite sorbent	42.53 95.31	43.82 97.07	45.65 97.32	45.65 97.63
80-100	Basecarbon Composite sorbent	40.48 97.53	41.18 98.21	46.23 97.76	48.45 98.10

Some batch equilibration tests were also carried out with this sorbent using a simulated salt loaded alkaline waste solution containing plutonium and uranium. The K_d value for plutonium was found to be 3.5 x10^3 mL/g.

3.6.2. Hydrous Titania and its Strontium Uptake Properties

Hydrous titania is a widely studied inorganic sorbent which was prepared in granular, column-usable form. Both batch equilibration and column tests were carried out for studying the strontium sorption behaviour of this sorbent.

3.6.2.1. Effect of solution pH on uptake of strontium

Batch equilibration experiments were conducted to study the effect of pH on uptake of radiostrontium by hydrous titania. Different pH values were obtained by adding HNO_3 or NaOH to the test solution. The results are shown in Table XIV. It is evident from Table 14 that uptake of radiostrontium by hydrous titania is strongly influenced by the pH of the solution. An increase in pH favours uptake with 99% of the activity being removed at pH > 12. Such high sorption even in the presence of large concentration of sodium ions in solution shows the strong affinity of this sorbent towards strontium.

TABLE XIV. EFFECT OF pH ON STRONTIUM UPTAKE BY HYDROUS TITANIA

Solution: 2.5 M $NaNO_3$ + 1.14x10^{-4} M $Sr(NO_3)_2$ + $^{85+89}Sr$ tracer

Equilibrium pH	4.2	6.7	8.1	9.1	10.7	11.5	12.9
%Uptake	13.8	76.6	85.9	92.2	96.8	97.8	99.0

3.6.2.2. Effect of Sodium Concentration on Uptake of Strontium

The salt content of intermediate level alkaline reprocessing wastes is mainly due to the presence of sodium salts. Hence it is important to know the effect of sodium concentration on the uptake of trace quantities of strontium ions by hydrous titania. From the results shown in Fig. 2 it is evident that K_d values (Fig. 2) decrease with increase in sodium concentration. However, even at 3.0 M concentration, the uptake is quite high ($K_d > 10^4$ mL/g). This shows the high selectivity of the sorbent for strontium ions in the presence of large concentration of sodium ions.

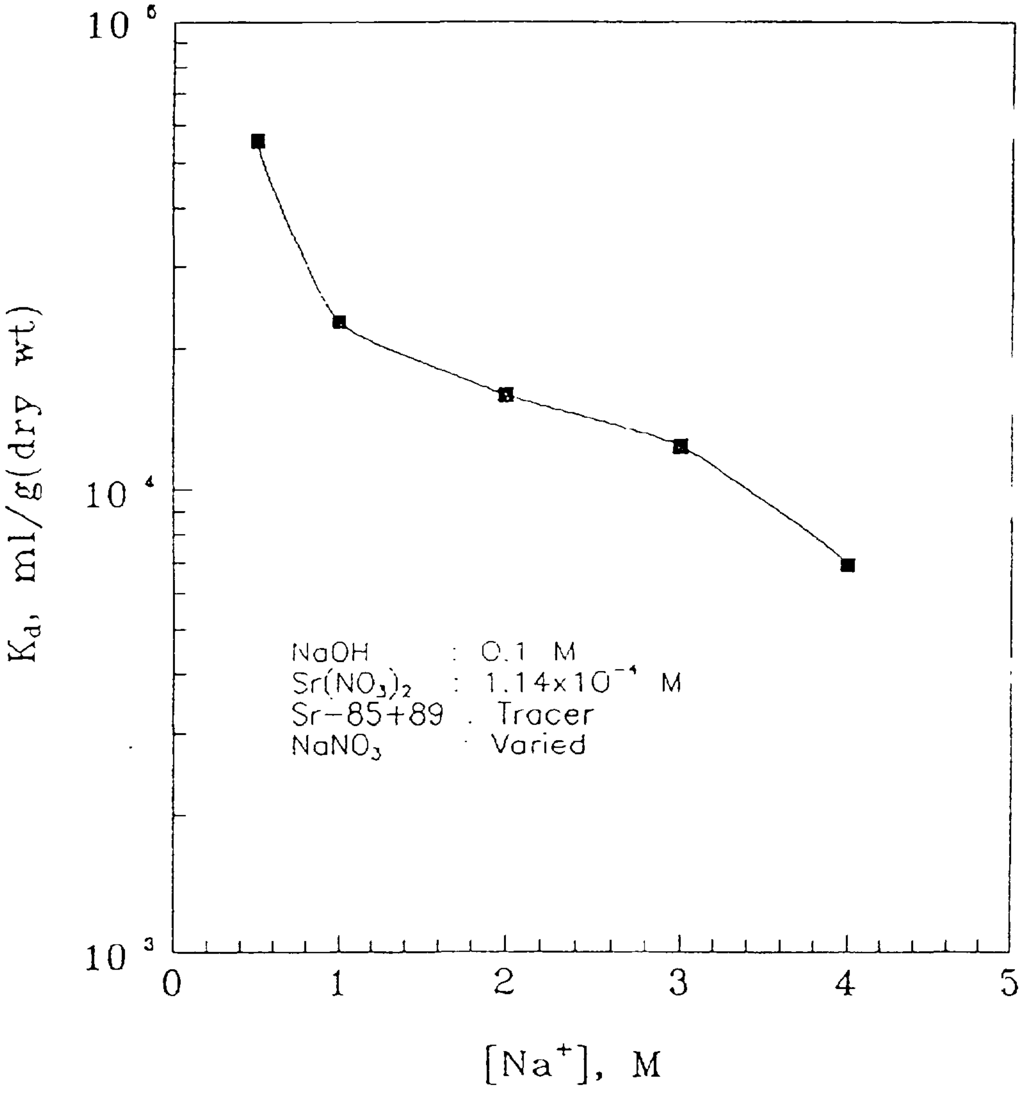

FIG. 2. Effect of sodium concentration on strontium uptake by hydrous titania

3.6.2.3. Effect of Strontium Concentration on its Uptake

The equilibration solutions in this experiment contained 1.0 M $NaNO_3$ + 0.1 M NaOH + $^{85+89}Sr$ with varying concentrations of $Sr(NO_3)_2$. It was found that K_d values remained high ($> 10^4$ mL/g) and almost independent of strontium concentration at very low concentration values (up to ca. 10^{-5} M). The K_d values decreased with further increase in concentration of strontium.

3.6.2.4. *Effect of electron beam irradiation on strontium uptake*

Water-soaked samples of hydrous titania were irradiated using 1.5 MeV electrons from an accelerator at a dose rate of about 1200 Gy/sec. Different cumulative absorbed doses were obtained by varying the duration of irradiation. The irradiated samples as well as an unirradiated control sample were then tested for their strontium sorption property from a simulated waste solution (Table XV). The results are given in Table XVI.

TABLE XV. COMPOSITION OF SIMULATED WASTE SOLUTION USED FOR TESTING OF IRRADIATED SAMPLES OF HYDROUS TITANIA

$NaNO_3$	2.5M	$Sr(NO_3)_2$	1.4×10^{-4}M
NaOH	0.1M	$^{85+89}Sr$	Tracer

TABLE XVI. EFFECT OF ELECTRON BEAM IRRADIATION ON STRONTIUM SORPTION BY HYDROUS TITANIA

Total dose Mrad	0	108	540	1080
K_d mL/g (dry wt)	1.87×10^4	2.03×10^4	2.47×10^4	2.02×10^4

It is seen that K_d values are not adversly affected by irradiation. Inorganic sorbents are generally known to possess high radiation stability. The above results show the remarkable radiation stability of hydrous titania. Even after 10^2 Gy absorbed dose, its capacity for sorption of strontium remains unaffected.

3.6.2.5. *Column test with simulated waste*

A column run was conducted to study the usefulness of this sorbent for removal of strontium from simulated salt-loaded waste solution of the same composition as that shown in Table XV. A small laboratory column containing 3.2 mL of hydrous titania was used in the experiment. Simulated waste of the above composition was passed through the column at a flow rate of 10 bed volumes per hour. In a continuous run lasting for 57 days, nearly 14000 bed volumes of solution was passed through the column. The results are given in the form of a breakthrough curve in Fig. 3. Very encouraging results were obtained in these studies. For example, up to about 5700 bed volumes a DF > 1000 ($< 0.1\%$ breakthrough) was obtained. The curve rises very slowly thereafter indicating that the bed has sufficient capacity even after 0.1% breakthrough. This experiment thus shows that hydrous titania, prepared in granular, column-usable form in the laboratory, can be effectively used for removal of radiostrontium traces from intermediate level reprocessing waste solutions.

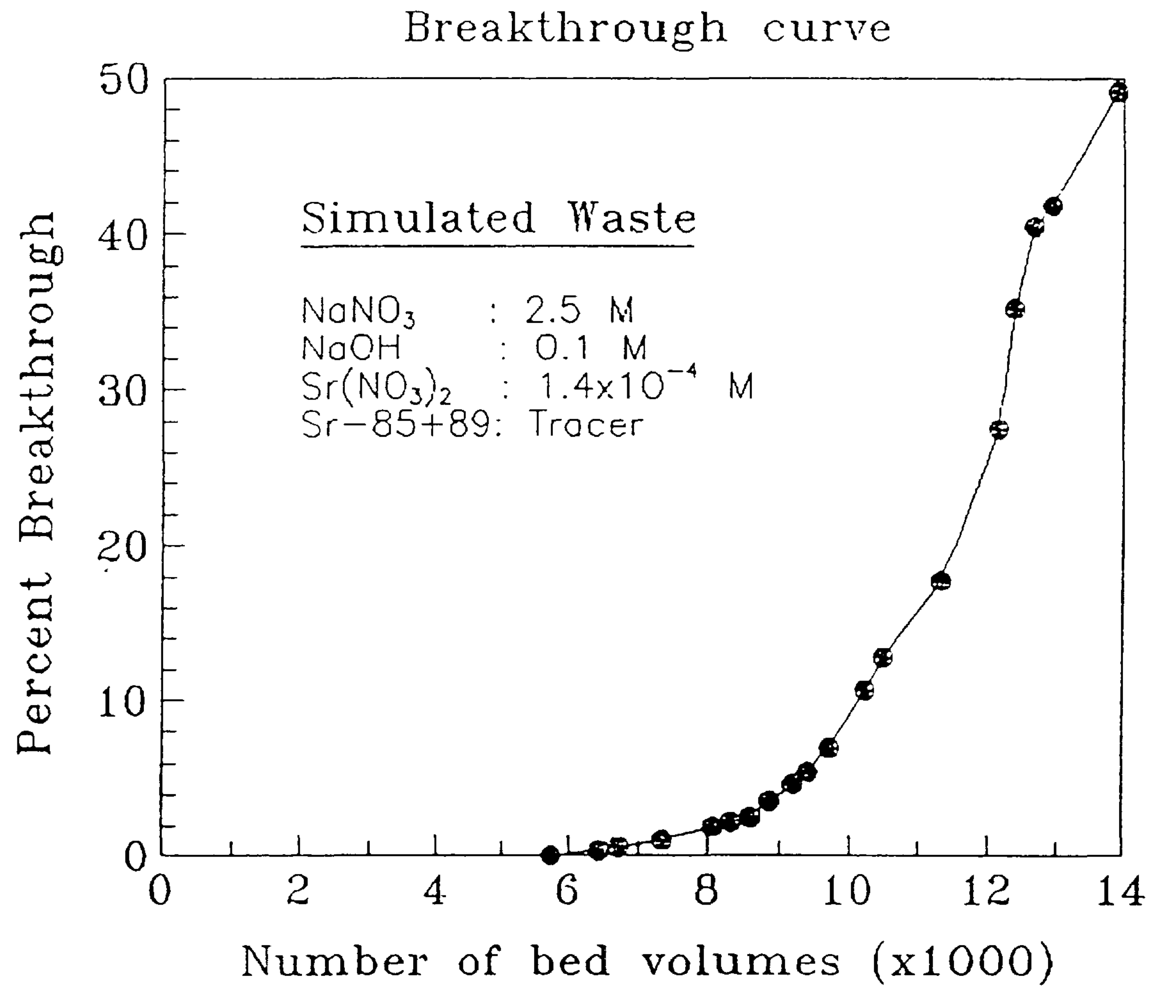

FIG. 3. Removal of strontium from simulated waste using hydrous titania

3.6.2.6. Column test with real waste sample

A column run was conducted to test the effectiveness of hydrous titania for removal of ^{90}Sr from a sample of real intermediate level alkaline waste solution stored in the waste tank farm of a spent fuel reprocessing plant. The composition of the waste solution is shown in Table XVII. The waste had uranium and plutonium contamination in addition to the fission products shown. The major radionuclide, ^{137}Cs, was removed by passing the waste sample through a column containing the granular inorganic sorbent potassium cobalt(II) hexacyanoferrate(II). The effluent from the column was treated with nitric acid to destroy carbonate and then the pH was raised by the addition of NaOH (pH 12-13). This resulted in the precipitation of uranium present in the waste as sodium diuranate. Almost all of the plutonium and a major portion of ^{90}Sr was also precipitated along with the uranium. The precipitate was separated by filtration. The filtrate was used as feed to the hydrous titania column for removal of residual strontium (^{90}Sr = 259Bq/mL). About 3 litres of this solution was passed through a small laboratory column containing about 5 mL of hydrous titania at a flow rate of 10 bed volumes per hour. The results showed that ^{90}Sr could be effectively removed by hydrous titania. After the passage of 3 litres of waste solution, the ^{90}Sr activity in the effluent was 3Bq/mL.

TABLE XVII. COMPOSITION OF REPROCESSING WASTE SOLUTION SAMPLE

TDS	267.2 g/L	^{137}Cs	74 kBq/mL
pH	9.2	^{90}Sr	16.3 kBq/mL
		^{106}Ru	0.07 kBq/mL

3.6.3. Hydrous Manganese Dioxide and its Strontium Uptake Properties

Hydrous manganese dioxide is well-known for its ability to sorb a variety of metal ions from aqueous solutions and hence is a potential candidate for use in the decontamination of radioactive waste effluents. As in the case of hydrous titania, characterization and testing of this sorbent for uptake of strontium was carried out.

3.6.3.1. *Effect of solution pH on uptake of strontium*

The equilibration solution had the following composition: 1.0 M $NaNO_3$ + 1.14×10^{-4} M $Sr(NO_3)_2$ + $^{85+89}Sr$ with varying pH. The strong dependence of strontium uptake on solution pH was evident in this case also. Very little uptake was observed at low pH values. However, high uptake (> 99%) of strontium was obtained at pH > 11 and thus, like hydrous titania, this sorbent is also effective only under highly alkaline conditions.

3.6.3.2. *Effect of sodium concentration on uptake of strontium*

From the results shown graphically in Fig. 4 it is seen that the K_d value is very high at low sodium concentration. With increase in sodium concentration, the K_d value decreases at first and then steadies. Even at 4.0 M sodium concentration, the K_d was > 10^4 mL/g and this shows the remarkable affinity of the sorbent for strontium even in solutions containing high concentrations of sodium salts.

3.6.3.3. *Effect of strontium concentration on its uptake*

The test solutions used were same as those used for studying the effect of strontium concentration on its uptake by hydrous titania. It was found that the K_d values decrease with increase in strontium concentration. For example, the K_d value decreased from about 10^4 mL/g at 10^{-5} M strontium concentration to less than 10^2 mL/g when the concentration was increased to 10^{-2} M.

3.6.3.4. *Column test with simulated waste*

Based on the results obtained in batch equilibration experiments, a column run was conducted to study the effectiveness of hydrous manganese dioxide in removing strontium from a simulated alkaline salt-loaded radwaste solution, the composition of which is given in Table XVIII.

About 3 mL of hydrous manganese dioxide taken in a small glass column was used in the experiment. The simulated waste solution of above composition was then passed through the column from top to bottom using a peristaltic pump at a flow rate of 11.0-11.5 bed

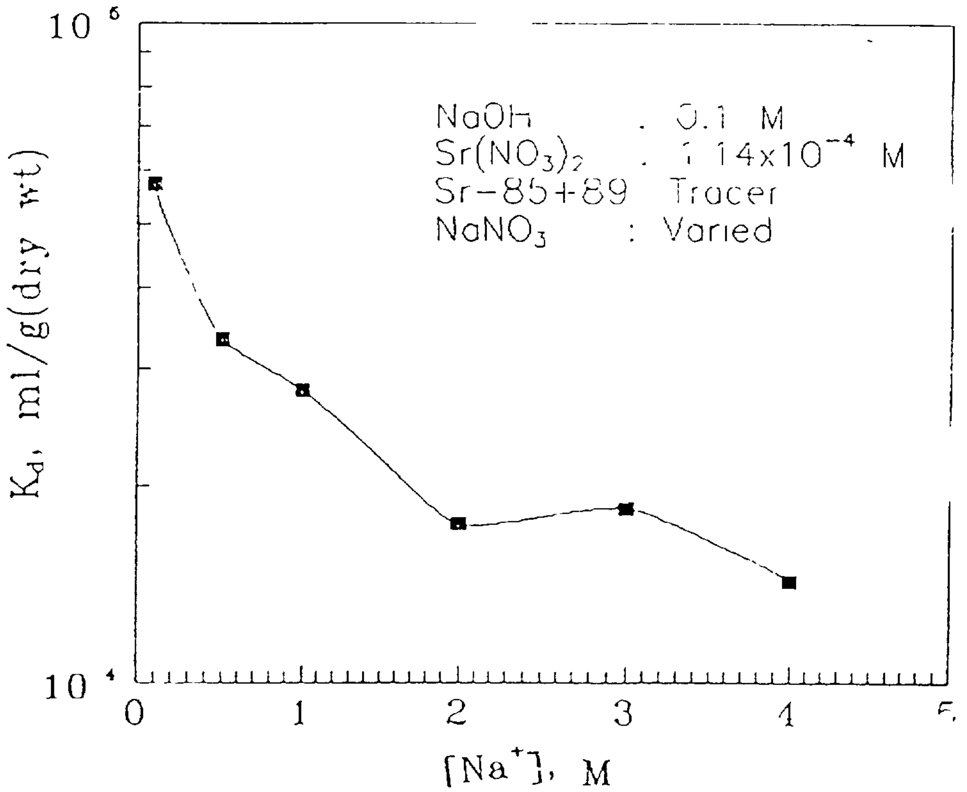

FIG. 4. Effect of sodium concentration on strontium uptake by hydrous manganese dioxide

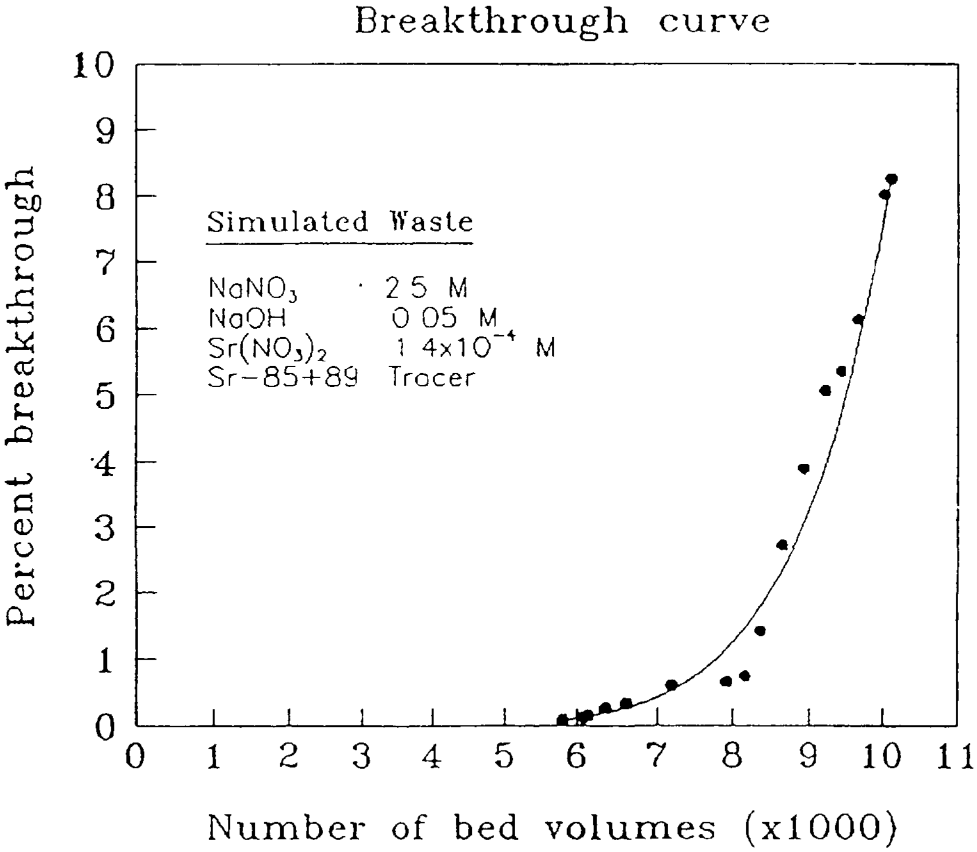

FIG. 5. Removal of strontium from simulated waste using hydrous manganese dioxide

TABLE XVIII. COMPOSITION OF SIMULATED WASTE FOR COLUMN RUN USING HYDROUS MANGANESE DIOXIDE

$NaNO_3$	2.5M	$Sr(NO_3)_2$	1.4×10^{-4}M
NaOH	0.05M	$^{85+89}Sr$	Tracer

volumes per hour. Effluent samples were collected periodically and monitored for gamma activity. During the coarse of the column run, nearly 10,000 bed volumes (about 30 litres) of waste solution was passed continuously over a period of 37 days. The results of the column run are shown in the form of a breakthrough curve in Fig.5. The breakthrough of radiostrontium was found to be $< 0.1\%$ (DF > 1000) up to nearly 6000 bed volumes. This shows that, like hydrous titania, hydrous manganese dioxide is also a very effective column-usable inorganic sorbent for removal of radiostrontium from alkaline sodium salt-loaded waste solutions of reprocessing plant origin. The 1% breakthrough level is reached after about 8000 bed volumes. At the termination of the run, after about 10,000 bed volumes, nearly 8% of the influent strontium activity was found in the effluent.

4. CONCLUSIONS

The synthetic zeolites 4A, AR1 and 13X of Indian origin can be considered as promising sorbents for removal of the critical radionuclides ^{90}Sr, ^{137}Cs and ^{60}Co, respectively, from low level waste solutions. The modified form of mordenite (AR1-H) can be used for removal of radiocaesium from mildly acidic effluents such as evaporator condensates.

The highly caesium selective inorganic sorbent ammonium molybdophosphate (AMP) was successfully granulated into column usable form and was found suitable for sorption of radiocaesium from acidic waste solutions. The granulated form of $CaSO_4$-$BaSO_4$ eutectoid was found promising for radiostrontium removal from mildly acidic/alkaline and salt-free waste solutions.

Batch equilibration tests have shown considerable sorption of strontium and plutonium from alkaline salt loaded waste solutions on hydrous ferric oxide - activated carbon composite sorbent.

Hydrous titania in granular form has been found to be promising for removal of radiostrontium from alkaline salt loaded solutions. Column studies using simulated intermediate level reprocessing waste solution have shown that this sorbent can very effectively remove strontium from such wastes with DF greater than 1000 being obtained for several thousand bed volumes. Tests with real reprocessing waste solution confirmed the effectiveness of this sorbent. Another inorganic sorbent, hydrous manganese dioxide was also prepared in granular, column-usable form. Batch and column studies showed this sorbent was also very effective in removal of radiostrontium from alkaline reprocessing waste solutions.

REFERENCES

[1] INTERNATIONAL ATOMIC ENERGY AGENCY, "Use of Inorganic Sorbents for Treatment of Liquid Radioactive Waste and Backfill of Underground Repositories", IAEA-TECDOC-675, International Atomic Energy Agency, Vienna (1992).

[2] A.N. PRASAD, M.K.T. NAIR, T.K. THEYYUNNI, V.V.S. MANI, "Thrust of Research and Development in the Indian Nuclear Waste Management Scenario", Proceedings, Indian Nuclear Society Conference on Advanced Technologies related to Nuclear Power, Bhabha Atomic Research Centre, Bombay, Feb 28 - Mar 2 (1994).

[3] T.K.THEYYUNNI, "Process Innovations in the Management of Radioactive Wastes", National Symposium on the Management of Radioactive and Toxic Wastes (SMART-95), Bhabha Atomic Research Centre, Bombay, Mar 2O-21 (1995).

[4] J. KENNEDY, J.W. PECKETT, R. PERKINS, "The removal of plutonium and certain fission products from alkaline media by hydrated titanium oxide", Report AERE-R-4516, Atomic Energy Research Establishment, Harwell (1964).

[5] Y. INOUE, H. YAMAZAKI, J. Nucl. Sci. Technol., 13 (1976) 85.

[6] M. TSUJI, M. ABE, Sola. Ext. Ion Each., 2 (1984) 253.

[7] S. JAIN, M. RAMASWAMY, T.K. THEYYUNNI, "Removal of cesium and strontium from low active waste solutions by zeolites", Report BAR/1994/E/ABBE, Bhabha Atomic Research Centre, Bombay (1994).

[8] I.J. SINGH, S. SATHI, T.K. THEYYUNNI, "Use of molecularsieves zeolite-4A for removal of caesium and strontium from low level waste effluents of BWR origin", Report BAR/1995/E/003, Bhabha Atomic Research Centre, Bombay (1995).

[9] C. SRINIVAS, M. RAMASWAMY, T.K.THEYYUNNI, "Wet oxidative destruction of spent ion exchange resins using hydrogen peroxide", Report BAR/1994/E/041, Bhabha Atomic Research Centre, Bombay (1994).

[10] S.K. SAMANTHA, M. RAMASWAMY, P. SEN, N. VARADARAJAN, R.K. SINGH, "Removal of radiocaesium from alkaline IL waste", National Symposium on Management of Radioactive and Toxic Wastes (SMART-93), Indira Gandhi Centre for Atomic Research, Kalpakkam, March 17-19 (1993).

[11] S.K. SAMANTHA, T.K. THEYYUNNI, B.M. MISRA, J. Nucl. Sci. Technol., 32 (1995) 425.

[12] S.K. SAMANTHA, T.K. THEYYUNNI, B.M. PAIL, G. THOMAS, N. VARADARAJAN, D.D. BAJPAI,"Potassium cobalt(II) hexacyano-ferrate(II) as a sorbent for selective removal of radiocaesium from reprocessing wastes", Nuclear and Radiochemistry Symposium, Indira Gandhi Centre for Atomic Research, Kalpakkam, Feb 21-24 (1995).

IMMOBILIZATION OF ^{137}Cs ON CEMENT-ZEOLITE COMPOSITES

XA9744282

L. THAMZIL, NUROKHIM
Radioactive Waste Management Technology Centre,
National Atomic Energy Agency,
Tangerang, Batan, Indonesia

Abstract

The research has been mainly concerned with the solidification of radioactive waste in cement based matrices to reduce the mobility of cesium in the solid form. Zeolite was fixed in a cement based matrix and exposed to synthetic ground water. The zeolite can replace sand materials that are used in the cement formulations. The influences of different weights of zeolite and sand on the diffusion coefficients for ^{137}Cs were studied using the solid waste form treated in ground water.

1. INTRODUCTION

A major concern in the disposal of solidified waste is that radionuclides may be leached from the solidified waste by groundwater, thus providing pathways for the distribution of radionuclides into the biosphere and the environment. Therefore, before emplacement of waste into a shallow land disposal facility, the liquid radioactive wastes must be immobilized into solid waste using hydraulic cement.

It is generally believed that the leaching process is a diffusion controlled process even though the mechanism of diffusion is still not completely understood. This is due to the complex microstructure of cement-bonded material, but studies on cement waste matrices have revealed that the rate of leaching of radionuclides is affected by many variables such as the composition of the radioactive waste and the host matrix, temperature, the chemical nature of the element diffusing out, the chemical nature of the leaching solution, such as deionized water, groundwater or seawater and radiation effects.

Zeolite was found to be an ideal choice of ion-exchanger for the treatment of liquid radioactive wastes because of its selectivity for Cs as well as its natural abundance, thermal stability and resistance to degradation by solutions of varying pH. This study was undertaken to evaluate the leachability of ^{137}Cs from solidified waste, containing zeolite and sand using the IAEA leaching test and to calculate the effective diffusion coefficient of ^{137}Cs from solid waste forms. In this test, a specimen (usually in cylindrical form) was exposed to a fixed volume of leaching solution. Samples of leaching solution were withdrawn periodically and analyzed to determine the quantity of radionuclide released from the specimens.

The diffusion transport equation in homogeneous medium for cumulative release of diffusing species is:

$$CFR = 2\frac{S}{V}\left[\frac{D}{\pi}\right]^{1/2} T^{1/2} + \beta \quad ..(1)$$

where,

CFR is cumulative fraction of radioactive species release,

S is the surface area of specimen [cm^2],

V is the volume of the specimen [cm^3],
D is the effective diffusion of the diffusivity species [cm^2/s],
T is the cumulative leaching time [s], and
β is the fraction initial activity [constant].

From equation 1, the effective diffusivity (D_e) can be calculated from the slope of the straight line curve of CFR versus $T^{1/2}$. To avoid the bias error problem in calculation by equation 1, an alternative method has been used based on fraction of initial activity released during each leach interval. The equation is :

$$D_n = \Pi\left[\frac{(IFR)n}{\Delta tn}\right]^2 .[\frac{V}{S}]^2 .T \text{............}(2)$$

where:
D_n is effective diffusivity for leach interval n [cm^2/s],
IFR is incremental fraction of initial fraction of radioactivity specimens release during leach interval n,
∇t_n is the duration of leach interval n [s] and
T is the "mean time" [s], [$1/2\ (t_n^{1/2} + t_{n-1}^{1/2})]^2$.

2. EXPERIMENTAL PROCEDURE

2.1. PREPARATION OF CEMENT BASED WASTE FORM CONTAINING ZEOLITE OR SAND

Zeolite from Bayah, West Java and sand obtained locally was used throughout the study. The zeolite was in its natural state and contained K as a major component. The Ordinary Portland Cement (OPC) was commercially produced by Tiga Roda Indo Cement Co. The particle size of the zeolite was in the range of 150-355 μm. The geometric surface area of the zeolite was 21.75 m^2/g.

2.2. LOADING OF ZEOLITE WITH ^{137}Cs

Zeolites (150 g) were loaded into 3 cm i.d x 30 cm length Pyrex columns and washed with 1 litre of deionized water. 1 litre of CsCl solution (0.15 M) containing approximately 0.4 MBq of ^{137}Cs was then introduced and allowed to percolate the zeolite bed under gravity flow over a period of 24 hours. The effluent was monitored and recycled until the activity remained constant. This conditioning required at least 2 cycles. Finally the zeolite bed was washed with 1 litre of deionized water to remove any residual activity in the reservoir and column. The wet bed was then slurried from the column, dried overnight and then stored in a desiccator for one week before use. In this way the specific activity of zeolite was defined. No activity decay correction was necessary because of its long half life.

2.3. PREPARATION OF CEMENT COMPOSITES CONTAINING ACTIVE ZEOLITE.

Before the cement composites could be prepared it was necessary to optimize the conditions and quantities of the various components. 19.5 g of total solids with a water to solid ratio (w/s) of 0.40 were used. This gave sufficient workable paste to fill a cylindrical mould 2.5 cm diameter x 2.5 cm height. This mixture gave a strong composite which could be removed from the moulds after 24 hours.

The cement composites were prepared by mixing zeolite, sand and cement with a zeolite to solid ratio as shown in Table I and II.

TABLE I. COMPOSITION OF CEMENT-ZEOLITE COMPOSITE

Sample number	mass zeolite, g	mass OPC, g	Zeolite to solution ratio
1B	1.95	17.55	0.1
2B	3.90	15.60	0.2
3B	5.85	13.65	0.3

TABLE II. COMPOSITION OF CEMENT-ZEOLITE-SAND COMPOSITE

Sample	mass	mass Sand	mass OPC	Zeolite to
4B	1.95	7.80	9.75	0.1
5B	3.90	5.85	9.75	0.2
6B	5.85	3.90	9.75	0.3

After 24 hours setting the composites were placed in a polyethylene bottle for curing in 100% relative humidity at room temperature. The bottles were capped, and the composites were not immersed in deionized water during this 28 days curing. Non-active composites were also prepared identically for measurement of compressive strength using a Perrier machine. The specimens (4 cm in diameter and 4 cm long on average) cured for 28 days, were subjected to slow loading until rupture occurred. Tests were also carried out on specimens without zeolite and sand. The composition of these specimens is listed in Table III.

Deionized water (7.2 mL) containing 40 kBq of ^{137}Cs was mixed with cement, sand and/or zeolite (non active) for one sample. This cement composite was prepared to the same composition as the cement composite prepared with active zeolite. The composition of these cement composites is shown in Table IV.

TABLE III. COMPOSITION OF ZEOLITE-SAND-CEMENT COMPOSITE FOR MECHANICAL STRENGTH TEST

Sample number	Mass zeolite, g	Mass sand, g	Mass OPC, g	Zeolite to solid ratio
1A	7.8	-	70.2	0.1
2A	15.6	-	62.4	0.2
3A	13.4	-	54.6	0.3
4A	31.12	-	46.8	0.4
5A	39	-	39	0.5
6A	7.8	31.2	39	0.1
7A	15.6	23.4	39	0.2
8A	23.4	15.6	39	0.3
9A	31.2	7.8	39	0.4
10A	-	-	78	-
11A		39	39	-

TABLE IV. COMPOSITION OF ZEOLITE AND/OR SAND CEMENT COMPOSITE USING DEIONIZED WATER SPIKED WITH ^{137}Cs

Sample number	Mass zeolite, g	Mass OPC, g	Mass sand, g	Cement to solid ratio
7B	-	19.50	-	1.00
8B	-	9.75	9.75	0.50

2.4. LEACHING EXPERIMENT

After curing at room temperature and 100% relative humidity (RH), the standard IAEA[1] leach method was employed to assess the leaching of ^{137}Cs from the cement composite. The specimen were placed in wide neck polyethylene bottles containing 200 mL of leachant. It was essential to place each specimen on its side so that the maximum surface area could be exposed to the leachant. The bottles were then kept at room temperature. The leachant used was synthetic ground water similar to the composition of local grown water in the Serpong area. The composition of the synthetic ground water is presented in Table V.

TABLE V. COMPOSITION OF SYNTHETIC GROUNDWATER

Component	g/liter
$NaHCO_3$	0.0255
KNO_3	0.0753
$Ca(NO_3)_2.4H_2O$	0.1095
$MgCl_2.6H_2O$	0.0603
$FeSO_4.7H_2O$	0.0102

The leachant was replaced with fresh solution during sampling, daily for the first three days, then weekly for 1 month and monthly thereafter. The leachant was removed carefully to avoid loss of any solids and 10 mL aliquots counted by liquid scintillation counting using Cerenkov technique. The pH was also measured periodically with Whatman pH paper.

The IFR and CFR can be calculated by the following equations;

$$IFR = \frac{An}{Ao} \cdot \frac{V\partial}{Vc} \text{.............(3)}$$

$$CFR = \frac{\Sigma An}{Ao} \cdot \frac{V\partial}{Vc} \text{..........(4)}$$

where

A_n is amount of the species in leachate [cpm],
A_o is amount activity in the solid sample at initial time [cpm],
$V\gamma$ is volume of leachant used [mL] and
V_c is volume of leachant counted by LSC [mL].

3. RESULT AND DISCUSSION

3.1. COMPRESSIVE STRENGTH AND DENSITY

The compressive strength was determined as failure load/cross section area (kN/cm^2). Table VI shows the effect of varying the zeolite, sand and cement in the solid on the bulk density and compressive strength of the specimen. The results indicate that the compressive strength decreased with increasing zeolite and/or sand to solid ratio. On the basis of the compressive strength it was found that a zeolite to solid ratio up to 0.2 was acceptable for replacing sand in the composite, which was in good agreement with previous work [3]. The substitution of zeolite for sand will decreases the compressive strength. The measurement shows that the density decreases with increasing zeolite and/or sand to solid ratio.

3.2. LEACHING TEST

All experiments were conducted at room temperature, treated identically and immersed in simulated ground water solution after 28 days curing at 100% RH. The leaching test results are presented in Figs. 1-3 as the cumulative fraction release versus the square root of total time $\sqrt{\sum t_n}$(day). Figs. 1-3 show respectively the data for zeolite-cement composite, zeolite-sand-cement composition and the cement composite without zeolite prepared with deionised waste.

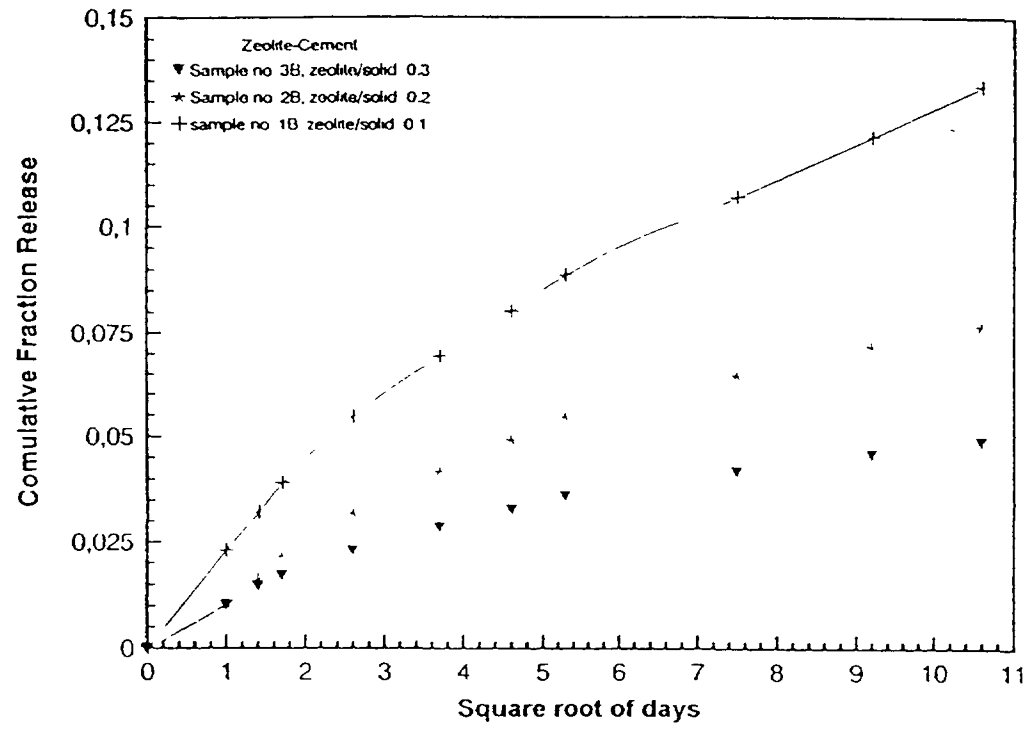

FIG. 1. CFR of ^{137}Cs from zeolite-cement composite

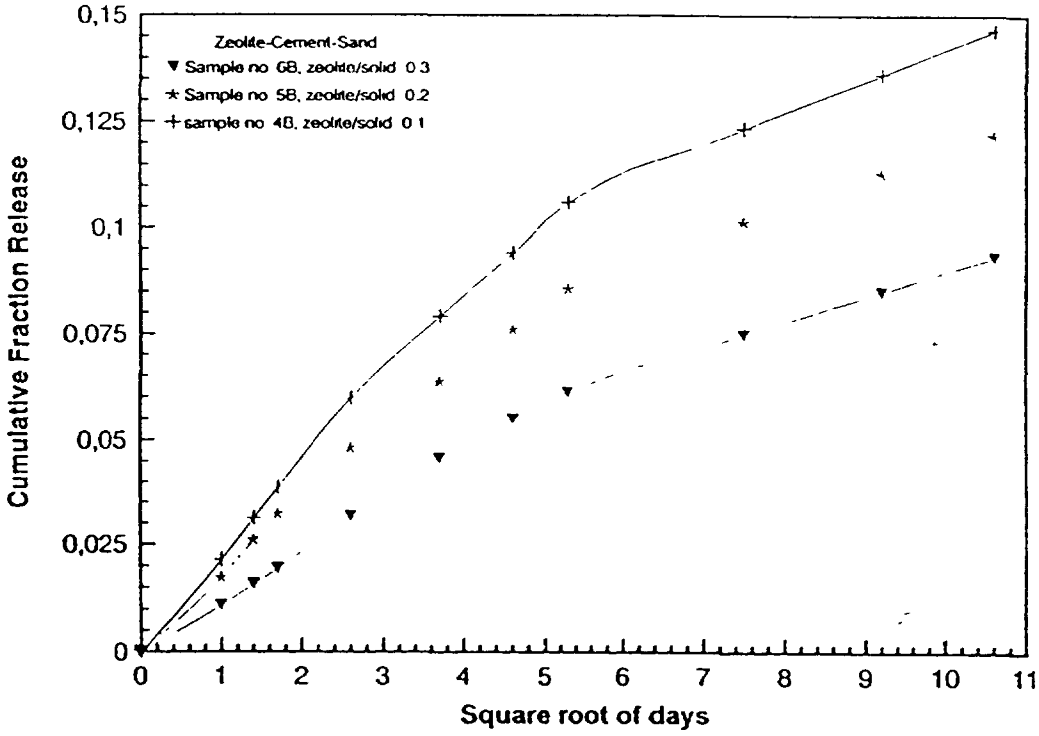

FIG. 2. CFR of ^{137}Cs from zeolite-cement-sand composite

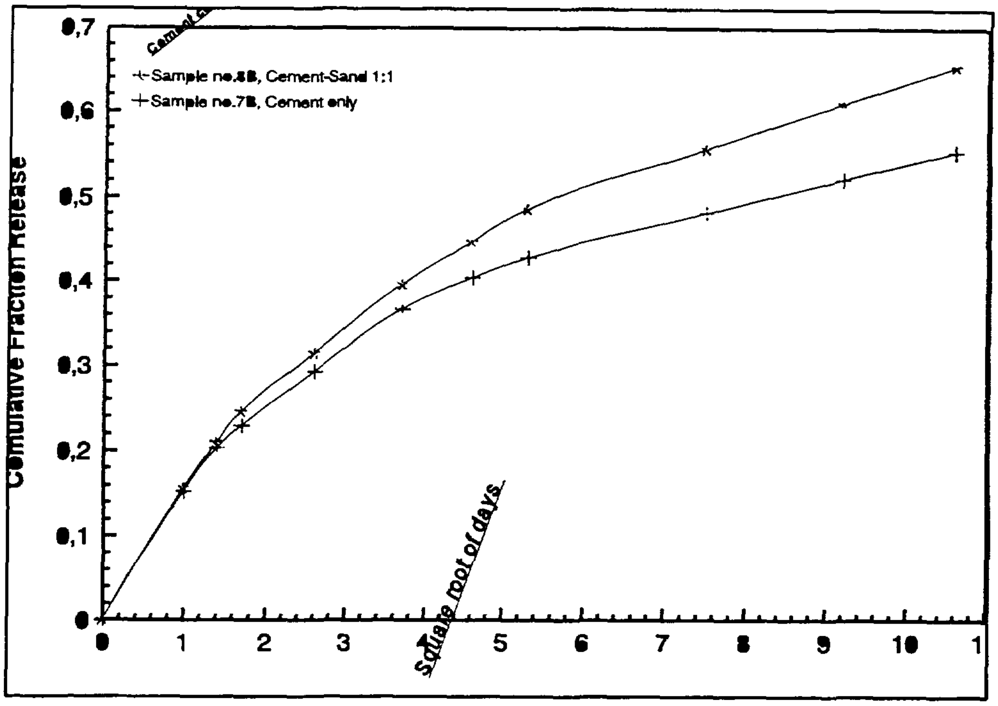

FIG. 3. CFT of ^{137}Cs from cement composite without zeolite prepared with deionized water containing ^{137}Cs

TABLE VI. BULK DENSITY AND COMPRESSIVE STRENGTH OF SPECIMEN

Sample number	Zeolite to solid ratio	Bulk density g/cm^3	Mechanical strength kN/cm^2
1A	0.1	1.884	2,20
2A	0.2	1.807	2,14
3A	0.3	1.795	2,01
4A	0.4	1.742	1,86
5A	0.5	1.666	1,76
6A	0.1	1.796	2,12
7A	0.2	1.763	2,03
8A	0.3	1.655	1,91
9A	0.4	1.635	1,87
10A	-	1.967	2,46
11A	-	1.861	2,19

As seen in Figures 1-3, the leaching process may be divided into two linear regions, a rapid initial region (less than 30 days) and a relatively slow region after 30 days (up to 112 days). The release of ^{137}Cs from zeolite-cement composites was slower than with the zeolite sand-cement composite. The leaching results were used to study the kinetics of leaching by calculation of the effective diffusion coefficient using Eq.1 and 2. The results of the calculations are presented in Table VII for the zeolite-cement composite (specimen 1B-3B) and for the zeolite-sand-cement composite (specimen 4B-6B). The specimen 7B-8B contained no zeolite. By comparison of the results it can be seen that there is no significant difference in the calculated D_e values for ^{137}Cs in simulated ground water. The D_e values for zeolite-cement composites was less than for zeolite-cement-sand composite. It was also shown that the D_e values for cement composite (zeolite absent) using the labelled deionized water was higher than in composite containing zeolite.

TABLE VII. DIFFUSION COEFFICIENT OF CESIUM IN SAMPLE SPECIMENS

Sample number	Average Diffusivity (cm^2/s)	Cumulative Effective Diffusivity (cm^2/s)	Coefficients of Linear CFR Equation	
			Slope ($s^{-1/2}$)	Intercept
t< 30				
1B	$(4.1\pm0.9)10^{-10}$	$3.613\ 10^{-10}$	$5.148\ 10^{-5}$	0.0111
2B	$(2.0\pm0.4)10^{-10}$	$1.620\ 10^{-10}$	$3.447\ 10^{-5}$	0.0026
3B	$(4.2\pm0.9)10^{-11}$	$5.309\ 10^{-11}$	$1.975\ 10^{-5}$	0.0061
4B	$(6.8\pm0.7)10^{-10}$	$6.111\ 10^{-10}$	$6.694\ 10^{-5}$	0.0039
5B	$(4.4\pm0.9)10^{-10}$	$3.909\ 10^{-10}$	$5.354\ 10^{-5}$	0.0039
6B	$(2.1\pm0.2)10^{-10}$	$2.277\ 10^{-10}$	$4.086\ 10^{-5}$	0.0009
7B	$(6.9\pm0.7)10^{-9}$	$6.342\ 10^{-9}$	$2.157\ 10^{-4}$	0.1113
8B	$(7.1\pm0.4)10^{-9}$	$8.885\ 10^{-9}$	$2.553\ 10^{-4}$	0.1033
t>90 (up to112)				
1B	$(1.4\pm0.3)10^{-10}$	$1.138\ 10^{-10}$	$2.889\ 10^{-5}$	0.0438
2B	$(3.1\pm1.1)10^{-4}$	$2.854\ 10^{-11}$	$1.447\ 10^{-5}$	0.0323
3B	$(9.6\pm1.7)10^{-12}$	$9.314\ 10^{-12}$	$8.265\ 10^{-5}$	0.0232
4B	$(9.5\pm0.4)10^{-11}$	$9.265\ 10^{-11}$	$2.607\ 10^{-5}$	0.0656
5B	$(6.5\pm1.1)10^{-11}$	$7.427\ 10^{-11}$	$2.334\ 10^{-5}$	0.0496
6B	$(7.5\pm1.2)10^{-11}$	$5.862\ 10^{-11}$	$2.073\ 10^{-5}$	0.0289
7B	$(7.5\pm0.8)10^{-10}$	$8.839\ 10^{-10}$	$8.051\ 10^{-5}$	0.3032
8B	$(2.2\pm0.8)10^{-9}$	$1.606\ 10^{-9}$	$1.085\ 10^{-5}$	0.3171

The effect of addition of zeolite into cement was to decrease the diffusion coefficient, but reduce the compressive strength. On the other hand, introduction of zeolite into sand cement composite did not increase the compressive strength of the composite and did not have a significant effect on the D_e values. Based on these results, the zeolite added to the cement composite should not exceed 30%.

These results clearly show that the calculated effective diffusion coefficient has little effect on the leachability of ^{137}Cs by synthetic ground water solution. The D_e values in zeolite cement composites was found to about 18 to 119 times lower than those in cement without zeolite and the D_e values in zeolite-sand-cement composites was about 15 to 39 lower than in cement without zeolite (see Table VIII).

TABLE VIII. COMPARISON OF DIFFUSION COEFFICIENT OF ^{137}Cs IN ZEOLITE SPECIMENS

Zeolite-Cement composite (ZC) to cement composite only (CC).

Zeolite to solid ratio	D_e ratio of CC to ZC	
	t < 30 days	t > 30 days (until 112)
0.1	17.55	7.77
0.2	39.14	30.97
0.3	119.45	94.91

Zeolite-Sand-Cement composite (ZCS) to Cement-Sand composite (CS).

Zeolite to solid ratio	D_e ratio of CC to ZCS	
	t < 30 days	t > 30 days (until 112)
0.1	14.54	17.33
0.2	22.73	21.62
0.3	39.02	27.40

4. CONCLUSION

By comparing the leaching data from all experimental results, some conclusions may be made as follows :

- Both zeolite and sand were able to fix the ^{137}Cs into cement composite, even though the zeolite was in it natural form.
- Low effective diffusion coefficients were obtained for the leaching process on zeolite-cement composites and were lower than those in zeolite-sand cement composite.
- The general trends showed that leachability of ^{137}Cs from cement composite (zeolite absent) in synthetic ground water was higher when compared with zeolite cement composites.
- Based on the compressive strength and leachability data, the zeolite-cement composite should not exceed 20% of the total solid composites.

ACKNOWLEDGEMENT

I wish to express my sincere gratitude to the Division of Nuclear Fuel Cycle, IAEA for financial support and to Dr. A. Tsarenko for providing the opportunity to be involved in the Research Co-ordination Programme.

My thanks to all my colleagues in the group of "Waste Treatment and Immobilization Technologies Involving Inorganic Sorbents" for their valuable discussion.

REFERENCES

[1] E.D. HESPE, IAEA, Leach testing of immobilized radioactive waste solids", a proposal for a standard method, ed Atomic Energy Rev. 9 (19), 1971.

[2] C.V MCISAAC AND S.T. CRONEY, Waste Management Vol 11, pp 271-282 1991.

[3] T. LAS , PH. D THESIS, University of Salford, Manchester, England, 1989

SOL-GEL PREPARATION OF HIGH SURFACE AREA POTASSIUM TETRATITANATE FOR THE IMMOBILIZATION OF NUCLEAR WASTE METAL IONS

K.T. JUNG, Y.G. SHUL, J.K. MOON, W.J. OH
Department of Chemical Engineering,
Yonsei University,
Seoul, Republic of Korea

Abstract

Potassium tetratitanates($K_2Ti_4O_9$) were synthesized by using the sol-gel method to produce ion-exchangeable materials with high surface area. The effects of mole ratios of K/Ti and H_2O/Ti were examined. $K_2Ti_4O_9$ was obtained at 740°C by the sol-gel method, which uses a lower temperature than the melting method. After calcination at 800°C, K_2Ti_4O exhibits a needle shape which is quite different from the shape of $K_2Ti_6O_{13}$ powder. The surface area of $K_2Ti_4O_9$ was 15 m^2/g by the sol-gel method after calcining at 800 C. The enhancement of BET area to 25 m^2/g was obtained after supercritical drying using EtOH as solvent. By using the sodium alginate method, needle type potassium titanate 10μm in length, the longest aspect ratio of $1,3x10^3$, could be obtained. There are variations in the Sr^{2+} ion exchange rate and capacity according to the preparation method. Larger BET surface area provides fast ion exchange and larger capacity for Sr^{2+} ion in the order; sol-gel process with supercritical drying > sol-gel process > melting process.

1. INTRODUCTION

Potassium titanates [$K_2O.nTiO_2(n=1\text{-}8)$] have cage, tunnel or layered structures, which consist of TiO_6 octahedra joined by sharing corners, edges and/or faces [1]. Among these titanates; potassium dititanate ($K_2Ti_2O_5$), potassium tetratitanate ($K_2Ti_4O_9$) and potassium hexatitanate ($K_2Ti_6O_{13}$) are well known [2-3].

Potassium tetratitanate, is used as a catalyst, filter materials, reinforcing material, heat insulator, automotive brake lining material and acoustic absorbing material as well as an ion exchanger [4,5]. When potassium ions, the ion-exchangeable sites, are replaced by protons a hydrous titanium dioxide is obtained. These hydrous titanium dioxides, which can be represented as $(H^+.H_3O)Ti_4O_9$, have a large ion exchange capacity for alkali metal ions [6], alkaline earth metal ions [7] and divalent transition metal ions [8]. These ion-exchange properties are due to the fact that hydrous titanium dioxide has exchangeable protons and hydronium ions in an interlayer structure. The acid treatment process to make crystalline hydrate titanate and the ion exchange process are well established and known to be reversible to some extent [9]. The acid treatment process and the ion exchange equation is denoted as follows:

$$K_2Ti_4O_9 + 2H^+ + nH_2O. \rightarrow H_2Ti_4O_9 .nH_2O+2K^+ \ldots(1)$$
$$xM^+(aq) + H_2Ti_4O_9\ yH_2O \rightarrow M_xH_{(2-y)}Ti_4O_9 .yH_2O(s) + xH^+(aq)\ (2)$$

when M means metal ion.

Some reports have been published for sorption of Sr^{2+}, Cs^+, and other ions with sodium titanate [10]. In treating Sr^{2+} and Cs^+, the advantage of high distribution coefficient(Kd) value is reported at high pH; the disadvantage of this process is the slow exchange rate due to the low surface area of the powder(< 10 m^2/g).

Potassium tetratitanate has been synthesized at about 900-1000°C by using a melting method and the powder has a low surface area due to the high temperature treatment. Surface area, particle size, and pore size, which have an influence on ion exchange capacity, decrease with increase of temperature. Therefore, only powder of low surface area (α10m^2/g or rem) was obtained due to rapid densification of particles during the course of crystallization at this high temperature condition.

To prepare potassium tetratitanate with high surface area, the sol-gel process was found to be an excellent method since it provides many advantages over the conventional process [11]. In general, the sol-gel process is applicable to the low temperature synthesis of ceramics since the formation of an amorphous phase is promoted by the new intermediates present in a ceramic sol at low temperature. Therefore, if we make a homogeneous mixture of potassium and titanium in the sol state we can obtain a solid phase with large surface area at low temperature by suppressing the densification of a crystalline structure at high temperature. Up to now, few studies have been made on multicomponent systems. Recently, we have reported sol-gel synthesis of potassium hexatitanate to provide a large BET surface area [12].

Recently, a new process of preparing ceramic fibre by using sodium alginate has been employed by various workers [13]. This process is based on ion exchange and gelation of sodium alginate $(C_5H_7O_4COONa)_x$ yH_2O, which is well known as an ion exchangeable organic polymer. The alginate method does not require a ceramic powder as a starting material. In addition, the viscous solution of the sodium alginate has an advantage in that it gels in any shape such as fibre, film, and bead by ion exchange with protons or multivalent metal ions. Alumina-silica, hydroxyapatite, YBCO fibre was synthesized using this method [13].

In this study, sol-gel synthesis of potassium tetratitanate was attempted under various conditions. To enhance the surface area of potassium tetratitanate, supercritical drying was attempted for the precursor sol. Ion exchange of Sr^{2+} was tested with samples prepared by different methods; melting process, sol-gel process, and sol-gel process adopted with supercritical drying. To make long potassium titanate long fibres, synthesis of potassium tetratitanate using sodium alginate was also tested.

2. EXPERIMENTAL

The experimental scheme is shown in Fig. 1. Sol-gel reaction was carried out in a glove box under N_2 atmosphere. At first, the potassium precursor, water and catalyst were dissolved in 0.5 the theoretical amount of EtOH. Then titanium precursor dissolved in the remaining EtOH was added to partially hydrolyzed potassium alkoxide sol to make a homogeneous sol mixture. After making a homogeneous potassium-titanate sol mixture, the hydrolysis reaction proceeded and was subsequently aged at room temperature for 1-7 days to make a gelled structure. After drying the sample, it was calcined up to 800°C to obtain a crystalline potassium tetratitanate.

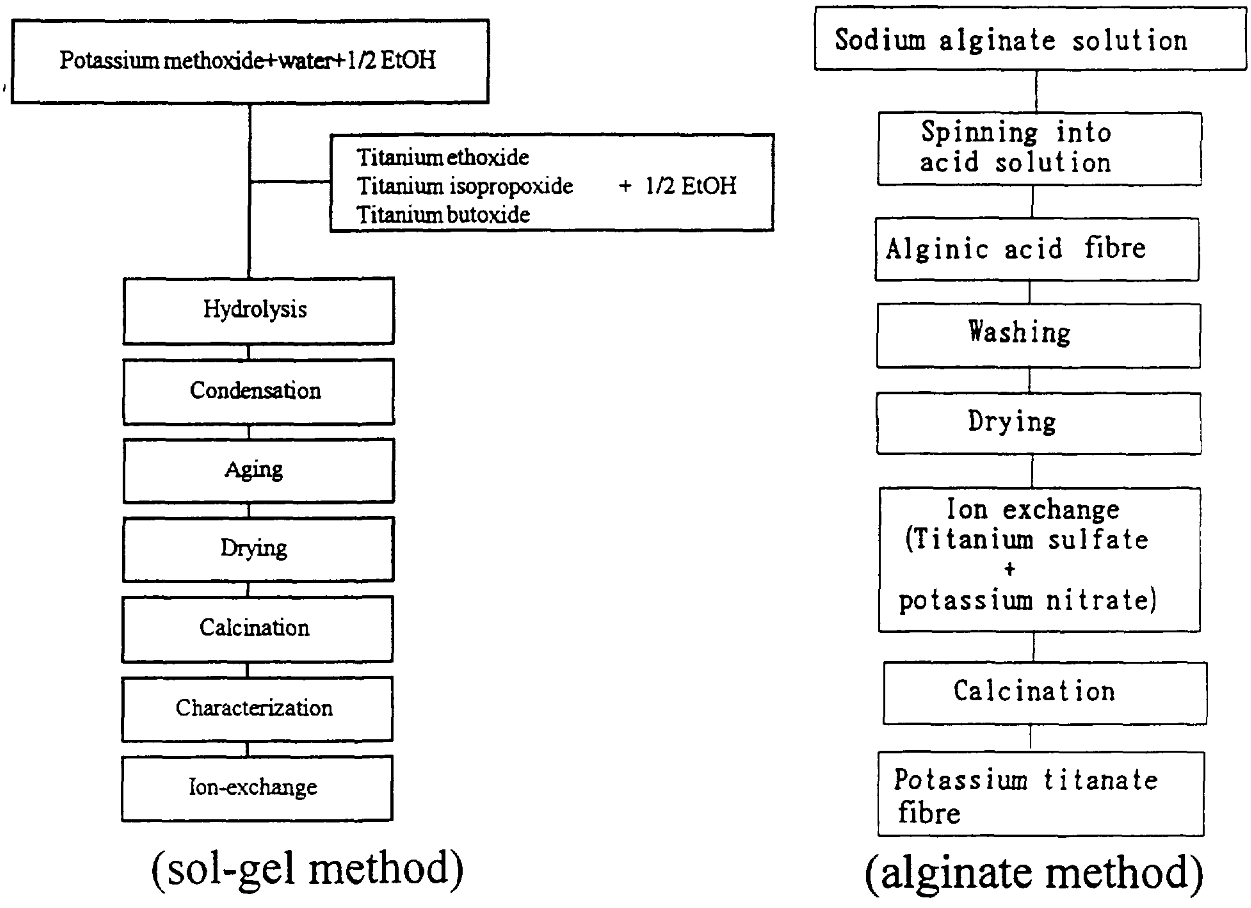

FIG. 1. Preparation of potassium titanate by sol-gel method and alginate method.

The experimental apparatus for supercritical drying (SCD) is shown in Fig. 2. As a solvent for SCD, EtOH(Tc=243.0℃, Pc = 925.8 psi) was used. Potassium tetratitanate sol was fed into the reactor(50 vol%) with EtOH solvent and the high pressure reactor was heated with a heating rate of 1°C/min up to 300°C. When the temperature reached 300°C, the autoclave was held for 1h to ensure complete thermal equilibration (300°C, 1700 psig). After that, the pressure was decreased isothermally to atmospheric pressure by venting the solvent. To avoid condensation of solvent on the samples, the autoclave was flushed with nitrogen at atmospheric pressure from 300°C to room temperature.

An aqueous solution of 5% sodium alginate was extruded from a nozzle with a 2 mm inner diameter into 1M-HCl. The extruded sodium alginate sol gelled as an alginic acid fibre through ion exchange of its sodium ions with protons in the HCl solution, and the alginic acid fibre was rinsed 5 times in de-ionized water and then immersed in a solution of titanium sulphate and KNO_3 for more than 10 hours. The K-Ti-alginate fibre was rinsed in de-ionized water, dried at ambient temperature and then fired at 800°C for 3 hours in air.

Ion exchange experiments were executed for the kinetic measurements using a batch contact technique. 0.3g samples of potassium tetratitanate hydrate treated with 0.1M HCl were immersed in 200 mL of 0.005M strontium nitrate solution.

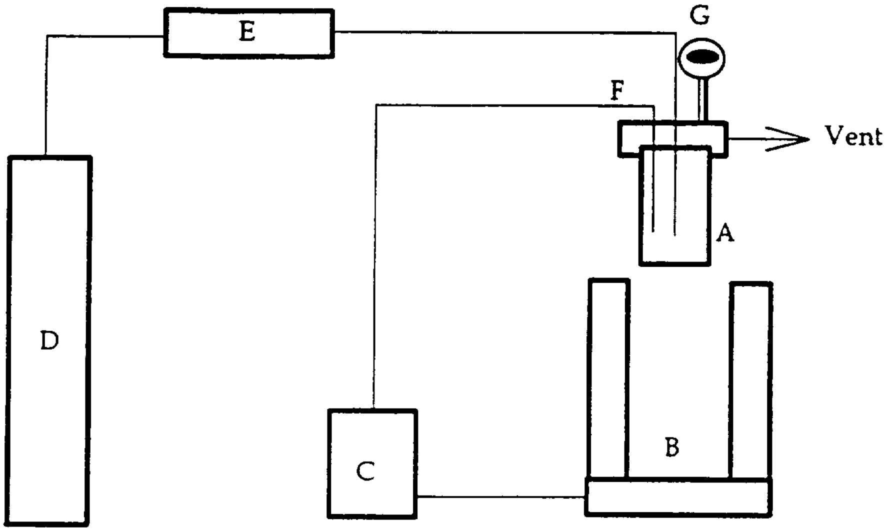

FIG. 2. Supercritical drying apparatus.
A: Reactor B: Furnace C: Thermocouple controller
D: Nitrogen E: Trap F: Thermocouple G: Pressure gauge

The surface area was estimated, using nitrogen adsorption, by a surface area analyzer 848 (Micrometrics Co.) and the particle size and shape of particles were observed by SEM (JEOL). To characterize thermal behavior and crystalline temperature, differential thermal analysis and thermal gravimetric analysis (TG-DTA, Thermoflex, Rikagu) of the powder were carried out. X-ray diffraction (XRD, D-Max. 3, Rigaku) was used for the identification of the crystalline phase. Strontium concentrations in the solution were determined by atomic absorption spectrometry (AAS, Perkin Elmer) using the flame technique.

3. RESULT AND DISCUSSIONS

To apply potassium titanate, which has ion exchangeable sites, for the immobilization of nuclear waste, various synthetic methods were attempted such as a melting method [9], sol-gel method [11], sol-gel method adopted with super critical drying process, and sodium alginate method.

3.1. MELTING METHOD

Potassium titanate was prepared by the reaction of titanium dioxide (rutile) and potassium carbonate. When the molar ratio K/Ti was 0.5, potassium tetratitanate was obtained at 950°C after 50 hours heating. However, potassium hexatitanate was synthesized over the temperature range 950-1050°C (K/Ti=0.3). Figure 3 shows SEM images of potassium titanate obtained by the melting method. The average length and the aspect ratio (length/diameter) of potassium tetratitanate fibre is 5μm and 10-15, respectively. In the case of potassium hexatitanate, the average length and the aspect ratio was smaller than that of potassium tetratitanate. Normally, those samples prepared by the melting method have a low BET surface area ($< 10m^2/g$).

3.2. SOL-GEL METHOD

3.2.1. Synthesis of potassium tetratitanate from CH_3OK-$Ti[O(CH_2)CH_3]_4$

Figure 4 shows the TG-DTA profiles of potassium tetratitanate ($K_2Ti_4O_9$) synthesized by CH_3OK as a potassium precursor and $Ti[O(CH_2)CH_3]_4$ as a titanium precursor. Changes of TG-DTA profile are compared according to $[H_2O]/[Ti]$ ratio and drying method. In the case of (a) and (b), it is shown that weight loss was about 30% at 100-150°C and two endothermic peaks were assigned to desorption peaks of physisorbed water and chemisorbed water 100-150°C and 350-150°C, respectively. The exothermic peak at 559°C and 745°C without weight loss is due to the phase transition of amorphous powder to crystalline intermediate and intermediate to potassium tetratitanate respectively. This was proven by XRD patterns of the potassium tetratitanate after calcination at 800°C as shown in Figs. 5 and 6. This kind of low crystallization temperature was not feasible in conventional synthesis starting with solid powders. The exothermic peak (Fig. 4) at 559°C corresponds to an intermediate phase and peak at 745°C is assigned to the phase transition temperature from an intermediate to potassium tetratitanate. It proves that, unlike potassium hexatitanate, potassium tetratitanate is synthesized through an intermediate phase.

In the case of the supercritical dried sample, the weight loss was lower than that of atmospheric drying due to the extraction of water absorbed in the gel powder during the supercritical drying process and a broad exothermic peak appeared near 830°C. As shown in Fig. 7, the shape of potassium tetratitanate gel powder in the pure gel state is spherical. However, after calcination at 800°C, potassium tetratitanate is needle shaped. According to Y. Fujiki et. al [14], they synthesized potassium tetratitanate by a flux (K_2MoO_4) and cooling method at 1150°C. The size of fibres obtained was 1mm in length and 0.01mm in diameter on average. However, in our case, the fibre have a length of 0.5-5μm and a thickness of 0.05 - 0.2μm. The shape of the potassium tetratitanate is quite differ from the shape of potassium hexatitanate powders obtained by the melting process. Figure 8 reveals that the morphology of potassium tetratitanate changes with preparative method. In the melting method the spherical shape of potassium tetratitanate is mixed with needle shape potassium tetratitanate. The shape of potassium tetratitanate, supercritical dried process (Fig. 8 (c)), is even thinner and shorter than that from other methods(melting and sol-gel process).

3.2.2. Effect of K/Ti ratio

The effects of initial K/Ti ratios on the final properties of products are shown in Table 1 for different titanium alkoxides. Potassium hexatitanate converted to potassium tetratitanate on increasing the K/Ti ratio from 0.3 to 2. In this hydrolysis and condensation reaction of metal alkoxides, potassium should also act as a base catalyst to form colloid type particles instead of the polymeric types which can be observed in acid catalysis [15]. As shown in Fig. 9, the gel powder shows a spherical shape of agglomerate which should come from a colloidal type of primary particles, potassium titanate sol. When the K/Ti ratio is 2.0, the XRD patterns show potassium tetratitanate(K/Ti=0.5) as a main phase and small amount of potassium hexatitanate (K/Ti=0.3). The amount of potassium incorporation into the titanium framework is decreased as the K/Ti ratio is increased. It seems difficult to obtain pure potassium tetratitanate under these conditions because all the potassium is not incorporated with titanium ion in the sol state. The excess potassium should remain in solution or deposit on the surface of the titanium sol. It is noteworthy that the surface area of titanate gel powder

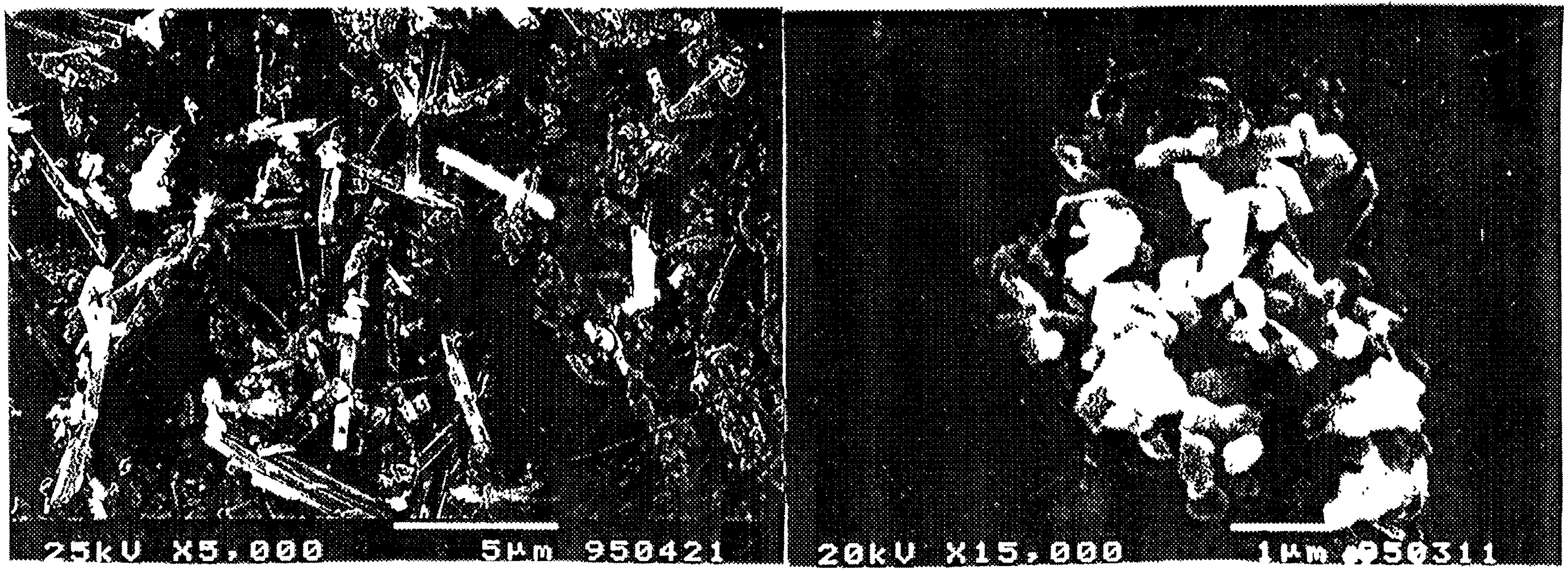

(a)

(b)

FIG. 3. SEM images of potassium titanate synthesized by melting method
(a) $K_2Ti_4O_9$ *(b)* $K_2Ti_6O_{13}$

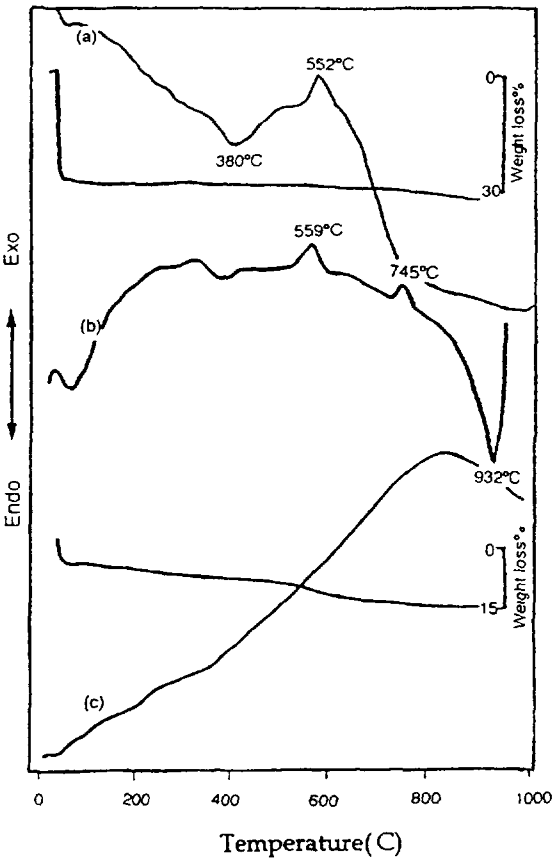

FIG. 4. TG-DTA curves of potassium titanate
(a) $H_2O/Ti=0$ (b) $H_2O/Ti=0$
(c) $H_2O/Ti=10$, supercritical drying

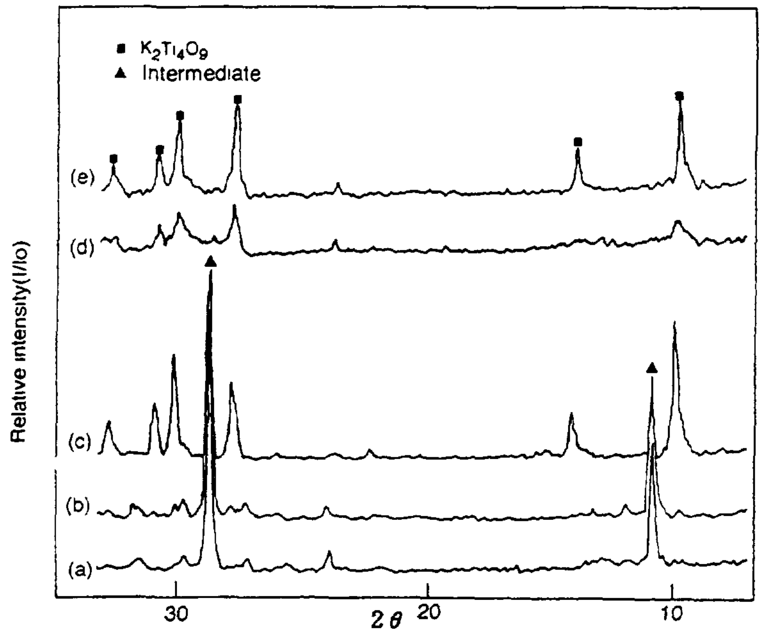

FIG. 5. Changes of XRD pattern with calcination temperature.
($[H_2O]$ {Ti]=0)
(a) after supercritical drying (300°C, 140 bar)
(b) 700°C, 10min (c) 800°C, 1.5hrs

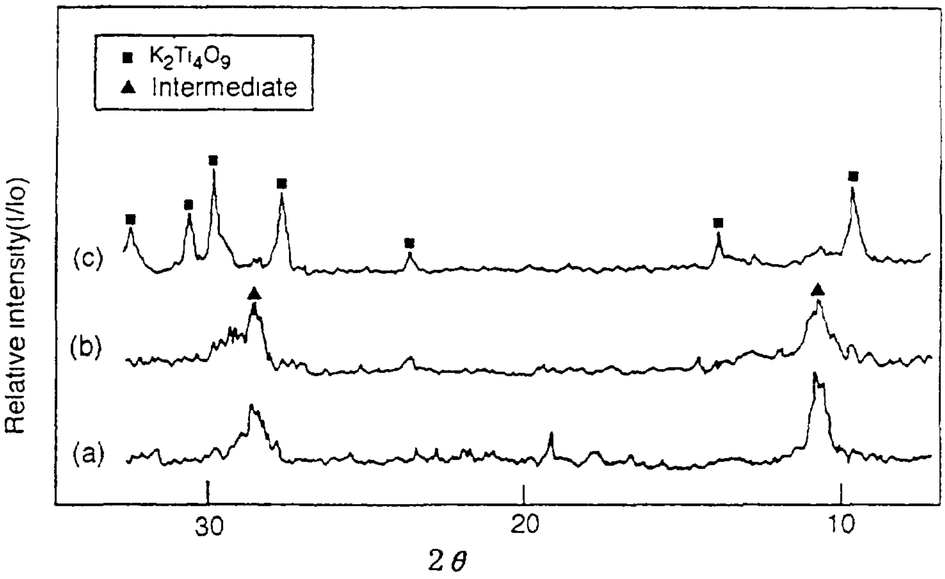

FIG. 6. Changes XRD patterns with calcination temperature
(H_2O/Ti=10, 270°C, 118 bar)
(a) after supercritical drying (b) 700°C, 10 min (c) 800°C, 1.5hrs

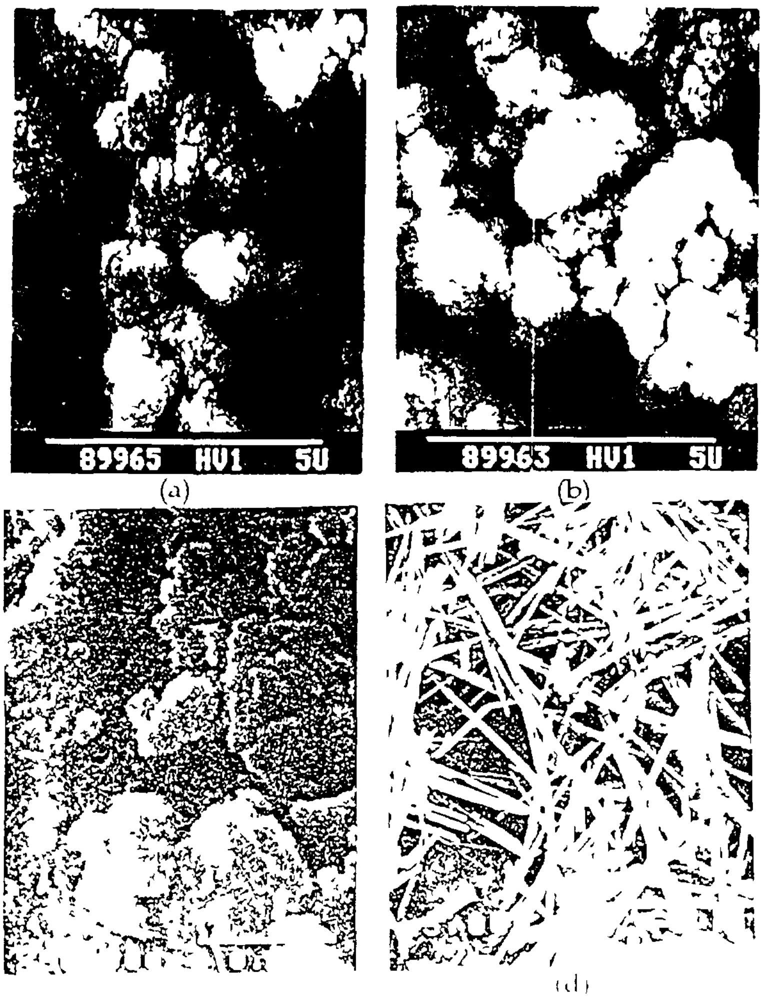

FIG. 7 SEM images of potassium titanate
(a) $K_2Ti_6O_{13}$ gel powder (b) crystalline $K_2Ti_6O_{13}$
(c) $K_2Ti_4O_9$ gel powder (d) crystalline $K_2Ti_4O_9$

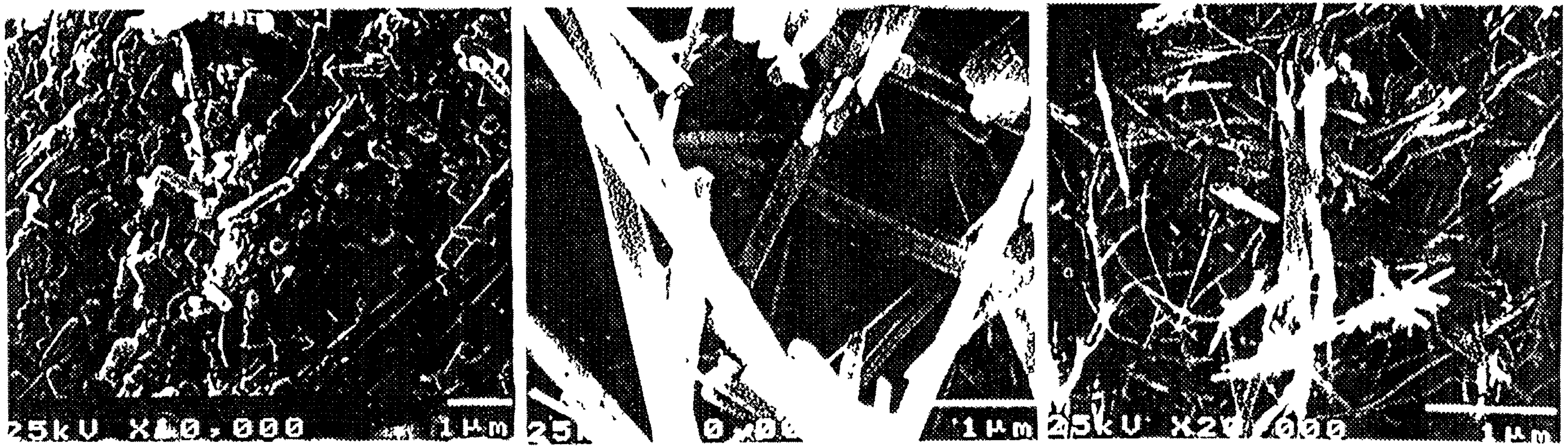

(a) (b) (c)

*FIG. 8. SEM images of potassium titanate by different preparative methods
(a) melting method (b) sol-gel method (c) sol-gel method, supercritical drying*

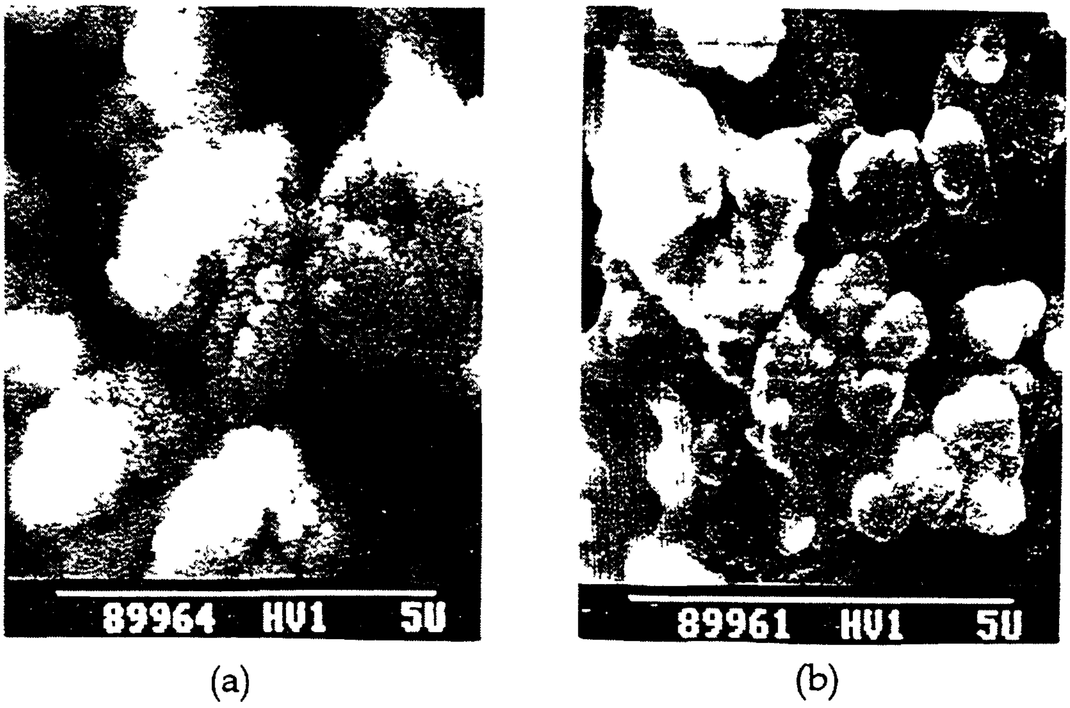

FIG. 9. SEM images of potassium titanate gel powders with different K/Ti ratios (a) K/Ti=0.3 (b) K/Ti=1.0

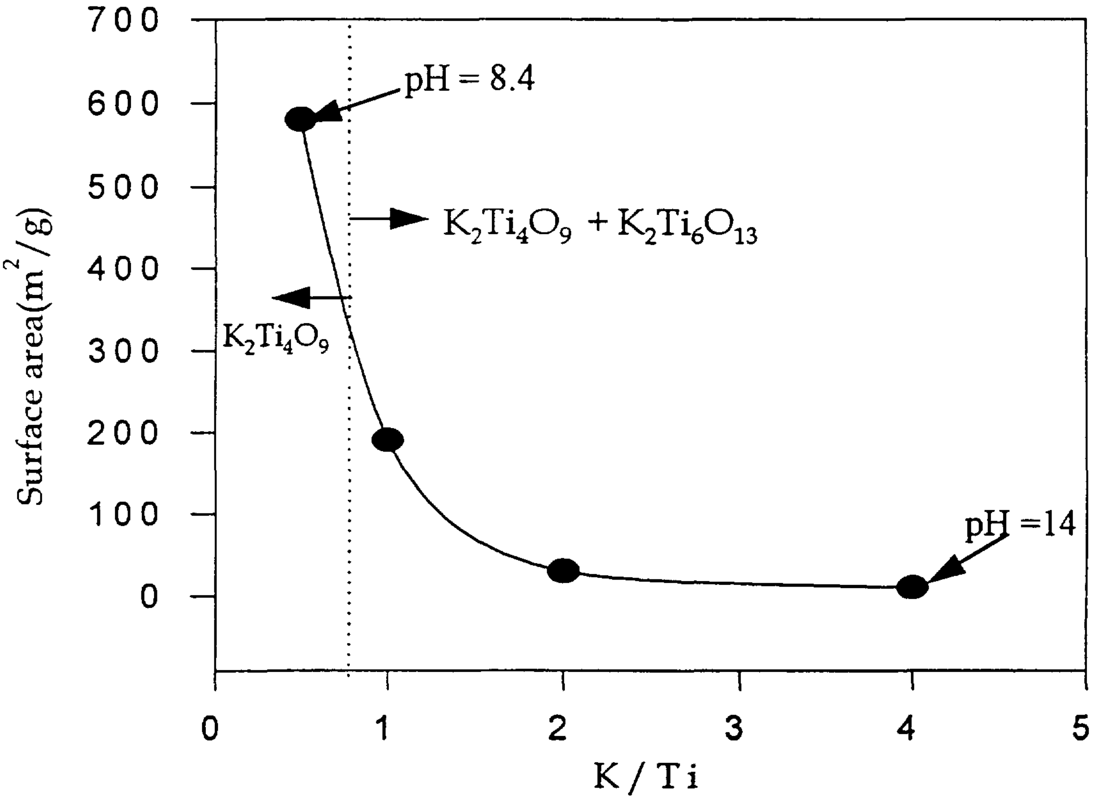

FIG. 10. Effects of K/Ti ratio on the surface area of potassium titanate gel powders.

dropped drastically as K/Ti ratio increased as shown in Fig. 10. When the K/Ti ratio is less than 1 more than 200m^2/g area is obtained. Concurrently, when the K/Ti ratio increased, the pH of the solution increased from 8.3 (K/Ti=0.5) to 14 (K/Ti=4).

3.2.3. Effect of H_2O/Ti ratio

In the hydrolysis reaction, the H_2O/Ti ratio is an important parameter in determining the final properties of the sample because the hydrolysis reaction rate changes with water content of the solution. The titanium alkoxides are known to be sensitive to water content due to the rapid hydrolysis of titanium alkoxide in the presence of water [11]. The change of surface area of potassium titanate gel is shown in Fig. 11. It shows clearly that the large surface area of gel powder is obtained at high H_2O/Ti ratio after room temperature drying in the case of potassium hexatitanate. However, the surface area of potassium tetratitanate was not dependent on the ratio of H_2O/Ti. This is an unexpected result and we should find other ways. Among them, the supercritical drying process is one way to get a high surface area because it can minimize the liquid-vapour interfacial(capillary) force during the drying process. In Fig. 12, the surface area of the supercritical dried sample was compared with that obtained using the melting method. More than 25m^2/g of surface area is obtained at 800°C by the supercritical drying.

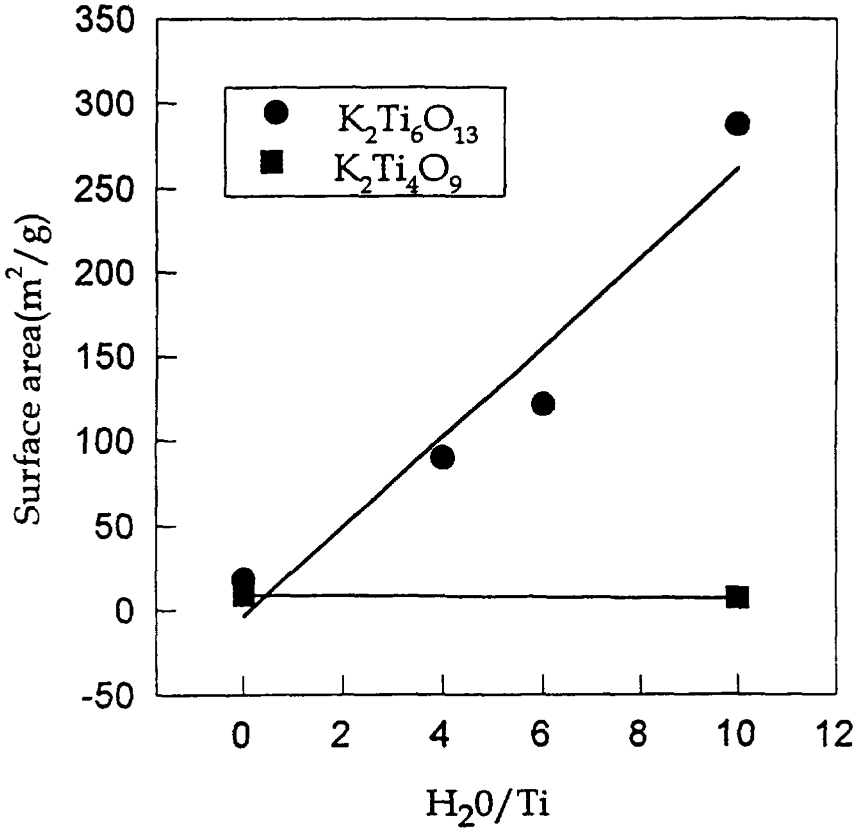

FIG. 11. Changes of surface area with H_2O/Ti in potassium titanate gel powders (25C drying)

3.2.4. Effect of titanium precursors

The effect of titanium alkoxides on the types of potassium titanates is shown in Fig. 13. The product ratio was calculated from the representative peak intensity of XRD. (200) and (001) were used as the representative planes of potassium hexatitanate and potassium tetratitanate respectively. As the alkyl chain length(R) of the titanium alkoxide increased, the potassium tetratitanates to potassium hexatitanate ratio increased at the given K/Ti ratio (=0.5). It suggests more potassium is incorporated as the chain length of alkoxide increased.

In the alkoxide system, the alcohol exchange reaction occurs readily with metal alkoxide precursors and exchange is facilitated when δ(electrical negativity)(M) > G1. For a series of titanium alkoxides, the alcohol exchange reaction occurs as follows:

$$Ti(OR)n + xEtOH \rightarrow Ti(OR)n\text{-}x(OEt)x + xROH \quad \text{---- (3)}$$

According to Bradley et al, alcohol exchange rate decreases with the alkyl chain length, consistent with the steric effect expected for an associative SN reaction mechanism. The molecular complexity of titanium alkoxide is decreased with increasing chain length of alkyl group (i.e., when R=Et, n=2.4; R=Pr, n=1.4 and R=Bu, n=1.0[16]) as shown in Fig. 13. In our case, the alcohol exchange rate of $Ti(OBu)_4$ should be slow in comparison with $Ti(OEt)_4$ and $Ti(OPr)_4$ which may be ascribed to a steric factor of the alkyl group. Therefore, facts imply that the hydrolysis reaction of titanium alkoxide might be dependent on the chain length of alkoxide. It is possible that potassium methoxide incorporation into titanium alkoxide to form more Ti-O-K bonds before the formation of Ti-O-Ti bond is increased which increases the chain length of titanium alkoxide in the course of hydrolysis and condensation reaction. As a result, we can get a high yield of potassium incorporation into the titanium matrix (potassium tetratitanate) with $Ti(OBu)_4$.

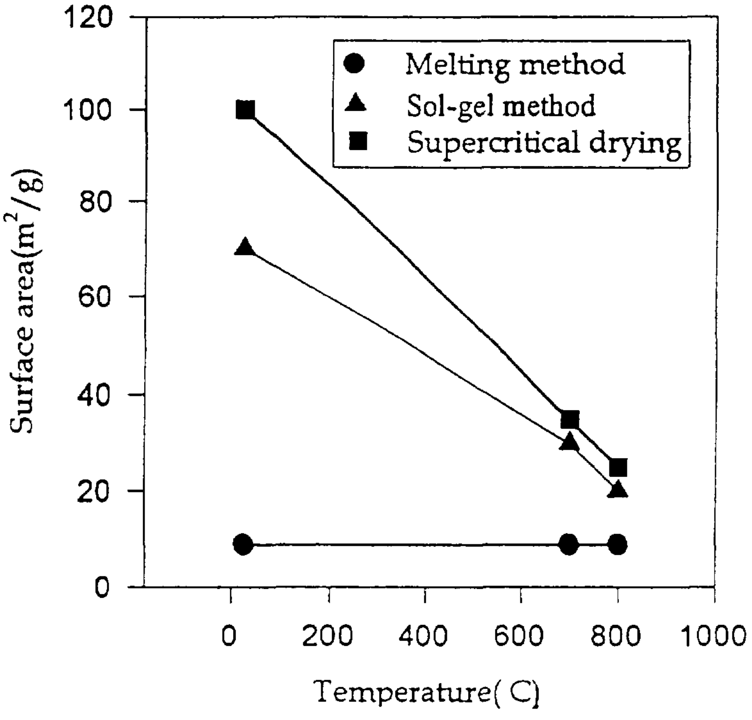

FIG. 12. Changes of surface area with calcination temperature ($K_2Ti_4O_9$, $H_2O/Ti=10$)

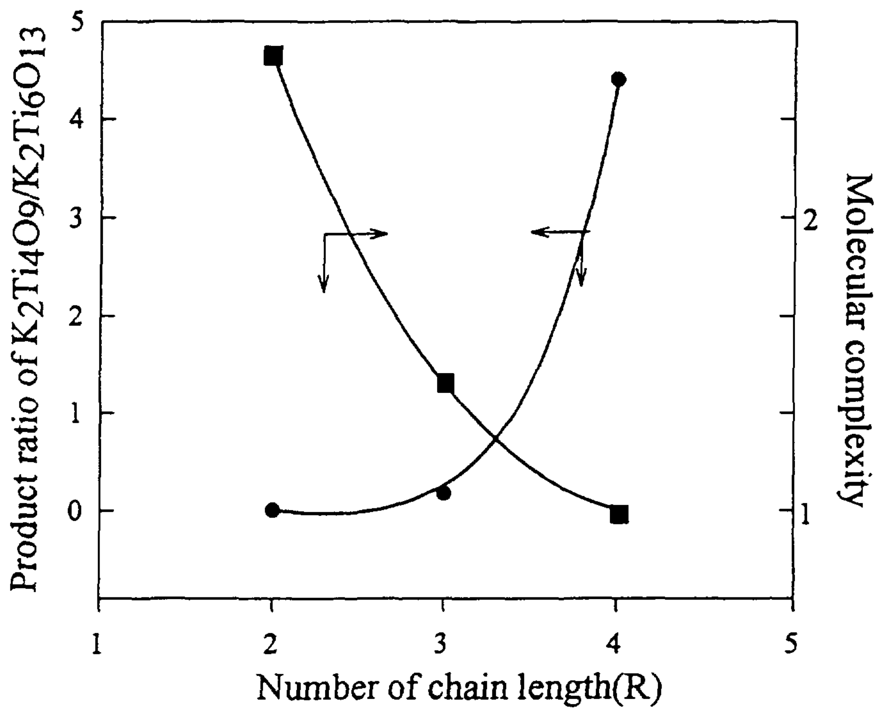

FIG. 13. Effect of alkyl chain length on the product ratio of $K_2Ti_4O_9$ to $K_2Ti_6O_{13}$ (K/Ti=0.5, 1000°C)

3.3. SODIUM ALGINATE METHOD

After ion exchange with metal ions, the alginic acid fibre becomes K-Ti-alginate because protons are exchanged for K and Ti ions. Figure 14 shows the changes of XRD patterns with the K/Ti ratio. We could obtain potassium titanate when the K/Ti ratio is more than 5, which is higher than that of the theoretical ratio(K/Ti=0.3). In the case of K/Ti=25, potassium tetratitanate phase is present as shown in Fig. 15 (c). This result suggests that ion selectivity for titanium ion is higher than that for potassium ion when using alginic acid [17]. These results show that a greater excess of potassium is necessary for the formation of potassium titanate in alginate and sol-gel method.

Figure 15 shows SEM images of potassium titanate after calcining the K-Ti-alginate at 800°C. The average length and thickness of potassium tetratitanate is about 2cm and $150\mu m$, respectively. The aspect ratio of this fibre is about $1.3\text{x}10^3$, which is the highest aspect ratio of potassium titanate among the various synthetic methods. This result also implies the possibility of formation of continuous fibre in the potassium titanate system.

Figure 16 shows the morphological changes of potassium tetratitanate depending on the synthetic methods. It should be noted that the needle type of potassium titanate, which has the largest length in size and the highest aspect ratio, is generated from K-Ti-alginate fibre.

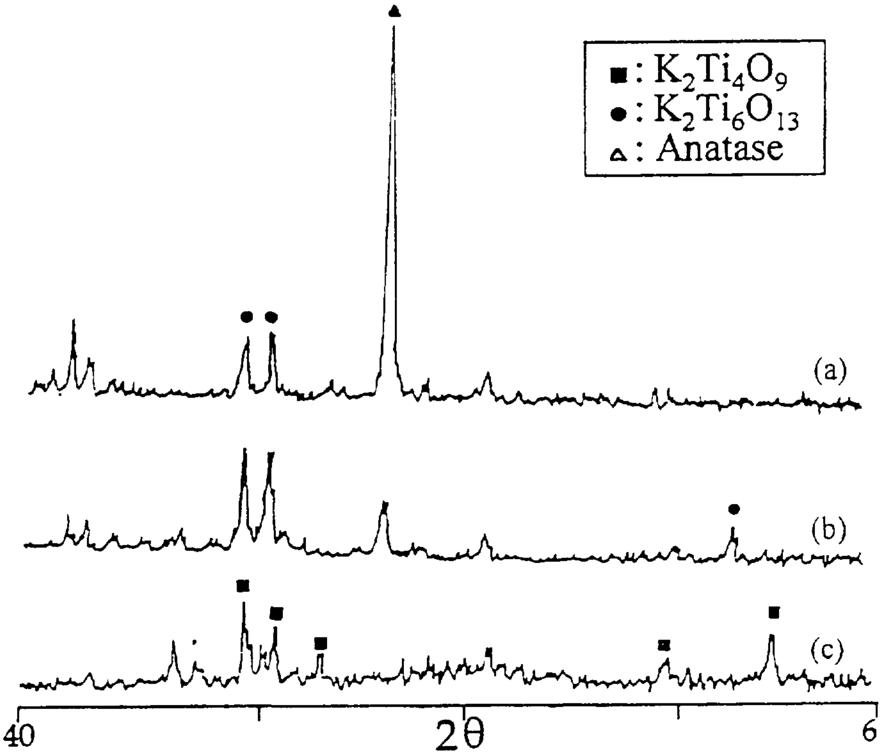

FIG. 14. Changes of XRD patterns with K/Ti ratio in alginate method.
(a) K/Ti=5 (b) K/Ti=10 (c) K/Ti=25

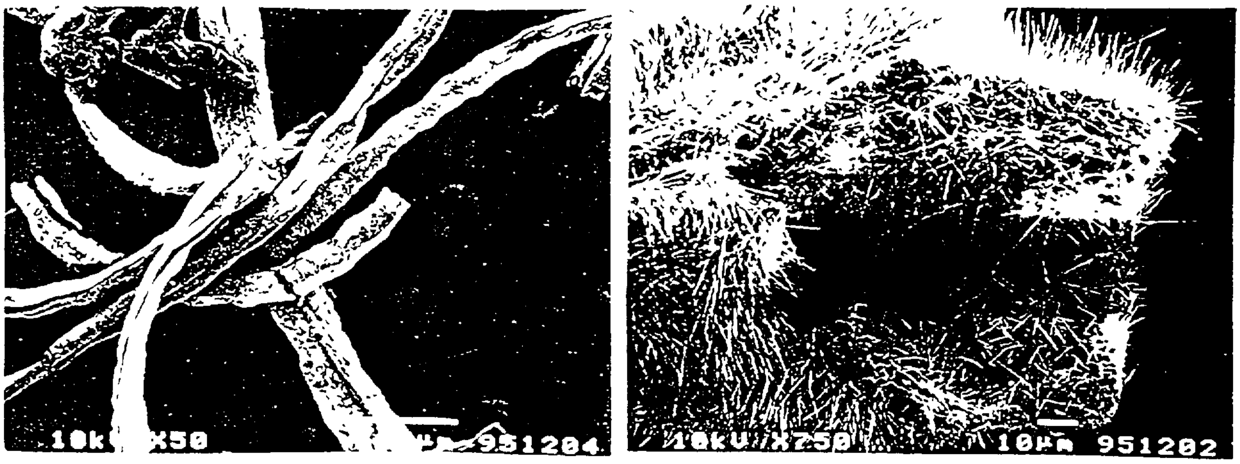

(a)

(b)

FIG. 15. SEM images of potassium tetratitanate synthesized by using alginate method (K/Ti=25, calcining at 100C).

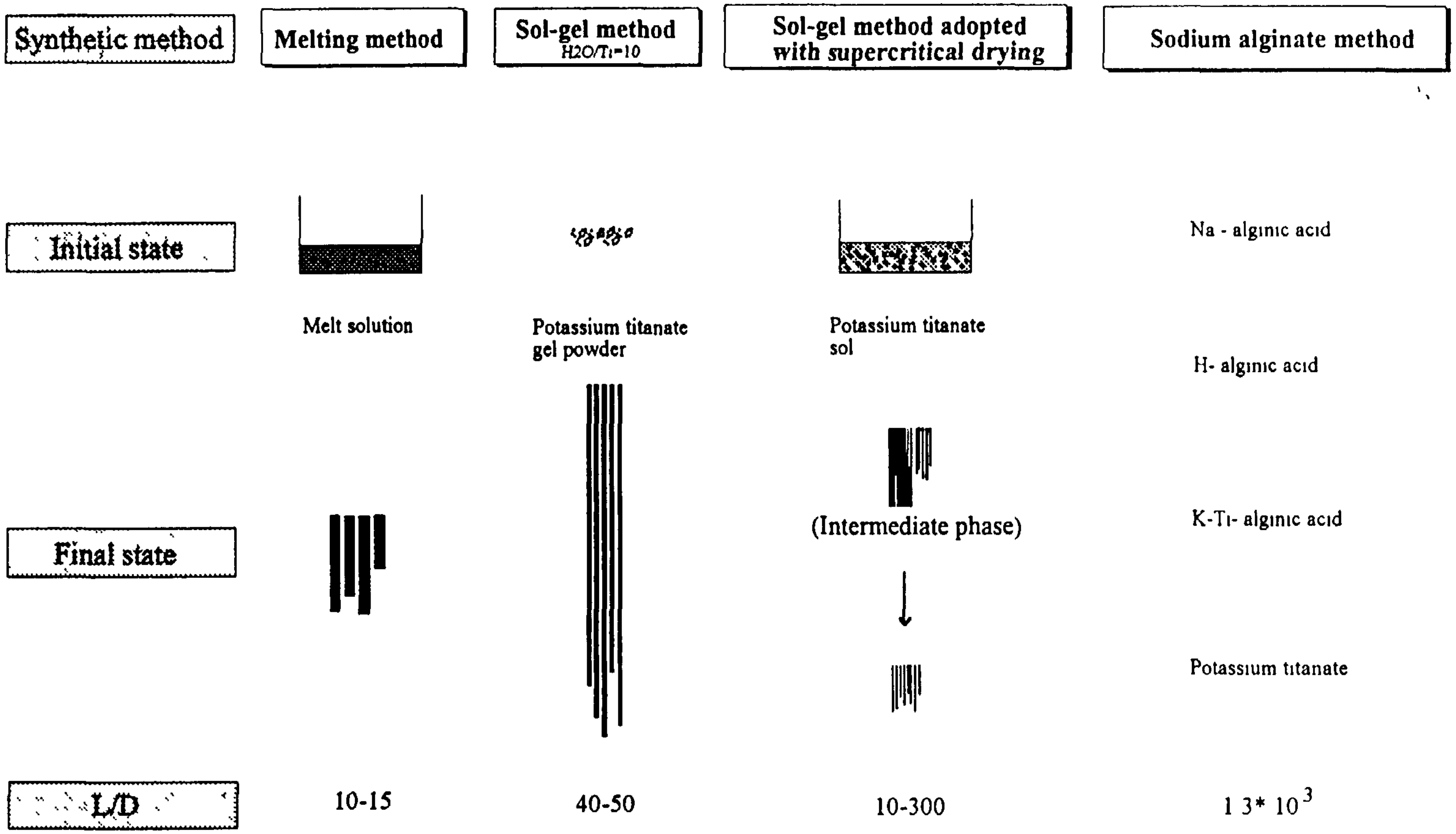

FIG. 16. Morphological changes of potassium tetratitanate depending on the synthetic methods.

3.4. ION EXCHANGE OF STRONTIUM ION

Ion exchange of strontium ions was examined for potassium titanate samples prepared by various methods. The HCl treated sample was obtained by replacing the interlayered potassium ion to proton ion and hydronium ion from the potassium tetratitanate as shown in eq. (4).

$$xSr^+(aq) + H_2Ti_4O_9\,yH_2O \rightarrow Sr_xH_{(2-y)}Ti_4O_9\,yH_2O(s) + xH^+(aq) \quad (4)$$

Strontium ion uptake on acid treated potassium tetratitanate as a function of time is presented in Fig. 17. Adsorption capacity depends on the pretreatment. The sample dried at 200°C shows higher Sr^{2+} ion exchange capacity (0.186 mmol/g) than that dried at 50°C (0.04 mmol/g). Figure 18 shows the degree of dispersion of acid treated potassium titanate in aqueous phase. Samples dried at 50°C are agglomerated to each other to form larger secondary particles. Therefore, degree of dispersion seems to have marked effect on ion exchange capacity.

Figure 19 shows the ion-exchange capacity of hydrous titanium dioxide as a function of pH. An increase in ion exchange capacity of hydrous titanium dioxide synthesized by the sol-gel method is observed with increasing pH. The maximum ion exchange capacity, 4.0meq/g, was obtained at pH 12, which is highly alkaline. From the point of view of the chemical process, not only the ion exchange capacities but also the exchange rate are important parameters. Strontium ion uptake on hydrous titanium dioxide as a function of time is presented in Fig. 20. Equilibrium is attained after 10 minutes with the samples of the melting method while 5 minutes is enough to reach equilibrium with sample of the sol-gel method. The ion exchange rate of acid treated potassium tetratitanate is increased in the order; supercritical drying >sol-gel method >melting method. As for ion exchange capacity, the melting method samples are lower than those of the sol-gel method combined with the supercritical drying process.

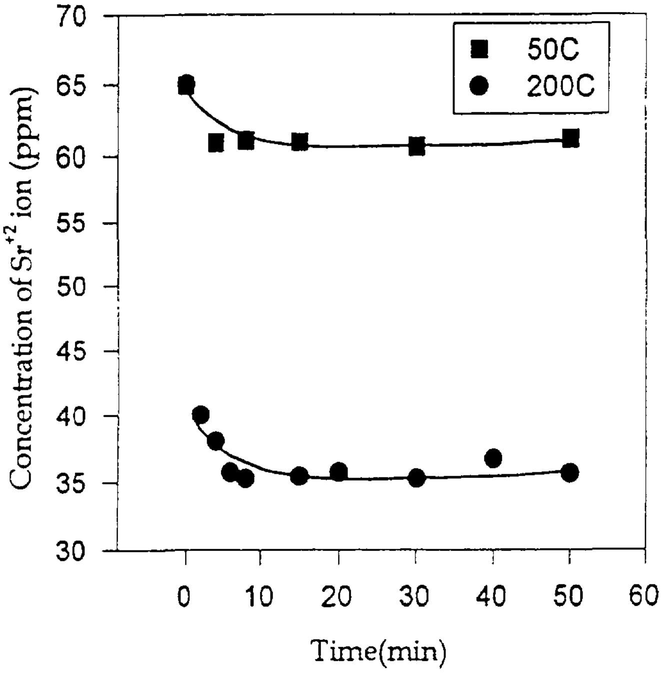

FIG. 17. Changes of Sr^{+2} ion concentration with ion exchange period.
($H_2O/Ti=10$)

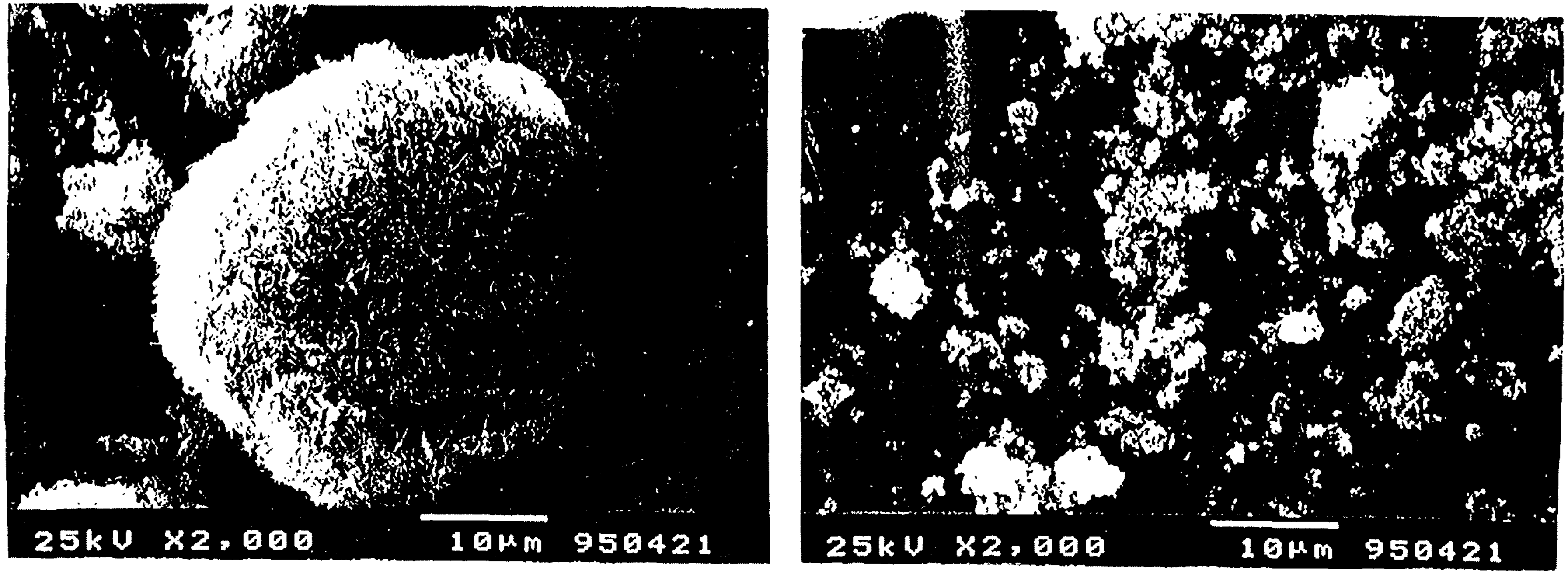

(a)

(b)

FIG. 18. SEM images of acid treated $K_2Ti_4O_9$
(a) drying at 50C (b) drying at 200C

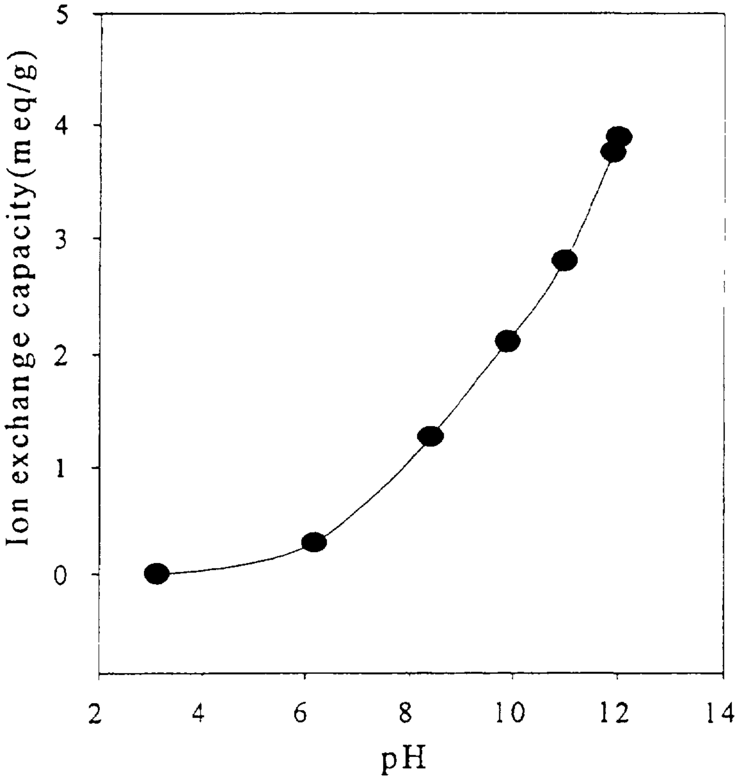

FIG. 19. Changes of strontium ion exchange capacity of hydrous titanium dioxide with pH

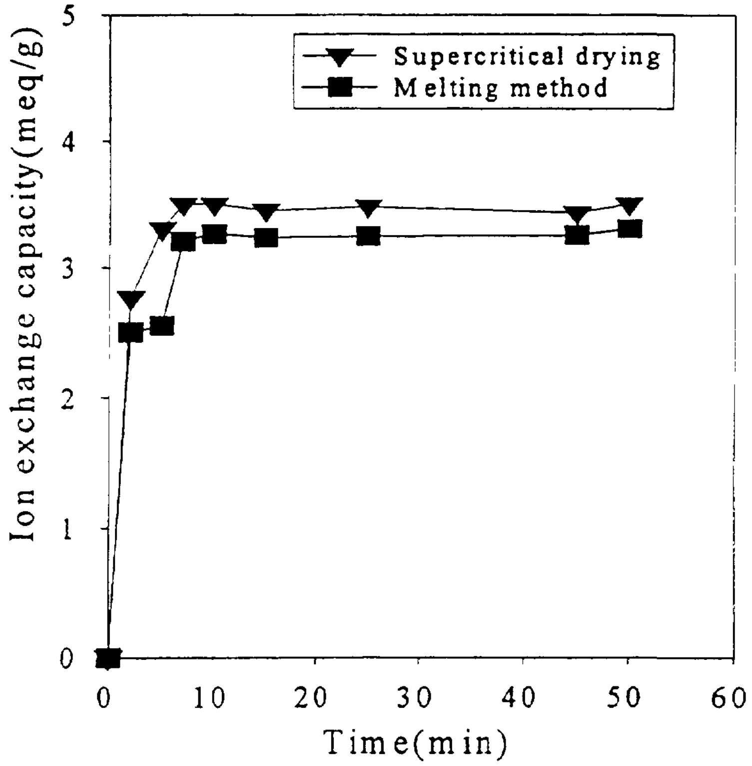

Fig. 20. Changes of Sr ion exchange capacity of hydrous titanium dioxide with preparaticve method as a function of time

This shows the advantages of the sol-gel process against the melting method. Namely, one can enlarge the BET surface area and change the morphology of potassium titanate using sol-gel process conditions.

To confirm the phase change behavior of exchanged sample, the strontium ion exchanged sample was calcined up to 1000°C. Figure 21 shows the change of XRD patterns of the strontium ion exchanged sample with calcination. At 1000°C, anatase, rutile, and strontium titanate were present. This shows that the following reactions proceed during the thermal process with the sintering of exchanged sample.

$$SrTi_4O_9 \rightarrow SrTiO_3 + 3TiO_2 \quad (4)$$

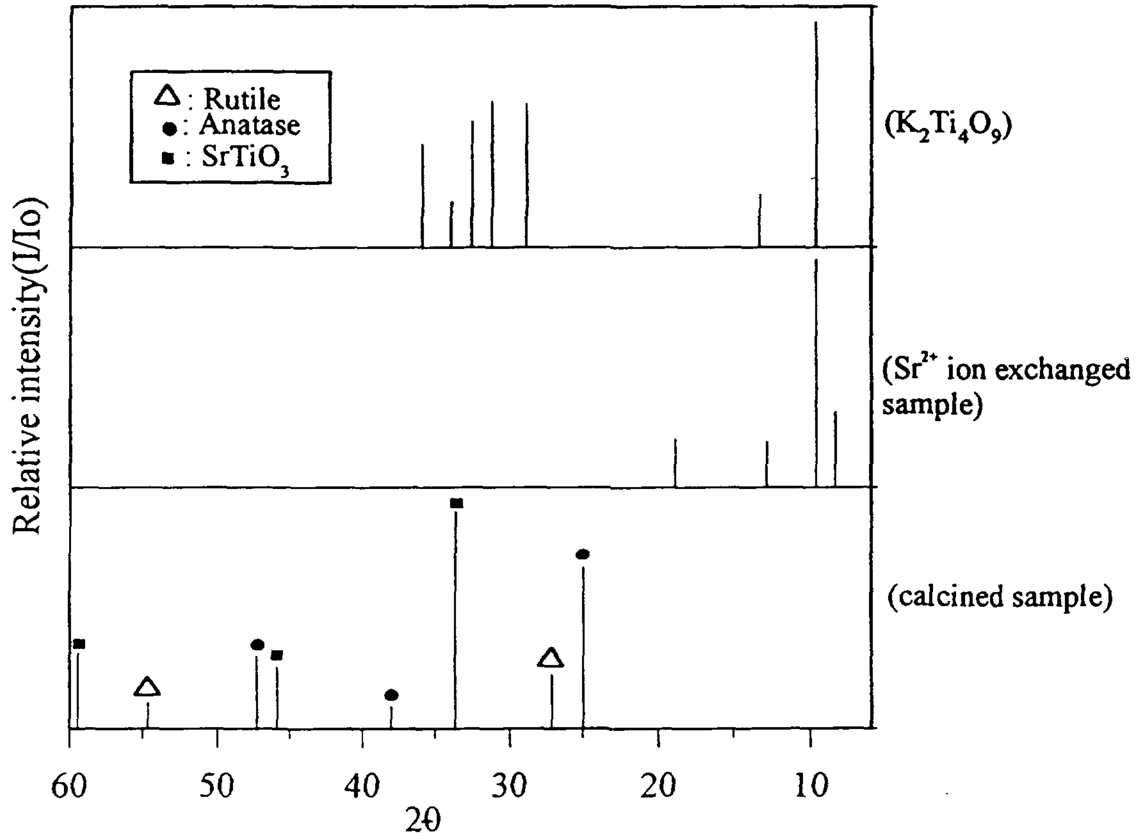

FIG. 21. Phase change behaviours of strontium ion exchanged sample after calcination at 1000C.

4. CONCLUSIONS

(1) In this experiment potassium tetratitanates with high surface area about 25 m^2/g were obtained at 800°C by using a sol-gel process combined with supercritical drying.

(2) The morphology and aspect ratio of potassium tetratitanate were varied depending on the preparation method. The sodium alginate method provided the largest aspect ratio.

(3) The greater BET area of potassium titanate provides more rapid ion exchange and a greater ion exchange capacity for the immobilization of a nuclear waste metal ion (Sr^{2+}).

TABLE I. EFFECT OF TITANIUM PRECURSORS ON THE FORMATION OF POTASSIUM TITANATES

Mole ratio of CH_3OK/Ti	$Ti(OC_3H_5)_4$	$Ti(OCH(CH_3)_2)_4$	$Ti(OCH_3)_3CH_3)_4$
20	20	20	20
20	20	20	20
20	20	20	20
20	20	20	20
20	20	20	20

REFERENCES

[1] FUJIKI, Y., KOMATSU Y., OHTA, N. : Chem. Lett. 1023-26(1980)

[2] MUTO, F., NAKAGOMI, T., TAKS, S.: Yogyo-Kyokai-Shi, 86(19) 443 (1978)

[3] SHIMIDZU, T., HASHIMOTO, K., YANAGIDA, H.:Yogyo-Kyokai-Shi,

[4] SHIMIDZU, T., YANASIDA, T., HORI, M., HASHIMOTO, K. , NISHKAWA, Y.: Yogyo-Kyokai-Shi, 87(5), 272(1979)

[5] MUTO, F., NAKAOMI T., TAKI, S.: Yogyo-Kyokai-Shi,86(10),443(1978)

[6] PARTLOW, D.P. AND YOLDAS, B.E.: J. Non-Cryst. Solids,46153(1981)

[7] FUJIKI, Y., IZUMI, F., OHSAKA, T., WATANABE, M.: Yogyo-Kyokai-Shi, 85(10), (1977)

[8] KOMATSU,Y., FUJIKI, Y. AND SASAKI, T. Japan Analist Sect E31, E225 (1982)

[9] FUJIKI, Y., WATANABE, M., SASAKI, T., MITSUHASHI, T., ONOSA, Y., YOSHIKADO, S., OHACHI, T.: Yogyo-Kyokai-Shi,94(9),1021(1986)

[10] HEINONEN, OO.J., LEHTO, J., MIETTINEN, J.K. Radiochimica Acta 28,93-96(1981)

[11] DISLICH, H: New routes to multicomponent oxide glasses,Angew. Chem. Int. Ed.,10,363(1971)

[12] JUNG, K.T., SHUL, Y.G. J. Sol-gel science and technology, accepted.

[13] SUGIMOTO, A., SANO, T., KANEKO, Y. J. Jpn. Chem. Soc., 2 (1994)126 .

[14] FUJIKI, Y., SASAKI, T. J. Solvent Extraction and Ion Exchange, 11(1), 159-169(1993)

[15] CANHAM, L.T., CULIIS, A.G., PICKERING, C., DOSSER, O.D., COX, T.I., LYNCH, T.P., J. of Nature, 368, 10, (1994) 133.

[16] BRADLEY, D.C., MEHROTRA, R.C., GAUR, D.P. Metal alkoxides(Academic press, NY, 1978)

[17] IWASAKI, H., KANEKO, Y. J. Soc. Mat. Sci. Jpn. 37 (1988)60.

XA9744284

SYNTHESIS AND ION EXCHANGE PROPERTIES OF VARIOUS FORMS OF MANGANESE DIOXIDE: STUDIES ON SELECTIVITY FOR CATIONS OF GROUPS I AND II

B. BARTOS, A. BILEWICZ
Department of Radiochemistry,
Institute of Nuclear Chemistry and Technology,
Warsaw, Poland

Abstract

Various crystalline forms of manganese dioxide were synthesized by redox reaction between alkali metal permanganates and manganese sulphate. The crystalline structure of samples precipitated from $KMnO_4$, $RbMnO_4$ and NH_4MnO_4 solutions showed good agreement with that reported for α-crystalline MnO_2 and exhibited high selectivity for cations of the given ranges of ionic radii: 135 - 155 pm (K^+, NH_4^+, Rb^+, Ba^{2+} and Ra^{2+}). The high ion exchange affinity for Ra^{2+} cations is only shown by MnO_2 samples precipitated in the presence of cations with similar ionic size (K^+, NH_4^+ and Rb^+). These sorbents have the memory size effect of these cations. The samples precipitated from $NaMnO_4$ and $CsMnO_4$ were identified as the γ form of MnO_2 and exhibit a much smaller affinity for Ra^{2+} cations. The highly selective α-crystalline MnO_2 samples can also be obtained from $NaMnO_4$ in strongly acidic solutions ($[H^+] > 8M$). The α-MnO_2 samples can be applied in new procedure for the determination of $^{226,228}Ra$ in natural water at very low level.

1. INTRODUCTION

Manganese oxides possess highly diverse crystallographic morphologies. Many compounds with layered and tunnel structures with the MnO_6 octahedra structural unit are possible. Manganese dioxide occurs in many minerals and several crystalline forms of MnO_2 have been synthesized [1]. Recently, an α-crystalline form of MnO_2 in the H^+ form has been shown to have excellent ion-exchange selectivity towards cations with a crystal ionic radius of 130-150 pm, e.g. K^+, NH_4^+, Rb^+ and Ba^{2+} [2-5]. This high selectivity can be attributed to the well-defined 2x2 tunnel structure which is composed of double chains of edge-shared MnO_6 octahedra and corner sharing of the double chains [6]. Related MnO_2 minerals are cryptomelane (with K^+ as tunnel cation) and hollandite (with Ba^{2+} as tunnel cation). The synthetic cryptomelane MnO_2 was obtained by redox reaction between $KMnO_4$ and $MnSO_4$. The product obtained contains Mn(IV) and Mn(III) ions, and the negatively charged framework is organized around the exchangeable K^+ cations which can be readily removed by acid [6]. We suggest that, after exchange of K^+ ions, the cryptomelane MnO_2 exhibits a memory effect of the cation size and in our opinion this is the source of its high selectivity for K^+ and for cations with similar ionic radii. A similar effect has been observed in complexation of metal cations by macrocycles obtained in template synthesis [7].

The aim of the present work is to study the possibility of synthesis of cryptomelane MnO_2 exhibiting special selectivity for certain cations. When permanganates other than $KMnO_4$ are used for synthesis, i.e. $NaMnO_4$, NH_4MnO_4, $RbMnO_4$, and $CsMnO_4$, the framework will also be organized around monovalent metal cations and after removal of the cations we should obtain sorbents with special selectivity for Na^+, NH_4^+, Rb^+ and Cs^+ respectively. Special attention will be paid to synthesis of MnO_2 selective for Ra^{2+}. Due to the fact that the ionic radius of NH_4^+ ($r_i = 143$ pm) and Rb^+ ($r_i = 152$ pm) is similar to the radius of Ra^{2+} ($r_i = 148$

pm), it is expected that sorbents obtained using NH_4MnO_4 and $RbMnO_4$ should exhibit special affinity for Ra^{2+}. Similarly, in the case of MnO_2 synthesis in the presence of the Na^+ ions (r_i=102 pm), we should obtain a sorbent selective for Ca^{2+} (r_i=100 pm), Cd^{2+} (r_i=96 pm), etc.

The practical goal of the studies is to synthesize selective sorbents for radium radionuclides. The pollution from Ra^{2+} released with water from coal mines is an important radioecological problem in Poland and also, although to a lesser extent, in some other countries. The cryptomelane MnO_2 samples obtained on the basis of NH_4MnO_4 and $RbMnO_4$ should selectively adsorb radium radionuclides from saline waters and also in the presence of Ba^{2+} ions.

2. EXPERIMENTAL

2.1. REAGENTS

Commercial $KMnO_4$ and $NaMnO_4$ were obtained from Fluka. The less soluble permanganates of $RbMnO_4$, $CsMnO_4$ and NH_4MnO_4 were precipitated from mixture of $NaMnO_4$ with Rb_2SO_4, Cs_2SO_4 and $(NH_4)_2SO_4$ respectively at low temperature (around 0°C). The permanganates obtained were washed with cold water and acetone and air-dried at room temperature. Other chemicals were commercially available.

2.2. RADIONUCLIDES

Gamma emitting ^{24}Na, ^{42}K, ^{86}Rb, ^{137}Cs, ^{85}Sr, ^{133}Ba and ^{223}Ra and beta emitting ^{45}Ca radiotracers were used. The ^{223}Ra was obtained from the Ac generator at the Institute of Nuclear Physics, Orsay (France), and the other radionuclides were supplied from the Radioisotope Center at Swierk (Poland).

The measurements of γ-activities were carried out with the use HPGe detector, and that of the β-emitter ^{45}Ca, by GM counter.

2.3. SYNTHESIS OF VARIOUS FORM OF MANGANESE DIOXIDE

α-crystalline MnO_2 samples were synthesized according to the procedure by Tsuji and Abe [8]. The precipitates were obtained by adding the appropriate permanganate solution (250 mL of 0.5M $KMnO_4$, $NaMnO_4$, NH_4MnO_4, $RbMnO_4$ or $CsMnO_4$ in 1M H_2SO_4) to 250 mL of a solution of 1M $MnSO_4$ and 1M H_2SO_4 at 60°C. The precipitates were aged overnight and washed with 6M HNO_3 (50 mL), followed by water washing until the wash liquor became neutral. The product was dried at ca 70°C for three days, and then it was ground and sieved. The fraction of 0.1-0.5 mm in diameter was collected for adsorption experiments. Any residual alkali metal and SO_4^{2-} ions were removed from the crude product by percolating concentrated HNO_3 through a glass column filled with the material, until the concentration of alkali metal cations in the effluent was lower than 10^{-4} M. The solid was then washed with water and air-dried at room temperature.

For studies on the transformation of α-MnO_2(Rb) to its hydrogen form, the sorbent labelled with radioactive ^{86}Rb was synthesized. The Rb^+ cations labelled by ^{86}Rb were eluted from precipitated $MnO_2(Rb)$ by concentrated HNO_3. 20 mL of HNO_3 was sufficient for full transformation of $MnO_2(Rb)$ to $MnO_2(H)$. Similar results were obtained in the case of $MnO_2(K)$ where the amount of K^+ in the $MnO_2(K)$ phase was determined using neutron activation analysis.

2.4. X-RAY DIFFRACTION STUDIES

Structural investigations of the MnO_2 samples were made using the X-ray diffractometer URD-6 (Zeiss) equipped with lithium drifted silicon X-ray detector (Silena), using Mo K_a radiation (40 kV, 20 mA) at the diffraction angle range $2\Theta=6\text{-}50°$.

2.5. CHEMICAL ANALYSIS OF THE SAMPLES.

Synthesized samples have been analyzed for alkali metal content by neutron activation analysis with a neutron flux of 2.5×10^{13} N cm^{-2} s^{-1} in the nuclear reactor ORPHEE at CEN Saclay (France).

2.6. DETERMINATION OF DISTRIBUTION COEFFICIENT (K_d).

Batch distribution studies of alkali and alkaline earth metal cations from aqueous nitric acid solutions were carried out by shaking 50 mg of adsorbent with 5 - 10 cm^3 samples of solution containing radiotracer. After attaining the distribution equilibrium (48 h shaking), aliquots of solution were measured for their radioactivity and compared with those of the initial solution.

The distribution coefficients K_d have been calculated from the equation:

$$K_d=\frac{(A_i-Aeq)}{Aeq}\cdot\frac{V}{m}$$

where:

A_i and A_{eq} denote the measured activities of the aliquots - initial and at equilibrium, respectively,

V is the volume of the solution (mL), and

m is the mass of the adsorbent (g).

3. RESULTS AND DISCUSSION

3.1. INFLUENCE OF CATIONS PRESENT IN THE SYNTHESIS SOLUTION ON PROPERTIES OF MnO_2 SAMPLES

3.1.1. Structural characterization of the adsorbent

Table I presents the results of X-ray diffraction studies of MnO_2 samples precipitated from $NaMnO_4$, $KMnO_4$, NH_4MnO_4 and $RbMnO_4$. The interlayer distances have been

TABLE I. X-RAY DIFFRACTION DATA OF THE γ-MnO_2, CRYPTOMELANE AND SYNTHESIZED MnO_2 SAMPLES

MnO_2(K)	MnO_2(Rb)	MnO_2(NH_4)	CRYPTOMELANE [ASTM card 29-1020]
d (Å) I	d (Å) I	d (Å) I	d (Å) I/Io
7.06 40	7.07 20	7.00 40	6.94 25
4.93 43	4.87 25	4.96 40	4.90 30
3.13 32	3.10 51	3.12 30	3.10 65
2.38 62	2.39 64	2.40 70	2.38 100
2.15 17	2.15 33	2.16 15	2.14 15
1.83 24	1.83 25	1.83 29	1.82 12
MnO_2(Na)	γ-MnO_2 [ASTM card 14-644]		
d (Å) I	d (Å) I/Io		
3.99 28	3.95 100		
2.42 24	2.42 100		
2.33 weak	2.32 80		
2.13 23	2.12 80		
1.63 17	1.63 80		
	1.60 60		
	1.42 60		

calculated from the individual peaks and compared to the literature data for various crystalline form of MnO_2.

The X-ray diffraction pattern of our samples, except MnO_2(Na) show a good agreement with that reported for cryptomelane, which belongs to a body-centered tetragonal system with the lattice parameters: $a_o = 9.77$ Å , and $c_o = 2.85$ Å [2]. The ion exchange sites of the dimension 2.68 and 2.84 Å along the a_o and c_o axes, respectively [3], assure selective adsorption of metal ions of radii close to 1.4 Å (140 pm) [2-5].

In the case of MnO_2(Na) the sample was identified as the γ form of MnO_2.

3.1.2. Chemical characterization of the adsorbent

The amounts of alkali metal cations in synthesized MnO_2 samples before and after acid treatment (MnO_2(H)) are presented in Table II.

TABLE II. NUCLEAR ACTIVATION ANALYSIS OF MnO_2 SAMPLES

Sample	Alkali metal
MnO_2(K) MnO_2(H)	2.12 0.10
MnO_2(Rb) MnO_2(H)	0.76 0.10
MnO_2(Na) MnO_2(H)	0.01 0.007
MnO_2(Cs) MnO_2(H)	0.27 0.01

The results in Table II indicate that the framework of MnO_2(K) and MnO_2(Rb) is organized around the exchangeable K^+ and Rb^+ cations which can be easily removed by acid. The amount of alkali metal cations in MnO_2(Na) and MnO_2(Cs) is very low and the exchangeable cations in these sorbents are probably H_3O^+ ions.

The ion exchange capacity of MnO_2(K) for K^+ ions, calculated as the difference of K^+ content before and after HNO_3 washing, is equal to 2.0 mmol g^{-1}. In the case of MnO_2(Rb) the capacity is lower, equal to 0.6 mmol g^{-1}.

3.1.3. Distribution studies of Ra^{2+} and related cations on MnO_2

The dependence of K_d for Ra^{2+} and Ba^{2+} on the molar concentration of nitric acid is shown in Fig.1. The slopes are close to -2 on a log-log scale (in the 0.1 - 1.0 molar concentration range) and indicate an ion exchange mechanism for the adsorption of both ions.

The K_d values of alkali metal cations in 1M HNO_3 solution were plotted as a function of ionic radius (Fig.2). The values of ionic radius (r_i) were taken from Shannon's table for coordination number 6 [9]. In all cases a maximum of K_d can be seen at the r_i of approximately 140 pm, between the r_i of K^+ and Rb^+. As mentioned by Tsuji and Abe [8], the high selectivity of cations with r_i of 140 pm is related to the steric effect of the exchanger which has ion exchange size with diameter 270 pm Due to the rigid MnO_2 structure the cations exchange in partially or fully dehydrated form Small cations like Na^+ are strongly hydrated and require a large amount of energy to be dehydrated K^+ and Rb^+ can shed their hydration shell more readily and enter the exchanger phase The r_i of Cs^+ (169 pm) is too large and Cs^+ cannot enter the MnO_2 phase through the tunnels with smaller radius

The ion exchange efficiency of the MnO_2 sorbents decreases in the order

$MnO_2(K) = MnO_2(NH_4) = MnO_2(Rb) >> MnO_2(Na) > MnO_2(Cs)$

The high ion exchange affinity for K^+ and Rb^+ was exhibited only by MnO_2 samples precipitated in the presence of cations with similar ionic size (K^+, NH_4^+ and Rb^+) These sorbents demonstrated probably the memory size effect of the cations. The MnO_2(Na) and MnO_2(Cs) sorbents have a different crystalline form and exhibit much smaller affinity for the K^+ and Rb^+ cations

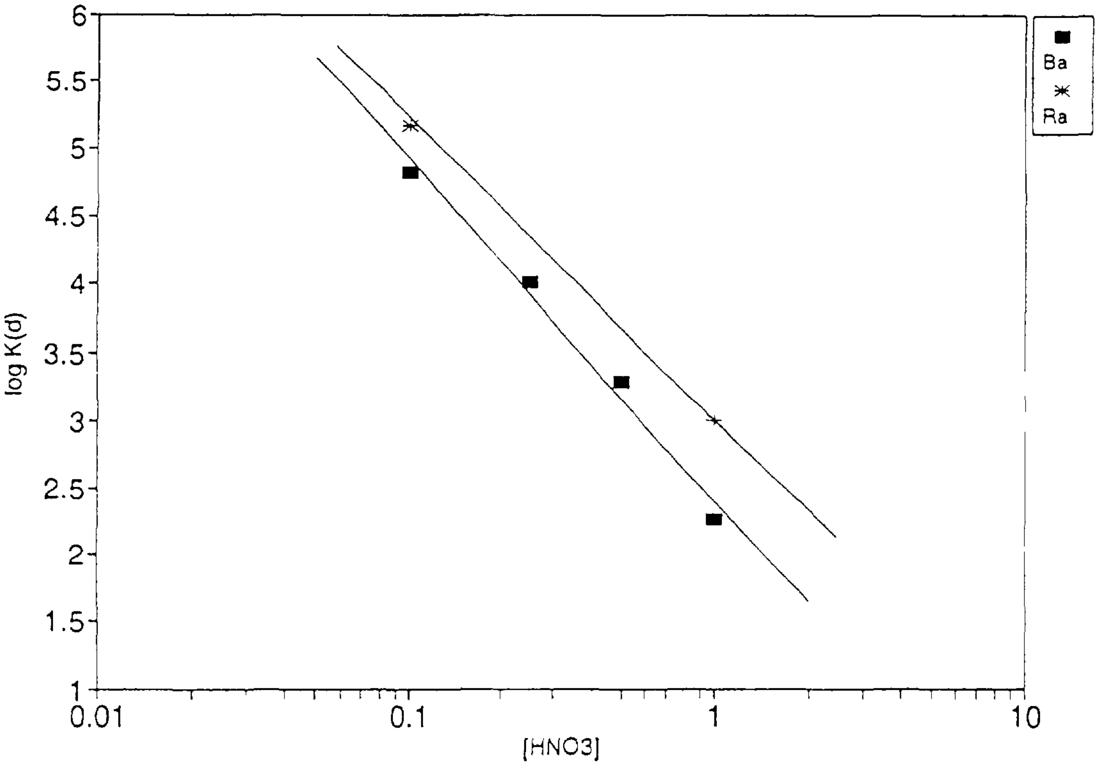

FIG 1 Dependence of K_d for Ra^{2+} and Ba^{2+} on HNO_3 molar concentration.

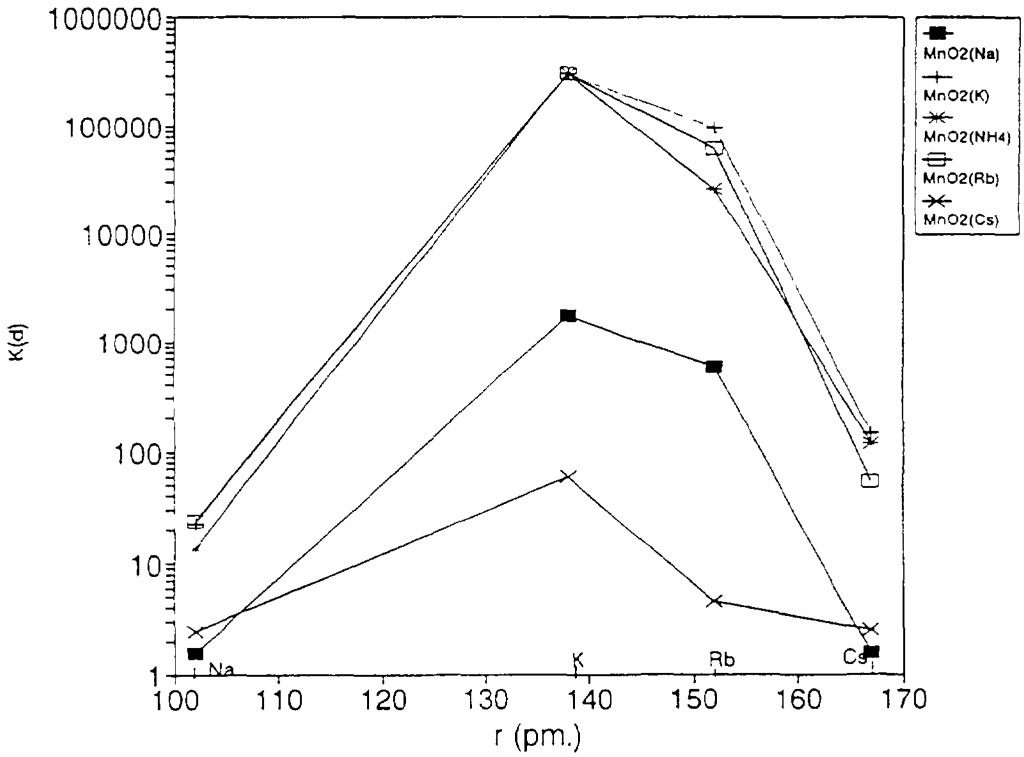

FIG 2 Distribution coefficient values for alkali metal cations in 1M HNO_3 as a function of their ionic radius (Coordination Number = 6).

Similar dependence has been observed for group 2 metal cations (Fig 3), where also a high maximum for cations with r_i = 140 pm (Ba^{2+} and Ra^{2+}) has been found

Due to fact that the r_i of Ba^{2+} and Ra^{2+} are very similar, the K_d values are very close and separation of these cations is very difficult Table III presents the separation factor value $\alpha = K_d(Ra^{2+})/K_d(Ba^{2+})$ for various MnO_2 sorbents.

TABLE III SEPARATION FACTOR (α) FOR THE Ra^{2+} - Ba^{2+} CATIONS COUPLE

sorbent	$MnO_2(K)$	$MnO_2(NH_4)$	$MnO_2(Rb)$
α	2 17	3 28	4 48

The selectivity series for MnO_2 samples is as follows

$MnO_2(Rb) > MnO_2(NH_4) > MnO_2(K) >> MnO_2(Na)$

As was reported previously, the high ion exchange selectivity for Ra^{2+} cations is exhibited only by MnO_2 samples precipitated in the presence of cations with similar ionic size (K^+, NH_4^+ and Rb^+) These sorbents have the memory size effect of the cations The $MnO_2(Na)$ and $MnO_2(Cs)$ have another crystalline form and exhibit much smaller affinity for the Ra^{2+} cations The selectivity is based on a particular framework structure of α-MnO_2 stabilized by large ions such as Ba^{2+}, Rb^+, NH_4^+ or K^+ which enter the tunnels of an appropriate diameter [4] Due to the fact that the ionic radius of Ra^{2+} (148 pm) is close to the radius of Rb^+ (152 pm), the selectivity of MnO_2 precipitated from $RbMnO_4$ was greatest of the all samples studied

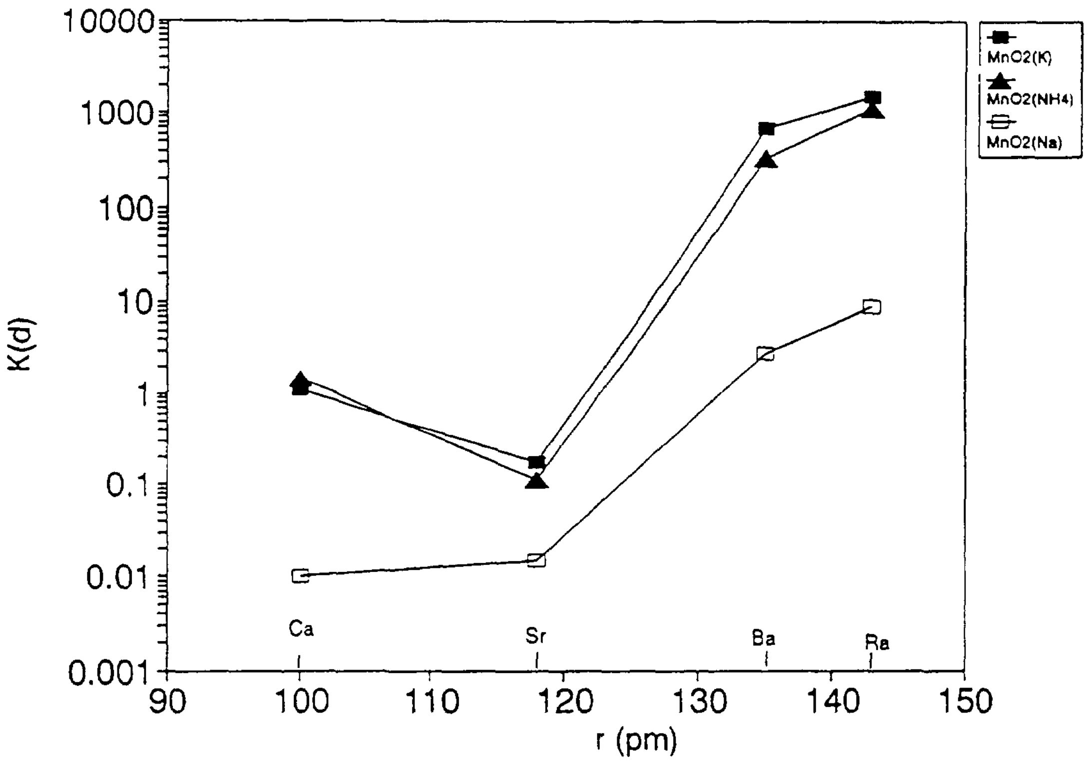

FIG. 3. Distribution coefficient values for alkaline earth metal cations in 1 M HNO_3 as a function of their ionic radius (Coordination Number = 6).

3 2 INFLUENCE OF ACID CONCENTRATION IN SYNTHESIS SOLUTION ON CRYSTALLINITY AND ION EXCHANGE PROPERTIES OF MnO_2 SAMPLES

The MnO_2 samples precipitated from $NaMnO_4$ in 1M H_2SO_4 solution exhibit very little ion exchange properties Because the synthesis redox reaction is very sensitive to the concentration of H^+ ions, studies of the influence of acid concentration on the ion exchange properties of synthesized samples of MnO_2 were performed The samples obtained have been structurally examined

TABLE IV SAMPLES PRECIPITATED AT VARIOUS ACID CONCENTRATIONS

1M H^+		2 M H^+		4 M H^+		8 M H^+	
d(Å)	I/Io	d(Å)	I/Io	d(Å)	I/Io	d(Å)	I/Io
3 99	97	3 99	100	6 94	52	7 0	68
2 42	100	2 42	86	4 85	56	4 93	61
2 33	51	2 34	weak	3 99	78	3 13	45
2 12	59	2 13	82	3 49	30	2 40	100
1 63	87	1 63	61	3 07	30	2 12	39
				2 41	100	1 81	39
				2 39	96		
				2 13	65		
				1 63	70		

The data in Table IV shows that the structure of the MnO_2 samples changed with increasing concentration of H^+ ions in the synthesis solution At low acid concentrations ($[H^+]$ <4M) the structure of the MnO_2 samples is that of the γ form In high acid concentrations ($[H^+]$8M) the precipitated samples were identified as the α-form of MnO_2, very similar to natural hollandite or cryptomelane

The ion exchange properties of MnO_2(Na) samples precipitated at various acid concentrations were tested for adsorption of monovalent and divalent cations In Fig 4 distribution coefficients (K_d) values for alkali metal cations in 1M^3 HNO_3 solution are plotted as a function of ionic radius The ion exchange properties are highest in samples precipitated from a solution with H^+ concentration higher than 8 In all cases, as with cryptomelane [5], a maximum in the K_d value is observed at the r_i of approximately 140 pm, between the r_i of K^+ and Rb^+

Figure 5 presents the Kd values for Ba^{2+} adsorption on MnO_2 samples precipitated from solution with various acid concentration As in the case of monovalent cations, ion exchange affinity for Ba^{2+} increases with increasing H^+ concentration in the synthesis solution

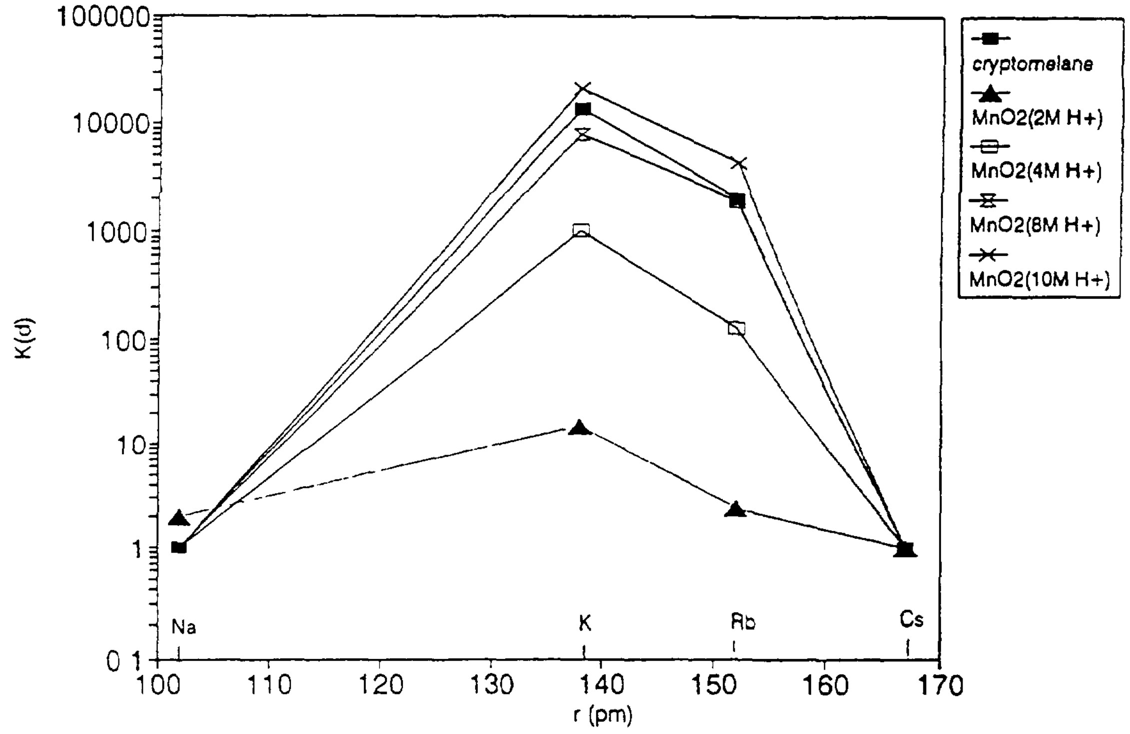

FIG 4 Distribution coefficient values for alkali metal cations in 1 M HNO_3 as function of their ionic radius (Coordination Number = 6). MnO_2 samples were precipitated from $NaMnO_4$ solution at various H^+ concentration.

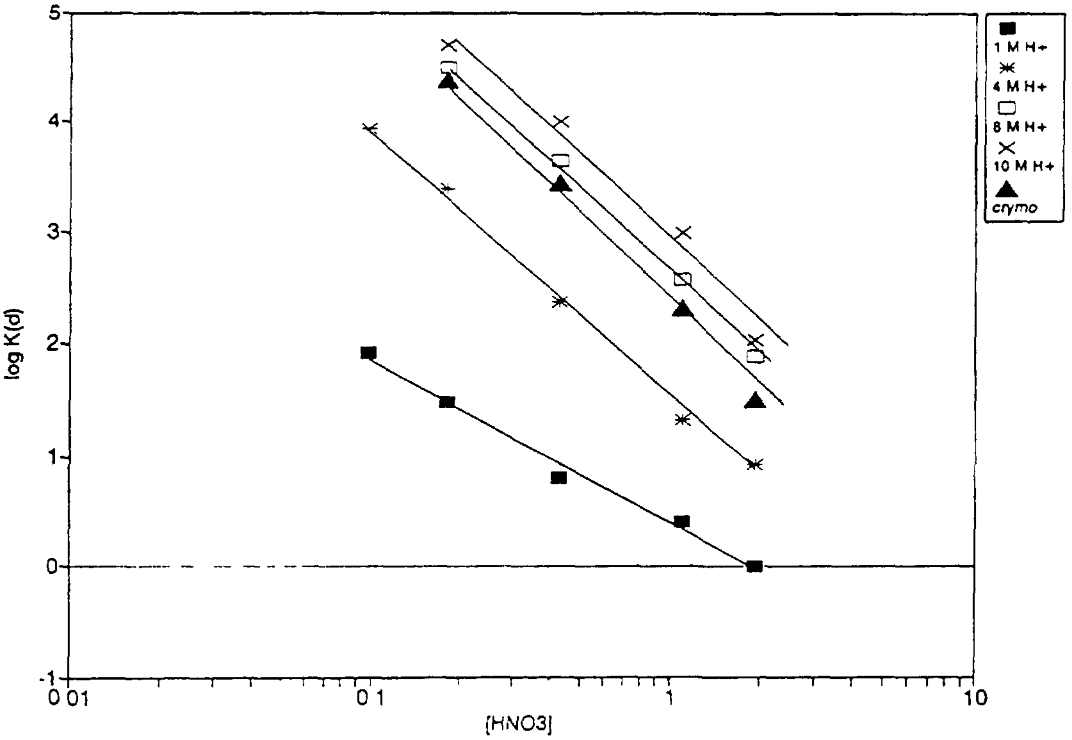

FIG 5 Dependence of distribution coefficient values of Ba^{2+} on HNO_3 concentration. MnO_2 samples were precipitated from $NaMnO_4$ solution at various H^+ concentrations

In natural or synthetic cryptomelane the structure is stabilized by exchangeable heavy mono or divalent cations (K^+, Ba^{2+} etc) In the case of the MnO_2 samples precipitated from $NaMnO_4$ we did not identify (using neutron activation analysis) any metal cations other than manganese Due to the fact that the MnO_2(Na) samples obtained from high acid concentrations have ion exchange properties like cryptomelane we suggest that structure of the MnO_2 samples is stabilized by H_3O^+ cations which have a radius very similar to the K^+ , Ba^{2+} or Ra^{2+} cations The formula of the samples is probably $H_3OMn(III)Mn(IV)_7O_{16}$ by analogy to the formula of cryptomelane $KMn(III)Mn(IV)_7O_{16}$ [6] In the case of cyptomelane, the exchangeable ions are K^+ cations In α-MnO_2 samples precipitated from $NaMnO_4$ at high acid concentration the exchangeable cations are H_3O^+

The presented studies can also have a practical aspect The MnO_2 samples obtained using $NaMnO_4$ exhibit an affinity for radium nuclides similar to synthetic cryptomelane A big advantage of these samples is that they were synthesized in the H^+ form which can be use directly for Ra^{2+} adsorption In the case of cryptomelane the samples before adsorption must be converted into the hydrogen form by percolating a large volume of concentrated HNO_3 over a long period of time The MnO_2 samples obtained can be applied in a new procedure for the determination of $^{226,228}Ra$ in natural water at very low level The utilization of the new sorbents for removal of radium nuclides from the high activity aqueous streams is also planned

REFERENCES

[1] GMELIN HANDBUCH DER ANORGANISCHEN CHEMIE, Mangan Teil C1, Springer Verlag, Berlin 1973, pp. 345-355

[2] M.TSUJI, M ABE, Bull Chem Soc.Jpn., 58, 1109 (1985)

[3] TSUJI, M , KOMARNENI, S J Mater Res., 8, 611 (1993).

[4] TSUJI, M., KOMARNENI, S., ABE, M. Solvent Extr.Ion Exch , 11, 143 (1993)

[5] BILEWICZ, A , FUKS, L. Chem.Anal (Warsaw), 38, 331 (1993)

[6] YUAN-GEN YIN, WEN-QUING XU, R DEGUZMAN, S L SUIB, C I O'YOUNG, Inorg Chem , 33, 4384 (1994)

[7] DIETRICH, B , VIOUT, P , LEHN, J -M Macrocyclic Chemistry, VCH Verlag, Weinheim, 1993, p 108-112.

[8] TSUJI, M , ABE, M Solvent Extr.Ion Exch , 2, 253 (1984)

[9] SHANNON, R D Acta Cryst. A32, T51 (1976)

[10] WELLS, A F. Structural Inorganic Chemistry, 4-th ed , Clarendon Press, Oxford, 1975, p 459

A STUDY OF THE PROPERTIES OF HEXACYANOFERRATE SORBENTS AND THEIR USE FOR SORPTION OF CAESIUM AND STRONTIUM

V.I. KARETA, A.I. GRIVKOVA, T.N. ARTEMOVA,
L.I. MIZINA, E.P KRASAVINA
Institute of Physical Chemistry of the Russian Academy of Sciences,
Moscow, Russian Federation

Abstract

A method of deposition of zinc, copper, and nickel hexacyanaferrates on silica-containing substrate (clinoptilolite) has been developed to produce mechanically strong sorbents for cesium and strontium separation from solutions of different compositions The modification of clinoptilolite increases its sorption capacity for both cesium and strontium Sorption behaviour of radionuclides was studied both in static and kinetic conditions

1. INTRODUCTION

For the final removal of the long-lived radionuclides ^{137}Cs and ^{90}Sr in processes connected with the treatment of radioactive wastes and operation of nuclear power plants it is often recommended to use sorption columns with inorganic sorbents We investigated some types of hexacyanoferrate sorbents to purify the aqueous wastes from cesium and strontium

Nickel hexacyanoferrates are known to be effective sorbents of cesium [1-4] This is accounted for by the stabilizing effect of large cesium ions on the structure of nickel hexacyanoferrates and by a resulting decrease in solubility of the product

Our study is concerned with the effect of the chemical composition of nickel hexacyanoferrates, their solubility and their tendency to peptization on the sorption of cesium microquantities Since the exchange of cesium for alkali metal ions in nickel hexacyanoferrates occurs more readily than that for nickel ions, the nature and content of the alkali metal in the hexacyanoferrate composition may have an appreciable effect on cesium sorption Therefore, nickel hexacyanoferrates of various composition were prepared and investigated

2. EXPERIMENTAL RESULTS AND DISCUSSION

Nickel hexacyanoferrates were produced by mixing the solutions 0 1 M $Ni(NO_3)_2$ (A) and 0 1 M $Na_4Fe(CN)_6$ (B1), or 0 1 M $K_4Fe(CN)_6$ (B2), or 1 6 M NH_4NO_3 (B3), or 0 1 M $Na_4Fe(CN)_6$, 0 2 M $CsNO_3$ (B4) Table I gives the volume ratios of the solutions and the order in which they were mixed and also the literature references to the conditions of preparation In experiment 8 the product was labelled with ^{137}Cs The composition of the products was determined by chemical analyses for nickel [9] and ferrocyanide [10], as well as radiometric analysis for ^{137}Cs in solutions before and after precipitation A direct analysis of the compounds obtained was also made after their decomposition by a mixture of sulphuric and nitric acids The concentrations of nickel and iron ions in the solution were determined using an AS-503 atomic absorption spectrometer

The air-dried compounds were investigated using the X-ray powder diffraction technique on an ADP-10 diffractometer with CuK$_\alpha$-radiation The solubility of the compounds was determined by analysis for nickel ions in the solution after equilibration using a Plasma-40 spectrophotometer (the method of emission spectroscopy with ICP- inductively coupled plasma) When determining the solubility of nickel, the release of Cs from the sample containing ^{137}Cs was also determined radiometrically

In batch equilibration experiments, the sorbents (0 01 g) were mixed by shaking for 20 days (with night breaks) with 500 mL of the 0 1 M solution of sodium nitrate containing 4 10^4 Bq/L of ^{137}Cs After equilibration the solutions were centrifuged and an aliquot of the supernatant was gamma-counted using a NaI(Tl) crystal detector at a NRG-603 gamma-automate facility (Tesla)

TABLE I CONDITIONS OF PREPARING NICKEL FERROCYANIDES

N	Order of mixing	$Ni^{2+}:Fe(CN)_6^4$	Conditions of preparation
1	B_1 added to A	10 1	[5]
2	A to B_1	1 5 1	[6]
3	A to B_1	0 1 1	[5]
4	A to B_2	1 33 1	[3]
5	A to B_2	0 1 1	-
6	A to B_3	1 33 1	[7]
7	A to B_3	0 1 1	-
8	A to B_4	1 1	[8]

The compositions of the compounds obtained under the conditions given in Table I corresponded to those listed in Table II The content of water in them was not determined, because it could hardly affect their sorption properties

The composition of products of mixed nickel hexacyanoferrates for one and the same alkali metal ion depends on the ratio of the reagents being mixed, and the tendency of alkali metals to enter into the residue composition increases with the radius of their ions

$Na_2NiFe(CN)_6$ is only formed at the ratio Ni^{2+} $Fe(CN)_6^4$ = 0 1 1, while $Cs_2NiFe(CN)_6$ is already formed at a ratio of 1 1

The X-ray diffraction pattern of all the compounds prepared confirmed the earlier conclusion, that nickel, sodium and nickel, potassium hexacyanoferrates formed one isostructural group Small differences in the X-ray diffraction patterns of these compounds are only observed in the values of relative band intensities (Fig 1)

TABLE II COMPOSITIONS OF NICKEL HEXACYANOFERRATES PREPARED

N	**Ni^{2+}:$Fe(CN)_6$ in the product**	**Compound**	**Colour of the residue**
1	1 95	$Ni_2Fe(CN)_6$	brownish green
2	1 48	$Na_2Ni_3[Fe(CN)_6]_2$	grass green
3	1 00	$Na_2NiFe(CN)_6$	--"--
4	1 32	$K_4Ni_4[Fe(CN)_6]_3$	greenish blue light
5	1 00	$K_2NiFe(CN)_6$	--"--
6	1 30	$(NH_4)_4Ni_4$ $[Fe(CN)_6]_3$	greenish blue
7	1 00	$(NH_4)_2NiFe(CN)_6$	blue
8	1 00	$Cs_2NiFe(CN)_6$	light green

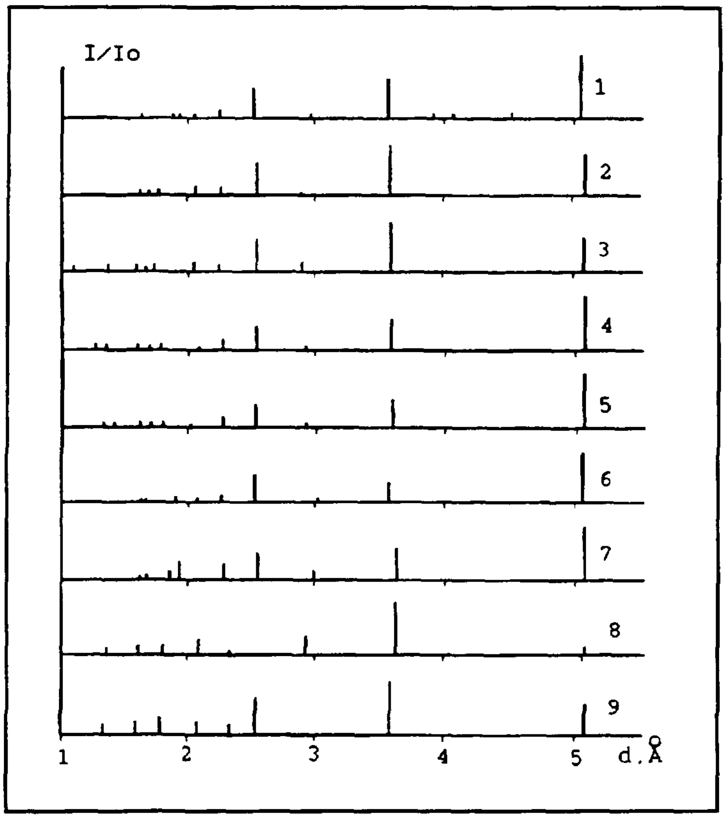

Fig. 1. X-ray diffraction patterns of nickel hexacyanoferrates:
1-$Ni_2Fe(CN)_6$, 2-$K_4Ni_4[Fe(CN)_6]_3$, 3-$K_2NiFe(CN)_6$, 4-$(NH_4)_4Ni_4[Fe(CN)_6]_3$, 5-$(NH_4)_2NiFe(CN)_6$, 6-$Na_2NI_3[Fe(CN)_6]_2$, 7-$Na_2NiFe(CN)_6$, 8-$Cs_2NiFe(CN)_6$, 9-sorbent

Determining the solubility of nickel hexacyanoferrates presents certain difficulties that are related not only to their very low solubility but also to their tendency to peptization, particularly for compounds of the composition $Me_2NiFe(CN)_6$, and transition to the solution of the colloidal form of the material

In this work the solubility of the product was determined under the conditions excluding the penetration of the colloidal form of the residue (Table III) The residue, sealed in a dialysis film, was placed into a test tube with distilled water, stirred and changed after each five days. Equilibration was determined by the constant concentration of nickel ions in water The experiments were conducted at 20°C

TABLE III SOLUBILITY OF NICKEL HEXACYANOFERRATES

Compound	**Equilibrium concentration of Ni^{2+}, mg/L**	**Solubility, mol/L**
$Ni_2Fe(CN)_6$	0 080+/- 0 006	7 0 10^{-7}
$Na_2Ni_3[Fe(CN)_6]_2$	0 079+/- 0 005	4 5 10^{-7}
$Na_2NiFe(CN)_6$	0 041+/- 0 006	7 0 10^{-7}
$K_4Ni_4[Fe(CN)_6]_3$	0 023+/- 0 003	1 0 10^{-7}
$K_2NiFe(CN)_6$	0 026+/- 0 003	4 5 10^{-7}
$(NH_4)_4Ni_4[Fe(CN)_6]_3$	0 016+/- 0 002	7 0 10^{-8}
$(NH_4)_2NiFe(CN)_6$	0 012+/- 0 002	2 0 10^{-7}
$Cs_2NiFe(CN)_6$	0 001+/- 0 0003	2 0 10^{-8}

The values obtained show that the solubility of nickel hexacyanoferrates is very low The higher literature values for $Ni_2Fe(CN)_6$ - 2 6 10^{-5} mol/L [12] are probably due to the presence in the solution of the colloidal form of the solid As the radius of the monovalent ion increases from sodium to cesium, the solubility of the mixed nickel hexacyanoferrates decreases The lowest value was obtained for $Cs_2NiFe(CN)_6$ - 2 0 10^{-8}mol/L

The value of the ^{137}Cs distribution coefficient (Kd, mL/g) was determined in a 0 1 M solution of sodium nitrate labelled with ^{137}Cs This composition of the solution was chosen to prevent possible peptization of the residues and to exclude its effect on Kd (Table IV)

The measurements showed that there was no correlation between the solubility of compounds and their sorption behaviour Obviously, not only the solubility of the compounds but also the nature and the content in the compound of monovalent ions competing with cesium affect cesium sorption Therefore, the highest Kd values were obtained for mixed nickel, sodium hexacyanoferrates

During cesium adsorption from solutions containing compounds that attack the sorbent (alkalis, carbonates, phosphates, oxalates and the like) the solubility of the sorbents determines

TABLE IV. ^{137}Cs DISTRIBUTION COEFFICIENTS OF NICKEL HEXACYANOFERRATES

Compound	**Kd,mL/g**
$Ni_2Fe(CN)_6$	1.4 10^7
$Na_2Ni_3[Fe(CN)_6]_2$	2.6 10^7
$Na_2NiFe(CN)_6$	2 6 10^7
$K_4Ni_4[Fe(CN)_6]_3$	1.0 10^7
$K_2NiFe(CN)_6$	0.2 10^7
$(NH_4)_4Ni_4[Fe(CN)_6]_3$	1.3 10^7
$(NH_4)_2NiFe(CN)_6$	0.3 10^7

their stability and Kd values. Therefore, to prepare cesium selective inorganic sorbents stable in salt solutions of complex composition, the least soluble nickel, ammonium and nickel, potassium hexacyanoferrates were chosen. The sorbent obtained by depositing these residues on silica gel contained 25 mg/g of nickel and 70 mg/g of hexacyanoferrates. ^{137}Cs Kds on this sorbent are rather high and equal to 2-3 10^5 mL/g even at the Na_2CO_3 or $H_2C_2O_4$ concentration to 2 g/L.

The 0.1 M sodium nitrate labelled with ^{137}Cs (4 10^4 Bq/L) was passed through the sorbent placed in a column to a depth of 10 cm at a flow rate of 0.025 cm/s. The volume of the purified solution was 30000 times as much as the sorbent volume, and the decontamination factor was 1000.

We investigated also the sorption on clinoptilolite modified by hexacyanoferrates. The final selection of sorbents is made according to the results of experiments under dynamic conditions. These experiments normally take a long time and complicate a comprehensive study of the sorption process. In this work, the possibility of a faster assessment of the properties of inorganic sorbents was studied. This assessment is based on a study of the initial regions of sorption yield curves at high solution flow rates and on establishing the dependence of the time of operation of the column, before the breakthrough of radionuclides, on the solution flow rate.

Extensive information is available from the literature on the use of sorbents prepared on the basis of transition-metal hexacyanoferrates (MeCF) for the extraction of ^{137}Cs [13-16]. For the extraction of ^{90}Sr, a natural zeolite-clinoptilolite (CP) is recommended [17, 18]. Methods of depositing hexacyanoferrates on CP were also proposed [19-21]. We developed our own method of depositing MeCF on a silicon-containing carrier. This method allows mechanically strong sorbents to be produced. Depending on the porosity of the carrier, these sorbents may contain from 3 to 50 wt % MeCF. We used this method for the deposition of zinc, copper, and nickel hexacyanoferrate precipitates on clinoptilolite (Dzegvi deposit, Georgia) particles. The resulting sorbents are listed in Table V.

The sorption properties of the prepared sorbents were studied in mains water of the following composition (mg/L) Na^+, 6 4, K^+, 3 9, Mg^{2+} 10, Ca^{2+}, 42, Cl^-, 4 6, SO_4^{2-}, 48, HCO_3^-, 157.

TABLE V. PARAMETERS OF THE MODIFIED CLINOPTILOLITE

Sorbent	**Concentration in sorbent, mg/g**		**Bulk density,g/cm^3**	**Particle size,nm**
	Me	**$Fe(CN)_6$**		
ZFCP	13.2	32	1.1	0.25-0.50
NFCP	9.0	26	1.1	0.25-0.50
CFCP	10.5	20	1.1	0.25-0.50

Note: ZFCP, NFCP, and CFCP are sorbents prepared by the deposition of zinc, nickel, and copper hexacyanoferrates, respectively.

Radioactive tracers (either ^{137}Cs or ^{90}Sr) were added to the water up to a specific activity between 3.7 and 37 KBq/L. The liquid-solid phase ratio during the determination of the distribution ratios (DR) was 10000 for ^{137}Cs and 500 for ^{85}Sr. The time of stirring was 5 days. In addition, the cesium and strontium distribution ratios in water with an increased Ca^{2+} concentration (400 mg/L) were determined (Table VI).

TABLE VI. ^{137}Cs AND ^{90}Sr DISTRIBUTION RATIOS ON MEFCP-TYPE SORBENTS

Sorbent	**Main water, 40 mg/L Ca^{2+}**		**Main water, 400 mg/L Ca^{2+}**	
	DR $_{137}$Cs	**DR $_{85}$Sr**	**DR ^{137}Cs**	**DR ^{85}Sr**
CP	1.8 10^4	0.7 10^3	6.0 10^4	2.0 10^2
ZFCP	1.8 10^5	2.7 10^3	2.0 10^5	7.0 10^2
NFCP	2.5 10^5	1.1 10^3	2.2 10^5	3.2.10^2
MFCP	2.6 10^5	0.7 10^3	3.3 10^5	2.2 10^2

The modification of clinoptilolite with MeCF precipitates increases the affinity of clinoptilolite not only for cesium , but in some cases, for strontium, especially for the ZFCP sorbent. To determine the reason for the increase in the ^{85}Sr distribution ratio on ZFCP, we studied the ^{85}Sr distribution ratio on clinoptilolite in the zinc form [the sample was prepared by the treatment of clinoptilolite with a solution of $Zn(NO_3)_2$ (1 mol/L)], as well as on $Zn_2Fe(CN)_6$ and $Na_2Zn_3[Fe(CN)_6]_2$. The distribution ratios obtained were equal to 7 10^2, 1.2 10^2 and 1.3 10^3 respectively. Consequently, the precipitation of the mixed zinc-sodium salt on the clinoptilolite increases its affinity for strontium.

The cesium and strontium sorption under dynamic conditions was studied on the ZFCP sorbent. The sorbent (2 cm^3) was placed in a column with a diameter of 0.7 cm, and the solution was passed through from bottom to top. The solution flow rate was varied from 400 to 1600 column volumes/h in experiments with ^{137}Cs and from 20 to 85 column volumes/h in experiments with ^{85}Sr. Figure 2 shows the initial regions of the ^{137}Cs sorption curves.

As shown in [23], the system of the sorption dynamics equations in the case of outside diffusion and a convex sorption isotherm, which is the case with the ^{137}Cs sorption on ZFCP, allows the yield curve to be represented as a straight line:

$$\ln Z = K_1 t + K_0 \ (1) \text{ or } \ln A/A_0 = \beta(A/\alpha)\tau - \beta(h/\omega) - 1 \ (2),$$

where A and A_0 are the specific activities at the inlet and outlet of the column, α is the specific activity of the sorbent, ω is the linear solution flow rate; cm/s; **h** is the height of the sorbent, cm; τ is the time; and β is the kinetic coefficient of the outside diffusion, s^{-1}.

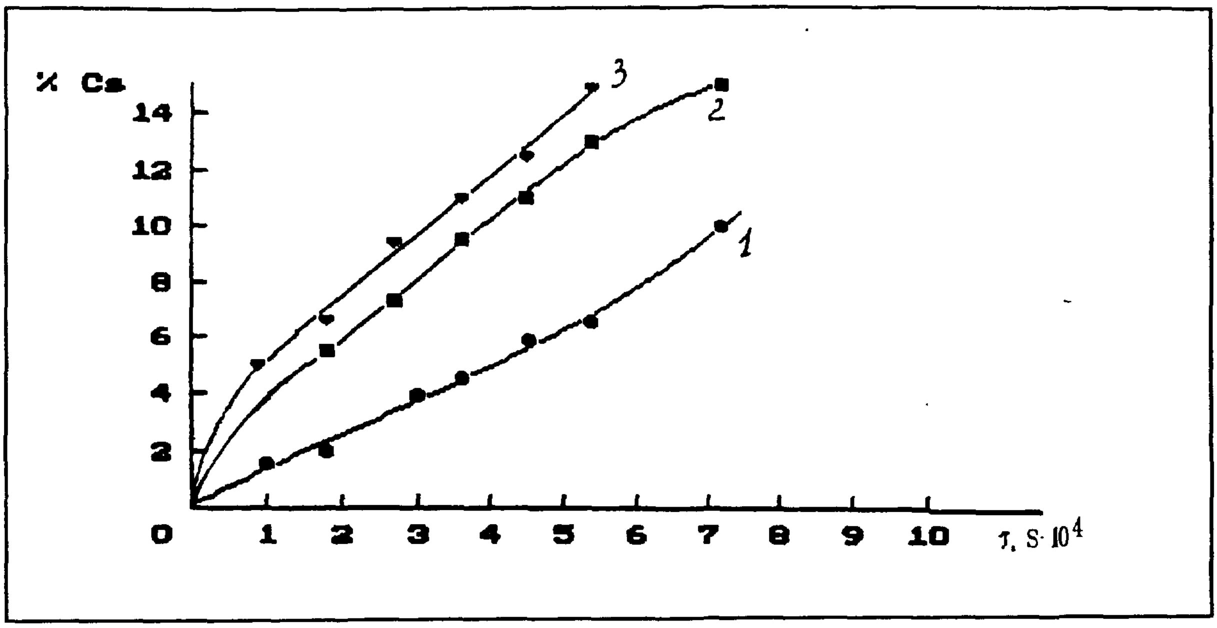

Fig.2. The dependence of ^{137}Cs sorption on flow rate using ZFCP sorbent.
1-400 column volumes/hour;
2-826 column volumes/hour;
3-1600 column volumes/hour.

The initial regions of the experimental yield curves for the ^{137}Cs sorption, calculated on the $\ln(A/A_0) = f(\tau)$ coordinates, are straight lines (Fig. 3).

This fact confirms the validity of using equation (2) for the description of this sorption process. From these data, the K_0 and K_1 coefficients in equation (1) were calculated using the least-squares technique. The kinetic coefficient of the outside-diffusion mass transfer was determined from K_0

$$\beta = (1 - Ko)\omega/h, \text{ (Table VII, Fig. 3)}$$

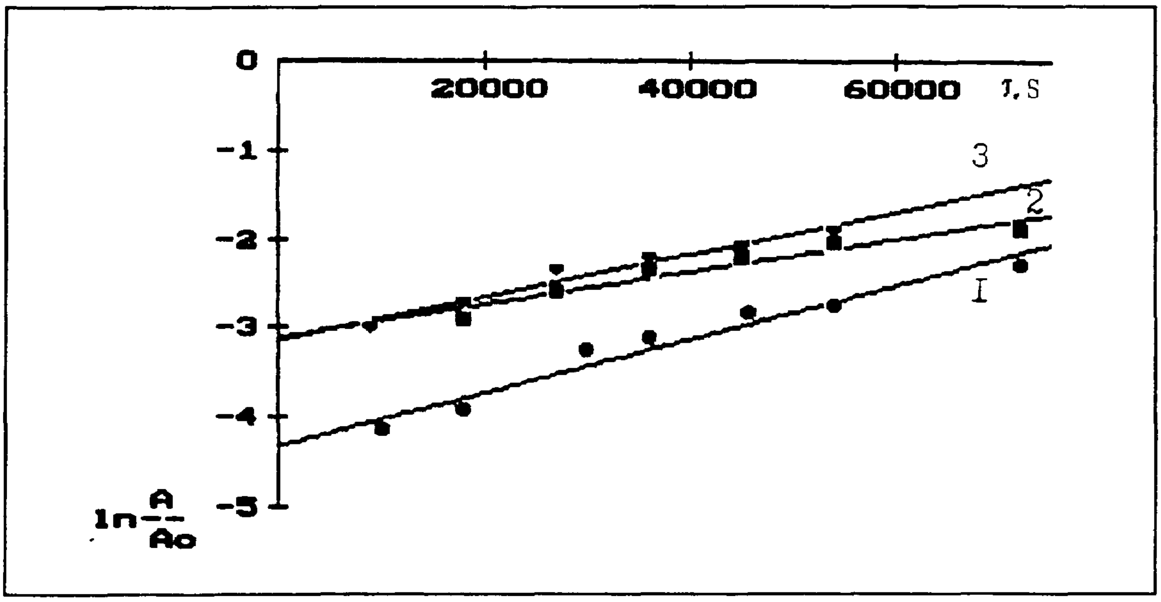

Fig. 3. The dependence of ^{137}Cs sorption on flow rate using ZFCP sorbent in the ln(A/A$_0$) = f(τ) coordinates.

1-400 column volumes/hour;
2-826 column volumes/hour;
3-1600 column volumes/hour.

TABLE VII. DEPENDENCE OF THE KINETIC COEFFICIENT OF OUTSIDE DIFFUSION B ON THE SOLUTION FLOW RATE Ω FOR ^{137}Cs SORPTION ON THE ZFCP SORBENT IN MAIN WATER

ω, cm/s	lnω	β, s^{-1}	lnβ
0.203	-1.590	0.366	-0.999
0.419	-0.870	0.481	-0.723
0.811	-0.209	0.948	-0.053

The established dependence on the flow rate can be written as:

$$\ln\beta = 0.68 \ln \omega + 0.011.$$

The experiments on strontium sorption were carried out at a significantly lower flow rate because the rate of the ^{85}Sr sorption is significantly lower than that of ^{137}Cs. A comparison of the yield curves for sorption by ZFCP sorbents and nonmodified clinoptilolite in hard mains water (100 mg/L Ca^{2+}) confirmed the results obtained under equilibrium sorption conditions. Initial regions of three yield curves for ^{85}Sr sorption in mains water at different flow rates were obtained (Fig. 4).

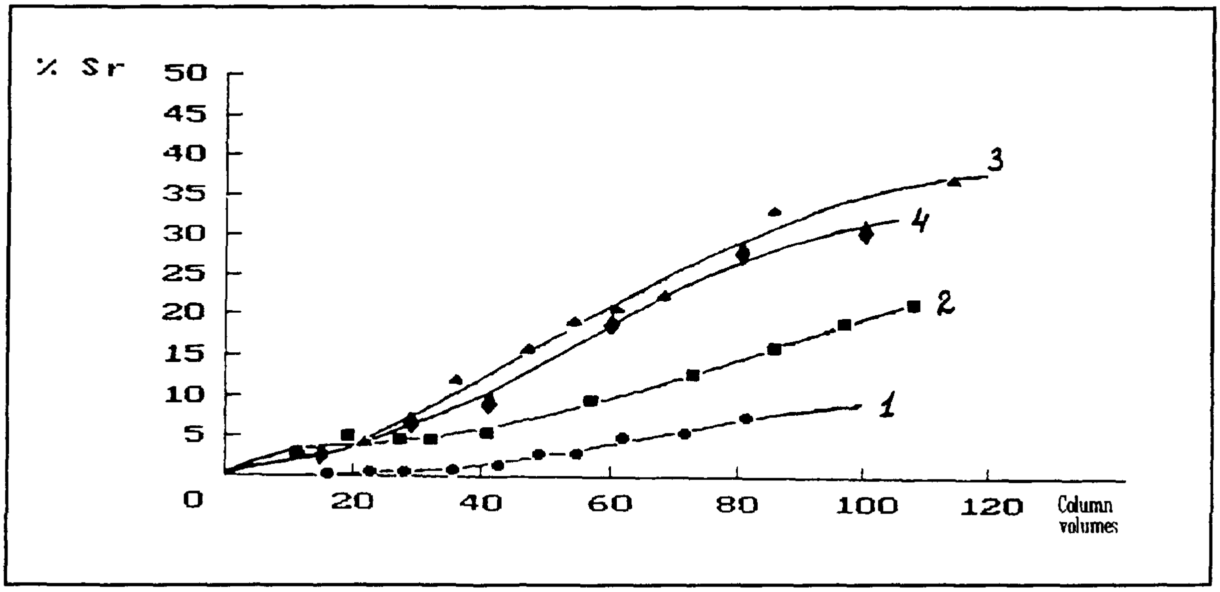

Fig.4. The dependence of the ^{85}Sr sorption on flow rate using ZFCP sorbent
1-20 column volumes/hour;
2-41 column volumes/hour;
3-85 column volumes/hour.
4-The dependence of ^{85}Sr sorption using clinoptilolite, flow rate - 20 column volumes/hour

On the lnA/A$_0$ coordinates, these regions are also linear (Fig.5).

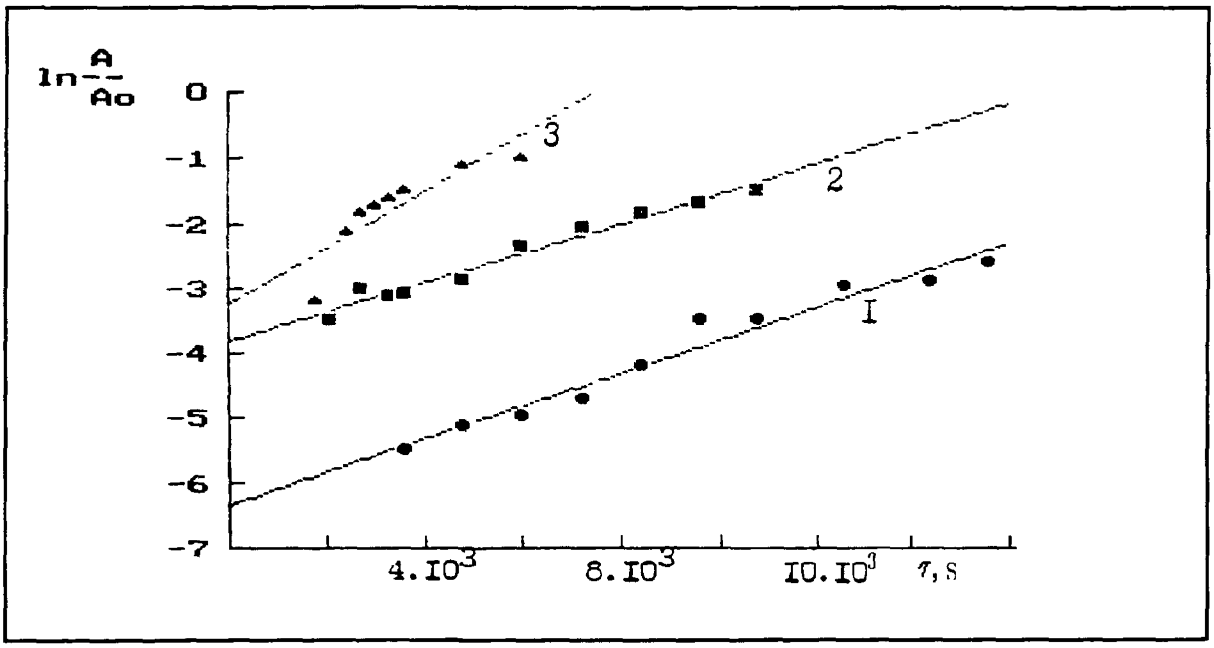

Fig.5. The dependence of ^{85}Sr sorption on flow rate using ZFCP sorbent in the ln(A/A$_0$) = f(τ) coordinates.
1-20 column volumes/hour;
2-41 column volumes/hour;
3-85 column volumes/hour.

Nevertheless, attempts to fully linearize the yield curves for ^{85}Sr were unsuccessful. The outside diffusion is likely to be the limiting stage of the sorption process only at the initial moment of time. The dependence of the diffusion coefficients on the solution flow rate is described by the following equation

$$\ln\beta = 0.4 \ln \omega - 1.7.$$

Thus, the results obtained show that the ZFCP sorbent can be used for a simultaneous removal of ^{137}Cs and ^{90}Sr. In this process, the rate of solution flow through the sorbent is determined by the sorption of ^{90}Sr, which is a slower stage. The equations establishing the dependence of the β coefficients on the flow rate allow the calculation of the time of the protective effect of the column for selected flow rates.

CONCLUSIONS

- A method of the deposition of zinc, copper, and nickel hexacyanoferrates on a silica-containing substrate has been developed. This method allows mechanically strong sorbents to be produced. Depending on the substrate porosity, these sorbents may contain from 3 to 50 wt % MeCF.

- The modification of clinoptilolite increases its sorption capacity relative to both cesium and strontium.

- For selected flow rates (for cesium 100 - 3000 column volumes/hour; for strontium, 10 - 100 column volumes/hour), the extent of the protective action of the sorption column can be calculated from the experimental data according to the equation establishing the dependence of the coefficient b on the flow rate.

REFERENCES

[1] ROGINSKIY S.Z., YANOVSKIY M.I., MALININA E.I.,ALTSHULER O.V. RADIOKHIMIYA, 2 (1960), 438.(in Russian).
[2] KOURIM V., RAIS J., MILLION B. J.Inorg.Nucl.Chem. 26 (1964), 1111.
[3] VOLKHIN V.V., KOLESOVA S.A. ZhNKh, 40 (1967), 342 (in Russian).
[4] BAETSLE L.H. e.a. J.Inorg.Nucl.Chem. 26 (1964), 1329.
[5] KAWAMURA S., SHIBATA S., KUROTAKY K. Anal.Chim.Acta 81 (1976),91.
[6] TANANAEV I.V., LEVINA M.I. ZhNKh, 1 (1946), 231 (in Russian).
[7] DOLESAL J., KOURIM V. Radioc.Radioanal.Lett., 1 (1969), 295.
[8] KUZNETSOV V.G., POPOVA Z.V., SEIFER G.B. ZhNKh, 15 (1970), 1084 (in Russian).
[9] SHVARTSENBAKH G. "Kompleksometriya", GNTN Khim.Litt., M., (1958).
[10] KOLGOF I.M., BELCHER R. et al. Obyomniy analiz, 3 (1961), 64 (in Russian).
[11] BASINSKI A., ROZWADOWSKI M. ROCZNIKI Chem. 34 (1960), 47.
[12] TANANAEV I.V., GLUSHKOVA M.A., SEIFER G.B. ZhNKh, 1 (1956),66 (in Russian).
[13] ZAITSEV, B.A., SOBOLEV, I.A., KHOMCHIK, L.M., et al., Removal of Long-Lived Radionuclides from Concentrated Liquid Radioactive wastes Using Selective

Inorganic Sorbents, Proceedings of V Symposium of the Council of Mutual Economic Assistance, Marianske Lazne, 1981, Prague . 14.Zaitsev, B.A., Malinina, E.I., Plisko, V.N., et al., Removal of Radioactive Cesium and Strontium Isotopes on Selective Inorganic Sorbents, Proceedings of II Symposium of the Council of Mutual Economic Assistance , Kolobzheg, 1972, Warsaw, 1973.

[15] PROUT, W.E., RUSSEL, E.R., GROH, H.J., Ion-Exchange Adsorption of Cesium by Potassium Hexacyanocobalt(II) Ferrate(III), J. Inorg. Nucl. Chem., 27, 1965, 473.

[16] KRYLOV, V.N., BORISOV, M.S, BUROV, A.G., Cesium Sorption by Hexacyanoferrate, Radiokhimiya, 1988, no. 5, p. 644.

[17] PESKOV, G.I., DANEV, KH.T., GRADEV, G.D., MILANOV, M.V., A Study of Natural Calcium Clinoptilolite to Be Used for Purification of Water Containing Cesium , Strontium, and Cobalt Isotopes, Proceedings of IV Science and Technology Conference of the Council of Mutual Economic Assistance, Moscow, 1976; Atomizdat, 1978.

[18] CHERNYAVSKAYA, N.V. Strontium Sorption on Clinoptilolite and Heulandite, Radiokhimiya, 1985, no.5, p. 618.

[19] GVOSHEV, G.S., DANEV, KHR. T., ALEKSIEV, A.N., SIMOVA, N.N. ^{137}Cs Sorption on Carrier Treated with Hexacyanoferrates(II), Yadern. Energ., 1987, vol. 24, p. 74-78. 21. Kawamura et al., Nucl. Technol., 1982, vol. 58, no. 2, p. 242.

[20] US Patent no. 4448711 BOIJ 27/24, 15.05.1984.

[21] VENETSIANOV, E.V., RUBINSHTEIN, R.N. Dinamika Sobtsii iz Zhidkikh Sred (Dynamics of Sorption from Liquid Media), Moscow: Nauka, 1983, p. 237.

XA9744286

STUDY OF THE SORBTION OF NUCLEAR FUEL FISSION PRODUCTS USING NON-ION EXCHANGE POLYMERIC AND INORGANIC MATERIALS

P. MANORIK
L.V. Pisarzhevskij Institute of Physical Chemistry,
Kiev, Ukraine

Abstract

New tetrazamacrocycle and crown-ether poly-styrene and divinylbenzenepolystyrene derivatives (P-TAM and P-CE respectively) have been synthesized and studied as chemisorbents for Cs, Sr (P-CE) and Ru, Co (P-TAM) radioisotopes. It has been found that the tetraazamacro cycle modifier concentration in such material is about $5x10^{-4}$ M/g material. Model solutions, containing Ru and other platinoid salts, and also Co salts, were used in experiments at concentrations of $5x10^{-3}$ - $5x10^{-6}$ M/L. It was shown that P-TAM quantitatively removes Ru and other platinoids from the water solution at pH=0-1 during 1-2 days and practically all modifying groups participate in the sorption process. It was established that in alkaline solutions this sorbent also adsorbs Co, Cr and other 3d-metal ions. P-TAM also demonstrates a very high platinoid sorption selectivity (close to 100%) from solutions containing, for example, platinoids in the presence of a large excess of 3d-metal ions. ^{137}Cs sorption by some types of P-CE and IN-CE from Ringer-Locka model waste solution was also studied and it was found that K_d (Bq/g) strongly depends not only on the crown-ether ring size but also on the form in which crown-ethers exist on the surface, for example when the modifier was in the form of the complex such as P-CE-L(L=$K_3Fe(CN)_6$ or L=$K_4Fe(CN)_6$) there was an increase in K'_d value (Bq/mole of CE). The results of a study of ^{85}Sr removal by P-CE and IN-CE show that the chemisorption capacity strongly depends not only on the "hole"size of crown-ethers but also on the nature of encapsulated complexes, including ferrocyanides of different types. In our opinion, the most likely way to increase chemisorption capacity is by using an inorganic matrix, such as SiO_2, modified by macrocyclic ligands (these ligands are introduced into the matrix at the stage of gel texture formation), in which the characteristics (hydrophobicity, size of ligand and of chelating "hole", nature of donor atoms) have a strong influence on pore size and volume and on the surface area characteristics.

1. INTRODUCTION

An amount of low and intermediate level radioactive liquid wastes and the presence of some radionuclides in natural waters in the Ukraine after the Chernobyl accident makes the study of the sorption of radionuclides on different materials necessary.

Our research was based on our opinion that we can use some ligands, which form in water (or mixed water-organic) solutions very stable complexes (lgK>20) with some of the radionuclides, as modifiers of polymeric or inorganic sorbent surfaces. Our results show that we can produce polymeric or inorganic materials which are able to extract some radionuclides (Ru, Cs, Sr, Co etc) quantitatively from water solutions.

2. LITERATURE DATA

A literature survey was undertaken to identify suitable ligands for modification of inorganic or polymeric materials in order to produce materials with a strong and maybe selective affinity for radionuclides. Stability constants for complexes formed between alkali, alkaline-earth and rare-earth, 3d, 4d, 5d, 4f metal ions and different types of ligands containing O,N,S donor atoms were reviewed [1-10] (Fig.1). It was decided, the most promising ligands are: some crown ethers (Fig.1,b,c) (for Cs, Sr) and some tetraaza (Fig. 1, e-g) and pentaaza-macrocyclic ligands (for Ru, Rh, Co, Cr). These macrocycles are also of interest for this purposes but they are very expensive.

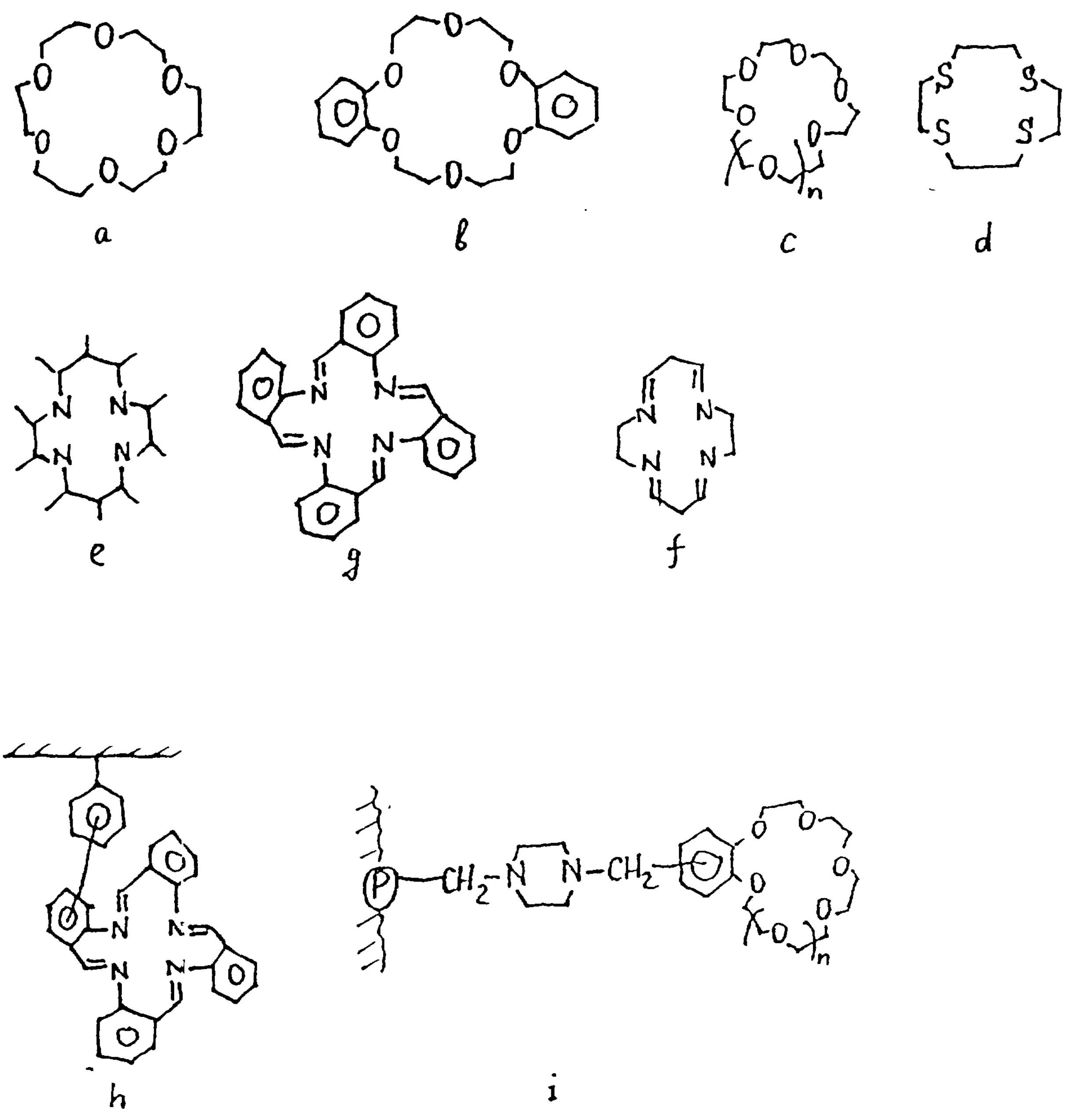

Fig. 1. The types of macrocyclic ligands tested as prospective modifiers for polymeric and inorganic matrixes: oxygen-containing crown-ethers without aromatic rings (a) with aromatic rings (b) with different number of oxygen atoms and ethylene bridges (c) sulphur-containing macrocycles (d) different types of tetraazamacrocycles with different number of ethylene and propylene bridges and substitutes (e) and double bonds (f) and tetraazaannulenes (g) modified with tetraazaannulene polystyrene (h) mofyied with crown-ethers divinylbenzene copolymer of polystyrene (I).

The criteria for selection of these ligands was:

1) high stability constants of their complexes with the metal ions;
2) the presence in their molecules of potentially active centers, which may be used for linking them with inorganic and polymeric matrices;
3) their thermal stability and stability in acids and alkalies.

We also reviewed inorganic and polymeric materials [11,12,13]. Among the inorganic materials we selected gels, which may have a large pores (the SiO_2 , Al_2O_3 , TiO_2, ZrO_2 derivatives). Among polymeric materials we selected polystyrene and its copolymer with divinylbenzene, because there was a good possibility of modifying them with different chelating and macrocyclic ligands. They also have a density less than 1 and may be readily separated from water.

3. EXPERIMENTAL

3.1. PREPARATION OF MODIFIED POLYMERIC MATERIALS AND STUDY OF THEIR CHEMISORPTION ABILITY

3.1.1. Tetraazaderivatives

10 tetraazamacrocyclic ligands were synthesised in accordance with [14], each containing four nitrogen donor atoms and different substituents in carbon links (Fig.1a). They were analysed for C,H,N and their IR, UV and ^1H NMR-spectra were determined which supported their chemical composition. One of them (M1) had very good characteristics for use for the modification of a polymeric matrix (t_{melt} 298° C, high stability over the whole pH range, common with donor atoms π-system, sublimed without destruction,insoluble in water, alcohol, ether, has moderate solubility in DMFA, DMSO, CCl_4 , CH_3CN, $CHCl_3$).

The complex formation processes of ligand M1 with the noble metals (Pt, Pd, Ru, Os, Ir) and 3d-metals (Co, Cr) in solution were studied using spectrophotometry and the complexes with tetraazamacrocycle (M1) were synthesised and identified.These complexes with noble metals have very high stability constants (lg $K^M_{ML} > 30$, with 3d-metals - lg $K^M_{ML} > 15$). They may be formed at pH 0-1 in contradiction to Co,Cr complexes which are formed in alkaline solutions. We expected that this would also be the case on the surface of a modified polymer.

The commercial product polystyrene was used as matrix for immobilization of tetraazamacrocyclic ligands using a multistep synthetic procedure:

polystyrene polystyrene-NO_2 $\xrightarrow{SnCl_3}$ polystyrene-NH_2 $\xrightarrow{NaNO_2}$ polystyrene-diazonium salt + macrocycle $\xrightarrow{Lewis.acid}$ polystyrene-macrocycle (M1).

Using the IR, UV, VIS spectroscopy technique, it was estimated that the concentration of modifier (macrocycle) on the surface of the sorbent was about 5.10^{-4} M/g of sorbent.

The complex formation reactions with this material (P-M1, Fig.1h) were studied using spectrophotometry.

Some of these results are shown in Fig.2-5.

The study of chemisorption of noble metal salts on P-M1 sorbent involved mixing 100mL solution of one of the salts ($C_M = 5 \cdot 10^{-3}$ M) with 2g of powdered P-M1 (which is lighter than water) and stirring with constant velocity. Samples of the solution (2 mL) were filtered off every 30 minutes and their VIS-spectra recorded on Karl Zeiss Specord M-40.

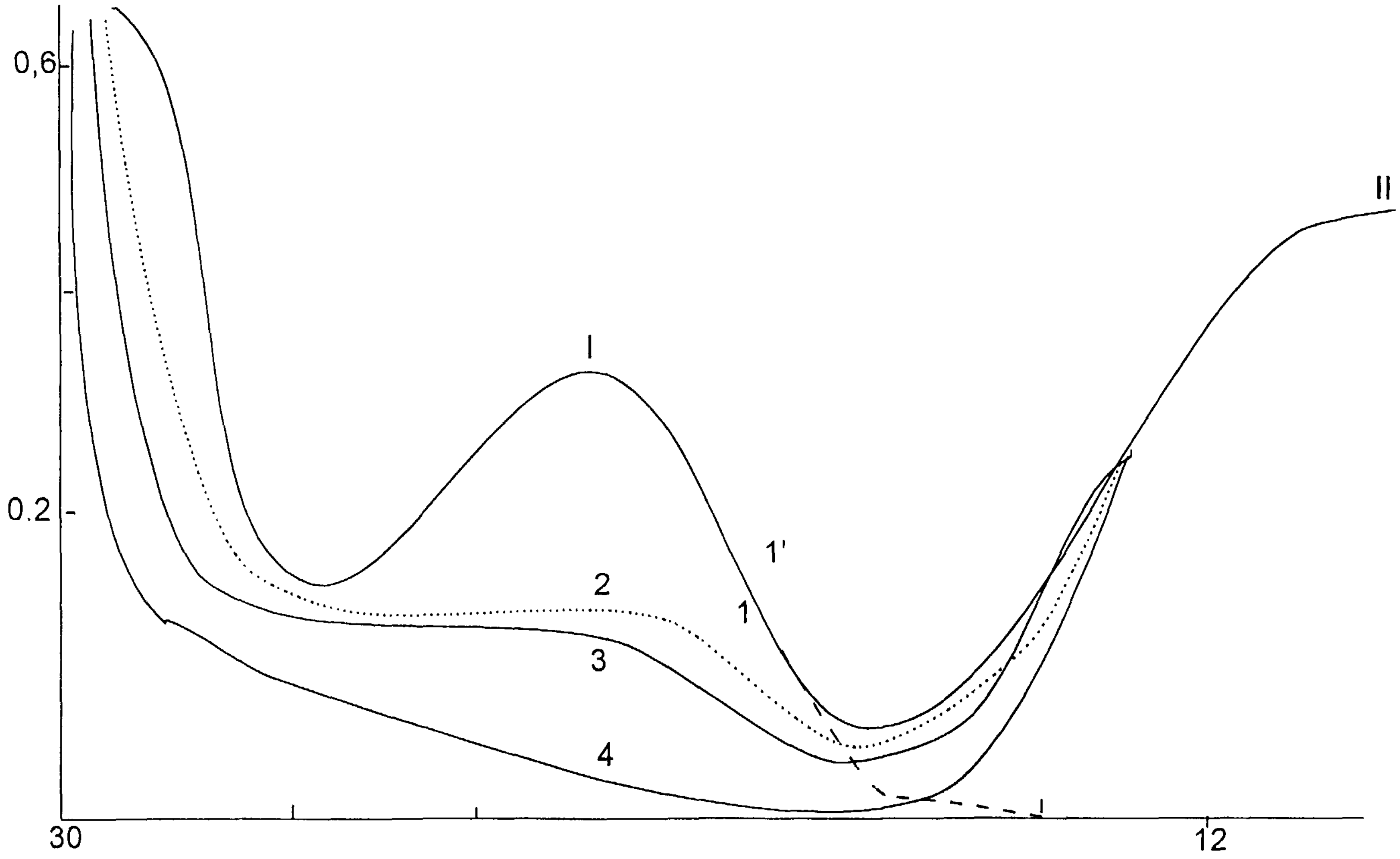

Fig. 2. Visible spectra data for H_2PdCl_4 (1') water solutions and its mixtures (1-4) with $CuCl_2$. $CH_2PdCl_4 = 5.10^{-4}$ M,

$C_{CuCl_2} = 1.10^{-2}$M, 1=1 cm
1'-initial solution of H_2PdCl_4;
(1) - mixture of H_2PdCl_4 with $CuCl_2$; t=0 h;
(2) t=12 h; (3) t=18 h; (4) t=25 h.

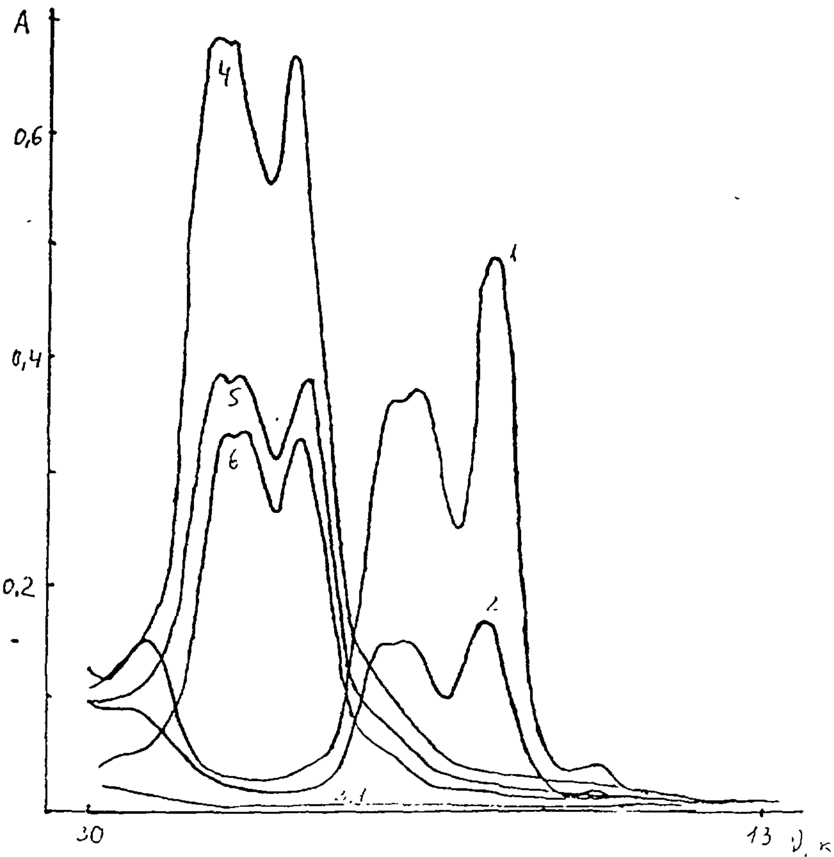

Fig. 3. Visible spectra data: (a) for Na_2IrCl_6 (1-3) water solutions; (1) t=0 h; (2) t=10 h; (3) t=40 h; $C_{Na2IrCl6} = 5.10^{-4}$ M,

(B) for Na_2OsCl_6 (4-7) water solutions; (4) t=0 h; (5) t=10 h; (3) t=11 h; (7) t=48 h; $C_{Na2OsCl6} = 5.10^{-4}$ M, 1=1 cm.

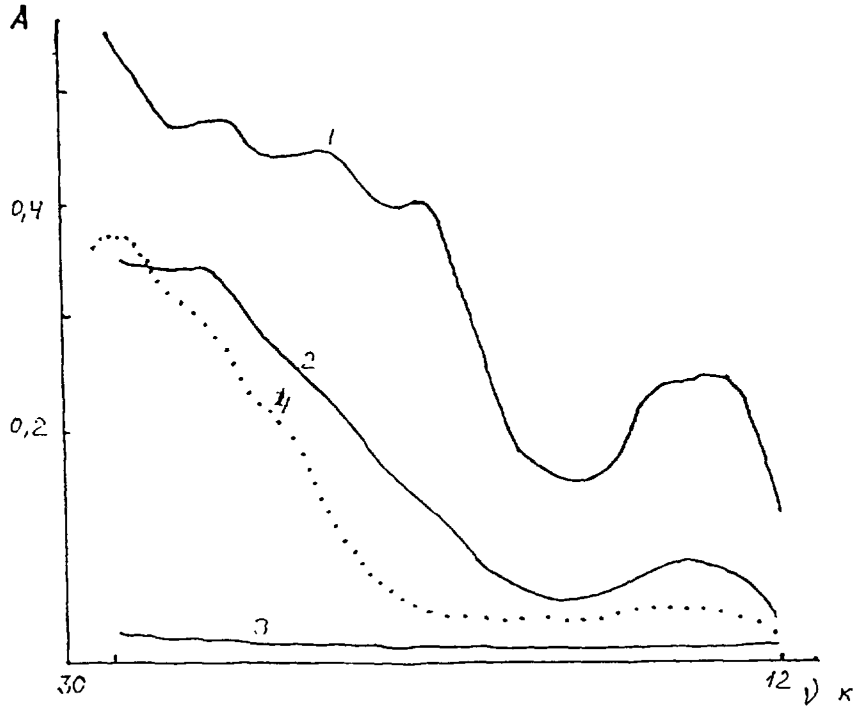

Fig. 4. Visible spectra data for $RuCl_3OH$ (1-3) water solutions; (1) t=0 h; (2) t=2 h; (3) t=46 h; (4) the sample (2) recorded after heating during 10 minutes under 50°C. $C_{RuCl3OH}=5.10^{-4}$ M, 1=1 cm.

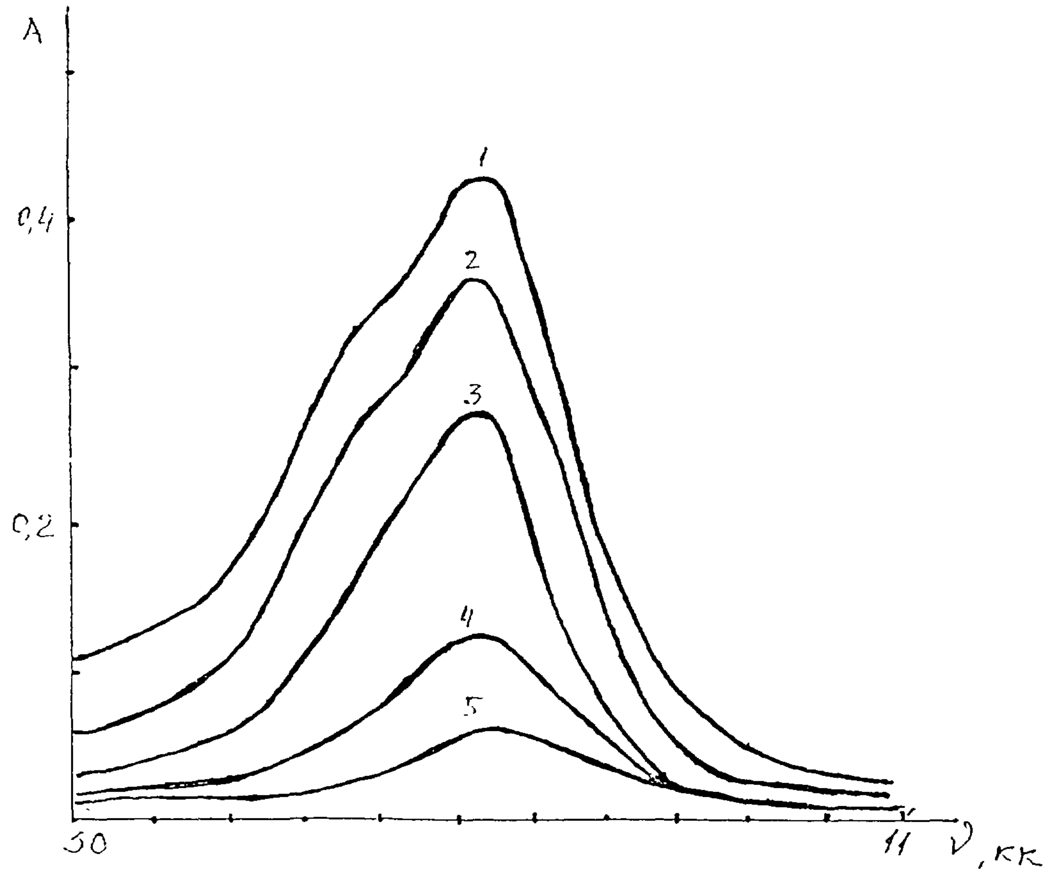

Fig. 5. Visible spectra data of $CoCl_2$ sorbtion process on P-M1 sorbent:
1 - initial solution ($C_{CoCl2}=5.10^{-2}$ M), t=0 h;
2 - initial solution + P-M1, t=2 h; (3) t=4 h; (4) t=10 h; (5) t=12h

It was found, that at pH 0-1, chemisorbent P-M1 quantitatively bound all noble metals (Pt, Pd, Ir, Rh, Ru, Os). The time of sorption depends on the nature of the metal ion (on its kinetic characteristics) and its oxidation state.

Figure 2 shows some of the experimental curves, illustrating the process of chemisorption of H_2PdCl_4 on P-M1. After 30 hours at room temperature the concentration of H_2PdCl_4 was below the limit of detection by VIS-spectroscopy. This was also the case with Os(IV) (Fig.3), Ir(IV) (Fig.3), Pd(IV) (Fig.2), Ru(IV) (Fig.4) salts. In the case of Ru(IV) we also tried to increase the velocity of chemisorption by heating the solution to 50°C, but because of hydrolysis of $RuCl_4$ (Fig.4, curve 4) this process could not be studied.

From the practical point of view it was interesting to study the selectivity for sorption of noble metal salts, first of all Ru, in the presence of a large excess of 3d-metal ions. For this purpose we prepared model solutions containing noble metal salts (Ru or Os, Pt, Pd, Ir) and salts of Co (or Cu or Ni), which were taken in great excess (for example C_{Ru}/C_{Co} 1:100 to 1:1000). The most illustrative example of the results of these experiments is the study of chemisorption of the mixture of H_2PdCl_4 in the presence of 100 times excess of $CuCl_2$ (Fig.2) because in VIS spectra these metal ions have practically non-overlapping bands (I and II respectively). Fig.2 shows that the chemisorption of Pd(II) in the presence of Cu occured with high selectivity (near 100%) at pH 0-1.

In another series of experiments the chemisorption of 3d-metals (Co, Cr, Cu, Ni) on P-M1 was studied. Figure 5 presents the results of chemisorption of Co(II) on P-M1 at pH=9 and illustrates the high affinity of P-M1 for Co.

The optimal conditions for chemisorption of noble radionuclides and 3d-nuclides (Co, Cr) by P-M1 were examined. For noble radionuclides they are pH=1, time of sorption 30 hours, stirring; for 3d-nuclides (Co, Cr): pH=8-9, time of sorption 10 hours, the presence of oxygen containing chelating ligands, stirring.

3.1.2. Crown-ether derivatives

A technique for adsorption of macrocycles onto silica-based C_{18} columns or polystyrene divinylbenzene packing has been reported [15]. Appropriate macrocycles have a hydrophobic tail or other moiety that promotes strong adherence to the stationary phase. Specifically, some authors adsorbed dodecylsubstituted 12-crown-4, 15-crown-5, 18-crown-6 ligands to silica based C_{18} columns as well as the cryptand decyl-2.2.2 [15,16]. Polymeric crown ether stationary phases were formed in two ways: formation of solid polymer particles or by coating macrocycle polymer onto a solid support. Blasius also made a caesium selective exchanger by forming a condensation polymer with dibenzo-24-crown-8 [17] and he also used polymeric polyamide-18-crown-6 to perform separations [18], which were unsuccessful in separating cations. Separations of lanthanides, Cu, and UO_2 have also been achieved [19,20] by grafting nitrogen-containing crown ethers to styrene-divinylbenzene copolymer.

The dibenzo-crown ether polymers were reacted with the silanol groups or with chloromethylated polystyrene to form an anchored polymeric resin for HPLC separation of alkali metals. Recently there was reported the use of crown ethers loaded on solid supports for Cs, Sr and Ba separations of interest to the nuclear industry [21,22].

Analyzing these data and the literature values of stability constants for different metal ions with many types of linear and cyclic ligands [1-10], we selected some types of crown-ethers which may be used for development of the polymeric materials for the immobilization of Cs, Sr: Benzo-15-crown-5, Benzo-18-crown-6, DB-18-crown-6, DB-24-crown-8.

We synthesized four polymer materials containing crown ethers. Taking into account the well known influence of different types of metal ions and their complexes on cation binding ability of crown ethers we also prepared a few materials using polymers modified by crown-ethers with encapsulated different types of complexes. Investigation of sorption ability toward ^{137}Cs from aqueous solutions was undertaken using four pure polymer-bonded crown ethers (Fig.1i) and for encapsulated samples.The data given in Table I show the ligands themselves to be less effective than the corresponding complexes of those with metal salts. For the sorption experiments aqueous solutions of Ringer-Locka containing 93,68 Bq/mL of ^{137}Cs were used. The distribution constants K_d in Table I are given as quantities of ^{137}Cs bound per gram of the sorbent.

Since PDB18C6 $K_3Fe(CN)_6$ complex appeared to be the most active agent of all polymer-bonded crown ethers studied, two types of complexes - L $K_3Fe(CN)_6$ and L $K_4Fe(CN)_6$ were formed in order to examine their sorption of ^{137}Cs. In Table II the results obtained are reported as K_d and also as K'_d which is the quantity of ^{137}Cs bound per mole of the crown ether in the sample. The starting concentration of ^{137}Cs in an aqueous solution of Ringer-Locka type was 51,600 Bq/mL.

3.1.3. Synthesis and chemosorbtion processes study of inorganic matrices modified by macrocyclic ligands

Previously we have synthesised and studied new materials, containing macrocyclic ligands(crown ethers, tetreaazaannulens) which were chemically linked to a polymeric matrix. Such samples, because of the ability of crown ethers to bind the alkaline-earth and alkali metal ions, strongly demonstrated an ability to remove Sr and Cs from aqueous solutions and, because of the high ability of tetraaza- annulens to bond 3d,4d,5d-transition metal ions, were good sorbents for Ru, Co, Cr etc. The processes of synthesis of such materials are quite difficult and expensive. Because of this we tried to find other ways of preparing new materials containing macrocyclic ligands. We used silica gels as matrix for macrocyclic ligands and studied different ways of modifying it by macrocycles without stages of chemical modification.

Preparation of modified materials

Different methods of synthesising macrocycle modified silica gels were used: 1) traditional method of impregnation (samples 1,2,6,7) and 2) coprecipitation (sol-gel method, samples 2'-5, 7'-10). In the first group of experiments we used previously prepared samples of SiO_2, characterized with different size pores and surface area (samples 1,2,6,7). In the second group of experiments the process of gel formation and modification was combined (samples 2'-5, 7'-10).

Sample 1. For its preparation commercial silica gel was used. ($S=300$ m^2/g, $v=0,8$ cm^3/g, $d=120$ Å). 250 mL of DB18C6 alcohol solution was mixed with 1,13 g of SiO_2. After 4 days the DB18C6 concentration in solution was determined (using spectrophotometry) as 5,7 10^{-3} M i.e. SiO_2 adsorbed 1,5 10^{-4} M of DB18C6/1 g.

Sample 2. 20 mL of tetraethoxysilane were mixed with 6 mL of H_2O, 40 mL of an ethanol and 1 mL of initiator. After a few days the gel was dried for 3 hours at 110-120°C. The prepared gel ($S=800$ m^2/g, $V=0,3$ cm^3/g, $d=20$ Å) 1,132 g was mixed with 120,6 mL of DB18C6 (5,89.10^{-3} M). After a few days the DB18C6 concentration in solution was determined (using spectrophotometry), as 5,82 10^{-3} M/dm^3, i.e. SiO_2 adsorbed 7 10^{-6} M of DB18C6/1 g.

Samples 2'. 20 mL of tetraethoxysilane were mixed with 6 mL, H_2O, 40 of a mL ethanol solution of DB18C6 (1 g) and L ml of initiator. After a week, the gel product was dried for 3 hours at 110-120°C. The gel ($S=800$ m^2/g, $V=0,3$ cm^3/g, $d=20$ Å) contained DB18C6 in amount 0,456 10^{-4} M/g (Table 1).

Sample 3. 20 mL of tetraethoxysilane were mixed with 6 mL H_2O, 400 mL of an ethanol solution of DB18C6 (1 g) and 1 ml of initiator. The solution was evaporated on a water bath until viscous. After a few days, the prepared gel was dried for 3 hours at 110-120°C. The gel ($S=120$ m^2/g, $V=1,23$ cm^3/g, $d=410$ Å) contained DB18C6 in amount 2,023 10^{-4} M/g (Table I).

Sample 4. 4 mL of tetraethoxysilane were mixed with 1,2 mL H_2O, 400 mL of an ethanol solution of DB18C6 (1 g) and 16 mL of initiator. The solution was evaporated on a water bath until viscous. After a few days, the prepared gel was dried for 3 hours at 110-120°C. The gel ($S=100$ m^2/g, $V=1,42$ cm^3/g, $d=570$ Å) contained DB18C6 in amount 3,07 10^{-4} M/g (Table 1).

Sample 5. 2 mL of tetraethoxysilane were mixed with 0,6 mL H_2O, 400 mL of an ethanol solution of DB18C6 (1 g) and 32 mL of initiator. The solution was evaporated on a water bath until viscous. After a few days, the prepared gel was dried for 3 hours at 110-120°C. The gel (S=75 m^2/g, V=1,53 cm^3/g, d=820 Å) contained DB18C6 in amount 3,707 10^{-4} M/g (Table I).

Sample 6. For its preparation commercial silica gel was used (S=300 m^2/g, v=0,8 cm^3/g, d=120 Å). 250 mL of DB24C8 alcohol solution was mixed with 1,13 g of SiO_2. After 4 days, the DB24C8 concentration in solution was determined (using spectrophotometry), as 5,7 10^{-3} M, i.e. SiO_2 adsorbed 1,4 10^{-4} M of DB24C8/1 g.

TABLE I. THE DISTRIBUTION CONSTANTS K_D (AS QUANTITIES OF ^{137}Cs BOUND PER GRAM OF THE SORBENT) FOR SOME CROWN-ETHER MODIFIED POLYMERIC MATERIALS

Sorbent	**K_d, Bq/g**
PDB18C6	10,2
PDB24C8	4,3
PDB18C6 KPic	14,6
PDB18C6 $CaPic_2$	42,2
PDB18C6 $K_3Fe(CN)_6$	263,23
PDB24C8 KPic	8,4
PDB24C8 $CaPic_2$	12,2

Sample 7. 20 mL of tetraethoxysilane were mixed with 6 mL H_2O, 40 mL of an ethanol and 1 mL of initiator. After a few days the prepared gel was dried during 3 hours under 110-120°C. The resulting gel (S=800 m^2/g, V=0,3 cm^3/g, d=20 Å) 1,132 g was mixed with 120,6 mL of DB24C8 (5,89·10^{-3} M). After a few days the DB18C6 concentration in solution was 5,82·10^{-3} M, i.e. SiO_2 adsorbed 7·10^{-6} M of DB24C8/1 g.

Samples 7'. 20 mL of tetraethoxysilane were mixed with 6 mL H_2O, 40 mL of an ethanole solution of DB24C8 (1,3544 g) and 1 ml of initiator. After a week received gel was dried during 3 hours under 110-120°C. Received gel (S=790 m^2/g, V=0,3 cm^3/g, d=20 Å) contained DB24C86 in amount 0,456 10^{-4} M/g (Table 1).

Sample 8. 20 mL of tetraethoxysilane were mixed with 6 mL H_2O, 400 mL ethanol solution of DB24C8 (1,3544 g) and 1 ml of initiator. The solution was evaporated on a water bath until viscous. After a few days the gel product was dried for 3 hours at 110-120°C. The gel product (S=95 m^2/g, V=1,27 cm^3/g, d=460 Å) contained DB24C8 in amount 2,019 10^{-4} M/g (Table 1).

TABLE II. THE DISTRIBUTION CONSTANTS K_D (AS QUANTITIES OF ^{137}Cs BOUND PER GRAM OF THE SORBENT) AND K'_D (AS QUANTITIES OF ^{137}Cs BOUND PER GRAM OF THE CROWN-ETHER IN THE SAMPLE) FOR SOME CROWN-ETHER (WITH INCAPSULATED FERRO- AND FERRICYANIDES) MODIFIED POLYMERIC MATERIALS

Sorbent	**K_d, Bq/g**	**K'_d, Bq/mol**
PB15C5 $K_3Fe(CN)_6$	110,0	2890,00
PB15C5 $K_4Fe(CN)_6$	152,9	3520,0
PB18C6 $K_3Fe(CN)_6$	37,9	1860,0
PB18C6 $K_4Fe(CN)_6$	147,7	3520,0
PDB18C6 $K_3Fe(CN)_6$	215,2	3490,0
PDB18C6 $K_4Fe(CN)_6$	3649,5	4970,0
PDB24C8 $K_3Fe(CN)_6$	624,6	4630,0
PDB24C8 $K_4Fe(CN)_6$	392,3	4350,0

Sample 9. 4 mL of tetraethoxysilane were mixed with 1,2 mL H_2O, 400 mL of an ethanol solution of DB24C8 (1,3544 g) and 16 mL of initiator. The solution was evaporated on a water bath until viscous. After a few days the gel product was dried 3 hours at 110-120°C. The gel (S=89 m^2/g, V=1,46 cm^3/g, d=680 Å) contained DB24C8 in amount 3,071 10^{-4} M/g (Table 1).

Sample 10. 2 mL of tetraethoxysilane were mixed with 0,6 mL H_2O, 400 mL of an ethanol solution of DB24C8 (1,3544 g) and 32 ml of initiator. The solution was evaporated on a water bath until viscous. After a few days, the gel product was dried for 3 hours at 110-120°C. The gel product (S=70 m^2/g, V=1,58 cm^3/g, d=850 Å) contained DB24C8 in amount 3,702 10^{-4} M/g (table 3).

Sample 11. 2 mL of tetraethoxysilane were mixed with 0,6 mL H_2O, 400 mL of an ethanol solution of tetraazamacrocyclic (Fig. 1, h) ligand (1,3678 g) and 32 ml of initiator. The solution was evaporated on a water bath until viscous. After a few days the gel product was dried for 3 hours at 110-120°C. The gel product (S=75 m^2/g, V=1,58 cm^3/g, d=850 Å) contained ML in amount 4,59 10^{-4} M/g .

For samples 1-10, dynamic sorption was studied (see for example Fig. 6, for sample 4).

The chemisorption of Sr on samples 1-5 was examined by mixing 0,5 g of sorbent with 25 mL of the Sr solution (80 mg/L) during 2 hours. After this, the solutions after filtration were analysed for Sr concentration using atomic-adsorption technique (results are listed in Table III)

TABLE III. SAMPLES 1-10 SURFACE AREA, PORE SIZE, AND CHEMISORPTION PARAMETERS

No	Method	Static chemisorption capacity for Sr^{2+}, mg/g	DB18C6 (1-5), DB24C8 (6-10), $x10^{-4}$ M/g	S, m^2/g	V, cm^3/g	d, Å
1	Impregn.	12,62	1,440	300	0,8	120
2	Impregn.	0,61	0,072	800	0,3	20
2'	Coprecip.	3,90	0,456	800	0,3	20
3	Coprecip.	17,70	2,023	120	1,23	410
4	Coprecip.	26,90	3,070	100	1,42	570
5	Coprecip.	32,48	3,707	75	1,53	820
6	Impregn.	12,45	1,420	300	0,8	120
7	Impregn.	0,66	0,074	800	0,3	20
7'	Coprecip.	0,66	0,074	800	0,3	20
8	Coprecip.	4,10	0,451	790	0,3	20
9	Coprecip.	28,32	3,071	89	1,46	680
10	Coprecip.	35,81	3,702	70	1,58	850

The chemisorption of Sr was also studied using a solution of ^{85}Sr (500 mL, pH=1,7 (HNO_3)); the activity of the solution was 132,5 Bq/mL. To a 0,5354 g of sample 2 and 0,543 g of sample 5 were added 50 mL of ^{85}Sr solution. The sealed vessels were placed in a shaker and at 20, 50, 60, 90, 120, 180 minutes contact 1 mL sames were taken and analysed. The results are listed in Table IV.

In order to determine what factors (surface area, pore size) are affected by the modification of SiO_2 matrix with a macrocyclic ligand we used two types of previously prepared silica gels: one of them had low surface area (300 m^2/g) but quite large pore size (120 Å) and the other a high surface area (800 m^2/g) and small pore size (20 Å). The quantity of DB18C6 in these two samples were 1,44 10^{-4} M/g and 7,2 10^{-6} M/g respectively (Table III). It is clear that the pore size is more imporant for acceptance of the crown-ether. The samples 1,2 which were synthesized using the impregnation method, demonstrated low chemisorption capacity (Table III) because of their poor ability for macrocyclic ligands acceptance. In order to increase the quantity of crown-ether in the SiO_2 matrix we decided to introduce it into the SiO_2 on the stage of gel formation. Under these conditions, the ligand must participate in the SiO_2 lattice, surface and pore formation. Taking into account the results obtained for samples 1,2, we used such experimental conditions that would ensure the formation of SiO_2 gel with large pore size and containing a large amount of macrocyclic ligand.

TABLE IV. STATIC CHEMISORPTION CAPACITY OF SAMPLES 1-5 TOWARD ^{85}Sr AND ^{137}Cs, Bq/g OF SORBENT

No: Method	**Static chemisorption capacity (Bq/g) for**		**polymeric materials by crown-ether**	**Static chemisorption capacity for ^{137}Cs, Bq/g**
	^{85}Sr	**^{137}Cs**		
1 Impregn.	28862,26	30,4	PDB18C6	10,2
2 Impregn.	1395,09	2,4	PDB24C6	4,3
2' Coprecip.	8914,40	15,6	PDB18C6 $K_3Fe(CN)_6$	263,23
3 Coprecip.	40480,40	77,8	PDB18C6 $K_4Fe(CN)_6$	3649,5
4 Coprecip.	61520,99	85,3	PDB24C8 $K_3Fe(CN)_6$	624,6
5 Coprecip.	74282,61	109,1	PDB24C8 $K_4Fe(CN)_6$	392,3

Sample activity for ^{85}Sr was measured on γ-spectrometer ATKAM-300 (EG&G ORTEC), time of measuring - 200 sec. Sample activity for ^{137}Cs was measured on γ-spectrometer with semiconductor detector DGDK and impulse analyser AC-1024-95-16.

Comparing the results obtained for samples 2'-5 (Table III), it is apparent that increase of pore size leads to increase of macrocyclic ligand content in the prepared materials. They have a different static chemisorption capacity for Sr: the highest value was obtained with sample 5,which has the maximum pore size. Comparing data for samples 2'-5 it is clear that an increase in DB18C6 concentration does not vary linearly with increase in pore size. In our opinion it is connected with saturation of the SiO_2 matrix by DB18C6 and self-association of DB18C6. As a result, on the surface are present "active" and "non-active" crown-ether molecules. The quantity of "active" DB18C6 was measured by the static chemisorption capacity for Sr^{2+}.

The data listed in Table IV shows that the prepared samples are quite good sorbents for ^{85}Sr and ^{137}Cs, and the best among them is sample 5, which contains a greater amount of DB18C6. It is interesting that their Cs and Sr ions decontamination ability does not correlate with the amount of DB18C6 in the sample and is quite different for crown-ether modified polymers which we have previously synthesized and which are a good sorbents for Cs.

This suggests that the nature of matrix has an effect on chemisorption. For example, comparing the data for samples 1, 5 and PDB18C6, we can see that the concentration of DB18C6 in samples 1, 5 is only 2 and 5 times greater then for PDB18C6, but their chemisorption ability is 3 and 10 times greater respectively. Here the pore size of SiO_2 matrix has a large effect, which is better than polymeric matrices, because of it own sorption properties.

These results are in a good agreement with data obtained for SiO_2 samples containing DB24C8 (Table V).

All these samples (6-10), despite different contents of DB24C8 (Table I), have higher decontamination properties compared to PDB24C8 and are more effective than even samples 1-5 respectively. In our opinion this is connected with the influence of SiO_2 matrix characteristics on chemisorbtion (which are dependent of the initial concentrations of reagents). These characteristics also depend on the nature of the crown.

Looking at the results in Tables I-III we think that it is very interesting to synthesize such samples as 4,5,9,10 with encapsulated ferricyanides in order to increase their chemisorption ability.

TABLE V. STATIC CHEMISORPTION CAPACITY OF SAMPLES 6-10 (CONTAINING DB24C8) FOR ^{85}Sr AND ^{137}Cs, Bq/g OF SORBENT

No	**Method**	**Static chemisorption capacity (Bq/g) for**		**Crown-ether polymeric materials modified by crown-ether**	**Static chemisorption capacity for ^{137}Cs, Bq/g**
		^{85}Sr	**^{137}Cs**		
6	Impregn.	25683,1	30,4	PDB18C6	10,2
7	Impregn.	1125,02	4,2	PDB24C8	4,3
7'	Coprecip.	9112,10	18,7	PDB18C6 $K_3Fe(CN)_6$	263,23
8	Coprecip.	41356,30	81,4	PDB18C6 $K_4Fe(CN)_6$	3649,5
9	Coprecip.	63720,40	89,3	PDB24C8 $K_3Fe(CN)_6$	624,6
10	Coprecip.	77381,50	125,4	PDB24C8 $K_4Fe(CN)_6$	392,3

This year we also continued work in the field of the removal of Ru and other noble radionuclides and also Co, Cr. We synthesized and characterised, by IR, NMR, UV, VIS-spectroscopy, elemental analysis and thermogravimetry, a few samples containing tetraazamacrocycles. However the quantity of ligands in the prepared sorbents was quite small (by comparison with corresponding polymeric materials). This is due to poor solubility of the macrocycles in alcohol and because of this we can use only the impregnation method. We are now working on modifying the sol-gel method for preparing SiO_2 azamacrocycles samples.

The first step was the synthesis of sample 11 containing a tetraazamacrocycle. The concentration of ligand in this sample was quite high and close to that of the macrocycle in P-M1. This sample had good chemisorption characteristics (even higher than for P-M1) for Co, Cr decontamination. It was tested using cobalt and chromium salts where the metal ions are in oxidation states II and III respectively. For oxidation state II the process of decontamination was very fast, but for oxidation state III the process of decontamination was slow and was accelerated by heating.

4. CONCLUSION

Some inorganic (IN) and polymeric (P) materials, containing tetraazamacrocycles (TAM) and crown ethers (CE) have been synthesized:

IN-TAM, IN-CE, P-TAM, P-CE

They have been studied as sorbents for binding of Ru (and other noble radionuclides), Co, Cu, Ni (IN-TAM, P-TAM),Cs, Sr (IN-CE , P-CE) from model waste solutions. It has been established that polystyrene modified with tetraazamacrocycle (P-M1) quantitatively binds Ru and other noble metal ions at pH 0-1 and 3d-metal ions at $pH > 7$. P-M1 showed selectivity for noble and 3d-metal ions which was pH dependent.

The results of a study of sorption of ^{137}Cs from a model waste solution by polystyrene or its copolymer with PB15C5-crown-5 or PDB18C6-crown-6, PDB24C8-crown-8 showed that all of them remove ^{137}Cs from the solution with different K_d values. The most effective sorbent was obtained when the modifier was present on the surface of the sorbent as complex with metal salts and the best result was obtained with PDB18C6-$K_3Fe(CN)_6$ and PDB24C8-$K_4Fe(CN)_6$.

The results obtained for two types of new inorganic sorbents (IN-CE, IN-TAM) containing macrocyclic ligands as chelating groups and silica-gel as a matrix show that these materials are able to sorb even trace amounts of Sr and Cs from aqueous solutions. It was established that pore size is more important for acceptance of the crown-ether and correspondingly for efficiency of Sr, Cs chemisorption process and their decontamination. The best results in ^{85}Sr, ^{137}Cs decontamination were obtained with material containing the maximum quantity of DB18C6. But with IN-CE materials, Cs and Sr ions decontamination ability did not correlate with the amount, for example of DB18C6, in the sample. This poi to the role of the inorganic matrix and its texture on the process of chemisorption.

The results obtained during examination of the new materials (IN-CE, IN-TAM, P-CE, P-TAM) show that such materials have potential for Cs, Sr, Ru, Co etc. decontamination. The results also pointed to ways of increasing the decontamination properties of such materials.

The information on this work is also presented in the following publications:

1. MANORIK, P.A., MUSICHENKO, V.I., BOYKO, A.N. The Ru and platinoids chemosorbtions on the new tetraazamacrocycles modificated po materials.- Ukrainian Chemical Jornal, 1993 (in press).

2. MANORIK, P.A., MUSICHENKO, V.I., BOYKO, A.N., YATSIMIRSKII, K.B. New tetraazamacrocycles modificated polymeric materials for 3d,4d,5d-metal ions selective immobilization.- Dokladi Academii nauk Ukraine, 1993 (in press).

3. MANORIK, P.A., MUSICHENKO, V.I., BOYKO, A.N., YATSIMIRSKII, K.B. New tetraazamacrocycles modificated polymeric materials for 3d,4d,5d-metal ions selective immobilization.- Nuclear and hazardous waste management inter topical meeting "Spectrum-94", was held in Atlanta, Georgia, USA, August 14-18, 1994.

4. TALANOVA, G.G., YATSIMIRSKII, K.B., MANORIK, P.A. New crown-ethers modificated materials for Cs, Sr immobilization.- Nuclear and hazardous waste management international topical meeting "Spectrum-94", was held in Atlanta, Georgia, USA, August 14-18, 1994.

REFERENCES

[1] MANORIK, P.A., MUSICHENKO, V.I., BOYKO, A.N. The Ru and others platinoids chemosorbtions on the new tetraazamacrocycles modificated polystyrene materials.- Ukrainian Chemical Jornal, 1993 (in press).

[2] MANORIK, P.A., MUSICHENKO, V.I., BOYKO, A.N., YATSIMIRSKII, K.B. New tetraazamacrocycles modificated polymeric materials for 3d,4d,5d-metal ions selective immobilization.- Dokladi Academii nauk Ukraine, 1993 (in press).

[3] MANORIK, P.A., MUSICHENKO, V.I., BOYKO, A.N., YATSIMIRSKII, K.B. New tetraazamacrocycles modificated polymeric materials for 3d, 4d, 5d-metal ions

selective immobilization.- Nuclear and hazardous waste management international topical meeting "Spectrum-94", was held in Atlanta, Georgia, USA, August 14-18, 1994.

[4] TALANOVA, G.G., YATSIMIRSKII, K.B., MANORIK, P.A. New crown-ethers modificated materials for Cs, Sr immobilization.- Nuclear and hazardous waste management international topical meeting "Spectrum-94", was held in Atlanta, Georgia, USA, August 14-18, 1994.

[5] MANORIK, P.A., PHEDORENKO, M.A., KAGANOVSKII, V.A. New crown-ethers modificated materials for Sr immobilization.- Ukrainian Chemical Jornal, 1994 (in press).

[6] MANORIK, P.A., PHEDORENKO, M.A., KAGANOVSKII, V.A., BLYZNUKOVA, E.I. SiO_2, ZrO_2, Al_2O_3 matrixes with incapsulated crown-ethers as a sorbents for Sr immobilization.- Theoreticheskaya and experimentalnaya chimia, 1994 (in press).

[7] MANORIK, P.A., PHEDORENKO, M.A., BLYZNUKOVA, E.I. The principales of modificating ligands screening which are suitable for sorbents preparation.- Theoreticheskaya and experimentalnaya chimia, 1994 (in press).

[8] KAGANOVSKII, V.A., MANORIK, P.A., PHEDORENKO, D.A., MAKOVSKAYA, T.F., PHEDORENKO, M.A., BLYZNUKOVA, E.I. Synthetic condations influence on functional sorbents topochemistry forming.- Theoreticheskaya and experimentalnaya chimia, 1995 (in press).

[9] MANORIK, P.A., TALANOVA, G.G., YATSIMIRSKII, K.B., MUSICHENKO, V.I., PHEDORENKO, M.A., BLYZNUKOVA , E.I. New types of polymeric sorbents containing macrocycles (crown-ethers and tetraaza ligands) for Cs and noble radionuclides decontamination.- Dokladi Academii nauk Ukraine, 1995 (in press).

[10] MANORIK, P.A., KAGANOVSKII, V.A., YATSIMIRSKII, K.B., ZAITZEV, JU.P., TALANOVA, G.G., PHEDORENKO, D.A., MAKOVSKAYA, T.F., PHEDORENKO, M.A., BLYZNUKOVA, E.I. New types of polymeric and SiO_2 sorbents containing crown-ethers for Cs, Sr decontamination.- Dokladi Academii nauk Ukraine, 1995 (in press).

[11] MARTELL, A.E., SMITH, R.M. Critical stability constants, vol.1: Aminoacids.- New York: Plenum Press, 1974.-469p.

[12] MARTELL, A.E., SMITH, R.M. Critical stability constants, vol.2 Amines.- New York: Plenum Press, 1975.-415p.

[13] MARTELL, A.E., SMITH, R.M. Critical stability constants, vol.3. Other organic ligands.- New York: Plenum Press, 1977.-495p.

[14] MARTELL, A.E., SMITH, R.M. Critical stability constants, vol.4. Inorganic complexes.- New York: Plenum Press, 1976.-257p.

[15] MARTELL, A.E., SMITH, R.M. Critical stability constants, vol.5. First supplement.- New York: Plenum Press, 1982.-604p.

[16] CHRISTENSEN, J.J., IZATT, R.M. Handbook of metal ligand keets and related thermodynamic quantities N.J.: Marcell Dekker, 1983.-783p.

[17] IZATT, R.M., BRADSHAW, J.S., NIELSON, S.A., LAMB, J.D., CHRISTENSEN, J.J. Chem.Rev.- 1985.- 85.- p.271-339.

[18] YATSIMIRSKII, K.B., LAMPEKA, Ya. The Physicochemistry of Metal Complexes with Macrocyclic Ligands.-Naukova Dumka: Kiev.-1985 (Russian)

[19] IZATT, R.M., PAWLAK, K., BRADSHAW, J.S. Thermodynamic and kinetic data for macrocycle interaction with cations and anions Chem. Rev.- 1991.-91.- p.1721-2085.

[20] MANORIK, P.A. Mixed-ligand biocoordination metal compounds in the chemistry, biology, medicine.- Naukova Dumka: Kiev.-1985 (Russian).

[21] POPOV, V.V. The formation of disperce oxide, oxohydroxide and hydroxide systems.- NIITEHIM.-1991.-7.- p.1-75 (Russian)

[22] MYASOEDOV, B.F., SAVVINA, S.I. Chelateforming sorbents.- Nauka: Moscow.-1985 (Russian).

[23] LAMB, J.D., SMITH, R.G. Application of macrocyclic ligands to ion Chromatography. Proceeding of the international ion chromagraphy symposium, October 1990, San Diego, California.

[24] YATSIMIRSKII, K.B., KOLTCHINSKII, A.G., PAVLISHUCK, V.V., TALANOVA, G.G. The synthesis of macrocyclic compounds Naukova Dumka: Kiev, 1987

[25] KIMURA, K., HARINO, H., HAYATA, E., SHONO, T. Anal.Chem.-1986.- 58.-p.2233-2237.

[26] KIMURA, K., HAYATA, E., SHONOT, J. Chem. Soc. Chem. Commun.-1984.-p.271-272.

[27] BLASIUS, E., YANZEN, K.P. Topics in Current Chemistry.-1981.-98.- p.1[illegible]

[28] IGAWA, M., SAITO, K., TSUKAMOTO, J., TANAKA, M. Anal Chem.-53.- p.1942-1944.

[29] SUH, M., EOM, T., SUH, I. Bull.Korean Chem Soc.-1987.-8(5).-p.5-8. 20.

[30] JUNG, O., JUNG, H., KIM, J. Korean Chem.Soc. -1988.-32(4).-p.358-370.

[31] KREMLIAKOVA, N.Y., NOVIKOV, A.P., MYASOEDOV, B.F. J.Radioanal.Nucl.Chem., Letters.-1990.- 145(1).- p.23-28.

[32] PEIMLI, E.J. Radional. Nucl.Chem.,Letters.-1990.-144(1).- p.9-15.

INORGANIC SORBENTS FOR REMOVAL OF RADIOACTIVITY FROM AQUEOUS WASTE STREAMS:

1. Development of seeded ultrafiltration

2. Ion exchange properties of hydrous titanium oxide

3. The novel absorber evaluation club

E.W. HOOPER
Harwell Laboratory,
AEA Technology plc,
Harwell, Oxfordshire, United Kingdom

Abstract

This report describes briefly three areas of work involving inorganic sorbents that have been carried out at AEA Technology, Harwell during the course of the Co-ordinated Research Programme (CRP). 1. Seeded ultrafiltration, in which finely divided sodium nickel hexacyanoferrate (II), zirconium phosphate and a hydrous titanium oxide were used as a 'seed' cocktail, in combination with cross-flow membrane filtration, to decontaminate a simulate PWR primary coolant. All but one of the eight radionuclides present were reduced in concentration by a factor of ten or more. 2. Some data on the ion-exchange properties of hydrous titanium oxides are presented. These include the cation exchange capacity for barium (as a stand-in for radium), kinetics of sorption and Na:Ti ratio at different values of pH. 3. Some of the data collected from tests carried out by the Novel Absorber Evaluation Club are presented for a number of sorbents that have been examined during the period of this CRP.

1. DEVELOPMENT OF SEEDED ULTRAFILTRATION

1.1. INTRODUCTION

Ultrafiltration (UF) is a membrane separation process which uses pressure to force liquid through a fine membrane and thereby enables colloidal and fine precipitated materials at the nanometre level to be removed from liquid suspension. Fouling of the membrane surface by the solids is minimised by pumping the liquor across the surface of the membrane at high velocity (cross-flow) so as to produce a scouring action.

The development of membranes for industrial application has being ongoing since the 1960's with large scale processing examples being currently found in the dairy, paint, paper and metal finishing industries. The potential for the application of this technology to the treatment of liquid radioactive wastes has been recognised for a number of years and the Enhanced Actinide Removal Plant (EARP) at BNF plc, Sellafield, incorporates sufficient inorganic tubular ultrafiltration membranes to process upwards of 250 cubic metres of low level waste per day.

Nuclear power plant operation gives rise to a variety of liquid radioactive streams, most of which require some form of treatment to meet discharge authorisation limits to either the sea or inland waterways. Many of the radioactive nuclides in the wastes are present in colloidal form or adsorbed onto insoluble material and as such could be potentially removed by ultrafiltration alone. In other cases an alteration in the pH of the stream may lead to certain nuclides precipitating from solution making them compatible with ultrafiltration processing. Soluble species, however cannot be filtered directly without first being removed from solution. Work conducted by the Separation Technology Department at AEA Technology, Harwell has shown that by adding small quantities of finely divided ion exchange materials into the waste onto which soluble contaminants can be absorbed prior to filtration, higher decontamination factors can be achieved than by more conventional treatment such as flocculation/sedimentation. These materials are known generically as 'seeds' and the overall process 'seeded ultrafiltration'.

Over the last few years a continuing programme of work has been run in-house to investigate the potential application of seeded ultrafiltration. The objective of the programme is to identify seeds, or mixtures of seeds and the process conditions to give an optimised decontamination both in terms of reducing the levels of the radiologically important nuclides and the overall radiosotopic content.

1.2. RESULTS

Based on results obtained from a large number of small scale experiments, some pilot scale trials have been carried out using a simulated PWR primary coolant feed. The inactive components of the simulant are listed in Table I and this solution was spiked with radionuclides to the levels reported in Table II as 'Feed'.

TABLE I - INACTIVE COMPONENTS

Material	**Feed Level (mg/l)**	**Compound Added**
Boron	7000	H_3BO_3
Aluminium	0.05	$Al(NO_3)_3.9H_2O$
Calcium	0.05	$CaCl_2$
Magnesium	0.025	$MgCl_2.6H_2O$
Lithium	7.00	LiOH
Silicon	1.00	SiO_2
Chlorine	0.20	KCl
Fluorine	0.16	NaF
Sodium	0.19	NaF

The spiked simulated feed was treated by seeded ultrafiltration using a seed cocktail consisting of:

Sodium Nickel Hexacyanoferrate II	10 mg/L
Zirconium Phosphate	100 mg/L
Hydrous Titanium Oxide	100 mg/L

The solution pH was adjusted to 4 prior to ultrafiltration.

Table II lists the analytical data obtained in the experiment. The calculated decontamination factors (DF) show that more than 90% of each radionuclide, other than antimony, was removed from solution.

The permeate from the above experiment was adjusted to pH 11 using sodium hydroxide and then ultrafiltered without addition of seeds. This provided a further reduction in the levels of manganese and cobalt in the permeate (Table III).

TABLE II. SEEDED ULTRAFILTRATION AT pH 4

Isotope	Cr-51	Sb-125	Ru-106	Cs-137	Mn-54	Ag-110m	Fe-59	Co-60	Total
Sample	Activity (Bq/ml)								
Permeate 1	<0.02*	1.53	<0.05	<0.04	0.04	<0.02	<0.01	0.37	2.08
Permeate 2	0.17	3.88	<0.03	0.01	0.01	0.03	<0.01	0.18	4.32
Permeate 3	0.23	4.41	<0.02	0.02	0.01	<0.02	<0.02	0.17	4.90
Permeate 4	0.13	3.46	<0.02	<0.01	0.01	0.01	<0.02	0.10	3.76
Permeate 5	0.13	2.71	<0.08	<0.01	0.01	0.02	<0.01	0.09	3.06
Feed	3.30	4.80	1.68	17.6	0.17	10.7	0.19	14.7	53.2
Concentrate	66.0	16.3	47.5	455	3.09	384	7.44	312	1291
DF	20	1.5	>56	1764	17	669	>19	81	15

Run 5 - 650 litres of feed processed in 8.3 hours
Permeate samples taken at 1) 20 minutes, 2) 2 hours, 3) 4.2 hours, 4) 5.5 hours, 5) 8.3 hours
* Ignored in calculating DF

TABLE III. FILTRATION OF PERMEATE AT pH 11

Isotope	Cr-51	Sb-125	Ru-106	Cs-137	Mn-54	Ag-110m	Fe-59	Co-60	Total
Sample	Activity (Bq/ml)								
Permeate 1*	0.23	3.79	<0.01	1.35	0.01	1.48	<0.01	0.08	6.96
Permeate 2	0.18	2.59	<0.04	0.92	0.01	0.67	<0.04	0.03	4.48
Permeate 3	0.17	2.80	<0.04	0.80	0.01	0.45	<0.01	0.03	4.31
Permeate 4	0.17	2.36	<0.04	0.63	0.01	0.48	<0.01	0.03	3.73
Feed	0.16	2.99	<0.01	0.43	0.02	0.35	<0.02	0.20	4.18
Concentrate	2.12	4.39	2.08	1.40	0.15	4.78	0.29	4.30	19.5
DF	<1	1.2	-	<1	2	<1	-	6.7	<1

Run 6 - 530 litres of feed processed in 6.75 hours
Permeate samples taken at 1) 10 minutes, 2) 1.6 hours, 3) 5.25 hours, 4) 6.75 hours.
* Ignored in calculating DF

2. ION EXCHANGE PROPERTIES OF HYDROUS TITANIUM OXIDE

2.1. SYNTHESIS OF HYDROUS TITANIUM OXIDE (HTiO)

The standard method of synthesis that was developed involved the addition of molar sodium hydroxide to a known volume of 15% weight/volume titanium sulphate solution. The solution was stirred magnetically throughout, and the alkali added at a controlled rate until the pH remained stable at the desired value.

The slurry was centrifuged to remove the supernatant liquid and the precipitate then washed three times with deionized water in order to remove the sodium sulphate.

2.2. CATION EXCHANGE CAPACITIES (CEC) OF HTiO AT DIFFERENT pHs

To obtain information on the variation in ion exchange behaviour of hydrous titanium oxide, numerous batch tests using barium solutions spiked with ^{133}Ba were carried out.

To vary the pH, measured amounts of known molarity sodium hydroxide or hydrochloric acid were added to the barium solution with stirring before the HTiO was added, and the pH then recorded when stable (about 1-2 minutes) after the addition of the HTiO. The amounts added were sufficiently small to be ignored when considering the ionic strength. The mixtures were then shaken for one hour, filtered and -counted to obtain a value for the cation exchange capacity in milli-equivalents per gram of titanium. The results of the batch tests are shown in Fig. 1.

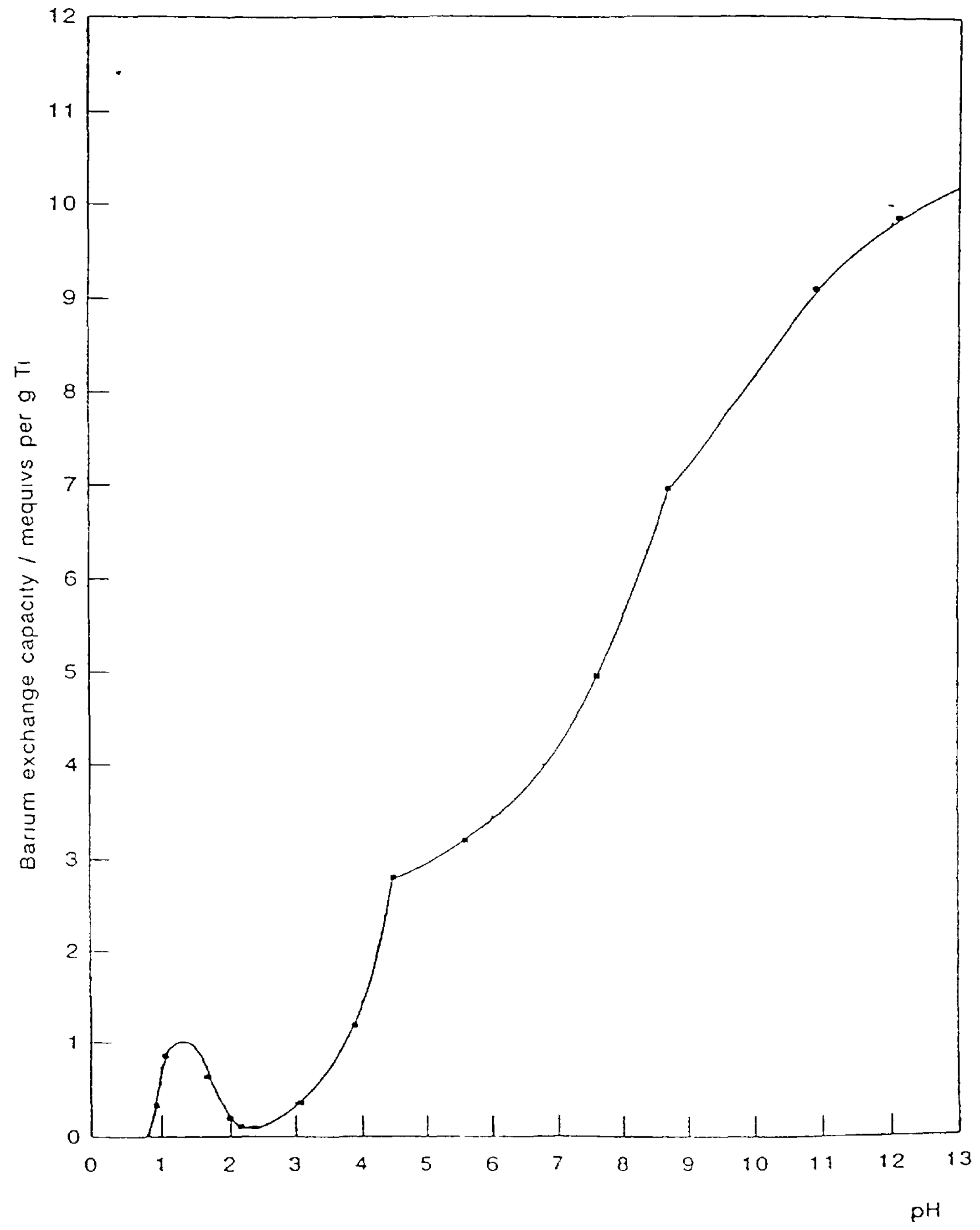

FIG. 1 Cation exchange capacity of HTiO vs pH

2.3. SODIUM TO TITANIUM RATIOS

Further experiments were carried out to determine the sodium to titanium ratio in the hydrous titanium oxide at different pHs. These were performed by adjusting the pH of some ^{22}Na labelled HTiO to the desired value, the mixture then being filtered through a MediaKap 10 filter and the sodium and titanium contents determined. The results obtained are shown in Fig. 2. In addition, the last point, not shown, was at pH 9.8 and Na:Ti 2.75.

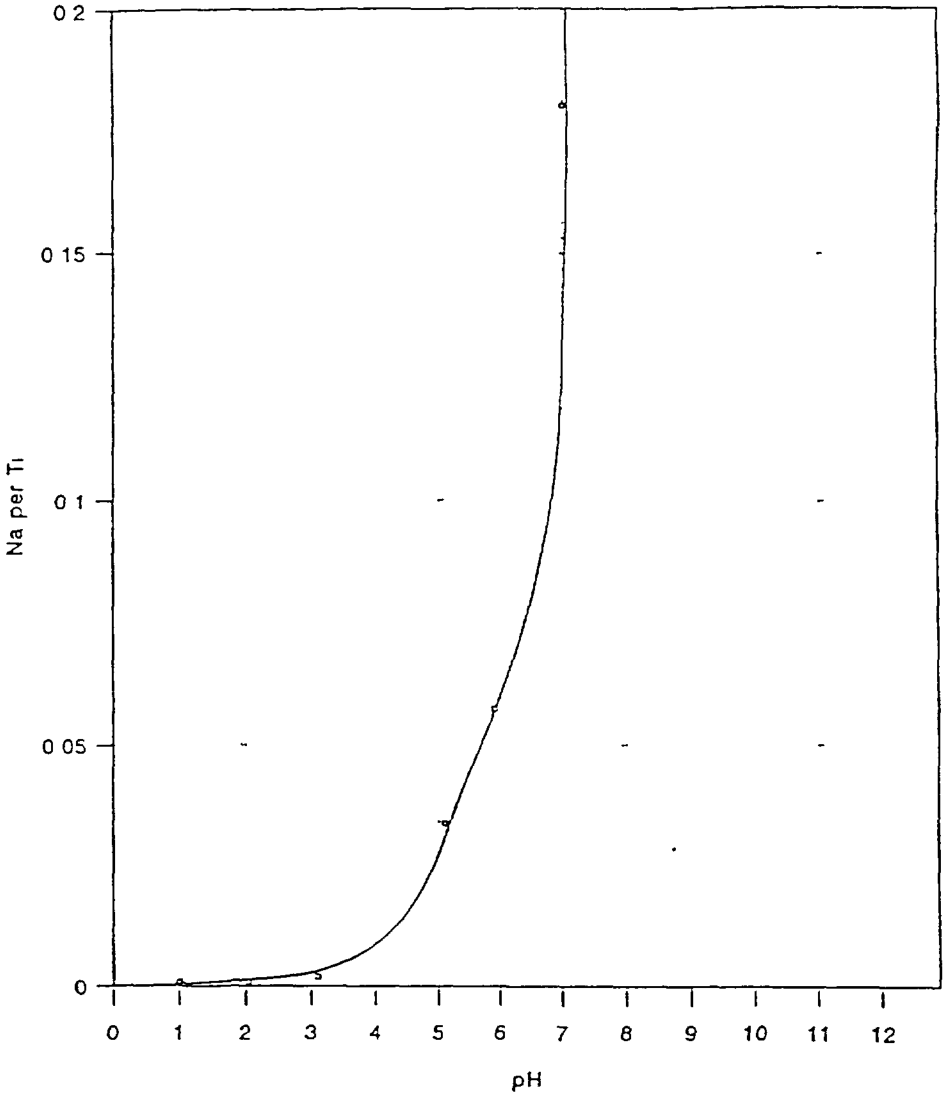

FIG. 2. Sodium: Titanium ratios vs pH

2.4. KINETICS OF SORPTION

Initial work using the batch test method had established that sorption by hydrous titanium oxide is extremely fast, almost maximum uptake being measured at twenty seconds, the fastest contact time that could be achieved under batch conditions. Hence to undertake any further investigation, a method enabling very short contact times would be necessary. To achieve this, a new experimental method was designed using a flow set-up. This is shown in Fig. 3.

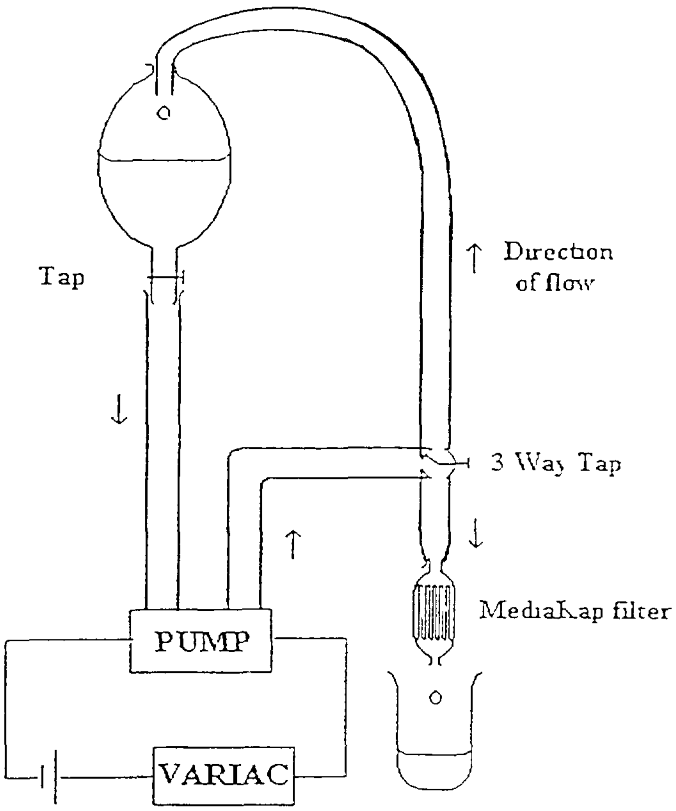

FIG. 3. Diagram to show apparatus for kinetic studies

A quantity of HTiO slurry, corresponding to 0.0279 g of titanium in 10 mls water, was laid down on a MediaKap 5 hollow fibre filter so that the HTiO coated the fibres through which the feed would pass The main flow system contained a standard, spiked, barium nitrate solution which had been neutralised to pH 7

This experiment was repeated at different pump speeds until values for the CEC over a range of residence times had been obtained The results are shown in Fig 4

The method outlined above and the results illustrated in Figure 4 were only able to attain residence times down to 0.37 seconds, at which time the CEC has already reached a significantly high, fairly stable, value. To reach residence times below this, two changes were made. Firstly, the filter used was changed to a MediaKap 2, with a 2cm^3 volume and a 35cm^2 surface area. The reduced filter volume would enable faster residence times for the same pump speeds Secondly to reduce the resistance exerted by the filter on the flow system, the amount of HTiO deposited was reduced by a factor of ten and the concentration of the barium stock reduced accordingly.

Since the surface area had been reduced by a factor of two, this meant that HTiO was laid down at a level of 0.08 x 10^{3} gTi/cm^2, a reduction of a factor of five, providing a reduction in the resistance of the filter and enabling shorter residence times in the filter to be attained.

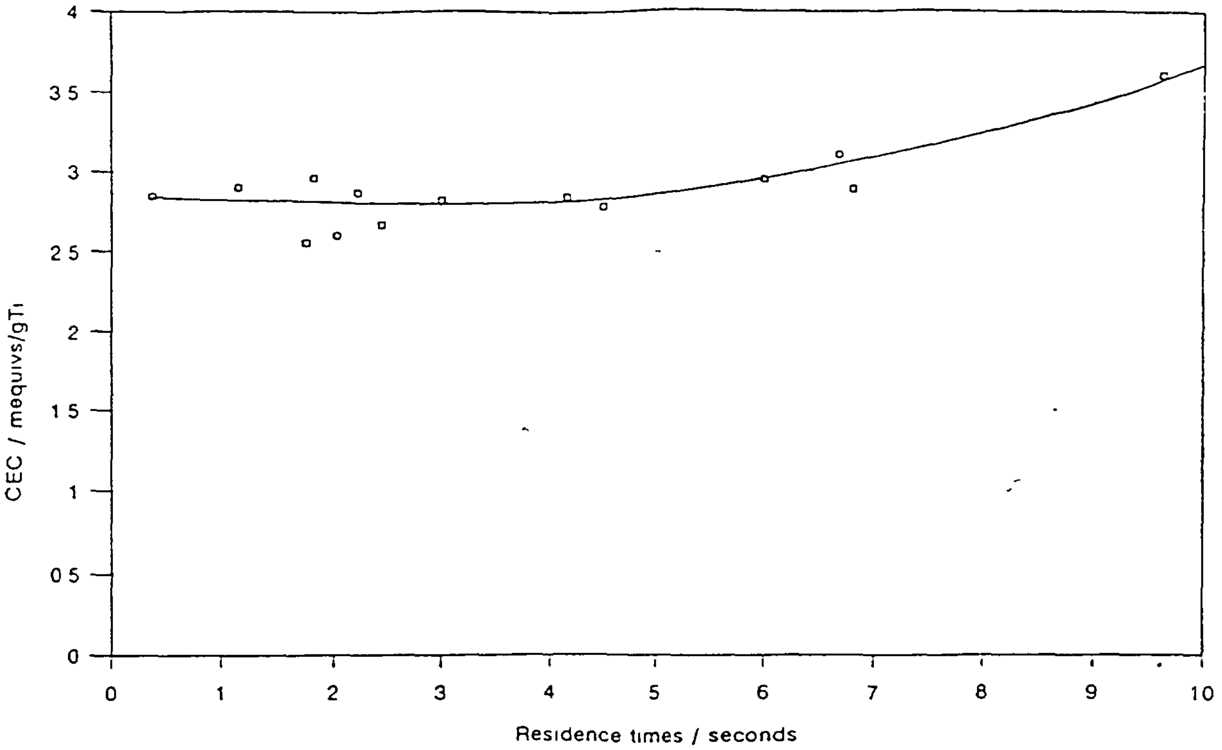

FIG. 4. Kinetic data: Residence Times vs CECs

The results obtained by this method are shown in Figure 5. These techniques have enabled residence times as low as 0.16 seconds to be attained.

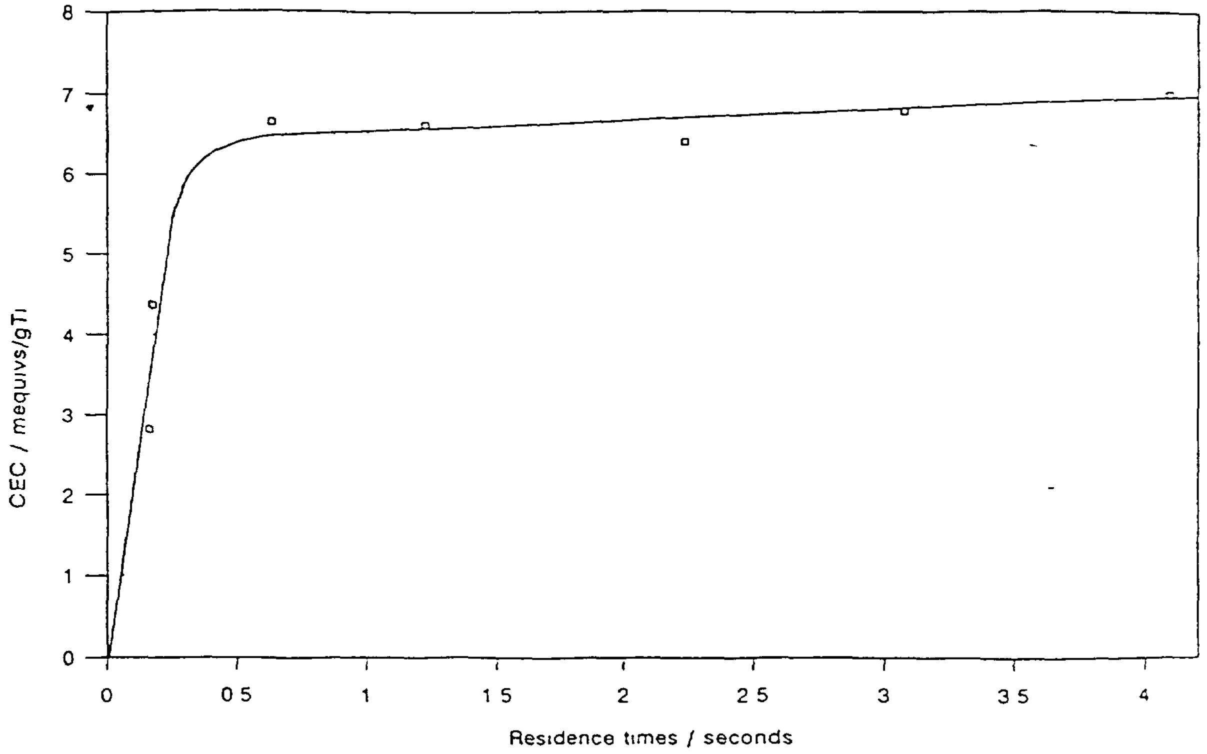

FIG. 5. Kinetic data: Residence vs CECs

3. THE NOVEL ABSORBER EVALUATION CLUB

3.1. INTRODUCTION

The separation processes of ion exchange and sorption have been widely used for many years throughout the nuclear industry to decontaminate aqueous waste streams. The two processes are analogous, both removing ions from solution either by exchange of a counter ion (ion exchange) or by direct physical removal (sorption). Standard formulations of sorbents are used world-wide to treat waste streams, but as new materials are manufactured and discharge authorisations are lowered, it becomes increasingly difficult for operators to adhere to the governing principles of ALARP *(as low as reasonably practicable)* and BATNEEC *(best available technology not entailing excessive cost)*. The objective of the Novel Absorber Evaluation Club is to remain aware of new sorbent developments and produce decontamination data on these products for direct comparison with standard 'benchmark' materials.

The Novel Absorber Evaluation Club (NAEC) was inaugurated in 1988 by AEA Technology on behalf of the UK Nuclear Industry as part of an overall requirement to minimise any environmental impact resulting from operations.

Membership of the NAEC is open to all parties with an interest in the decontamination of liquid radioactive effluents. The work programme of the NAEC is guided by the membership with a remit to provide quantitative experimental information of the ability of new and novel absorbent materials to remove radionuclides from solution.

Manufacturers and suppliers from industry and research are invited to submit materials for testing. Members prioritise the testing which comprises an initial screening of the material in a series of batch contacts with up to five standard NAEC reference waste streams. Further evaluation at suppliers request may include flow through packed beds or use as a finely divided addition in combination with membrane filtration. Test conditions may be varied by change of pH (in the range 3-11) and additions of organic contaminants or complexants.

With a membership covering the spectrum of the nuclear industry, the NAEC is in a unique position as an independent test facility with input from acknowledged experts in the field. Present members include British Nuclear Fuels plc, Nuclear Electric plc,

Ministry of Defence (represented by the Atomic Weapons Establishment, Aldermaston and Director General Submarines, Bath) and UKAEA Government Division. A parallel contract also exists with the Her Majesty's Inspectorate of Pollution for full exchange of information. Features of the Club programme include:

- Independent test facility for manufacturers of sorbents
- Utilisation and access to a database of results and reports generated since 1988
- Use of full radioactive facilities, experimental techniques and operator expertise
- NAEC methods and reference waste streams internationally recognised by IAEA

- Reference waste streams cover the range of radionuclides expected to be found in virtually any nuclear stream

- World-wide contacts through Club experience, membership and exchange of information with research centres

- Capability of tailoring an absorber recipe to optimise the decontamination of specified waste streams

This section will detail the tests carried out since 1991 and summarise the results obtained for the sorption of a range of elements including Mn, Co, Cr, Zn, Ru, Cs, Sr, Cd, Hg, Ag, Fe, Sb, Tc and alpha emitters (Pu + Am).

3.2. *TEST DETAILS*

3.2.1. Reference waste streams

Five reference waste streams are used in the test programme, known as NAEC (Novel Absorber Evaluation Club) S1, S2, S3, S4 or S5.

All waste streams are 0.05M in sodium nitrate to reduce peptisation of the sorbent.

NAEC S1 contains ^{137}Cs, ^{60}Co, ^{65}Zn, ^{51}Cr, ^{59}Fe, ^{54}Mn, ^{125}Sb, ^{106}Ru, ^{203}Hg, ^{109}Cd, ^{110m}Ag and ^{144}Ce at the 100 Bq/mL level.

This stream is analysed by gamma spectrometry with a limit of detection of 1Bq/mL or less i.e. a decontamination factor of 100 or more can be detected.

NAEC S2 contains ^{99}Tc as the pertechnetate (TcO_4^-) at the 100 Bq/mL level. Analysis is by beta scintillation counting.

NAEC S3 contains ^{239}Pu(IV) at 2 Bq/mL, ^{241}Am at 1 Bq/mL and ^{90}Sr at 5 Bq/mL Analysis is by both alpha and beta scintillation counting.

NAEC S4 is NAEC S1 plus 0.25 g/L ethylene diamine tetra-acetic acid added as sodium form, and 0.15 g/L citric acid. Analysis is by gamma spectrometry.

NAEC S5 Contains ^{239}Pu(IV), ^{241}Am and ^{237}Np (V) at 1 Bq/mL plus 1g/L $NaHCO_3$ to produce anionic carbonate species in alkaline solution.
Analysis is by alpha scintillation counting.

The test solutions are adjusted to the required pH value and then kept for at least 24 hours at room temperature before use so as to allow equilibration of ionic species.

The waste streams used in the test will depend on the type of sorbent being examined. NAEC S1, S3 and S4 will be generally used for cation absorbers and S2, S4 and S5 for anion absorbers.

3.2.2. Sorbent conditioning

Prior to use, sorbents are conditioned by washing with water adjusted to the experiment pH value using sodium hydroxide solution or dilute nitric acid. The washings are continued until the pH of the wash remains at its original value for 2-3 hours or preferably overnight.

The absorber is used in wet condition after decanting the wash liquor and removing excess moisture with a cellulose tissue.

3.2.3. Batch Contact Experiments

1 mL portions of the conditioned absorber are measured into 100 mL borosilicate conical flasks using a hypodermic syringe which has had the conical end removed to provide a 'full-bore' syringe. 50 mL of the reference waste stream are added and the flask sealed with a polythene stopper before placing in an agitated thermostatted water bath at 25°C. 1.5 mL portions of the liquid are removed after 1, 2, 4, 6 and 24 hours, centrifuged and then 1 mL removed for counting.

A control experiment, i.e. no sorbent present, is included to determine the extent of 'plate-out' on the walls of the container.

All experiments are performed in duplicate.

The analytical results are presented as Bq/mL and also as a calculated decontamination factor with reference to the original waste stream activity level:

$$\text{Decontamination Factor (DF)} = \frac{\text{activity per mL in feed}}{\text{activity per mL in sample}}$$

No correction is made for the volume changes resulting from sampling.

3.2.4. Column experiments

Glass columns of 1 cm bore are packed with 5 mL absorber. 500 mL of water adjusted to the test pH are washed through each column to condition the absorber. Each column is then allowed to stand for a further 5 days, the pH of conditioned effluent being checked daily and adjusted if necessary. The columns are operated at a throughput of 10 bed volumes per hour (approximately 400 mL per day) using reference streams NAEC S1, S2 and S3, as appropriate. The pooled effluent is sampled daily for analysis.

3.3. ABSORBERS TESTED

The absorbers tested by the NAEC have been provided by the following organisations (number of samples in brackets):

Duratek Corporation	(2)	USA
Toray Industries	(3)	Japan
Universal Chemicals	(2)	UK

Recherche Appliquee du Nord	(1)	France
MEL Chemicals	(2)	UK
Institute of Nuclear Chemistry	(4)	Poland
University of Reading	(8)	UK
Whatman Paper Ltd	(2)	UK
Tate & Lyle	(1)	UK
Rohm & Haas	(2)	USA
Termoxide Company	(3)	Russia
Technical University of Prague	(5)	Czech Republic
Allied Colloids	(1)	UK
BASF	(1)	Germany
Comenius University	(2)	Slovak Republic
Union Carbide USA		

The particular absorbers supplied by each organisation are identified in Table IV.

Absorbers to be tested in the future have been obtained from:

Eichrom	USA
Degussa	Germany
Sutcliffe Speakman	UK
Chemviron	UK

3.4. RESULTS

The results of tests carried out during 1988-1991 were reported at IEX '92'[1]

Table IV shows the results obtained with reference waste streams NAEC S1, S2 and S3 during the period 1992 to the time of writing. It should be noted that, for ease of scanning, the table shows either decontamination factor for each nuclide after 24 hours contact or mean effluent nuclide DF in the case of column experiments. These are indicated by either 'b' or 'c' respectively in column 2 of the table. In all cases, a > sign indicates that the nuclide was removed to below the limit of detection of the analytical method used.

All the results in Table IV were obtained at a solution pH of 9 except where stated.

Table V lists the Decontamination Factors obtained for selected absorbers after 24 hours contact with NAEC S1 at pH values of 3, 6 and 11.

Table VI shows the decontamination factors obtained with four absorbers contacted with NAEC S5 at pH values of 7, 9 and 11.

TABLE IV: DECONTAMINATION FACTORS AFTER 24 HOUR CONTACT

Absorber	batch/ column	Cr-51	Mn-54	Co-60	Zn-65	Ru-106	Cd-109	Sb-125	Cs-137	Hg-203	Fe-59	Tc-99	Sr-90	α
Clinoptilolite	b	11 4	6 0	9 1	25 6	>50	8 5	1 1	63	1 8	--	1 0	19 0	14 9
AW 500	b	12 2	49 6	37 6	>60	>60	>100	1 1	66	2 7	--	1 0	7 1	8 7
IRN 77/78 (pH 7)	b	--	2 5	2 8	>5	--	--	9 1	2 0	--	--	--	2 5	3 0
MEL Chemicals														
ZrP/ZrOH (9:1)	c	13 8	3 3	18 6	95 3	132	--	47 6	33 2	28 8	85	--	--	--
Inst. Nuclear Chemistry, Warsaw														
NiFC composite	b	4 1	2 4	4 1	13 1	3 4	--	1 1	35 4	--	--	--	--	--
CoFC composite	b	2 6	4 3	4 0	14 7	3 8	2 9	1 0	30 2	1 4	--	--	--	--
Polyan composite	b	1 9	5 7	5 4	12 2	3 2	3 0	1 0	1 0	1 4	--	--	2 3	2 8
TiFC composite (pH 6)	b	4 2	9 0	6 2	10 0	3 6	--	1 1	24 8	--	--	--	--	--
University of Reading														
Na Bentonite	b	1 6	1 8	1 8	2 7	1 4	--	1 0	1 3	--	>150	--	--	7 3
Ca Bentonite	b	1 7	2 1	2 1	3 3	2 6	--	1 0	1 2	--	6 0	--	--	13 6
Tin Hydrogen Phosphate	b	2 3	10 9	10 0	13 1	4 9	--	1 1	1 2	--	>150	--	--	2 1
Phosphatoantimonic acid	b	1 3	1 4	1 4	2 5	1 8	1 3	1 1	1 2	1 3	2 2	--	--	--
Oxide Y (pH 6)	b	3 4	5 7	7 4	11 1	4 8	--	1 2	1 1	--	15 4	--	31 5	54 5
LDH (pH 6)	b	1 9	4 5	4 5	4 0	2 5	2 8	1 0	1 1	1 6	3 1	--	1 6	--
Whatman Paper Ltd														
Partisil 4002	b	--	1 2	1 3	1 2	1 3	1 5	1 2	1 3	4 8	2 0	3 6	2 4	>150
Partisil 6002	b	--	1 1	1 0	1 0	1 0	1 1	1 2	1 2	2 8	1 4	2 0	1 6	15
Tate & Lyle														
Brimac 216 (milled)	b	1 8	8 5	7 4	>206	>254	--	1 2	1 0	--	--	--	1 0	>26
Brimac 216 (granular)	c	>123	36 4	21 2	>206	>254	--	1 9	1 1	--	--	1 1	3 2	80
Rohm & Haas														
Amberjet 1200	b	4 1	484	127	133	4 0	11 0	1 1	2 9	8 6	58 2	--	43 1	>1 5
Amberjet 4200	b	--	--	--	--	--	--	--	--	--	--	27 7	1 1	35 2

TABLE IV (cont): DECONTAMINATION FACTORS AFTER 24 HOUR CONTACT

Absorber	batch/ column	Cr-51	Mn-54	Co-60	Zn-65	Ru-106	Cd-109	Sb-125	Ag-110	Cs-137	Hg-203	Fe-59	Tc-99	Sr-90	α
Termoxid Company															
Termoxid 3A	b	80.8	71.5	38.7	69.2	3.8	18.2	--	55.4	>800	5.1	36.7	--	3.1	2.7
Termoxid 5	b	>194	>930	>890	180	>204	>128	--	144	1.9	95.6	110	1.0	25	107
Termoxid 231	b	--	--	--	--	--	--	--	--	--	--	--	1.3	8.1	>107
Technical University, Prague															
NiFC-PAN	b	2.3	1.9	2.0	--	3.0	>77	--	1.2	>1260	1.3	2.3	--	1.6	15
TiO-PAN	b	>312	1.2	1.2	--	>218	24.1	--	1.6	1.0	1.2	9.8	--	5.4	>110
NaTiO-PAN	b	1.9	3.4	1.4	--	2.7	2.3	--	3.5	12.0	17.5	13.1	--	8.0	2.0
MnO-PAN	b	1.6	2.7	3.6	--	2.8	10.4	--	1.6	3.9	4.3	3.0	--	8.4	2.3
Nm-PAN	b	2.2	2.7	2.7	--	2.9	>77	--	1.1	>1260	1.6	3.0	--	57	22
University of Reading, II															
Kanemite	b	2.0	6.7	6.1	68	1.9	10.6	--	1.4	3.7	4.8	--	1.1	4.6	1.9
HDS	b	--	--	--	--	--	--	--	--	--	--	--	1.3	1.6	86.7
LDH-X	b	--	--	--	--	--	--	--	--	--	--	--	1.2	--	--
Allied Colloids															
Beringite (fine)	b	2.4	3.6	2.4	5.8	2.9	3.8	1.3	1.4	2.8	2.2	--	--	1.1	>106
Beringite (coarse)	c	>107	>1450	573	>730	12.4	11.0	1.2	>97	2.7	112	>378	--	--	--
BASF															
Divergan HM	b	8.2	17.4	25.1	31.3	1.3	>69	--	>280	1.2	>65	3.8	--		
Comenius University, Bratislava															
Nalsit G	b	11.3	5.8	5.5	5.5	2.1	4.4	--	5.2	6.1	2.5	11.6	--	7.3	2.4
Y-sit (coarse)	b	11.6	2.7	3.0	3.4	1.9	3.7	--	3.7	8.0	1.6	17.3	--	5.9	1.7
Y-sit (fine)	b	9.6	6.0	8.1	13.9	2.3	18.6	--	108	22.6	3.0	9.1	--	32.8	11.5

TABLE V: EFFECT OF pH ON THE DECONTAMIANTION FACTOR - NAEC S1, 24 hr CONTACT

Absorber →	ZrP			ZrOH			Goethite			HTiO			NiFC			BRIMAC		
pH →	3	6	11	3	6	11	3	6	11	3	6	11	3	6	11	3	6	11
Cs-137	>200	9	>200	1	1	1 7	1	1	1	1	1.6	1.2	15	127	1.2	1.7	1.7	1.4
Fe-59	31	13	13	17	740	>8000	5	>1500	>8000	19	>1500	22	6	493	>8000	2	>1500	180
Co-60	231	290	7	27	290	23	1	>870	38	21	>870	15	9	290	140	132	435	58
Ag-110m	38	1 6	77	1 3	101	>2710	1	77	>2710	1.4	>1000	>2710	>114	10	1	1	101	12
Sb-125	1 3	1	-	29	>275	-	10	>275	-	1.5	1	-	1.3	1	-	1.2	1.8	-
Cr-51	4	5	3	6	>275	15	2	>275	6	4	>275	13	3	22	7	1.2	>275	18
Mn-54	116	>970	8	12	>970	55	1	>970	60	36	>970	17	7	23	86	3	>970	66
Zn-65	48	57	-	21	194	-	1	>970	-	16	243	-	6	323	-	22	323	-
Hg-203	1	3	4	2	10	214	13	5	65	11	25	17	5	>234	2	1	69	>904
Cd-109	8	6	22	5	16	54	12	49	>313	6	54	45	5	>70	>313	9	>70	>313
Ru-106	7	2 5	3	11	>110	44	25	>110	40	9	9	4	3	5	>886	>257	17	>886

Table VI: Decontamination Factors obtained with NAEC-S5, batch contacts, 24 hours

Sorbent	pH 7	pH 9	pH11
Milled Brimac 216	>216	216	>216
HTiO	4.5	6.4	9.6
Goethite	>258	>258	>258
Termoxid 5	2.4	2.8	3.1

3.5. SUMMARY

The results presented in this paper show only a fraction of the data collected by the Novel Absorber Evaluation Club. A regularly updated Data Base provides Members of the Club with relevant information on sorbents for the decontamination of radioactive waste streams.

The information obtained from the Club's Test Programme is also of value in designing treatment processes for the clean-up of industrial wastes to meet discharge authorisations, recover metal values and to allow water recycle.

REFERENCE

[1] E W Hooper 'Inorganic Sorbent for Aqueous Effluent Treatment" presented at IEX '92 Cambridge UK 12-17 July 1992.

PARTICIPANTS IN THE CO-ORDINATED RESEARCH PROGRAMME

Balek, V.	Nuclear Research Institute Řež plc, 250 68 Řež, Czech Republic
Bilewicz, A.	Dept. of Radiochemistry, Institute of Nuclear Chemistry and Technology, Ul. Dorodna 16, PL-03195 Warsaw, Poland
Chales Suárez, G.	Centro de Protección e Higiene de las Radiaciones, La Habana, Cuba
Davydov, Yu.P.	Institute of Radioecological Problems, Academy of Sciences of Belarus, 220108 Minsk Sosny, Belarus
El-Naggar, I.M.	Nuclear Fuel Technology Department, Hot Lab Centre, Atomic Energy Authority, P.O. Box 13759, Cairo, Egypt
Federici, V.	Centre de Cadarache, F-13108 Saint-Paul-lez-Durance Cedex, France
Hooper, E.W.	Harwell Laboratory, AEA Technology, Harwell, Oxon OX11 ORA, United Kingdom
Hutson, G.V.	BNFL UK Group, B229 Sellafield, Seascale, Cumbria CA20 1PG, United Kingdom
Kareta, V.I.	Institute of Physical Chemistry, Russian Academy of Sciences, Leninsky Prospect 31, Moscow 117919, Russian Federation
Lehto, J.	Laboratory of Radiochemistry, University of Helsinki, Unioninkatu 35, SF-00170 Helsinki, Finland
Manorik, P.	L.C. Pisarzhevskij Institute of Physical Chemistry, Academy of Sciences, Prospect Nauki, 252028 Kiev 28, Ukraine
Saarinen, L.	Laboratory of Radiochemistry, University of Helsinki, Unioninkatu 35, SF-00170 Helsinki, Finland
Samantha, S.K.	Process Engineering and Systems Development Division, Bhabha Atomic Research Centre, Trombay, Mumbai 400 085, India
Sebesta, F.	Faculty of Nuclear Science, Czech Technical University, Brehova 7, 115 19 Prague 1, Czech Republic

Shul, Y.G.	Dept. of Chemical Engineering, Yonsei University, Seodaemun-Ku 134-1, Seoul, Republic of Korea
Thamzil, L.	Radioactive Waste Management Technology Centre, National Atomic Energy Agency, Kawasan, Puspiptek Area, Serpong, Tangerang 15314, Batan, Indonesia
Tsarenko, A.	Division of Nuclear Fuel Cycle and Waste Management, International Atomic Energy Agency P.O. Box 100, A-1400 Vienna, Austria
Xianhua, Fan	China Institute of Atomic Energy, P.O. Box 275-93, Beijing, China

Research Co-ordination Meetings

Sellafield, United Kingdom: 11-15 October 1993
Beijing, China: 8-12 May 1995
Jakarta, Indonesia: 15-19 January 1996